



**NANYANG
TECHNOLOGICAL
UNIVERSITY**

**PROCESSING OF BIODEGRADABLE POLYMER
MICROPARTICLES FOR SUSTAINED DRUG
DELIVERY**

CHEN XI

SCHOOL OF CHEMICAL AND BIOMEDICAL ENGINEERING

2007

Processing of Biodegradable Polymer Microparticles for Sustained Drug Delivery

Chen Xi

School of Chemical and Biomedical Engineering

A thesis submitted to the Nanyang Technological University
in fulfilment of the requirement for the degree of
Doctor of Philosophy

2007

ACKNOWLEDGEMENTS

The author would like to express her sincere gratitude to her supervisor, Assistant Professor Ooi Chui Ping, for her consistent and thoughtful advice, continuous encouragement and help during the course of research. I especially appreciate her patience and kindness.

Thanks to Ms. Huang Yushu, Assistant Professor Tan Lay Poh, Dr. Santosh Kumar Rath, Mr. Goh Chin Foo and Mr. Zhao Xiaole for their help in ordinary work.

Thanks to all my friends in the lab, Mr. Tang Yonddan, Mr. Pan Jie, especially Ms. Wang Liwei and Ms. Yu Shucong for our support to each other.

Thanks to my final year project student of year 2004, Mr. Chan Tau Cheung for his work in the tablet format.

Thanks to all the technicians of AMRC lab 2, biomaterials lab, advanced materials characterization lab and polymer lab of SME for their technical support.

Thanks to my parents for their forever support to me, I miss them so much.

Finally I would like to thank my husband, for his wholeheartedly support and long lasting care.

CONTENTS

ACKNOWLEDGE	i
CONTENTS	ii
FIGURES AND TABLES	v
ABSTRACT	x
CHAPTER 1 INTRODUCTION	1
1.1 BACKGROUND	1
1.2 OBJECTIVES	4
1.3 SCOPE	5
1.4 OVERVIEW	6
CHAPTER 2 LITERATURE REVIEW	7
2.1 POLYMERIC BIOMATERIALS	7
2.1.1 Poly-glycolic acid/ (PGA)	10
2.1.2 Poly-lactic acid/ (PLA)	10
2.1.3 Copolymers/ (PLGA)	11
2.1.4 Summary	17
2.2 MECHANISMS OF POLYMER DEGRADATION AND EROSION	18
2.2.1 Hydrolysis	20
2.2.2 Polymer erosion	21
2.2.3 Degradation mechanism	24
2.3 CONTROLLED RELEASE	28
2.3.1 Release Mechanisms	28
2.3.2 Mathematical Models of Drug Release	32
2.3.3 Summary	38
2.4 MICROPARTICLE DRUG DELIVERY SYSTEMS	38
2.4.1 Emulsion	38
2.4.2 Preparation of Particulate Systems	42
2.4.3 Encapsulation of water-soluble compounds	45
2.5 POLYMERIC SYSTEMS FOR OPHTHALMIC DRUG DELIVERY	47
2.5.1 Structure of the eye	47
2.5.2 Drug Delivery Systems	47
2.6 CYTOMEGALOVIRUS	50
2.7 GANCICLOVIR	51
2.7.1 Current treatment of CMV retinitis	54
2.7.2 Summary	58
CHAPTER 3 EXPERIMENTAL METHODS AND TECHNIQUES	60

3.1 MATERIALS	60
3.2 SAMPLE PREPARATION	62
3.2.1 Ganciclovir-loaded microspheres	62
3.2.2 Pure microspheres	64
3.2.3 Particle size study	64
3.2.4 Laser Particle analyzer	65
3.3 DEGRADATION STUDIES	65
3.3.1 Changes in mass of microspheres	66
3.4 DRUG RELEASE STUDIES	66
3.5 MATERIALS CHARACTERIZATION	66
3.5.1 Thermal analysis	67
3.5.2 Scanning Electron Microscope (SEM)	70
3.5.3 Gel Permeation Chromatography (GPC)	70
3.5.4 Ultraviolet-visible Spectrometer	71
3.5.5 ¹³ C nuclear magnetic resonance (NMR) spectroscopy	72
3.5.6 X-Ray Photoelectron Spectroscopy (XPS)	74
CHAPTER 4 AS-RECEIVED MATERIALS AND MICROSPHERES	76
4.1 AS-RECEIVED MATERIALS	76
4.1.1 Thermo gravimetric Analyzer (TGA)	76
4.1.2 Modulated Differential Scanning Calorimetry (MDSC)	77
4.1.3 Gel Permeation Chromatography (GPC)	79
4.2 SIZE DISTRIBUTION OF MICROSPHERES	83
4.3 PURE MICROSPHERES	85
4.4 GCV-LOADED MICROSPHERES	87
4.4.1 MDSC	87
4.4.2 GPC	87
4.4.3 SEM	87
CHAPTER 5 HYDROLYTIC DEGRADATION OF BLANK MICROSPHERES	89
5.1 MODULATED DIFFERENTIAL SCANNING CALORIMETRY (MDSC)	89
5.1.1 Thermograms	89
5.1.2 Glass transition temperature, T _g	93
5.2 GEL PERMEATION CHROMATOGRAPHY (GPC)	98
5.3 CHANGES IN pH	105
5.4 CHANGES IN MASS	107
5.5 SEM	109
5.6 CONCLUSIONS	114
CHAPTER 6 HYDROLYTIC DEGRADATION OF DRUG LOADED MICROSPHERES	116
6.1 MODULATED DIFFERENTIAL SCANNING CALORIMETRY (MDSC)	121
6.1.1 Thermograms	121

6.1.2 Glass transition temperature, T _g	127
6.2 GEL PERMEATION CHROMATOGRAPHY (GPC)	134
6.2.1 % Normalized change in weight-average molecular weight	134
6.2.2 Polydispersity Index (PI)	143
6.3 CHANGES IN pH	146
6.4 CHANGES IN MASS	149
6.4.1 Comparison between molecular weight and changes in mass.	153
6.5 SEM	155
6.6 CONCLUSIONS	161
CHAPTER 7 CONTROLLED RELEASE OF DRUG LOADED MICROSPHERES	164
7.1 DRUG RELEASE STUDIES (IN VITRO)	164
7.1.1 Fractional Cumulative Release Curve of GCV-loaded microspheres	164
7.1.2 X-Ray Photoelectron Spectroscopy (XPS) study of GCV-loaded microspheres	171
7.1.3 Median effective dose (ED ₅₀) of GCV-loaded microspheres	173
7.2 RELEASE MECHANISMS OF GCV-LOADED MICROSPHERES	180
7.3 PHYSICAL MODEL OF DRUG RELEASE PROFILE	186
7.4 CONCLUSIONS	187
CHAPTER 8 DRUG LOADED POLYMERIC TABLETS	189
8.1 MODULATED DIFFERENTIAL SCANNING CALORIMETRY (MDSC)	190
8.2 CHANGES IN MASS	191
8.3 GEL PERMEATION CHROMATOGRAPHY (GPC)	192
8.4 CHANGES IN pH	195
8.5 FRACTIONAL CUMULATIVE RELEASE CURVE	196
8.6 RELEASE MECHANISMS OF GCV-LOADED TABLETS	202
8.7 SEM	205
8.8 CONCLUSIONS	208
CHAPTER 9 CONCLUSIONS	212
9.1 DEGRADATION STUDIES	212
9.1.1 Pure microspheres	212
9.1.2 GCV-loaded microspheres	214
9.2 DRUG RELEASE STUDIES	215
9.3 GCV-LOADED TABLETS	217
CHAPTER 10 FUTURE WORK	219
REFERENCES	222
BIBLIOGRAPHY	229

FIGURES AND TABLES

<u>FIGURE & TABLE</u>		PAGE
TABLE 3.1	POLYMER USED FOR THE FABRICATION OF THE MICROSPHERES	61
FIGURE 3.1	GCV CALIBRATION CURVE	72
TABLE 4.1	DECOMPOSITION TEMPERATURES FOR AS-RECEIVED POLYMER GRANULES	77
TABLE 4.2	GLASS TRANSITION TEMPERATURE (T_G) OF THE AS-RECEIVED POLYMER GRANULES	78
FIGURE 4.1	THERMOGRAM OF COMMERCIALY AVAILABLE GCV	79
TABLE 4.3	WEIGHT AVERAGE MOLECULAR WEIGHT (M_w), NUMBER AVERAGE MOLECULAR WEIGHT (M_n), POLYDISPERSITY INDEX (PI) OF THE AS RECEIVED PDLA AND PLGA POLYMERIC GRANULES	79
FIGURE 4.2	^{13}C NMR SPECTRA OF PLGA 75/25 I.V. 0.94 AND ASSIGNMENT OF THE GA CARBONYL RESONANCES	80
TABLE 4.4	R_{CMS} OF PLGA MICROSPHERES	82
TABLE 4.5	SIZE OF PLGA MICROSPHERES VARIES DIRECTLY WITH POLYMER CONCENTRATION	84
FIGURE 4.3	SIZE DISTRIBUTION OF PLGA 75/25 I.V. 0.94 MICROSPHERES	84
FIGURE 4.4	SEM PHOTOGRAPHS OF PLGA 50/50 I.V. 0.50 MICROSPHERES BEFORE DEGRADATION	86
TABLE 4.6	GLASS TRANSITION TEMPERATURE (T_G) OF THE GCV-LOADED MICROSPHERES PREPARED	87
FIGURE 4.5	SEM PHOTOGRAPHS OF A) GCV; B) PLGA 75/25 I.V. 0.94 7% GCV MICROSPHERES	88
FIGURE 5.1	THERMOGRAMS OF A) PDLA I.V. 0.22 MICROSPHERES BEFORE DEGRADATION AND AFTER DEGRADATION; B) PLGA 75/25 I.V. 0.94 MICROSPHERES BEFORE DEGRADATION AND AFTER DEGRADATION AND C) PLGA 50/50 I.V. 0.50 MICROSPHERES BEFORE DEGRADATION AND AFTER DEGRADATION IN PHOSPHATE BUFFERED SOLUTION AT 37 °C	90
FIGURE 5.2	GLASS TRANSITION TEMPERATURES (T_G) AS A FUNCTION OF DEGRADATION TIME FOR PLGA 75/25 I.V. 0.94 AND PLGA 75/25 I.V. 0.24 MICROSPHERES DEGRADED IN PHOSPHATE BUFFERED SOLUTION AT 37 °C	93
FIGURE 5.3	GLASS TRANSITION TEMPERATURES (T_G) AS A FUNCTION OF DEGRADATION TIME FOR PLGA 50/50 I.V. 0.50 AND PLGA 50/50 I.V. 0.22 MICROSPHERES DEGRADED IN PHOSPHATE BUFFERED SOLUTION AT 37 °C	95
FIGURE 5.4	GLASS TRANSITION TEMPERATURES (T_G) AS A FUNCTION OF DEGRADATION TIME FOR PLGA 75/25 I.V. 0.24, PLGA 50/50 I.V. 0.22 AND PDLA I.V. 0.22 MICROSPHERES DEGRADED IN PHOSPHATE BUFFERED SOLUTION AT 37 °C.	96
FIGURE 5.5	WEIGHT-AVERAGE MOLECULAR WEIGHT CHANGE OF PLGA 75/25 I.V. 0.94, PLGA 75/25 I.V. 0.24, PLGA50/50 I.V. 0.50, PLGA 50/50 I.V. 0.22 AND PDLA I.V. 0.22 MICROSPHERES AS A FUNCTION OF DEGRADATION TIME	98
FIGURE 5.6	NORMALIZED WEIGHT-AVERAGE MOLECULAR WEIGHT ($M_{\text{WT}}/M_{\text{W0}}$) FOR MICROSPHERES AS A FUNCTION OF DEGRADATION TIME. PLGA 75/25 I.V. 0.94, PLGA 75/25 I.V. 0.24, PLGA50/50 I.V. 0.50, PLGA 50/50 I.V. 0.22 AND PDLA I.V. 0.22	99
TABLE 5.1	TIME FOR WEIGHT AVERAGE MOLECULAR WEIGHT (M_w) OF THE PDLA AND PLGA MICROSPHERES TO DROP TO 10,000 DALTON	100
FIGURE 5.7	PLOT OF $\text{LN}(M_n)$ OF PDLA AND PLGA WITH HYDROLYTIC DEGRADATION TIME	102
TABLE	DEGRADATION RATE CONSTANT K' OF EACH PURE POLYMERIC	103

5.2	MICROSPHERES	
FIGURE 5.8	POLYDISPERSITY INDEX (PI) OF PLGA 75/25 I.V. 0.94, PLGA 75/25 I.V. 0.24, PLGA50/50 I.V. 0.50, PLGA 50/50 I.V. 0.22 AND PDLLA I.V. 0.22 MICROSPHERES AS A FUNCTION OF DEGRADATION TIME.	104
FIGURE 5.9	PH VALUE OF PDLLA I.V. 0.22, PLGA 75/25 I.V. 0.24, PLGA 50/50 I.V. 0.50 AND PLGA50/50 I.V. 0.22 MICROSPHERES AS A FUNCTION OF DEGRADATION TIME.	105
FIGURE 5.10	MASS CHANGE OF PDLLA I.V. 0.22, PLGA 75/25 I.V. 0.24, PLGA 50/50 I.V. 0.50 AND PLGA50/50 I.V. 0.22 MICROSPHERES AS A FUNCTION OF DEGRADATION TIME	107
FIGURE 5.11	SEM PHOTOGRAPHS OF PDLLA I.V. 0.22 MICROSPHERES A) 7 DAYS; B) 21 DAYS; C) 42 DAYS; AND D) 84 DAYS OF DEGRADATION	109
FIGURE 5.12	SEM PHOTOGRAPHS OF DEGRADED PLGA 75 /25 I.V. 0.94 MICROSPHERES A) 7 DAYS; B) 35 DAYS; C) 49 DAYS AND D) 77 DAYS.	110
FIGURE 5.13	SEM PHOTOGRAPHS OF PLGA 75 /25 I.V. 0.24 MICROSPHERES WITH RESPECT TO DEGRADATION TIME. A) 7 DAYS; B) 28 DAYS; C) 35 DAYS; D) 56 DAYS AND E) 63 DAYS	112
FIGURE 5.14	SEM PHOTOGRAPHS OF PLGA 50 /50 I.V. 0.50 MICROSPHERES WITH RESPECT TO DEGRADATION TIME. A) 7 DAYS; B) 21 DAYS; C) 28 DAYS AND D) 35 DAYS	113
TABLE 6.1	THERMAL PROPERTIES OF CRYSTALLINE PLLA, SEMICRYSTALLINE PLGA AND CRYSTALLINE GCV	116
FIGURE 6.1	SCHEMATIC DIAGRAM OF GANCICLOVIR MOLECULE IN DIFFERENT PH ENVIRONMENT	118
FIGURE 6.2	$\log \frac{[HGCV+]}{[GCV]}$ and $\log \frac{[GCV-]}{[GCV]}$ AS A FUNCTION OF PH VALUES	120
FIGURE 6.3	HEATING PROFILES OF GANCICLOVIR (GCV), BLANK PLGA 75/25 I.V. 0.94 MICROSPHERES AND GANCICLOVIR-LOADED (GCV-LOADED) PLGA 75/25 I.V. 0.94 MICROSPHERES OBTAINED FROM MODULATED DIFFERENTIAL SCANNING CALORIMETRY (MDSC) AT A HEATING RATE OF 5 °C/MIN.	121
FIGURE 6.4	THERMOGRAMS OF A) PLGA 75/25 I.V. 0.94 7% GCV MICROSPHERES BEFORE DEGRADATION AND AFTER 175 DAYS OF DEGRADATION AND B) PLGA 75/25 I.V. 0.94 18% GCV MICROSPHERES BEFORE DEGRADATION AND AFTER 154 DAYS OF DEGRADATION IN PHOSPHATE BUFFERED SOLUTION AT 37 °C	122
FIGURE 6.5	THERMOGRAMS OF A) PLGA 50/50 I.V. 0.50 5% GCV MICROSPHERES BEFORE DEGRADATION AND AFTER 42 DAYS OF DEGRADATION AND B) PLGA 50/50 I.V. 0.50 20% GCV MICROSPHERES BEFORE DEGRADATION AND AFTER 35 DAYS OF DEGRADATION IN PHOSPHATE BUFFERED SOLUTION AT 37 °C	124
FIGURE 6.6	THERMOGRAM OF A) PLGA 75/25 I.V. 0.24 5% GCV MICROSPHERES BEFORE DEGRADATION AND AFTER 56 DAYS OF DEGRADATION; B) PLGA 50/50 I.V. 0.22 7% GCV MICROSPHERES BEFORE DEGRADATION AND AFTER 35 DAYS OF DEGRADATION AND C) PDLLA I.V. 0.22 5% GCV MICROSPHERES BEFORE DEGRADATION AND AFTER 238S OF DEGRADATION IN PHOSPHATE BUFFERED SOLUTION AT 37 °C	126
FIGURE 6.7	GLASS TRANSITION TEMPERATURES (T_G) OF UNDEGRADED PURE, LOW PAYLOAD (5 - 7 % WT/WT) GCV-LOADED MICROSPHERES AND HIGH PAYLOAD (18-20 % WT/WT) GCV-LOADED MICROSPHERES. 1- PLGA 75/25 I.V. 0.94; 2- PLGA 75/25 I.V. 0.24; 3- PLGA 50/50 I.V. 0.50; 4- PLGA 50/50 I.V. 0.22; 5- PDLLA I.V. 0.22	127
FIGURE 6.8	GLASS TRANSITION TEMPERATURE (T_G) AS A FUNCTION OF DEGRADATION TIME FOR PLGA 75/25 I.V. 0.94 7% GCV, PLGA 75/25 I.V. 0.94 18% GCV AND PLGA 75/25 I.V. 0.24 5% GCV MICROSPHERES DEGRADED IN PHOSPHATE BUFFERED SOLUTION AT 37 °C	129
TABLE 6.2	THE GRADIENT VALUE K OF THE LINEAR T_G PLOTS WITH DEGRADATION TIME OF PURE AND GCV-LOADED POLYMERIC MICROSPHERES	130
FIGURE 6.9	GLASS TRANSITION TEMPERATURE (T_G) AS A FUNCTION OF DEGRADATION TIME FOR PLGA 50/50 I.V. 0.50 5% GCV, PLGA 50/50 I.V.	131

	0.50 20% GCV AND PLGA 50/50 I.V. 0.22 7% GCV MICROSPHERES DEGRADED IN PHOSPHATE BUFFERED SOLUTION AT 37 °C	
FIGURE 6.10	GLASS TRANSITION TEMPERATURE (T_G) AS A FUNCTION OF DEGRADATION TIME FOR PDLA I.V. 0.22 5% GCV, PLGA 75/25 I.V. 0.24 5% GCV AND PLGA 50/50 I.V. 0.22 7% GCV MICROSPHERES DEGRADED IN PHOSPHATE BUFFERED SOLUTION AT 37 °C	132
FIGURE 6.11	NORMALIZED CHANGE IN WEIGHT-AVERAGE MOLECULAR WEIGHT (ΔM_w) OF A) PDLA 0.22 5% GCV AND PDLA 0.22; B) PLGA 75/25 I.V. 0.94 7% GCV, PLGA 75/25 I.V. 0.94 18% GCV AND PLGA 75/25 I.V. 0.94; C) PLGA 75/25 I.V. 0.24 5% GCV AND PLGA 75/25 I.V. 0.24; D) PLGA 50/50 I.V. 0.50 5% GCV, PLGA 50/50 I.V. 0.50 20% GCV AND PLGA 50/50 I.V. 0.50; E) PLGA 50/50 I.V. 0.22 7% GCV AND PLGA 50/50 0.22 MICROSPHERES AS A FUNCTION OF DEGRADATION TIME.	135
FIGURE 6.12	$\ln(M_n)$ AGAINST DEGRADATION TIME BEFORE COMMENCEMENT OF SIGNIFICANT MASS LOSS FOR GCV-LOADED PDLA AND PLGA MICROSPHERES. A) PDLA I.V. 0.22 5% GCV; B) PLGA 75/25 I.V. 0.94 7% AND 18% GCV; C) PLGA 75/25 I.V. 0.24 5% GCV; D) PLGA 50/50 I.V. 0.50 5% AND 20% GCV; E) PLGA 50/50 I.V. 0.22 7% GCV MICROSPHERES	139
TABLE 6.3	DEGRADATION RATE CONSTANT k' OF EACH GCV-LOADED AND PURE POLYMERIC MICROSPHERES.	139
FIGURE 6.13	POLYDISPERSITY INDEX OF A) PDLA I.V. 0.22 5% GCV AND PDLA I.V. 0.22; B) PLGA 75/25 I.V. 0.94 7% GCV, PLGA 75/25 I.V. 0.94 18% GCV AND PLGA 75/25 I.V. 0.94; C) PLGA 75/25 I.V. 0.24 5% GCV AND PLGA 75/25 I.V. 0.24; D) PLGA 50/50 I.V. 0.50 5% GCV, PLGA 50/50 I.V. 0.50 20% GCV AND PLGA 50/50 I.V. 0.50; E) PLGA 50/50 I.V. 0.22 7% GCV AND PLGA 50/50 I.V. 0.22 MICROSPHERES AS A FUNCTION OF DEGRADATION TIME	144
FIGURE 6.14	PH VALUE OF A) PDLA I.V. 0.22 5% GCV AND PDLA I.V. 0.22; B) PLGA 75/25 I.V. 0.24 5% GCV AND PLGA 75/25 I.V. 0.24; C) PLGA 50/50 I.V. 0.50 5% GCV, PLGA 50/50 I.V. 0.50 20% GCV AND PLGA 50/50 I.V. 0.50; D) PLGA 50/50 I.V. 0.22 7% GCV AND PLGA 50/50 I.V. 0.22 MICROSPHERES AS A FUNCTION OF DEGRADATION TIME	147
FIGURE 6.15	MASS CHANGE OF A) PDLA I.V. 0.22 5% GCV AND PDLA I.V. 0.22; B) PLGA 75/25 I.V. 0.24 5% GCV AND PLGA 75/25 I.V. 0.24; C) PLGA 50/50 I.V. 0.50 5% GCV, PLGA 50/50 I.V. 0.50 20% GCV AND PLGA 50/50 I.V. 0.50; D) PLGA 50/50 I.V. 0.22 7% GCV AND PLGA 50/50 I.V. 0.22 MICROSPHERES AS A FUNCTION OF DEGRADATION TIME	150
TABLE 6.4	COMMENCE TIME OF MASS LOSS FOR PURE AND GCV-LOADED PLGA, PDLA MICROSPHERES	153
FIGURE 6.16	CHANGES IN PERCENTAGE OF NORMALIZED M_w AND NORMALIZED WEIGHT OF A) PDLA I.V. 0.22 5% GCV; B) PLGA 75/25 I.V. 0.24 5% GCV; C) PLGA 50/50 I.V. 0.50 5% GCV; D) PLGA 50/50 I.V. 0.50 20% GCV; E) PLGA 50/50 I.V. 0.22 7% GCV MICROSPHERES DURING DEGRADATION AT 37 °C.	154
FIGURE 6.17	SEM PHOTOGRAPHS OF PDLA I.V. 0.22 5% GCV MICROSPHERES A) 7 DAYS; B) AFTER 105 DAYS; C) 168 DAYS AND D) 182 DAYS OF DEGRADATION	156
FIGURE 6.18	SEM PHOTOGRAPHS OF PLGA 75/25 I.V. 0.94 7% GCV MICROSPHERES A) 7 DAYS; B) 105 DAYS; C) 119 DAYS AND D) 154 DAYS OF DEGRADATION	157
FIGURE 6.19	SEM PHOTOGRAPHS OF PLGA 75/25 I.V. 0.94 18% GCV MICROSPHERES A) 14 DAYS; B) 70 DAYS; C) 84 DAYS AND D) 98 DAYS OF DEGRADATION.	158
FIGURE 6.20	SEM PHOTOGRAPHS OF PLGA 75/25 I.V. 0.24 5% GCV MICROSPHERES A) 7 DAYS; B) 28 DAYS; C) 35 DAYS AND D) 42 DAYS OF DEGRADATION.	159
FIGURE 6.21	SEM PHOTOGRAPHS OF PLGA 50/50 I.V. 0.50 5% GCV MICROSPHERES A) 7 DAYS AND B) 14 DAYS OF DEGRADATION	159
FIGURE 6.22	SEM PHOTOGRAPHS OF PLGA 50/50 I.V. 0.50 20% GCV MICROSPHERES A) 7 DAYS AND B) 21 DAYS OF DEGRADATION	160
FIGURE 7.1	FRACTIONAL CUMULATIVE RELEASE OF GCV FROM THE PLGA AND PDLA MICROSPHERES IN PHOSPHATE-BUFFERED SOLUTION (PH 7.0)	164

	AT 37 °C. THE VALUES ARE SHOWN AS MEAN ± SD OF N = 5, PLGA 75/25 I.V. 0.94 7% GCV, PLGA 75/25 I.V. 0.94 18% GCV, PLGA 75/25 I.V. 0.24 5% GCV, PLGA 50/50 I.V. 0.50 5% GCV, PLGA 50/50 I.V. 0.50 20% GCV, PLGA 50/50 I.V. 0.22 7% GCV, PDLLA I.V. 0.22 5% GCV.	
TABLE 7.1	QUANTIFICATION REPORT OF SURFACE ANALYSIS OF GCV (CYMEVENE), PLGA 75/25 I.V. 0.94 7% GCV AND PLGA 75/25 I.V. 0.94 18% GCV MICROSPHERES.	173
FIGURE 7.2	SEMI LOGARITHMIC PLOTS OF GCV CONCENTRATIONS IN PHOSPHATE-BUFFERED SOLUTION (PH 7.0) AT 37 °C. THE VALUES ARE SHOWN AS MEAN OF N = 5, PLGA 75/25 I.V. 0.94 7% GCV, PLGA 75/25 I.V. 0.94 18% GCV, PLGA 75/25 I.V. 0.24 5% GCV, THE AREA BETWEEN THE TWO LINES (100 NG/ML, 3000NG/ML) INDICATES A 50% EFFECTIVE DOSE (ED50) OF GANCICLOVIR FOR HUMAN CYTOMEGALOVIRUS REPLICATION.	174
FIGURE 7.3	SEMI LOGARITHMIC PLOTS OF GCV CONCENTRATIONS IN PHOSPHATE-BUFFERED SOLUTION (PH 7.0) AT 37 °C. THE VALUES ARE SHOWN AS MEAN OF N = 5, PLGA 50/50 I.V. 0.50 5% GCV, PLGA 50/50 I.V. 0.50 20% GCV, PLGA 50/50 I.V. 0.22 7% GCV, THE AREA BETWEEN THE TWO LINES (100 NG/ML, 3000NG/ML) INDICATES A 50% EFFECTIVE DOSE (ED50) OF GANCICLOVIR FOR HUMAN CYTOMEGALOVIRUS REPLICATION.	174
FIGURE 7.4	SEMI LOGARITHMIC PLOTS OF GCV CONCENTRATIONS IN PHOSPHATE-BUFFERED SOLUTION (PH 7.0) AT 37 °C. THE VALUES ARE SHOWN AS MEAN OF N = 5, PDLLA I.V. 0.22 5% GCV, THE AREA BETWEEN THE TWO LINES (100 NG/ML, 3000 NG/ML) INDICATES A 50% EFFECTIVE DOSE (ED50) OF GANCICLOVIR FOR HUMAN CYTOMEGALOVIRUS REPLICATION.	175
TABLE 7.2	INITIAL GCV AMOUNT PER 10 MG OF MICROSPHERES BEFORE IMMERSION IN PBS SOLUTION.	176
FIGURE 7.5	SEMI LOGARITHMIC PLOTS OF GCV CONCENTRATIONS IN PHOSPHATE-BUFFERED SOLUTION (PH 7.0) AT 37 °C. THE VALUES ARE SHOWN AS MEAN OF N = 5, PLGA I.V. 0.24 5% GCV, PLGA 75/25 I.V. 0.94 18% GCV AND PLGA 75/25 I.V. 0.94 7% GCV MICROSPHERES. THE AREA BETWEEN THE TWO LINES (100 NG/ML, 3000NG/ML) INDICATES A 50% EFFECTIVE DOSE (ED50) OF GANCICLOVIR FOR HUMAN CYTOMEGALOVIRUS REPLICATION.	178
FIGURE 7.6	SEMI LOGARITHMIC PLOTS OF GCV CONCENTRATIONS IN PHOSPHATE-BUFFERED SOLUTION (PH 7.0) AT 37 °C. THE VALUES ARE SHOWN AS MEAN OF N = 5, PLGA 50/50 I.V. 0.50 5% GCV, PLGA 50/05 I.V. 0.50 20% GCV AND PDLLA I.V. 0.22 5% GCV MICROSPHERES. THE AREA BETWEEN THE TWO LINES (100 NG/ML, 3000NG/ML) INDICATES A 50% EFFECTIVE DOSE (ED50) OF GANCICLOVIR FOR HUMAN CYTOMEGALOVIRUS REPLICATION.	179
FIGURE 7.7	FITTING CURVES (BOTH MT/MINFINITE VERSUS T AND LOG (MT/MINFINITE) VERSUS LOG (T))OF A) PDLLA I.V. 0.22 5% GCV; B) PLGA 75/25 I.V. 0.94 7% GCV; C) PLGA 75/25 I.V. 0.94 18% GCV; D) PLGA 75/25 I.V. 0.24 5% GCV; E) PLGA 50/50 I.V.0.50 5% GCV; F) PLGA50/50 I.V. 0.50 20% GCV; AND G) PLGA 50/50 I.V. 0.22 7% GCV MICROSPHERES.	183
FIGURE 7.8	PHYSICAL MODEL OF DRUG RELEASE FOR THE GCV-LOADED MICROSPHERES. A) UPON IMMERSION INTO THE PBS SOLUTION. B) DURING THE DIFFUSION RELEASE PHASE. C) POLYMERIC MATRIX SWELLS AND CRACKS, SMALL PORES OR MICRO-CHANNELS FORMED WITH FURTHER DEGRADATION. D) FINAL BURST RELEASE PHASE.	186
TABLE 8.1	PARAMETERS FOR SAMPLE ANNEALING	189
FIGURE 8.1	GLASS TRANSITION TEMPERATURE (T _G) AS A FUNCTION OF DEGRADATION TIME FOR PDLLA I.V. 0.22 5% GCV TABLETS, PLGA 75/25 I.V. 0.94 7% GCV TABLETS, PLGA 75/25 I.V. 0.24 5% GCV TABLETS, PLGA 50/50 I.V. 0.50 5% GCV TABLETS AND PLGA 50/50 I.V. 0.22 7% GCV TABLETS DEGRADED IN PBS AT 37 °C.	190
FIGURE	CHANGES IN MASS AS A FUNCTION OF DEGRADATION TIME FOR	191

	8.2	PLGA 75/25 I.V. 0.24 5% GCV TABLETS, PLGA 75/25 I.V. 0.94 7% GCV TABLETS, PDLLA I.V. 0.22 5% GCV TABLETS, PLGA 50/50 I.V. 0.22 7% GCV TABLETS AND PLGA 50/50 I.V. 0.50 5% GCV TABLETS DEGRADED IN PBS AT 37 °C.	
FIGURE	8.3	NORMALIZED WEIGHT AVERAGE MOLECULAR WEIGHT (M_w) AS A FUNCTION OF DEGRADATION TIME FOR PLGA 75/25 I.V. 0.24 5% GCV TABLET, PLGA 75/25 I.V. 0.94 7% GCV TABLET, PDLLA I.V. 0.22 5% GCV TABLET, PLGA 50/50 I.V. 0.22 7% GCV TABLET AND PLGA 50/50 I.V. 0.50 5% GCV TABLET DEGRADED IN PBS AT 37 °C.	193
FIGURE	8.4	$\ln(M_n)$ VS. DEGRADATION TIME FOR PDLLA I.V. 0.22 5% GCV; PLGA 75/25 I.V. 0.94 7% GCV AND PLGA 75/25 I.V. 0.24 5% GCV TABLETS.	194
TABLE	8.2	DEGRADATION RATE CONSTANT 'K' OF THE TABLETS AND MICROSPHERES.	194
FIGURE	8.5	PH AS A FUNCTION OF DEGRADATION TIME FOR PLGA 75/25 I.V. 0.24 5% GCV TABLETS, PLGA 75/25 I.V. 0.94 7% GCV TABLETS, PDLLA I.V. 0.22 5% GCV TABLETS, PLGA 50/50 I.V. 0.22 7% GCV TABLETS AND PLGA 50/50 I.V. 0.50 5% GCV TABLETS DEGRADED IN PBS AT 37 °C.	195
FIGURE	8.6	FRACTIONAL CUMULATIVE RELEASE OF GCV FROM THE PLGA, PDLLA TABLETS IN PHOSPHATE-BUFFERED SOLUTION (PH 7.0) AT 37 °C. THE VALUES ARE SHOWN AS MEAN \pm SD OF N=5, PLGA 75/25 I.V. 0.24 5% GCV TABLET, PLGA 75/25 I.V. 0.94 7% GCV TABLET, PDLLA I.V. 0.22 5% GCV TABLET, PLGA 50/50 I.V. 0.22 7% GCV TABLET AND PLGA 50/50 I.V. 0.50 5% GCV TABLET.	196
TABLE	8.3	RELEASE TIME FRAME DIFFERENCES OF MICROSPHERES AND TABLETS.	197
FIGURE	8.7	GCV CONCENTRATION AS A FUNCTION OF TIME DURING DRUG RELEASE FOR PLGA 75/25 I.V. 0.94 7% GCV TABLET AND PLGA 75/25 I.V. 0.24 5% GCV TABLET.	199
FIGURE	8.8	GCV CONCENTRATION AS A FUNCTION OF TIME DURING DRUG RELEASE FOR PLGA 75/25 I.V. 0.94 7% GCV TABLET AND PLGA 75/25 I.V. 0.24 5% GCV TABLET AFTER MODIFICATION OF AMOUNT.	200
FIGURE	8.9	GCV CONCENTRATION AS A FUNCTION OF TIME DURING DRUG RELEASE FOR PLGA 50/50 I.V. 0.50 5% GCV TABLET AND PLGA 50/50 I.V. 0.22 7% GCV TABLET.	201
FIGURE	8.10	GCV CONCENTRATION AS A FUNCTION OF TIME DURING DRUG RELEASE FOR PLGA 50/50 I.V. 0.50 5% GCV TABLET AND PLGA 50/50 I.V. 0.22 7% GCV TABLET AFTER MODIFICATION OF AMOUNT.	201
FIGURE	8.11	FITTING CURVES (BOTH M_t/M_{∞} VERSUS t AND $\log(M_t/M_{\infty})$ VERSUS $\log(t)$) OF A) PDLLA I.V. 0.22 5% GCV; B) PLGA 75/25 I.V. 0.94 7% GCV; C) PLGA 75/25 I.V. 0.24 5% GCV; D) PLGA 50/50 I.V. 0.50 5% GCV AND E) PLGA 50/50 I.V. 0.22 7% GCV TABLETS.	204
FIGURE	8.12	SEM PHOTOGRAPHS OF PLGA 75/25 I.V. 0.24 5% GCV TABLETS A) 0 DAY; B) 49 DAYS; C) 70 DAYS AND D) 77 DAYS OF DEGRADATION.	206
FIGURE	8.13	SEM PHOTOGRAPHS OF PLGA 75/25 I.V. 0.94 7% GCV TABLETS A) 0 DAY; B) 70 DAYS; C) 98 DAYS AND D) 112 DAYS OF DEGRADATION.	207
FIGURE	8.14	SEM PHOTOGRAPHS OF PLGA 50/50 I.V. 0.22 7% GCV TABLETS A) 0 DAY; B) 14 DAYS OF DEGRADATION.	208
FIGURE	8.15	SEM PHOTOGRAPHS OF PLGA 50/50 I.V. 0.50 5% GCV TABLETS A) 0 DAY; B) 14 DAYS AND C) 42 DAYS OF DEGRADATION.	208

ABSTRACT

CMV Retinitis is the most frequently encountered HIV-related ocular opportunistic infection that affects 25% to 40% of people with AIDS¹. It is caused by cytomegalovirus (CMV), which if left untreated can destroy the entire retina in 3 to 6 months and cause blindness. Hence, it would be ideal to develop a biodegradable drug delivery system, which would deliver therapeutic levels of ganciclovir locally to the eye for a period of 1 to 3 months, after which the system would be absorbed by the body. The objective of this research is to develop a biocompatible, drug delivery system made from PDLLA and PLGA microspheres, of various LA to GA ratio and molecular weight. The effects of drug distribution and polymer degradation on the drug release profile were investigated. Pure PDLLA and PLGA microspheres and ganciclovir-loaded microspheres were prepared using an oil-in-water (O/W) emulsification technique. GCV-loaded PDLLA and PLGA microspheres were further compressed into tablets to investigate the corresponding degradation and drug release profile.

The *in vitro* degradation and drug release studies were carried out in phosphate buffered solution (pH=7.0) at 37 °C to model physiological conditions. The characterization techniques used include thermal analysis (DSC and TGA), scanning electron microscopy, gel permeation chromatography, UV-Vis spectroscopy, X-ray photoelectron spectroscopy and ¹³CNMR. PDLLA and PLGA microspheres and tablets degraded through hydrolytic chain scission of the ester linkages of the backbone when exposed to PBS solution at 37 °C. The decrease in average molecular weights was observed much earlier than the mass loss. The incorporation of GCV increased the polymer degradation rate constant, k' , but to a certain extent, where excess GCV decelerated and/or had no affect on the k' value. It was observed that auto-catalyst effect accelerating polymer degradation at the center of the microspheres did not play a major role in the GCV-loaded microspheres. The increase in k' in the GCV-loaded microspheres was instead due to basic-catalyst effect. The decrease in k' in high GCV-loaded microspheres was due to little and/or no auto-catalyst effect. Most of the GCV was released during the burst release phase through polymer degradation. However, the time taken for the complete release of GCV was determined by the length of the diffusive phase. For GCV-loaded PDLLA and PLGA 75/25 microspheres, release of GCV was through diffusion and was highly dependent on the amount of the GCV that remained in the microspheres. For GCV-loaded PLGA 50/50 microspheres, GCV was released through diffusion and polymer degradation. The time taken for GCV-loaded tablets to release all the GCV was significantly shorter than PLGA microspheres due to the early disintegration of the tablets. The following microspheres (PLGA 75/25 I.V. 0.94 18% GCV, PLGA 75/25 I.V. 0.24 5% GCV, PLGA 50/50 I.V. 0.50 5% and 20% GCV) and tablets (PLGA 50/50 I.V. 0.22 7% GCV and PLGA 50/50 I.V. 0.50 5% GCV) were ideal as sustained release intraocular devices for the treatment of CMV retinitis.

CHAPTER 1

INTRODUCTION

1.1 Background

The therapeutic effect of a drug is achieved by attaining a long-term appropriate drug concentration. There has been great interest in developing *controlled-release drug delivery systems (DDS)* which deliver drugs at constant rates to the body to generate constant plasma levels for long periods of time without reaching a toxic level or dropping below the minimum effective level. The difference between these two levels is known as the therapeutic index, which is usually based on a dose-response of the median 50 % of a population (ED_{50}). These DDS are called “zero order” systems since they release drug at a constant rate². Long-term drug therapy, the maintenance of certain plasma levels and site-specific delivery are the requirements which warrant the use of a sustained release dosage form. Additionally, sustained release would be advantageous for drugs with narrow therapeutic indexes and short half-life periods.

Controlled-release drug delivery design involves the application of physical and polymer chemistry to produce a well-characterized and reproducible dosage form that controls drug entry into the body within the specifications of the required drug delivery profile³. The controlled-release dosage form should be tailored so that variations in component characteristics lead to predictable alterations in release profiles.

Biodegradable polymers in medical devices have long been of interest, especially in controlled drug release technology because of their reabsorbing ability in the body. This alleviates the need for surgical removal of a drug release device. In general, the term

“degradation” refers to a chemical process resulting in the cleavage of covalent bonds of the polymers. Hydrolysis is the most common chemical process by which polymers degrade, but degradation can also occur via oxidative and enzymatic mechanisms.

Degradable materials must fulfill stringent requirements in terms of their biocompatibility. In addition to the potential problem of toxic contaminants leaching from the implant, one must also consider the potential toxicity of the degradation products and subsequent metabolites. As of 1999, the Food and Drug Administration (FDA) have approved only five distinct synthetic, degradable polymers for use in a narrow range of clinical applications. These polymers are poly (lactic acid), poly (glycolic acid), polydioxanone, polycaprolactone and a poly (PCPP-SA anhydride). A variety of other synthetic, degradable biomaterials currently in clinical use are blends or copolymers of these base materials such as a wide range of copolymers of lactic and glycolic acid⁴.

Among the biodegradable polymers approved by FDA, the most widely used and studied is the polyesters: poly (lactic acid), poly (glycolic acid), and their copolymers⁵, due to the extensive safety profile based on their use as sutures³. By far, the largest research effort utilizing PLGA in controlled drug delivery is in microparticulate systems⁶⁻¹⁰. These formulations, whether designed to be administered subcutaneously, orally, or transmucosally, have the tremendous advantage of supplying a continuous amount of drug over a long period of time. The delivery time usually ranges from weeks to months, and once the dosage is administered it is nearly impossible to reverse.

There are four routes of administrations, which can be used to deliver drugs to the posterior segment of the eye: topical, systemic, periocular and intraocular¹¹. The first three types of administration are indirect routes to the vitreous. The poor drug penetration

through the ocular tissue barriers often result in non-therapeutic levels of drug in the posterior vitreous, retina and choroids. Therefore, the direct intravitreal delivery of drugs is required for the effective treatment of some posterior segment diseases. One of such diseases is the cytomegalovirus (CMV) retinitis.

CMV Retinitis is an opportunistic infection that affects 25 % to 40 % of people with AIDS and is the most frequently encountered HIV-related ocular opportunistic infection. It is caused by cytomegalovirus (CMV), which if left untreated can cause blindness in 3 to 6 months¹. In Asia, as the number of patients with AIDS increases, the blindness resulting from CMV retinitis is a serious problem to overcome¹². The treatment of CMV retinitis is often through intravitreal injection via the pars plana, which facilitates direct delivery of drugs into the posterior segment of the eye. However, the half-lives of most drugs with low molecular weights in the vitreous cavity are as short as a few hours^{1,12}. Hence are needed and often result in poor outcomes. To overcome this, an intraocular controlled-release system can be used for such disease in which repeated local administration of drugs is likely to be effective.

A non-biodegradable implant, called Vitrasert® is commercially available for treatment of CMV retinitis. It provides a sustained-release delivery of ganciclovir (GCV) (Cytovene®, Roche Laboratories) directly into the eye. GCV is an antiviral medication for treating CMV retinitis in both oral and intravenous forms by interfering with the replication of CMV. The half-life of GCV is 2 to 6 hours¹³. The Vitrasert® implant delivers therapeutic levels of medication to the eye without exposing the patient to large systemic doses, which are frequently associated with adverse effects such as neutropenia and thrombocytopenia. The implant is effective for 5 to 8 months, after which, it is surgically removed and a new implant is placed¹⁴. Despite the good performance of the

available intraocular implant, a biodegradable implant would be a better alternative to the non-biodegradable device^{15, 16}. Degradation of the implant ensures that only one surgical procedure is needed to implant this device, thus eliminating the need for a second surgical intervention to remove the device. This helps reduce the trauma, the risk of infection and the cost of treatment borne by the patient.

Besides these surgical implants, a biodegradable injectable system could also be employed^{17, 18}. This injectable system was made up of biodegradable microspheres of PLGA containing GCV. Intravitreal injection of PLGA or PLA microspheres had shown no cytotoxicity on the retina electrophysiologically and histologically^{19, 20}. Injectable drug delivery devices are potentially less expensive than the surgical implants now available. Performing an intraocular injection requires a lower level of surgical sophistication than that needed to perform the delicate surgery for the placement of an intraocular implant. But the potential drawback of these microspheres was that the fluorosilicon oil (FSiO) and silicone oil (SiO) used in producing these microspheres^{17, 18} were non-biodegradable and would remain in the eye after the polymer disappeared.

1.2 Objectives

The main objective here was to develop a biodegradable drug delivery system, which would deliver therapeutic levels of drug locally to the eye for a period of 1 to 3 months, for treatment of ocular diseases. In fulfilling this main objective, the research was divided into three major parts.

The first part was to develop a range of drug-loaded poly (D, L-lactic) acid (PDLLA) and poly (lactic-co-glycolic) acid (PLGA) microspheres of suitable sizes for intraocular

injection. This was carried out by varying the emulsion techniques and the effects of polymer concentration on the size of microspheres were studied.

The second part was to study the hydrolytic degradation behavior of the pure and the drug-loaded PDLLA and PLGA microspheres. The effects of different lactic acid to glycolic acid (LA to GA) ratio, molecular weight on the degradation profile were investigated.

The third part was to study the release kinetics of the drug-loaded PDLLA and PLGA microspheres. The effects of pure drug diffusion or polymer matrix degradation on the release profile were investigated.

Finally the microspheres were compressed into tablets and their degradation and release profiles were investigated.

1.3 Scope

The following biopolymers were studied: PLGA 75/25 with intrinsic viscosity (I.V.) of 0.94, PLGA 75/25 I.V. 0.24, PLGA 50/50 I.V. 0.50, PLGA 50/50 I.V. 0.22 and PDLLA I.V. 0.22. The drug investigated was the commercially available ganciclovir (GCV). The effect of LA to GA ratio and molecular weight on degradation and drug release profile were investigated. To eliminate the effect of size of the microspheres on degradation and drug release profiles, the size was from 90 to 130 μm for both the pure and GCV-loaded microspheres.

The polymer properties that were of interests in this study were the molecular weight, the thermal and the morphological properties. The surface morphology was studied using the

scanning electron microscope (SEM), the thermal properties were studied using the modulated differential scanning calorimetry (MDSC) and the molecular weight using the gel permeation chromatography (GPC).

The pure and GCV-loaded microspheres were incubated at 37 °C in phosphate buffered solution (pH = 7.0) over a period of 4 to 12 weeks for the *in vitro* hydrolytic degradation studies. As for the *in vitro* drug release studies, only the GCV-loaded microspheres and tablets were incubated at 37 °C in phosphate buffered solution at pH 7.0 for up to 12 weeks.

1.4 Overview

The thesis will begin with the Literature Review, where a literature search on biodegradable polyesters, the hydrolytic degradation of these polyesters and controlled release kinetics are critically reviewed. The Materials and Methods of the experimentation follow the literature review and the experimental procedures are detailed in this section. The results obtained from the various characterization methods are reported, and discussed in the Results and Discussion chapters. Conclusions drawn from the present work are given, at the end of the thesis, along with the possible future works.

CHAPTER 2

LITERATURE REVIEW

2.1 Polymeric Biomaterials

The term biomaterials describe materials derived from biological sources or materials used for therapies in the human body. The use of polymers in medicine is as early as the birth of the field of polymer science. Nylon sutures were reported in the early 1940s and polymers such as poly (methylmethacrylate) (PMMA), Dacron polyester, and polyvinyl chloride were used in the mid-1940s. Bulk commodity polymers such as Teflon, high-density polypropylene and polyurethanes have also been used in medicine. These polymers remain important in clinical medicine as essential components of permanent prosthetic devices including hip implants, artificial lenses and large diameter vascular grafts⁵. However the stability and performance of these materials are not optimized and much of the research effort is employed to optimize them, *in vivo*.

Permanent implants almost always elicit a chronic inflammation called a foreign body response. This response is characterized by formation of a poorly vascularized fibrous layer similar to a scar at the material-tissue interface. The foreign body response is typically benign and sometimes desirable to anchor devices into host tissue. However it leads to some clinical complications. For example, infection of tissue that is considered as risks to be avoided in many applications. In the case of controlled drug delivery, it is undesirable to permanently leave an expired polymer device in the patient⁵. Hence degradable implants are required.

Tissue engineering and drug delivery rely primarily on materials that resorb or degrade in body fluids so that the device ultimately disappears with no ill effects. The materials currently employed in these areas are degradable polymers. Degradable polymers undergo extensive chain scission to form small soluble oligomers or monomers. Degradation may proceed by a biologically active process, which involves enzymes present in body fluids, or by passive hydrolytic cleavage of covalent bonds. The term “biodegradable” typically refers to materials in which active biological processes are involved. Degradable polymers gradually dissolve and are eliminated through the kidneys or other means. A wide variety of both solid and hydrogel-type polymers have been developed and many serve dual applications in drug delivery and tissue engineering⁵.

Recent research has led to a number of well-established investigational polymers that may find practical applications as degradable implants within the next decade⁴. It is an interesting observation that a large proportion of the currently investigated synthetic degradable polymers are polyesters⁴.

Polydioxanone (PDS) has gained increasing interest in the medical and pharmaceutical field due to its degradation to low-toxicity monomer *in vivo*. PDS has a lower modulus than PLA or PGA⁴.

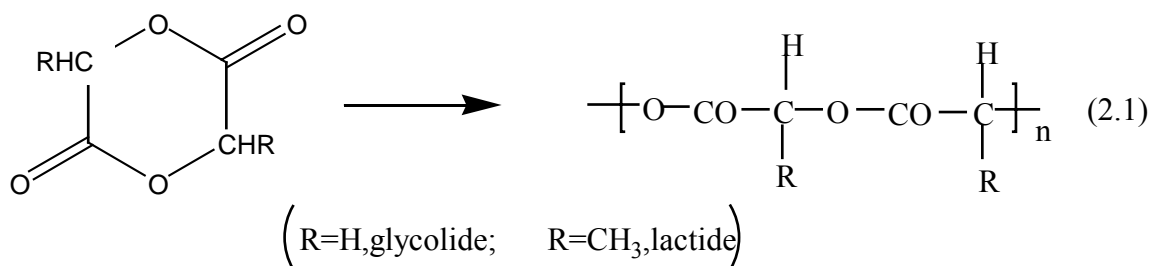
Polycaprolactone (PCL) is a semicrystalline polymer. The high solubility of PCL, its low melting point (59-64 °C), and its exceptional ability to form blends has stimulated research on its application as a biomaterial. PCL degrades at a slower pace than PLA and can therefore be used in drug delivery devices that are active for over a year⁴.

Polyanhydrides are among the most reactive and hydrolytically unstable polymers currently used as biomaterials. Aliphatic polyanhydrides degrade within days, whereas some aromatic polyanhydrides degrade over several years. Many polyanhydrides degrade by surface erosion without the need to incorporate various catalysts or excipients into the device formulation⁴.

Synthetic degradable polyesters were adopted in surgery 30 years ago as materials for sutures and bone fixation devices²¹. Degradable polyesters derived from three monomers, lactide, glycolide and caprolactone are in common clinical use. They are characterized by degradation times ranging from days to years depending on formulation and initial molecular weight⁴.

Biodegradable poly (α -hydroxyl acids) are polyesters derived from α -hydroxyl acids, $HO-CHR-COOH$. The commonly used α -hydroxyl acids are glycolic acid (GA, R=H) and lactic acid (LA, R = CH₃). The latter was a chiral compound and thus existed under two enantiomer forms, namely L and D (or S and R as referred to absolute configurations). These two isomers have similar intrinsic chemical properties but opposite configurational structures.

High molecular weight poly (α -hydroxyl acids) can be obtained by ring-opening polymerization of cyclic diesters only, according to the following equation



2.1.1 Poly-glycolic acid/ (PGA)

Poly (glycolic acid) (PGA) is the simplest linear aliphatic polyester. The repeating molecular structure of PGA consists of one nonpolar methylene group and a single relatively polar ester group. Relative to other biodegradable polymers, PGA is highly crystalline, with crystallinity typically reported in the range of 35 %– 75 %. The molecular and crystalline structures of PGA allow for very tight chain packing, and hence it has a high melting point and low solubility in organic solvents. The solvents for PGA are hexafluoroisopropanol (HFIP) and hexafluoroacetone sesquihydrate (HFASH). PGA was used in the development of the first totally synthetic absorbable suture by American Cyanamid²². PGA sutures have been commercially available under the trade name DEXONTM since 1970. The crystallinity of PGA in DEXONTM sutures is typically in the range of 46 %– 52 %²². A practical limitation of DEXONTM sutures is that they tend to lose their mechanical strength rapidly, typically over a period of 2 to 4 weeks after implantation.

PGA biodegrades by hydrolysis of the readily accessible and hydrolytically unstable aliphatic ester linkages.

2.1.2 Poly-lactic acid/ (PLA)

Lactic-acid is a chiral molecule, existing in L- and D- isomers where the L- isomer is the biological metabolite. Generally, L-PLA is employed more frequently than D-PLA, since the hydrolysis of L-PLA yields L (+)-lactic acid, which is the naturally occurring stereoisomer of lactic acid. Thus “polylactic acid” actually refers to a family of polymers: pure poly-L-lactic acid (L-PLA), pure poly-D-lactic acid (D-PLA), and poly-D, L-lactic acid (DL-PLA). The polymer PLA can exist in an optically active stereoregular form (L-PLA) and in an optically inactive racemic form (D, L-PLA). L-PLA is found to be semicrystalline in nature due to high regularity of its polymer chain while D, L-PLA is an

amorphous polymer because of irregularities in its polymer chain structure. The differences in the crystallinity of D, L-PLA and L-PLA have important practical ramifications. Since D, L-PLA is an amorphous polymer, it is usually considered for applications such as drug delivery, where it is important to have a homogeneous dispersion of the active species within the carrier matrix. On the other hand, the semicrystalline L-PLA is preferred in applications where high mechanical strength and toughness are required, for example, sutures and orthopaedic devices^{23, 24}.

Lactic acid is more hydrophobic than glycolic acid. In copolymers of glycolic and lactic acids (PLGA), the lactide-rich copolymers are more hydrophobic due to the hydrophobic nature of lactic acid. Hence these copolymers absorb less water²² when compared to glycolide-rich PLGA copolymers, giving rise to the slower degradation rate in the former copolymers²⁵. The methyl group in PLA reduces the polarity of the ester group, thus reducing the susceptibility to hydrolytic attack when compared to PGA.

2.1.3 Copolymers/ (PLGA)

It is now well established that LA-GA polymers are of great interest in human therapy for their outstanding biocompatibility and bioresorbability. Furthermore, a wide range of physical, thermal, mechanical and biological properties can be obtained by varying the composition and structural configuration in the polyester chain. PGA and LA-GA copolymers with low content of LA units were first introduced and developed as bioresorbable synthetic sutures in the 1960s and 1970s²⁶. Homopolymers, copolymers and stereocopolymers of lactic acid and glycolic acid are currently being investigated in several countries with respect to applications as temporary aids in bone surgery (osteosynthesis and bone reconstruction) and for the design of drug delivery systems²⁶. As with PGA and PLA homopolymers, the copolymers of lactide and glycolide are also

subjected to biodegradation because of the susceptibility of the aliphatic ester linkages to hydrolysis. However, biodegradation of the copolymers is normally faster than the homopolymers because copolymerization reduces the overall crystallinity of the polymer, thus giving the polymer a more open microstructure for easier moisture penetration.

Since the microstructure of a polymer can affect the physical behavior, i.e. solubility or degradation, of a polymer, it is a valuable property to be analyzed. A few studies examining the microstructure of PLGA copolymers using ^{13}C NMR have been reported²⁷⁻²⁹. Avgoustakis and Nixon²⁷ observed two resonances at 166.6 and 166.7 representing carbonyls of the glycolic acid (GA) unit of the copolymer in specific environments of GA-GA-GA and GA-GA-LA (lactic acid unit)²⁷. They concluded that the reported spectrum represents a blocky or heterogeneous copolymer and not a random or homogeneous copolymer (which should exhibit additional resonances near 166 ppm representing the LA-GA-LA and LA-GA-GA arrangements).

Similarly, Bendix²⁸ used ^{13}C NMR to compare PLGA polymers prepared by two methods; polycondensation of lactic and glycolic acids without catalyst, which is thought to produce totally random copolymers, and ring-opening melt condensation of lactide and glycolide, which produces more heterogeneous copolymers. By comparing relative intensities of the previously mentioned peaks, average poly(glycolide) block lengths ranging from 1 for the random polycondensation copolymers to about 4.6 for the heterogeneous ring-opening melt condensation copolymers were observed. These studies support the use of ^{13}C NMR as the chosen method to study comonomer ratios and sequence distributions of copolymers.

However, when Bendix²⁸ used the spectrometer at 75 MHz, they did not observe any differences between the spectra of different PLGA even though the average poly(glycolide) block lengths oscillated between 1 and 4.6, characteristic of homogeneous and heterogeneous polymers, respectively.

M Jesus Dorta *et al*²⁹ did not find any differences described by Avgoustakis and Nixon²⁷, when running the spectra at 50.32 and 100.61 MHz for PLGA 75/25 and PLGA 50/50 with the R_{cms} oscillating between 0.25 and 1, characteristic of heterogeneous and homogeneous polymers, respectively.

The claimed additional resonances near 166 ppm representing the LA-GA-LA and LA-GA-GA arrangements by Avgoustakis and Nixon²⁷ were not observed by other researchers^{28,29}. M Jesus Dorta *et al*²⁹ summarized that the degree of polymer heterogeneity could only be determined from the signals corresponding to the LA-GA and GA-GA units.

Three different monomers constitute the copolymer structure. The monomers are two stereoisomers (D- and L-lactic acid) and glycolic acid. It has been reported that PLGA does not possess a random distribution of D- (or L-) lactic acid and glycolic acid in its polymer backbone. Instead, it has a segregated structure because of the higher reactivity of the glycolic acid than that of L- (or D-) lactic acid during the ring opening polymerization²².

So, for a PLGA with high molecular weight through ring opening polymerization of the cyclic dimers, the average poly(glycolide) block lengths of 1 and 4.6, is the characteristic of homogeneous copolymer instead of random copolymer.

The understanding of the physical, chemical, and biological properties of the polymer is helpful, before formulating a controlled drug delivery device. The various properties of the polymer and the encapsulated drug directly influence other factors like the selection of the microencapsulation process, and the drug release from the polymer device.

The physical properties such as the molecular weight and the polydispersity index affect the mechanical strength of the polymer. These properties also control the biodegradation rate and hydrolysis of the polymers. The commercially available PLGA polymers are usually characterized in terms of intrinsic viscosity, which is directly related to their molecular weights.

The mechanical strength, swelling behavior, capacity to undergo hydrolysis, and subsequently the biodegradation rate are directly influenced by the crystallinity of the PLGA copolymer. The resultant crystallinity of the PLGA copolymer is dependent on the type and the molar ratio of the individual monomer components in the copolymer chain. It is noteworthy that there is no linear relationship between the ratio of glycolic acid to lactic acid and the physico-mechanical properties of the corresponding copolymers. With the exception of DL-PLA, all the homopolymers can be crystallized. The melting temperatures are above 160°C for PGA and L- or D-PLA^{22, 30, 31}. While PGA is highly crystalline, crystallinity is rapidly lost in copolymers of glycolic and lactic acid. These morphological changes lead to an increase in the rates of hydration and hydrolysis. Thus, copolymers tend to degrade more rapidly than PGA or PLA^{22, 25}. The fastest degradation is seen for copolymers with a 50:50 ratio of lactide to glycolide and with low molecular weights³². PLGA prepared from L-PLA and PGA containing more than 70 % glycolide is crystalline copolymers, while those from D, L-PLA and PGA are amorphous in nature.

The degree of crystallinity and the melting point of the polymers are directly related to the molecular weight of the polymer.

Values of glass transition temperature T_g for the homopolymers range from well above body temperature (L-PLA $\sim 55^\circ\text{C}$) to just below body temperature (PGA $\sim 35^\circ\text{C}$)^{22,30,31}. The glass transition temperature T_g of the PLGA copolymers is above the physiological temperature of 37°C and hence they are glassy *in vivo*. Hence they have a fairly rigid chain structure, which gives them significant mechanical strength to be formulated as drug delivery devices. The T_g of PLGA decreases with the decrease of lactide content in the copolymer composition and their molecular weight.

Both, *in vitro* and *in vivo*, the PLGA copolymer undergoes degradation in an aqueous environment (hydrolytic degradation or biodegradation) through cleavage of the backbone ester linkages. From the macroscopic viewpoint, degradation of aliphatic polyesters is regarded as homogeneous, the degradation occurs at uniform rate throughout the PLGA matrix. The PLGA biodegradation occurs through random hydrolytic chain scission of the swollen polymer. The carboxylic acid end groups present in the PLGA chains increase in number during the biodegradation process as the individual polymer chains are cleaved. These carboxylic acid end groups are known to catalyze the biodegradation process.

The biodegradation rate of the PLGA copolymers is dependent on the molar ratio of the lactic and glycolic acids in the polymer chain, molecular weight of the polymer, the degree of crystallinity, and the T_g of the polymer. The higher the glycolic acid content results in the faster the degradation rate. However, as the amount of glycolic acid in the copolymer is increased, crystalline domains of PGA may form, and solubility in

toxicologically acceptable solvents decreases; thus the highest amount of PGA normally used is about 50 mol %. Such copolymers have an average lifetime of about 2-4 weeks². The differences in degradation rates of different polymer compositions have been attributed to differences in the access of water to the ester bond rather than to differences in the intrinsic rates of ester cleavage³³. The hydrophilic versus hydrophobic character of the polymer, which is a function of the structure of the monomeric starting materials, can therefore have an overwhelming influence on the observed degradation rate. For instance, devices made of poly (glycolic acid) erode faster than identical devices made of the more hydrophobic poly (lactic acid), although the ester bonds have about the same chemical reactivity toward water in both polymers⁴.

From a chemical standpoint, absorbable devices are thought to undergo five general stages of degradation^{34, 35}. These stages are not discrete and may overlap.

First, hydration of the implant begins when the device is placed in the body. During this stage, the device absorbs water from the surrounding environment. Hydration of the amorphous segments of the polymer occurs faster than the crystalline segments.

The second stage of degradation is depolymerization or chemical cleavage of the polymer backbone which results in a reduction in mechanical properties (strength). In this process, water reacts with the polymer in a hydrolytic fashion resulting in cleavage of covalent chemical bonds and reduces the average molecular weight. The degradation of amorphous zones of the polymer matrix occurs initially, followed by the degradation of the more crystalline zones. During this degradation phase, the mass of the device remains essentially unchanged.

The third stage in the degradation process is loss of mass integrity which occurs when the cleaved polymer chains lose the cohesive strength and begins to fragment into pieces of low molecular weight polymer.

The fourth stage of degradation is absorption which occurs when further hydrolysis causes the fragment size to be suitable for assimilation by phagocytes or when further hydrolysis simply leads to soluble monomeric (lactate or glycolate) anions which dissolve into the intercellular fluid. It is during this stage that the implant undergoes significant loss in mass corresponding to the physical absorption.

The final stage of degradation is elimination. During this stage, L-lactate is converted into carbon dioxide and pyruvate. The majority of the elimination of PLA degradation products occurs through respiration (carbon dioxide) with only minor elimination via urine and/or feces. Final hydrolysis of PGA results in glycolate, some of which is excreted directly in the urine. Some glycolate may also be oxidized to glyoxylate which is then converted to glycine, serine, and pyruvate.

2.1.4 Summary

The high interest in the PGA, PLA and their PLGA copolymers is based mostly on the fact that these polymers have already been used successfully in a number of approved medical implants and are considered safe, nontoxic, and biocompatible by regulatory agencies in virtually all developed countries. Therefore, implantable devices prepared from PLA, PGA, or their copolymers PLGA can be brought to market in less time and for a lower cost than similar devices prepared from novel polymers whose biocompatibility is still unproven.

Amorphous D, L- PLA homopolymer and PLGA copolymer are usually considered for applications such as drug delivery, where it is important to have a homogeneous dispersion of the active species within the carrier matrix. The biodegradation rate of the PLGA copolymers is dependent on the molar ratio of the lactic and glycolic acids in the polymer chain, molecular weight of the polymer, the degree of crystallinity, and the T_g of the polymer.

Amorphous PLGA polymers of different LA to GA ratio and different molecular weight are investigated as drug carriers in this research on intraocular drug delivery device. Using ^{13}C NMR to examine the microstructure of these PLGA copolymers is engaged in this research.

2.2 Mechanisms of Polymer Degradation and Erosion

Currently four different terms (biodegradation, bioerosion, bioabsorption and bioresorption) are being used to indicate that a given material or device will eventually disappear after having been introduced into a living organism. However, when reviewing the literature, no clear distinctions in the meaning of these four terms are evident⁴.

The process of “degradation” describes the chain scission process during which polymer chains are cleaved to form oligomers and finally to form monomers. Hydrolysis is the most common chemical process by which polymers degrade, but degradation can also occur via oxidative and enzymatic mechanism. In contrast, “erosion” designates the loss of material owing to monomers and oligomers leaving the polymer³⁶. This often results in physical changes in size, shape, or mass of a device, which could be the consequence of either degradation or simply dissolution.

As all polymers degrade, the distinction between degradable and non-degradable polymers is not clear and is in fact arbitrary. It is the relationship between the time-scale of degradation and the time-scale of the application that differentiates the degradable from the non-degradable polymers. The term “degradable” is usually assigned to materials, which degrade during their application, or immediately after it. On the other hand, non-degradable polymers are those that require a substantially longer time to degrade than the duration of their application.

There are different types of polymer degradation such as photo-, thermal-, mechanical and chemical degradation³⁷⁻³⁹. All polymers share the property that they erode markedly under the influence of UV light or γ -sterilization, after which a significant loss of molecular weight can be observed⁴⁰. Thermal degradation plays a greater role for non-degradable polymers⁴¹. Mechanical degradation affects polymers that are subjected to mechanical stress, such as the non-degradable⁴² and biodegradable polymers⁴³ used as fixture or suture material.

All biodegradable polymers contain hydrolysable bonds. Their most important degradation mechanism is, therefore, chemical degradation via hydrolysis or enzyme-catalyzed hydrolysis. The latter effect is often referred to as biodegradation, meaning that the degradation is mediated at least partially by a biological system⁴⁴.

Hydrolysable polymeric biomaterials have functional groups consisting of carbonyls bonded to heterochain elements (O, N, and S). Examples include esters, amides, urethanes, carbonates, and anhydrides. Hydrolytically susceptible groups exhibit differing rates of degradation, which are dependent on the intrinsic properties of the functional group and on other molecular and morphological characteristics. Among the carbonyl

polymers, anhydrides display the highest hydrolysis rates followed, by esters and carbonates. Other carbonyl groups such as urethane, imide, amide and urea demonstrate long-term stability *in vivo* if contained in a hydrophobic backbone or highly crystalline morphologic structure⁴⁵.

2.2.1 Hydrolysis

The rate of hydrolysis tends to increase with a high proportion of hydrolysable groups in the main or side chain. Other factors that increase the hydrolysis rate include polar groups which enhance hydrophilicity, low crystallinity, low or negligible cross-link density, a high ratio of exposed surface area to volume, and mechanical stress. Factors that suppress hydrolysis rate include hydrophobic moieties (for example, hydrocarbon or fluorocarbon), cross-linking, high crystallinity due to chain order, thermal annealing or orientation, low stress, and compact shape. While the molecular weight of linear polymers by itself may not have a great effect on degradation rate, physical property losses may be retarded for a given number of chain cleavage events with relatively high molecular weight polymers. Property loss caused by chain cleavage is more pronounced in polymers with weak intermolecular bonding forces⁴⁵.

Among the factors that influence the rate of hydrolysis, the most important factors are the type of chemical bond (hydrolysable), pH, copolymer composition and water uptake. Chemical and physical changes go along with the degradation of biodegradable polymers, like the crystallization of oligomers and monomers or pH changes. Some of these factors can have a substantial feedback effect on the degradation rate. The change in molecular weight is the most important parameter for monitoring degradation. Besides loss of molecular weight, other parameters have been proposed as a measure for degradation, like loss of mechanical strength, complete degradation into monomers or monomer release.

All of these are related but do not necessarily obey the same kinetics. For example, complete degradation of poly (L-Lactic acid) is known to take substantially longer time than the loss of tensile strength⁴⁵. Furthermore, monomers from copolymers need not be released with identical kinetics during erosion. The specific relation between the erosion parameters varies according to the type of polymer.

2.2.2 Polymer erosion

The processes involved in the erosion of a degradable polymer are complicated. First, water enters the polymer bulk, which might be accompanied by swelling. The intrusion of water triggers the chemical polymer degradation, leading to the creation of oligomers and monomers. Progressive degradation changes the microstructure of the bulk through the formation of pores. The pH inside pores is controlled by degradation products, which typically have some acid-base functionality.

All degradable polymers share the property of eroding upon degradation. Degradation and erosion are the decisive performance parameters of a device made of such materials. Degradable polymers are clarified to surface and bulk eroding materials³⁵, which is illustrated in Figure 2.1. During an application, surface eroding polymers lose material from the surface only. They become smaller but keep their original geometric shape intact. For bulk eroding polymers, degradation and erosion are not confined to the surface of the device. Therefore, the size of a device will remain constant for a considerable length of time during its application. The advantage of surface eroding polymers is the predictability of the erosion process. This is desirable for drug delivery application, where the release of drugs can be related directly to the rate of polymer erosion. Polymers displaying surface erosion are polyanhydrides or poly (ortho ester).

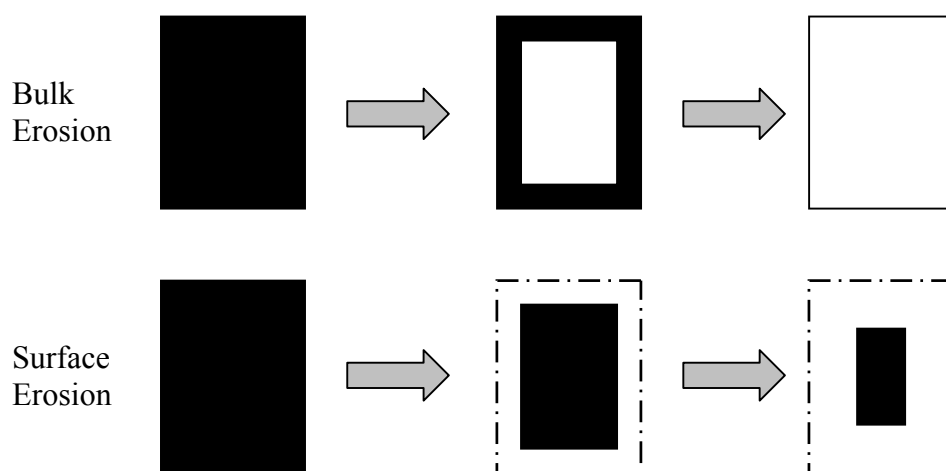


Figure 2.1 Schematic illustrations of bulk erosion and surface erosion³⁵

In the case of bulk eroding polymers, the specimen is homogeneous in the sense that the matter is the same regardless of the position in the specimen. Once placed in an aqueous medium, the specimen absorbs water and hydrolytic cleavage of the ester bonds starts, shown by molecular weight decrease. At the beginning, degradation is faster at the surface than in the core, according to the gradient of absorbed water. Degradation products are formed at the surface as well as in the inner part. However, soluble degradation products localized near the surface can dissolve more easily in the medium than those located in the core, which have to diffuse through the bulk of the polymer mass. Therefore, the concentration of carboxylic end-groups increases much more in the center than at the surface, resulting in surface/centre segregation. This leads to a faster degradation in the center than at the surface because of the catalytic effect of more numerous carboxylic end-groups, leading to a faster decrease in the molecular weight. When internal macromolecules are reduced to hydrosoluble oligomers and the surface becomes permeable, these oligomers diffuse through the surface and dissolve in the degradation medium. In consequence, a hollow structure is formed progressively⁴⁶. Finally, oligomers and monomers are released through the pores, leading to the weight loss of polymer devices.

Currently, the degradation of aliphatic polyester in contact with living tissues or with enzyme-containing body fluids is regarded by most people as resulting from abiotic hydrolysis of ester bonds only^{4,47}. Enzymatic degradation of aliphatic polyesters is said to occur only if mass loss and dimensional change are observed without a decrease in molecular weight. This rarely exists since enzymes can hardly penetrate deep into a dense polymer matrix. Surface erosion occurs when the rate of degradation is greater than the rate of diffusion of water into the polymeric mass. This is unlikely in the case of PLGA for which water uptake is always faster compared with the degradation rate⁴⁷.

The knowledge of the erosion mechanism is important for the successful application of a degradable polymer. Take for example, in tissue engineering, surface properties and porosity determine the performance of implantable scaffolds. In drug delivery, swelling and porosity are critical to the release behaviors of drugs with degradable polymers, the physical, morphological and mechanical properties of the polymers change with degradation time. Hence the knowledge of the degradation mechanism is crucial in the success of the implant.

2.2.2.1 Morphological changes

The first morphological changes during erosion are confined to the polymer surface. It has been observed for the autocatalytic degradation of poly (D, L-lactic-co-glycolic acid) rods and discs, the erosion proceeds from the bulk of the polymer to the surface⁴⁷. The preferential erosion of amorphous compared to crystalline regions was observed for enzymatic as well as non-enzymatic degradation⁴⁷.

2.2.2.2 Changes in pH

As mentioned earlier, the degradation rate depends strongly on pH. Through the chain scission, polymers are transformed into oligomers and monomers, which have different functional groups than the corresponding polymer. Thus, esters are cleaved into alcohols and carboxylic acids. The degradation products, therefore, influence pH in the degradation medium as well as inside the pores.

2.2.2.3 Changes in crystallinity

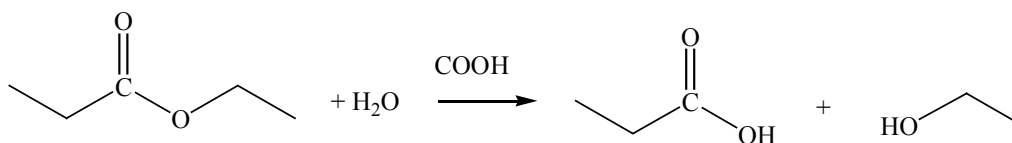
There are two general sources of crystallinity changes during polymer erosion. One is the generation of crystallized oligomers and monomers. Vert *et al*⁴⁷ and Li *et al*⁴⁸ observed that poly (D, L-lactic acid) was able to crystallize during its degradation. They identified the crystals as an oligomeric stereocomplex consisting of poly (D-lactic acid) and poly (L-lactic acid) chains. Monomers created by degradation have also been reported to crystallize during erosion^{47, 48}.

The other source of crystallinity change is from the behavior of partially crystalline polymers during erosion. Due to the faster erosion of amorphous regions compared to crystalline regions, the overall crystallinity of samples increases. This has been measured for poly (L-lactic acid)⁴⁹. Crystallinity also increased during the erosion of intrinsically amorphous polymers like quenched samples of poly (D, L-lactic acid).

2.2.3 Degradation mechanism

Once a PLGA device is placed in contact with an aqueous medium, water penetrates into the specimen and the hydrolytic cleavage of ester bonds starts. Each ester bond cleavage generates a new carboxyl end group that, in principle, can catalyze the hydrolytic reaction of other ester bonds as proposed in the case of the homogeneous degradation mechanism.

It is generally accepted⁵⁰ that the hydrolysis of most polyesters proceeds according to the reaction:



The kinetics of this reaction are given by

$$\frac{d[COOH]}{dt} = k[ester][H_2O][COOH] = k[COOH] \quad (2.2)$$

where $[COOH]$, $[ester]$ and $[H_2O]$ are the concentrations of carboxyl end groups, ester and water in the polymer matrix respectively, and it is assumed that in the early stages of the reaction the concentration of water and ester are constant. By assuming that $[COOH] = 1/M_n$, it can thus be shown that

$$\ln M_n = \ln M_{n,0} - kt \quad (2.3)$$

where $M_{n,0}$ is the initial number-average molecular weight of the polymer, and k is the rate constant of the biodegradation process. This equation represents the early degradation behavior of PLGA very well. The semi-logarithm plots of M_t versus time of hydrolysis are linear prior to the onset of weight loss.

Bulk erosion mechanism is responsible for the main degradation of biodegradable polyesters where random chain scission on the linkage of ester bonds in the polymer backbone proceeds homogeneously throughout the matrix. The bulk degradation pathway³⁵ has three major features in the polymer erosion profile, as observed in Figure

2.2. The first stage is the **incubation** stage, which is represented as (a) in Figure 2.2. In this stage, there are no changes in the mass and molecular weight (M_w) of the polymer, which reflects the time required for water penetration into the polymer matrix. The second stage (b) is **induction** stage, where the M_w decreases and a rapid increase is observed in the degree of matrix hydration followed by saturation. The third and final stage (c) is **polymer erosion**. In this stage, weight loss is observed.

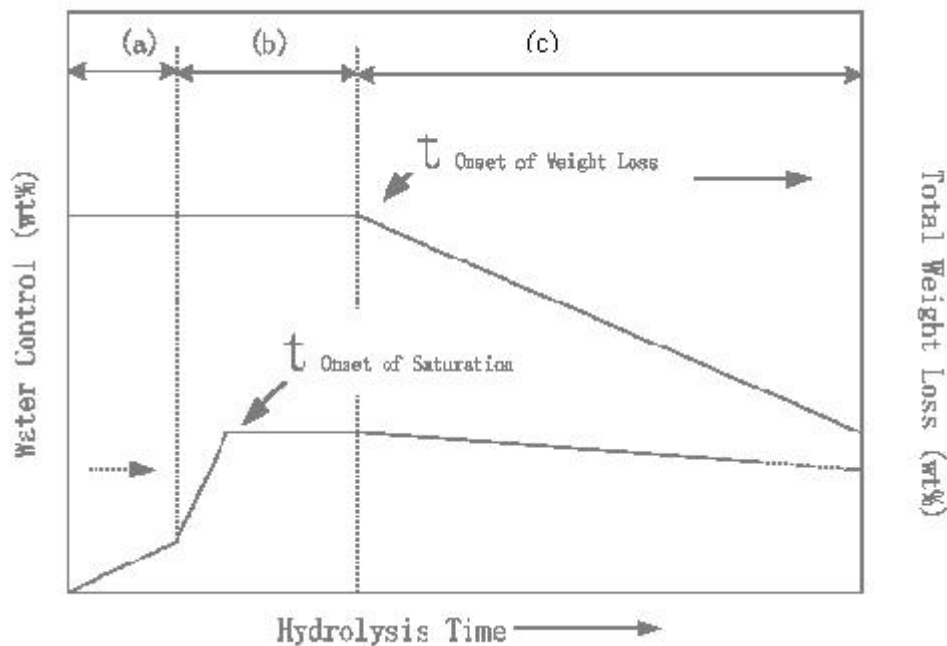


Figure 2.2 Descriptive hydrolytic bulk erosion profiles for semi-crystalline biodegradable polyesters: incubation. (b) induction (c) polymer erosion³⁵

During the onset of the polymer erosion stage, the partially degraded macromolecules remain insoluble in the surrounding aqueous medium, and the degradation proceeds homogeneously. However, as soon as the molecular weight of these partially degraded macromolecules becomes low enough to allow dissolution in the aqueous medium, diffusion starts within the whole bulk, with the soluble compounds moving slowly to and off the surface. This process, which combines diffusion, chemical reaction, and dissolution phenomena results in a differentiation between the rates of the degradation at the surface and the interior of the matrix. Oligomers from the surface can escape before total degradation, in contrast to those oligomers that are far inside. The result is a smaller

autocatalytic effect at the COOH-depressed surface with respect to the bulk. In buffered media, neutralization of terminal carboxyl might also contribute to a decrease in the surface degradation rate.

Grizzi *et al*⁵¹ reported that large devices of biodegradable polyesters degraded via a heterogeneous mechanism, that is, the degradation proceeded more rapidly in the center than at the surface. This was attributed to the autocatalytic action of the carboxylic acid end groups of degradation products that were trapped in the matrix. Due to this heterogeneous mechanism, the differences in degradation rates observed when comparing the degradation characteristics of films, powder, and microspheres issued from the same batch of PDLLA polymer⁵¹ showed that the smaller the polymer size, the slower the degradation rate. From the same logic, they concluded that porous systems degrade at a slower rate than dense ones, especially if dimensions of the considered device are millimetric.

There are four main factors that control the diffusion-reaction-dissolution phenomena: (a) the hydrolysis rate constant of the ester bond; (b) the diffusion coefficient of water within the matrix; (c) the diffusion coefficient of chain fragments within the polymeric matrix; and (d) the solubility of degradation products, generally oligomers, within the surrounding liquid medium. Additional factors, include temperature, additives in the polymeric matrix, additives in the surrounding medium, pH, buffering capacity, size and processing history, quenching or annealing, steric hindrance, and porosity⁵².

2.3 Controlled Release

When reviewing the literatures, most researchers^{2,11,53,54} consider terms known as “sustained release” or “prolonged release”, have been more recently called “controlled delivery”.

The drug delivery system (DDS) is designed to maintain drugs in target tissue at therapeutic concentrations with optimal spatiotemporal efficiency. Since the 1990s, an expanded concept of DDS has been developed in the following three areas: (1) controlled release of drugs administered locally; (2) drug targeting through a systemic route, and (3) enhancement of drug permeation through a barrier such as skin, epithelium, endothelium, connective tissue, and the cell membrane⁵⁴.

A controlled-release system is designed for local administration to achieve zero-order (slow, sustained) release, pulse release, or more intelligent biofeedback release, which responds to biologic signals. Drug modifications or external signals, such as magnetic and thermal stimuli, can increase the targeting of drugs to the targeted tissue (passive or active targeting) or inversely reduce targeting to other healthy tissues (inverse targeting). Alternatively, drug absorption is enhanced by modifying drugs or barriers that drugs must penetrate. One or a combination of these concepts might increase drug efficacy and attenuate side effects⁵⁴.

2.3.1 Release Mechanisms

According to Robert Langer⁵⁵, polymeric materials generally release drugs by a few mechanisms. The most common release mechanism is diffusion, whereby the drug migrates from its initial position in the polymeric system to the polymer's outer surface and then to the body. Diffusion may occur through a reservoir, in which a drug core is

surrounded by a polymer film, or in a matrix, in which the drug is homogeneously dissolved or dispersed within the polymeric system.

Drugs can also be released by chemical mechanisms such as degradation of the polymer, or the bonds between the drug and a polymer backbone are cleaved. Exposure to a solvent can also activate drug release. In this case, the drug may be locked into place by polymer chains, and, upon exposure to environmental fluid, the outer polymer regions begin to swell, allowing the drug to move outward.

Another mechanism that may be involved in the release of drugs by polymeric materials is osmosis. Water may permeate a drug polymer system as a result of osmotic pressure, causing pores to form and bringing about drug release. An attractive osmotic system that can provide constant release rates exists in the form of a pill that has a laser-drilled hole in the surface of a polymer coating. Some polymer systems can be externally activated to release more drug when needed, using forces such as magnetism. In this case, an external magnetic field causes polymer-embedded magnetic beads to “squeeze” drug containing pores, forcing more drug out of a matrix. Combinations of the above mechanisms are possible. The release rates from the polymer systems can be controlled by the nature of the polymeric material. Take for example, crystallinity or pore structure for diffusion-controlled systems while the liability of the bonds or the hydrophobicity of the monomers for chemically controlled systems. Besides that, the design of the system, for example, thickness and shape will also control the rate of drug release. The advantage of having systems with different release mechanisms is that each can accomplish different goals. For example, reservoir systems are able to produce near-constant release rates, whereas matrix systems are inexpensive to manufacture. Chemically controlled systems generally

result in the elimination of the polymer, whereas solvent-activated systems have release rates independent of pH^{56,57}.

Here, the diffusion controlled, chemically controlled and particular delivery systems are discussed in detail in the following sections.

2.3.1.1 Diffusion Controlled Delivery Systems²

There are two fundamentally different devices where the rate of drug release is controlled by drug diffusion. These are membrane-controlled devices and monolithic devices.

In a membrane-controlled reservoir delivery system, the active agent is contained in a core or “reservoir” which is surrounded by a thin polymer membrane. The release of the active agent to the surrounding environment occurs by diffusion through the rate-controlling membrane.

In a monolithic device, the therapeutic agent is uniformly dispersed or dissolved in a polymer matrix and its release is controlled by diffusion from the matrix. The matrix is assumed to be inert, i.e., non-swelling or fully swollen, and non-degrading.

In determining whether the reservoir or monolithic device is most appropriate for an intended application, this will depend upon the need for constant drug release rate, the manufacturing cost, and safety. Even though reservoir-type devices can yield zero order kinetics for long periods of time, the safety of this type of device may sometimes be of concern because rupture of the membrane can lead to sudden release of the drug within the core, especially when the core is either in a liquid state or is a fragile matrix. Thus, in such a situation, the amount of drug in the core and its toxicity must be considered.

Manufacture of reservoir-type devices is expensive and in many applications where device cost is an important factor, the less expensive matrix-type devices are used, even though release rate declines with time.

2.3.1.2 Chemically Controlled Delivery Systems²

In these systems, the drug is contained in the core of a solid implant covered by a biodegradable membrane. This DDS is identical to the reservoir system, except that the membrane surrounding the drug core is bioerodible or biodegradable. The bioerodible membrane must remain essentially unchanged over the duration of drug delivery. Significant bioerosion cannot take place until drug delivery has been completed.

In the development of bioerodible drug delivery systems, the matrix is usually made of biodegradable polymers such as PLA and PLGA, polyanhydrides, poly (ortho esters) and Poly(phosphoesters). The complex degradation process of these polymers does not yield a controlled release rate.

In the pendant-chain systems the drug is covalently attached to a biodegradable polymer backbone. Such systems are toxicologically complicated because the FDA requires unambiguous proof that the chemically attached drug is released in its native form and not as a chemical derivative. Pendant-chain systems are not currently under development with the exception of polymer conjugates used in tumor targeting.

2.3.1.3 Particulate Delivery Systems²

Under the particulate delivery systems, there are the microcapsules and the microspheres. A microcapsule has a well-defined core containing the therapeutic agent, and a well-defined polymer membrane surrounding the core. In controlled drug delivery

applications, such systems are of interest because drug release takes place by diffusion from the core through the rate-limiting membrane. Such systems fall under the category of membrane-controlled reservoir devices. Microcapsules are capable of extended zero-order drug release.

The attractiveness of achieving long-term zero-order drug release with microcapsules may be offset by their fairly expensive manufacturing method that limits the use of microcapsules to human therapeutics that are not price-constrained and the possibility of membrane rupture, giving rise to an abrupt release of the core material with the consequent overdosing potential.

Microspheres, on the other hand, are most often prepared by a simpler emulsion technique. In microspheres, there is no outer membrane and such devices are in effect matrix devices with the drug more or less uniformly distributed in the polymer matrix. Release kinetics is typical of diffusion from a matrix system. Particle size distribution is an important variable in the drug release profile.

Despite non-zero-order release kinetics, microspheres and microparticle delivery systems find wide application in both human and veterinary therapeutics because they can be inexpensive, are simple to manufacture and there is little danger of abrupt drug release.

2.3.2 Mathematical Models of Drug Release⁵⁸⁻⁶¹

A simple mathematical approach has been used to describe the observed *in vitro* drug release rates⁵⁸⁻⁶¹. This theory assumes that drug release is governed solely by diffusion, a mass transfer process which can be quantified using Fick's second law⁶²

$$\frac{\partial c}{\partial t} = \frac{\partial}{\partial x} \left(D \frac{\partial c}{\partial x} \right) + \frac{\partial}{\partial y} \left(D \frac{\partial c}{\partial y} \right) + \frac{\partial}{\partial z} \left(D \frac{\partial c}{\partial z} \right) \quad (2.4)$$

Here, c and D are the concentration and the diffusion coefficient of the diffusing species, respectively; t represents time, and x , y and z are the three spatial coordinates.

Considering the geometry of the investigated system and assuming: (i) constant drug diffusion coefficients; (ii) perfect sink conditions; and (iii) a uniform initial drug concentration that is smaller than the solubility of the drug within the system (monolithic solution), the following analytical solution of Fick's second law of diffusion as shown in equation 2.4 can be used to describe the resulting drug release rate⁶².

2.3.2.1 Fickian diffusion release from thin polymer slabs

Consider one-dimensional, isothermal solute release from a thin polymer slab of thickness l , where the system is initially maintained at a constant uniform drug concentration, C_1 , and its surfaces are kept at a constant drug concentration, C_0 . This situation is referred to as the *perfect sink condition*. For an assumed constant drug diffusion coefficient, D , with one-dimensional diffusion in the x direction, equation 2.4 can be expressed as

$$\frac{\partial c}{\partial t} = \frac{\partial}{\partial x} \left(D \frac{\partial c}{\partial x} \right) \quad (2.5)$$

where

$$t = 0 \quad -l/2 < x < l/2 \quad C = C_1$$

$$t > 0 \quad x = \pm l/2 \quad C = C_0$$

If M_t denotes the total amount of drug which was released from the slab at time t , and M_∞ is the corresponding amount of drug after infinite time, the fraction of drug release, M_t/M_∞ , which is useful for interpretation of short-time behavior can be expressed as^{56, 63}

$$\frac{M_t}{M_\infty} = 4 \left[\frac{Dt}{\pi l^2} \right]^{1/2} \left[\frac{1}{\pi^{1/2}} + 2 \sum_{n=1}^{\infty} (-1)^n \operatorname{ierfc} \frac{nl}{2\sqrt{Dt}} \right] \quad (2.6)$$

where $\text{ierfc } x$ represents the integrated complementary error function of x . For the early time approximation, which holds over the initial portion of the fractional release curves for Fickian diffusion, equation 2.6 reduces to

$$\frac{M_t}{M_\infty} = 4 \left[\frac{Dt}{\pi l^2} \right]^{1/2} \quad \text{for} \quad 0 \leq \frac{M_t}{M_\infty} \leq 0.6 \quad (2.7)$$

For the latter time approximation, which holds for the final portion of the fractional release curves for Fickian diffusion, equation 2.6 reduces to

$$\frac{M_t}{M_\infty} = 1 - \frac{8}{\pi^2} \exp\left(\frac{-\pi^2 Dt}{l^2}\right) \quad \text{for} \quad 0.4 \leq \frac{M_t}{M_\infty} \leq 1.0 \quad (2.8)$$

As indicated by equation 2.7, Fickian diffusion release from a thin slab is characterized by an initial $t^{1/2}$ time dependence of the drug released. The short-time approximation is valid for the first 60 % of the total released drug ($M_t/M_\infty \leq 0.60$).

2.3.2.2 Semi-empirical equation for drug released from thin polymer slabs⁵⁸⁻⁶¹

For Fickian diffusion in a thin slab, equation 2.7 indicates that the first 60 % of the fractional release at any time can be characterized by a constant multiplied by the square root of time. A second limiting case is one where the amount of drug released is linear-dependent of time and the drug release rate is concentration-independent, i.e., the kinetics is of zero-order. Such a situation can be described by a general equation of the form

$$\frac{M_t}{M_\infty} = k_1 t \quad (2.9)$$

Many situations of release processes fall between these limiting cases, i.e., they can be represented by coupling of a Fickian and a non-Fickian mechanism. A simple expression of this observation can be written by adding equations 2.7 and 2.9 to give:

$$\frac{M_t}{M_\infty} = k_1 \sqrt{t} + k_2 t \quad (2.10)$$

Where $k_1 = 4 \left[\frac{D}{\pi l^2} \right]^{1/2}$ and $k_2 = k'$.

A generalized expression of the previous equations can be thus written as

$$\frac{M_t}{M_\infty} = kt^n \quad (2.11)$$

where k is a constant incorporating characteristic of the macromolecular network system and the drug, and n is the diffusion exponent, which is indicative of the transport mechanism. Fickian diffusion in a thin slab is defined by n equal to 0.50 and non-Fickian by n greater than 0.50.

2.3.2.3 Fickian diffusion release from cylinders and spheres

For one-dimensional radial release from a cylinder of radius a and a sphere of radius a , under perfect sink initial and boundary conditions, with a constant drug diffusion coefficient D , equation 2.4 can be expressed as equation 2.12 and 2.13 respectively

$$\frac{\partial c}{\partial t} = D \left[\frac{\partial^2 C}{\partial r^2} + \frac{1}{r} \frac{\partial C}{\partial r} \right] \quad (2.12)$$

where

$$t = 0 \quad 0 < r < a \quad C = C_1$$

$$t > 0 \quad r = a \quad C = C_0$$

$$\frac{\partial c}{\partial t} = D \left[\frac{\partial^2 C}{\partial r^2} + \frac{2}{r} \frac{\partial C}{\partial r} \right] \quad (2.13)$$

where

$$t = 0 \quad 0 < r < a \quad C = C_1$$

$$t > 0 \quad r = a \quad C = C_0$$

The fraction of drug release, M_t/M_∞ , which is useful for interpretation of short-time behavior can be expressed as equation 2.14 and 2.15 respectively^{56,63}

$$\frac{M_t}{M_\infty} = 4 \left[\frac{Dt}{\pi a^2} \right]^{1/2} - \pi \left[\frac{Dt}{\pi a^2} \right] - \frac{\pi}{3} \left[\frac{Dt}{\pi a^2} \right]^{3/2} + \dots \quad (2.14)$$

$$\frac{M_t}{M_\infty} = 6 \left[\frac{Dt}{\pi a^2} \right]^{1/2} - 3 \frac{Dt}{a^2} \quad (2.15)$$

A graphical comparison of equation 2.14, 2.15 and 2.11 shows that an initial $t^{1/2}$ time dependence can not be used when analyzing data of solute release from cylindrical and spherical devices. This time dependence only predicts the first 15 % of the total fractional release. Hence equation 2.11 needs to be modified for application to the first 60 % of the fractional release curves for Fickian diffusion from a cylinder with $n = 0.451 \pm 0.004$ and a sphere with $n = 0.432 \pm 0.007$ ⁶⁴.

2.3.2.4 Dependence of the diffusion exponent on geometry⁵⁸⁻⁶¹

The relationship between the diffusion exponent, n , and the corresponding release mechanism is clearly dependent upon the geometry employed as shown in Table 2.1. However, a value of $n = 1$, means that the amount of drug released is linear-dependent of time and the drug release rate is concentration-independent and time-independent. In other words, the kinetics is of zero-order, regardless of the geometry.

Drug Release Mechanism	Diffusion exponent, n		
	Thin slab	Cylindrical sample	Spherical sample
Fickian diffusion	0.50	0.45	0.43
Anomalous (non-Fickian) transport	$0.50 < n < 1.00$	$0.45 < n < 1.00$	$0.43 < n < 1.00$
Zero-order release	1.0	1.0	1.0

Table 2.1 Diffusion exponent and mechanism of diffusion release from various non-swellable controlled release systems⁵⁹

In systems where the shapes range from a flat disk or tablet (where the radius a is much larger than the sample thickness l) to that of a cylindrical rod (where the length of the sample l is much larger than the radius a), the aspect ratio is defined as $2a/l$, Figure 2.3 shows the diffusion exponent, n , for Fickian diffusion as a function of the aspect ratio⁵⁹.

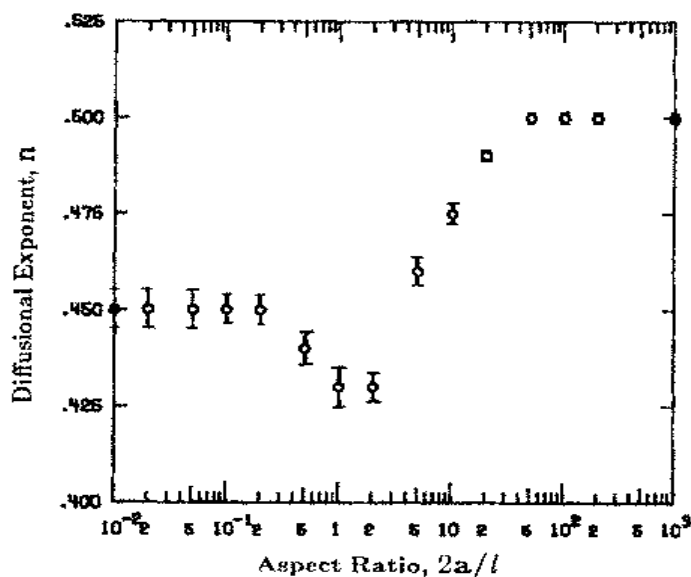


Figure 2.3. Diffusion Exponent, n , as a function of their aspect ratio, $2a/l$ ⁵⁹

For slabs which are defined by an aspect ratio greater than 50 the diffusion exponent n is equal to 0.5. Thus an aspect ratio of 50 defines the minimum aspect ratio for which one-dimensional diffusion in a slab can be assumed. Similarly, for cylinders which are defined by an aspect ratio smaller than 0.2, the diffusion exponent n is equal to 0.45. Hence, an aspect ratio of 0.2 defines the maximum aspect ratio for which the assumption of one-dimensional diffusion in a cylinder is valid. The transition from one-dimensional diffusion in a slab to one-dimensional diffusion in a cylinder is not represented by a linear function as shown in Figure 2.3. Instead, the diffusion exponent, n , passes through a minimum value of 0.43 at an aspect ratio of 1, which corresponds to spheres⁵⁹.

2.3.2.5 Semi-empirical equation for drug released from different geometries⁵⁸⁻⁶¹

The empirical equation 2.11 can be used to relate the amount of the drug released as an exponential function of time. The diffusion exponent, n , specifies the mechanism of the release. In the case of pure Fickian release, the exponent n has the limiting values of 0.50, 0.45, and 0.43 for release from slabs, cylinders and spheres, respectively. For tablets, the

Fickian diffusion mechanism is described by $0.43 < n < 0.50$, depending on the aspect ratio.

In theory this equation should only be applicable to the first 60 % of the fractional release from thin slabs, for which the assumption of one-dimensional diffusion under perfect sink conditions is valid. In practice, however, the equation has been applied to systems of different geometries, where one-dimensional diffusion cannot be assumed, and perfect sink boundary conditions are not maintained⁵⁹.

2.3.3 Summary

Matrix-type or monolithic-type DDS are inexpensive, simple to manufacture and little danger of abrupt drug release compared to reservoir-type or membrane-type DDS. Microspheres made from hydrophobic biodegradable polymers are in effect matrix devices with the drug more or less uniformly distributed in the polymer matrix. Release kinetics is typical of diffusion from a matrix system. A simple semi-empirical equation 2.11 expresses the general drug release behavior for the first 60 % of the fractional release from polymeric DDS. The diffusion exponent, n , specifies the mechanism of the release (Fickian diffusion or non-Fickian diffusion). No successful modeling has yet been established for the remaining 40 % of the fractional release.

2.4 Microparticle drug delivery systems

2.4.1 Emulsion⁶⁵

An emulsion is defined by Becher⁶⁶ as “a heterogeneous system, consisting of at least one immiscible liquid dispersed in another in the form of droplets, whose diameters, in

general, exceed 0.1 mm. Such systems possess a minimal stability, which may be accentuated by additives such as surface-active agents or finely divided solids.”

Since in almost all cases, at least one liquid is water or an aqueous solution, an emulsion is commonly described as being either oil-in-water (O/W) or water-in-oil (W/O), where the first phase represents the dispersed phase and the second the continuous phase⁶⁵.

The presence of a liquid/liquid interface induces an imbalance of forces that alters the energetic situation of molecules at or near that interface, usually giving molecules in that region a higher net energy than those in the bulk. The drive to lower the energy of the system results in the preferential adsorption of materials such as surfactants at the interfaces. The action of the adsorbed materials in lowering the free energy of the two-phase system reduces the energy required to generate new interfacial area and therefore facilitates the preparation of emulsified systems⁶⁵.

The nature of the interfacial film plays an important role in the long-term emulsion stability. The interfacial film has to withstand the pressures of droplet contacts, while acting as a barrier between the dispersed and continuous phase. The role of surfactants in the preparation and stabilization of emulsions is discussed⁶⁵.

2.4.1.1 Surfactant structure and emulsion performance⁶⁵

The surfactant must exhibit sufficient surface activity to ensure significant adsorption at the oil-water interface. The presence of materials such as electrolytes and polymers can greatly alter the role of the surfactant in stabilizing an emulsion as well as in controlling the type of emulsion formed. The surfactant should produce a strong interfacial film,

consistent with their ability to produce the required droplet size under the conditions of emulsification⁶⁵.

On a molecular level, the choice of surfactant is dependent on the type of emulsion desired and the nature of the oil phase. Oil soluble surfactants will preferentially produce W/O emulsions while water soluble surfactants yield O/W systems. Because of the role of the interfacial layer in emulsion stabilization, it is often found that a mixture of surfactants with widely differing solubility properties will produce emulsions with enhanced stability. The more polar the oil phase, the more polar surfactant is required to provide optimum emulsification and stability⁶⁵.

The **Hydrophile-Lipophile Balance (HLB)** system by Griffin⁶⁷ is a quantitative way of correlating the chemical structure of surfactant molecules with their surface activity. Griffin attempted to place the choice of the optimum nonionic surfactant for the stabilization of a given emulsion on a more quantitative, and theoretical basis. The system calculates the HLB number, within a range of 0 to 20. At the high end of the scale (8-18), lies hydrophilic surfactants, which possess high water solubility and generally act as good solubilizing agents, detergents, and stabilizers for O/W emulsions. At the low end (3-6), surfactants with low water solubility are placed, which act as solubilizers of water in oils and good W/O emulsion stabilizers. In the middle are materials that are very surface-active, in terms of lowering surface and interfacial tensions, but generally perform poorly as emulsion stabilizers, possibly because of their balanced solubility characteristics in the two phases. The effectiveness of a given surfactant in stabilizing a particular emulsion system would then depend on the balance between the HLB of the surfactant and the oil phase involved.

2.4.1.2 Polymeric Emulsifiers and Stabilizers⁶⁵

In nature as well as in technology, polymeric emulsifiers and stabilizers play a major role in the preparation and stabilization of emulsions. Natural materials such as proteins, starches, gums, cellulose, and their modifications, as well as synthetic materials such as **polyvinyl alcohol (PVA)**, polyacrylic acid, and polyvinylpyrrolidone, have several characteristics that make them extremely useful in emulsion technology. By the proper choice of chemical composition, such materials can be made to adsorb strongly at the interface between the continuous and dispersed phases. By their presence, they can reduce interfacial tension and/or form a barrier (electrostatic and/or steric) between drops. In addition, their solvation properties serve to increase the effective adsorbed layer thickness, increase interfacial viscosity, and introduce other factors that tend to favor the stabilization of the system.

The effectiveness of polymeric materials at lowering interfacial tensions is usually quite limited. More important to their function is the fact that polymers can form a substantial mechanical and thermodynamic barrier at the interface that retards the approach and coalescence of individual emulsion droplets. The polymeric nature of the materials means that each molecule can be strongly adsorbed at many sites on the interface. As a result, the chance of desorption is greatly reduced or effectively eliminated, and the interfacial layer attains a degree of strength and rigidity not easily found in systems of monomeric materials. In addition, the presence of polymeric materials in the system can retard processes such as creaming by increasing the viscosity of the continuous phase thereby reducing the rate of droplet encounters that could lead to flocculation or coalescence.

2.4.1.3 Multiple emulsions⁶⁵

Multiple emulsions are composed of droplets of one liquid dispersed in large droplets of a second liquid, which is then dispersed in a final continuous phase. Typically, the internal

droplet phase will be miscible with or identical to the final continuous phase. Because they involve a great variety of phases and interfaces, multiple emulsions are inherently unstable, even more so than conventional emulsions. Their surfactant requirements are such that two stabilizing systems must be employed: one for each oil-water interface. Each surfactant or mixture must be optimized for the type of emulsion being prepared, but must not interfere with the companion system designed for the opposite interface.

2.4.2 Preparation of Particulate Systems

Emulsion technique has been successfully used to produce poly (DL-lactide-co-glycolide) micro/nano particles⁶⁸⁻⁷⁰.

2.4.2.1 Double Emulsion Solvent Evaporation

This technique is used in encapsulating hydrophilic drugs and proteins within microparticles. It has also been applied to nanoparticles, where a pressure homogenization device was used to prepare nanoparticles with low size polydispersity⁷¹.

Typically, PLGA was first dissolved in an organic solvent such as dichloromethane (DCM). The hydrophilic drug was dissolved in distilled water to its maximum solubility. The aqueous drug solution was then added to the PLGA organic solution and water-in-oil (W/O) emulsion was formed by sonication over an ice bath using a probe-type sonicator at 50-55 W power output for 10 min. This W/O emulsion was further added to a polyvinyl alcohol (PVA) aqueous solution with sonication to achieve the (water-in-oil)-in-water (W/O)/W double emulsion system. The organic solvents were allowed to evaporate while being stirred first at atmospheric pressure for 16 hours and then at gradually reduced pressure (from 100 mmHg to 30 mmHg) for 2 hours. The evaporation of organic solvent could also be carried out under vacuum using a rotation evaporator⁷².

The solidified nanoparticles were then collected by ultracentrifugation and washed three times with distilled water to remove any residual PVA and drug. The final product was dried by lyophilization⁷³. This method is shown schematically in Figure 2.4⁶⁸.

2.4.2.2 Modified spontaneous emulsification solvent diffusion method:^{72,74-76}

This technique has also been successfully used to encapsulate hydrophilic drugs and proteins in PLGA microspheres^{72,74-76}. This technique is divided into three main steps. The first step was quasi-emulsification, where 500 mg of PLGA was dissolved in 12.5 ml of the solvent mixture consisting of acetone plus dichloromethane, ethanol, or methanol. The polymer solution obtained was then added into 50 ml of aqueous PVA solution using a peristaltic pump at a flow rate of 2.0 ml/min while the mixture was stirred at 400 rpm with a propeller mixer.

The second step was the purification. Here, the dispersion formed was transferred into a 1000-ml glass flask and 500 ml purified water was added. The dispersion was then condensed to 25 ml by means of an ultrafiltration, and purified water was added up to 500 ml. This dilution-condensation process was repeated three times to remove the residual PVA and organic solvents.

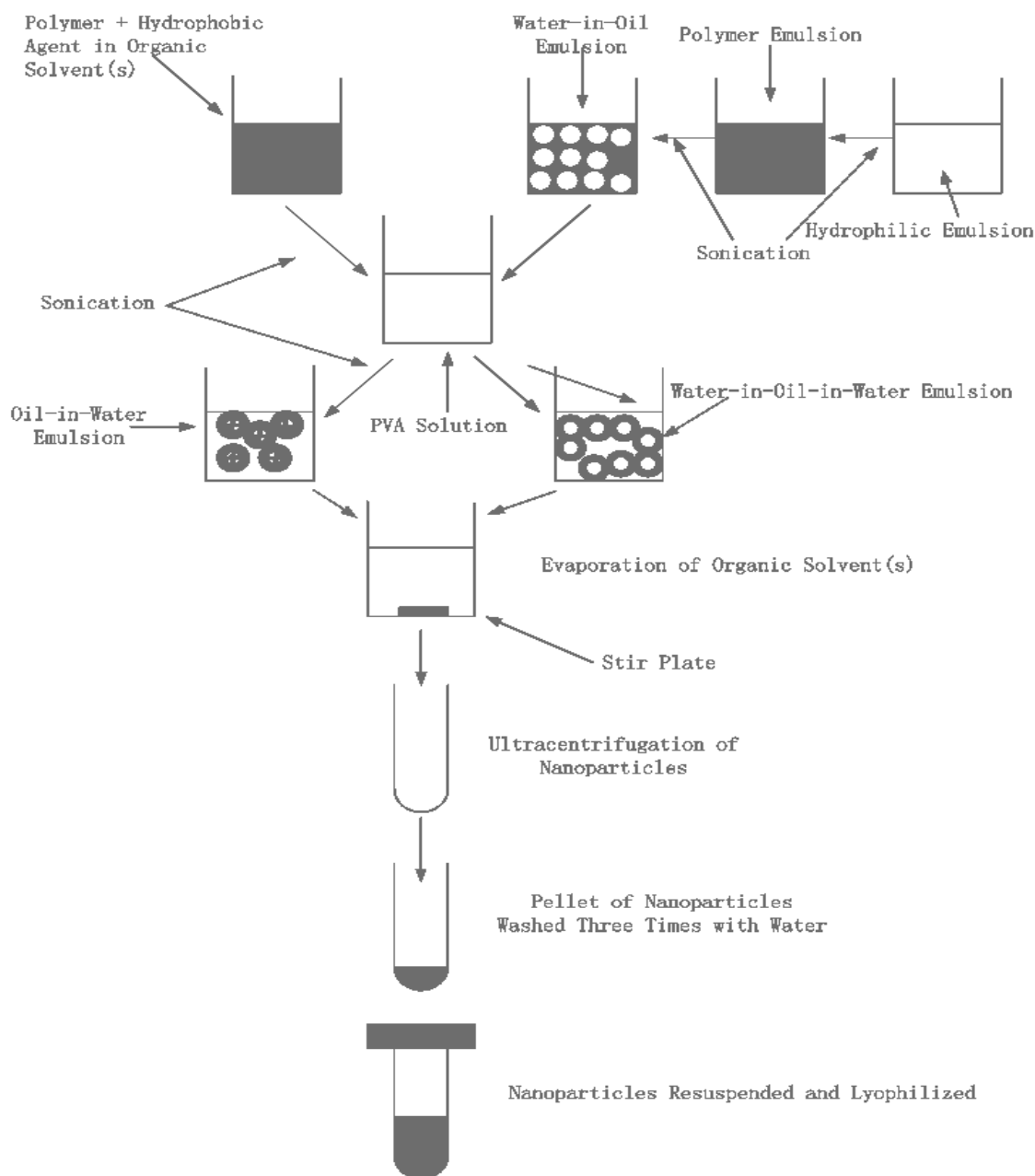


Figure 2.4 Strategies for formulation of PLGA nanoparticles with hydrophobic and hydrophilic agents⁶⁸.

The last step was freeze-drying. The 25ml condensed aqueous dispersion was passed through a 100-mesh sieve to remove aggregates and then freeze-dried in a vacuum to obtain powdered nanoparticles. The yield of nanoparticles was represented by the percent weight fraction of the powdered nanoparticles relative to the total weight of PLGA used for the preparation.

2.4.2.3 Salting-out method^{73,77-79}

This method has been reported in the preparation of PLGA nanoparticles^{73,77-79}. In this method, an aqueous gel containing PVA and magnesium acetate tetrahydrate was added under vigorous stirring to an acetone solution of PLGA and drug, leading to the formation of a water-in-oil emulsion. Despite the miscibility of water with acetone, a liquid-liquid two-phase system was formed due to the presence of the salting-out agent (magnesium acetate). Upon further addition of the aqueous phase, an oil-in-water emulsion was obtained. Finally, pure water was added to allow diffusion of acetone into the aqueous phase, leading to the formation of spherical nanoparticles. The nanoparticulate suspension was purified by cross-flow filtration using a Sartocon Mini device mounted with a polyolefin cartridge filter with a 100 nm pore size. The nanoparticles were freeze-dried and stored at -25°C until use.

2.4.3 Encapsulation of water-soluble compounds

In cases where the drug to be encapsulated is not soluble in the organic solvent used, there are two options. The drug may either be incorporated as solid submicrometer particles within the polymeric microparticles, or a tri- or multiphase preparation method may be used. This water-in-oil-in-water technique is extremely useful for incorporation of highly water-soluble drugs. An aqueous drug solution is dispersed within the initial polymer/solvent solution that then becomes the central core of the resulting microparticle or microcapsule. One of the limiting factors in using this technique is the solubility of the drug in the two aqueous phases of the microparticle preparation system. A high solubility in the internal aqueous phase is highly desirable as this will give microparticles with high final drug loadings. However, it is preferable to have low drug solubility in the external, continuous aqueous phase so that the maximum amount of drug will remain in the microparticles and not dissolve in the continuous, external aqueous solution.

Another variation of the solvent evaporation technique utilizes an oil-in-oil emulsion method to encapsulate ganciclovir¹⁷. A suspension of ganciclovir sodium salt (equivalent to 25mg of free ganciclovir) in FSiO (100 μ l) was added to acetone solution (0.8ml) of PLGA (250mg). The mixture was dispersed by agitation in a vortex for 1 min and sonication for 5 min at high frequency. This dispersion was then immediately sonicated for 25 sec at high frequency with a 2 ml aliquot, a solution of SiO (45ml) in acetone (5ml) and the surfactant DMSiEPO (100 μ l). After the sonication, the mixture was added to the remaining amount of SiO-acetone-surfactant solution and stirred. The mixture was stirred overnight in the fume hood at room temperature until the acetone evaporated and the solid microspheres were formed. The microspheres were filtered and washed twice with hexane to remove residual SiO, and then separated in size fractions using sieves. Finally, the microspheres were dried over anhydrous CaSO₄ in a vacuum desiccator for at least 48 hours before they were used for the drug-release assays.

Other research groups have expanded the principle behind preparing biodegradable microparticles using multiple emulsions to prepare water-in-oil-in-oil-in-oil formulations⁸⁰. These formulations began with water-soluble compounds dissolved in an aqueous phase which is emulsified in soybean oil to form a first stable emulsion. This emulsion is dispersed in a PLGA/acetonitrile solution that is then dispersed in a hardening solution of light mineral oil. This method protects the water-soluble drug from exposure to organic solvents with a layer of oil. Microparticles have also been made using a potentiometric dispersion technique that resulted in more uniform particles and higher drug loadings. Higher drug loadings may also be achieved, especially with lower stirring rates which produce larger microparticles. The particles produced using this method were all spherical and smooth, with cross-sections of these multiphase microspheres showing numerous internal spheres within the microparticles.

2.5 Polymeric Systems for Ophthalmic Drug Delivery

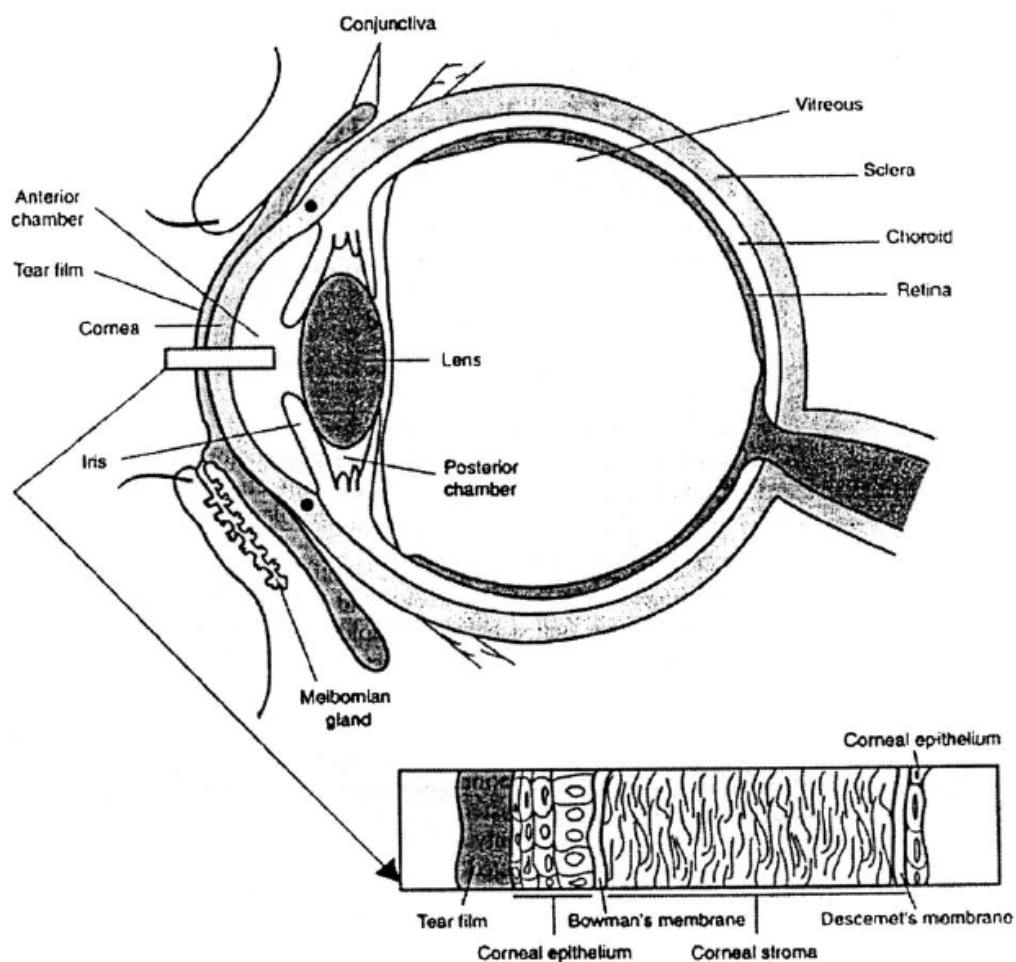
2.5.1 Structure of the eye

The eye is anatomically divided into the anterior and posterior segments. The former includes the cornea, the anterior chamber, the iris, the posterior chamber, the ciliary body, and the lens; the latter is composed of the vitreous, the retina, the retinal pigment epithelium, and the choroids. The eye has an environment that is specific to itself in terms of pharmacokinetics: the inner and outer blood-retinal barriers separate the retina and the vitreous from the systemic circulation. The vitreous body, which physiologically has no cellular components, occupies the vitreous cavity and reduces practical convection of molecules⁵³.

2.5.2 Drug Delivery Systems

The unique structure of the eye requires many therapies designed especially to treat difficult vitreoretinal diseases.

The administration of drugs for ophthalmic use may be either the external structures or the interior of the eye. Intraocular drug absorption occurs primarily via the cornea, but substantial absorption may occur via the sclera and conjunctival tissues⁸¹.

Figure 2.5 Structure of the eye⁸²

The most commonly used topical ophthalmic formulations are eyedrops, ointments, and, less frequently, inserts. Aqueous solutions have the disadvantage that most of the instilled drug is lost due to drainage via the nasolacrimal duct within the first 15-30 s after instillation⁸³.

It is much harder to deliver drugs to the posterior segment because of the longer diffusion distance and counter-direction intraocular convection from the ciliary body to Schlemm's canal. To overcome difficulties in achieving drug delivery into the posterior segment by topical administration, a controlled-release system may be required⁵³.

Intravitreal injection via the pars plana facilitates direct delivery of drugs into the posterior segment. Formerly, antibiotics⁸⁴ and antiviral drugs (e.g. ganciclovir)⁸⁵ were injected in eyes with endophthalmitis and Cytomagalovirus (CMV) retinitis, respectively. However, the half-lives of most drugs with low molecular weights in the vitreous cavity are as short as a few hours¹. Repeated injections often result in poor outcomes. The blindness resulting from CMV retinitis in increasing number of patients with AIDS is a serious problem to overcome. Therefore, urgent improvement of treatment modalities is required.

The drug delivery system (DDS) for vitreoretinal diseases has three major goals: enhances drug permeation (example, by iontophoresis and transscleral DDS), controlled release of drugs (example, using microspheres, liposomes, and intraocular implants), and targets drugs (example, prodrugs with high molecular weight and immunoconjugates)⁵³.

An ideal ophthalmic delivery system must

1. Prevent rapid elimination from the site of administration
2. Have optimum and reproducible drug release kinetics to achieve the required bioavailability profile
3. Be well tolerated and easy to use with a maximum of once-a-day administration

In view of this, various controlled release drug delivery systems have been investigated since the latter half of the 1980s. For the following decade, liposome formulations containing drugs⁸⁶, microspheres composed of biodegradable polymers⁸⁷, and implants made of non-biodegradable⁸⁸ or biodegradable⁸⁹ polymers have been developed.

Polymer devices for controlled release include (1) a homogeneous mixture of drugs and polymers (referred to as the “monolithic-type” or “matrix-type”), (2) polymer hydrogel binding drugs with chemical or ionic bonds (the “binding-type”), and (3) an outer shell of polymers packed with drugs (the “reservoir-type”)⁵³. The polymers used are classified as biodegradable or non-biodegradable polymers. Both materials can assume various forms, as injectable solution with the ability to form a gel or suspension of micelles, lipid emulsions (microspheres), liposomes, micro(nano)spheres, or micro(nano)capsules. They can even ensure the form of implantable devices in the shape of sheet, pellet, disc, rod, or plug. Table 2.2 lists the various ophthalmic controlled release systems.

DDS	Biodegradable polymers		Non-biodegradable polymers	
Monolithic -type	Injectable	Microspheres (emulsion)	Injectable	Gelling solution
	Implantable	Plug, disc, pellet, rod, sheet	Implantable	Pellet, sheet
	PLA, PLAGA, polyanhydrides, poly(ortho esters), etc.		Methylcellulose, polyacrylamide, poly-HEMA, etc.	
Binding -type	Injectable	microspheres		
	Implantable	Disc, sheet		
	Gelatin, collagen, albumin, chitosan, starch, dextran, etc			
Reservoir -type	Injectable	Microcapsule (PLA, PLGA)	Implantable	Disc, osmotic pump (PVA, EVA, silicon laminate, etc.)
		Liposome, micelle		

Table 2.2 A variety of controlled release systems⁵³

2.6 Cytomegalovirus

Cytomegalovirus (CMV) is responsible for the most common viral opportunistic infection in persons with acquired immunodeficiency virus syndrome (AIDS). Clinical disease due to CMV has been recognized in up to 40 % of patients with advanced HIV diseases^{1,90,91}. CMV retinitis is the most common ocular infection in AIDS and is the most important

cause of morbidity. With better treatment of the primary HIV infection, and a resultant longer survival, the prevalence of CMV retinitis appears to be increasing⁹². Patients may present with symptoms of blurred vision, a scotoma or dark area covering part of the visual field, light flashes, or floaters.

2.7 Ganciclovir⁹³

Ganciclovir is a synthetic guanine derivative active against cytomegalovirus (CMV). CYTOVENE-IV and CYTOVENE are the brand names for ganciclovir sodium for injection and ganciclovir capsules, respectively.

CYTOVENTE-IV is available as sterile lyophilized powder in strength of 500 mg per vial for intravenous administration. Each vial of CYTOVENE-IV contains the equivalent of 500 mg ganciclovir as the sodium salt (46 mg sodium). Reconstitution with 10ml of sterile water for injection yields a solution with pH 11 and a ganciclovir concentration of approximately 50 mg/ml. Further dilution in appropriate intravenous solution must be performed before infusion.

CYTOVENE is available as 250 mg and 500 mg capsules. Each capsule contains 250 mg or 500 mg ganciclovir, respectively, and inactive ingredients, croscarmellose sodium, magnesium stearate and providone. The mixture is contained in hard gelatin shells made up of gelatin, titanium dioxide, yellow iron oxide and FD&C Blue No.2.

Ganciclovir is a white to off-white crystalline powder with a molecular formula of $C_9H_{13}N_5O_4$ and a molecular weight of 255.23. The chemical name for ganciclovir is 9-[[2-hydroxy-1-(hydroxymethyl)ethoxy]methyl]guanine. Ganciclovir is a polar hydrophilic compound with a solubility of 2.6 mg/ml in water at 25°C and an n-octanol/water

partition coefficient of 0.022. The pK_a (acid dissociation constant) values for ganciclovir are 2.2 and 9.4. Ganciclovir is a neutral drug (but not zwitter ions) that has low protein binding (1 % - 2 %) efficiency.

According to Dr. Thomas L. Tarnowski⁹⁴ in Drug Metabolism and Pharmacokinetics department of Roche Palo Alto, zwitter ions occur when a molecule has 2 pK_a values and in neutral pH solution both are ionic (one positive and the other negative). Although the molecule is neutral, it may be polar if they exist in both the ionic forms.

In very acidic medium (pH less than 2.2), ganciclovir is protonated and therefore has a single positive charge. In solutions of pH between 2.2 and 9.4 (such as pH 7.4), ganciclovir is mainly neutral, with no charged groups. It is not zwitterionic. In strongly basic solution (pH greater than 9.4), ganciclovir is deprotonated and has a single negative charge⁹⁴.

Despite its neutrality at physiological pH values, ganciclovir is small and polar and is somewhat resistant to crossing lipid membranes. The low bioavailability of ganciclovir is a manifestation of this. The low distribution into cerebrospinal fluid, where it is only 24 to 70 % of the corresponding plasma concentrations, is further evidence of this effect. Within cells, ganciclovir becomes mono-, di- and tri-phosphorylated (it is the triphosphate that interferes with viral DNA synthesis)⁹⁴.

Since the pH of most tissues is in the neutral range and generally quite far from the pH values required to produce charged species from ganciclovir, the small difference in organ pH values within the neutral range seem unlikely to account for significant differences in organ distribution of ganciclovir⁹⁴.

In Cytovene IV, Ganciclovir is formulated as monosodium salt. It is a white to off-white lyophilized powder with a molecular formula of $C_9H_{13}N_5NaO_4$, and a molecular weight of 277.22. The chemical name for ganciclovir sodium is 9-[[2-hydroxy-1-(hydroxymethyl)ethoxy]methyl]guanine, monosodium salt. The lyophilized powder has an aqueous solubility of greater than 50 mg/ml at 25°C. At physiological pH, ganciclovir sodium exists as the un-ionized form with a solubility of approximately 6 mg/ml at 37°C⁹³. This suggests that the negatively charged sodium form is obtained at pH 11 and the un-ionized form exists at the physiological pH of around 7.4. The sodium form of ganciclovir increases the solubility of ganciclovir drastically, which is more convenient upon infusion.

The chemical structures of ganciclovir sodium and ganciclovir are:

Ganciclovir sodium (i) and Ganciclovir (ii)

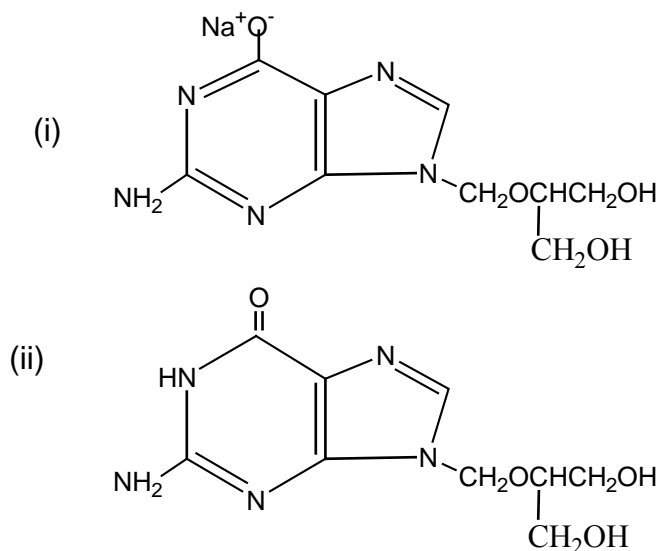


Figure 2.6: Chemical structure of (i) Ganciclovir sodium (ii) Ganciclovir

Ganciclovir is a nucleoside analog which inhibits herpes virus DNA polymerase. The drug is virustatic against CMV. Thus, when treatment for disease is stopped, viral spread and progression of disease characteristically recur¹.

2.7.1 Current treatment of CMV retinitis

The medication ganciclovir (GCV) is compressed into a tablet 2.5 mm in diameter by approximately 1 mm thick, coated on all sides with polyvinyl alcohol (PVA) and then coated with a discontinuous film of ethylene vinyl acetate (EVA). The entire assembly is then coated again with PVA, and a suture tab made of PVA is attached. The EVA coating is impermeable to ganciclovir, while the semipermeable PVA coating allows for drug diffusion into the eye. The rate of drug release is influenced by the solubility of the medication and the extent of EVA coating. This is similar to a membrane-controlled reservoir delivery system. A well-controlled (zero-order) sustained release of drug is enabled. This device has no final burst of inner drug in its release profile. This kind of non-biodegradable, sustained-release drug delivery device was the first commercial system established for clinical use to treat ocular diseases¹⁴. The device, however, is relatively large and required a 4-5mm sclerotomy at the pars plana for implantation. Because it is non-biodegradable, it has to be removed during a second surgery or reimplanted during a second surgery. Complications in the posterior segment, including vitreous hemorrhage, and cystoid macular edema with epiretinal membrane developed in 13 of 110 eyes (12 %) after implantation of this device⁹⁵. These problems should not be ignored because postoperative complications are associated with decreased visual acuity despite treatment.

In 2000, Japanese researchers evaluated biodegradable sclera implants as a controlled intraocular delivery system of GCV for the treatment of cytomegalovirus retinitis in rabbits^{15,16}. The sclera implants (weighing 8.5 mg) with length of 5 mm and diameter of 1 mm were made of PLA or PLGA and contained various amounts of GCV^{15,16}. The sustained release of GCV into the vitreous cavity with this biodegradable sclera plug that can be inserted through a 1-mm sclerotomy site was effective for the treatment of experimental CMV retinitis in rabbits^{15,16}. The sclera implants were prepared by dissolving the polymer and GCV in acetic acid, followed by lyophilizer to obtain a homogeneous cake. The cake was then compressed into a sclera implant on a hot plate at 80 °C to 100 °C.

Similar to the biodegradable microspheres, the drug-release profile of these devices, which underwent bulk erosion, had three phases⁵³: first was an initial burst of drugs followed by a diffusive phase and finally, another burst release of drugs was observed.

The diffusive phase following the initial burst exhibits stable drug release achieved by the outward diffusion of drugs newly dissolved by water under osmotic pressure and accompanying the surface erosion of the matrix. This phase is well controlled by the speed of polymer degradation as well as the total surface area of the device, the percentage of the loaded drug, and the hydrophilicity of the drug.

The bulk erosion accompanies hydrolysis of polymers throughout the matrix during the diffusive phase, resulting in the final burst. A highly compressed matrix, as was used in this case, would disintegrate and rapidly release most of the remaining drug when inner hydrolysis of polymers proceeded to a critical point. The higher the ratio of the volume to the total surface area of the matrix, the more intense the burst release.

The uncontrollable final burst of the drug load resulting from bulk erosion is undesirable and possibly problematic. This has been a critical disadvantage of a controlled-release system using biodegradable polymers compared with non-biodegradable polymers. When comparing to particulate delivery systems, because the total surface area/mass ratio of the implant is much smaller than that of microspheres, devices should be composed of polymers with a higher degradation speed or loaded with a larger amount of drug to achieve a drug-releasing rate comparable to that of microspheres. However, the devices made of polymers with higher degradation speed subsequently have a shorter diffusive phase and the devices with higher drug load lose most of the drug in the initial burst because a smaller amount of polymer cannot efficiently trap drug longer^{15,16}.

To overcome these problems, a new device was developed that combines biodegradable polymers with different molecular weights. This device could provide both a higher release rate of drugs and a prolonged diffusive phase as well as eliminate the final burst⁹⁶. In this device, polymers with a higher molecular weight act as a framework and gradual, constant hydrolysis of polymers with a lower molecular weight regulates the drug release. This improvement in biodegradable implants enables sustained release comparable to that of non-biodegradable implants.

(a) Injectable particles

For clinical use, microspheres should pass through 20-23-gauge needles. Generally, the size should be smaller than 150 μm in diameter⁵³. Microspheres larger than 2 μm tend to sink as the result of gravity or be suspended in residual vitreous body and, therefore, intravitreal injections of the suspension may be clinically feasible. Intravitreal injection of microspheres of PLGA or PLA causes no cytotoxicity on the retina electrophysiologically and histologically^{19,87}.

Rocio Herrero-Vanrell and Miguel F. Refojo of Harvard Medical School^{17,18} have obtained a sterilized formulation of microparticles using an oil-in-oil-in-oil double emulsion method (FSiO and SiO). They also have reviewed the current status of biodegradable microspheres for vitreoretinal drug delivery¹¹. Among the biodegradable polymers that have been investigated to make microparticles for drug delivery are gelatin, albumin, polyortho-esters, polyanhydrides, and polyesters, particularly PLA and PLGA¹¹. Several *in vitro* and *in vivo* rabbit studies of ganciclovir-loaded PLGA microspheres have been reported. Generally, the microspheres were fabricated by the solvent evaporation method^{17,18}.

Like biodegradable implantable devices, the general drug-release profile of degradable microspheres undergoing bulk erosion has three phases⁵³.

The initial burst came from drugs distributed on and near the surface of the polymer matrix and is dependent on the total surface area of the device, the percentage of loaded drug, and the hydrophilicity of the drug. This burst may be undesirable, especially when drugs are cytotoxic at high concentrations. Nevertheless, the burst can be minimized by pre-incubation with saline solution for several hours before use.

A wide total surface area of microspheres tends to result in a severe initial burst of drugs, when hydrophilic drugs are loaded. Because the solvent evaporation method does not involve the process of compression used in the fabrication of implantable devices, solvent enrichment during drying may also result in the initial burst.

The drug release in the diffusive phase is affected by the molecular weight and the composition of the polymers, the amount of drug loading, the hydrophilicity of drug, and

the size (the total surface area) of the microspheres. Generally, small microspheres contain a lower drug load and release drugs faster than larger ones.

The final burst, even from microspheres composed of polymers undergoing bulk erosion process, is likely to be minimal because the ratio of the volume to the total surface area of the matrix is much lower compared with implantable devices.

Microspheres gradually degrade through bulk erosion and subsequently form small pores and cracks that may affect drug release. The polymer degradation is also affected by the homogeneous distribution of drugs in the matrix. Hydrophilic drugs may dissolve faster than the polymers and subsequently make the structure of the polymer matrix more permeable. Other possible factors that affect polymer degradation involve the molecular weight and the composition of the polymer and the size of the microspheres.

2.7.2 Summary

Rocio Herrero-Vanrell *et al*^{11,17} and Amadeo *et al*¹⁸ were the major researchers in the study of ganciclovir loaded PLGA microspheres. The ganciclovir sodium used had much higher water solubility (50 mg/ml) than ganciclovir (2.6 mg/ml). This was the major reason for the development of the oil-in-oil-in-oil double emulsion method. The GCV loading obtained was 68.1 µg GCV/mg microspheres with the microspheres having the size range from 53 µm to 103 µm and 76.4 µg GCV/mg microspheres of size range from 106 µm to 212 µm, respectively.

The goal of this research was to prepare GCV-loaded microspheres of around 100 µm, with comparable GCV loading to the GCV-loaded microspheres prepared by

Rocio *et al*^{11,17,18}. A simple water-in-oil emulsion method was used, and the relatively low water soluble ganciclovir was chosen.

The release of drugs from microparticles takes place through several mechanisms¹¹, including diffusion through the polymer network and/or through the fluid-filled pores in the particles, physical erosion and/or hydrolysis of the polymer, ion-exchange, or by a combination of several of these mechanisms. The release kinetics of a drug is dependent on the polymers used, the rate of degradation of the polymer matrix, the solubility of the drug, the amount of drug loading, and the size and method used for the preparation of the particles.

In each of the drug-loaded polymer microparticles, in this case, the GCV-loaded PLGA and PDLA microspheres, the effects of the drug GCV loading and the PLGA copolymer ratio along with molecular weight on the release profiles and degradation kinetics are studied.

CHAPTER 3

EXPERIMENTAL METHODS AND TECHNIQUES

3.1 Materials

The anti-viral drug used was ganciclovir purchased from Roche Products Limited, (Welwyn Garden City, United Kingdom) in the form of Cymevene®. The drug ganciclovir is contained in a capsule and the contents of each capsule appear as a white powder consisting of about 90 % ganciclovir (GCV) and the remaining 10 % being povidone/K90, croscarellose sodium, magnesium stearate and purified water.

Table 3.1 summarizes the five polymers used in the fabrication of the ocular implant and their corresponding intrinsic properties. It was noted from the table that the intrinsic viscosity of the polymer granules increased with the weight average molecular weight. The poly(D,L-lactide-co-glycolide) 75:25, intrinsic viscosity (I.V.) of 0.94 dl/g, weight average molecular weight of 130,000 dalton, was purchased from Purac Far East, Singapore (manufactured in Holland). It had aliphatic alcohol end groups instead of carboxylic acid end groups. The other polymers were purchased from Absorbable Polymer Technologies, Inc., where their carboxylic acid end groups were uncapped.

Polymer	Intrinsic Viscosity (dl/g)	M _w (Daltons)	Synonym
Poly(DL-lactic acid co glycolic acid) ; molar ratio of lactic/glycolic acids, 75:25	0.94	130,000	PLGA 75/25 I.V. 0.94
Poly(DL-lactic acid co glycolic acid) ; molar ratio of lactic/glycolic acids, 75:25	0.24	23,000	PLGA 75/25 I.V. 0.24
Poly(DL-lactic acid co glycolic acid) ; molar ratio of lactic/glycolic acids, 50:50	0.50	37,000	PLGA 50/50 I.V. 0.50
Poly(DL-lactic acid co glycolic acid) ; molar ratio of lactic/glycolic acids, 50:50	0.22	11,000	PLGA 50/50 I.V. 0.22
Poly(DL-lactic acid)	0.22	20,000	PDLLA I.V. 0.22

Table 3.1 Polymer used for the fabrication of the microspheres

When the concentration c , expressed in g/L, is sufficiently low, the viscosity η of the solution is not much different from the viscosity η_s of the pure solvent. The ratio of η to η_s is called the relative viscosity, η_r as shown in equation 3.1.

$$\eta_r = \frac{\eta}{\eta_s} = 1 + [\eta]c + K_v c^2 + \dots \quad (3.1)$$

The linear coefficient $[\eta]$ is called the **intrinsic viscosity**⁹⁷. It can be obtained as the slope in the plot of η_r as a function of c in the low concentration limit. The dimension of $[\eta]$ is (concentration)⁻¹. The reciprocal of the intrinsic viscosity is often used to represent the overlap concentration of a given polymer: $c^* = 1/[\eta]$. In a rough approximation, each linear polymer chain occupies a space of a sphere or a cube of a linear dimension of R_g (radius of gyration). At low concentrations, these spheres or cubes are separated from each other. As the concentration c (mass concentration) increases, they become congested and eventually touch each other. At the so-called overlap concentration (c^*), the whole volume of the solution is packed with these spheres⁹⁷.

The intrinsic viscosity $[\eta]$ is a quantity characteristic of a polymer. It represents an increase in the solution viscosity when the concentration is raised to a certain level. As expected, a polymer molecule with a greater dimension has a larger $[\eta]$. Experimentally, it is expressed by Mark-Houwink-Sakurada equation⁹⁷:

$$[\eta] = K_M (M)^\alpha \quad (3.2)$$

where K_M is a constant of the unit of L/g, M is the molecular weight of the unit of g/mol and α is called a Mark-Houwink-Sakurada exponent. The value of α is around 0.7–0.8 for flexible chains in the good solvent and exceeds 1 for rigid chains. In the theta solvent, the flexible chain has $\alpha = 0.5$. α is greater for a more extended conformation because a polymer molecule with a greater dimension for a given contour length will experience a greater friction to move in the solvent.

The samples were degraded in phosphate buffered solution of pH 7.00 at 20°C, obtained from Merck Chemicals Ltd. (KGaA, Darmstadt, Germany).

Methylene chloride or dichloromethane (DCM) from Merck Chemicals Ltd. (KGaA, Darmstadt, Germany) and poly (vinyl alcohol), (87 % - 89 % hydrolyzed, average molecular weight 13,000-23,000) from Aldrich Chemical Company Inc. (Milwaukee, USA) were used as received.

3.2 Sample Preparation

3.2.1 Ganciclovir-loaded microspheres

The oil-in-water emulsion technique¹⁸ was applied for the preparation of ganciclovir-loaded microspheres. The dispersed phase was prepared by adding 100 mg of the drug

into a polymer solution. The polymer solution was prepared by dissolving 1000 mg of polymer in dichloromethane (DCM). The concentration of the polymer in dichloromethane was varied to keep the viscosity of the polymer solution the same. This was to avoid the effect of viscosity on the droplet size of the dispersed phase and the particle size of the microspheres. The mixture was stirred continuously for 24 hours with the help of a magnetic stirrer. The polymer-ganciclovir suspension was then added to 100 ml aqueous solution containing 1 % PVA. An oil-in-water (O/W) emulsion was formed with the help of a homogenizer at the speed of 1,000 rpm for 30 minutes. The organic solvent was allowed to evaporate under an aspirating hood at room temperature for 4 hours, leaving behind solid microspheres. The microspheres were collected and washed three times with distilled water to remove any residual PVA. The microspheres were then dried under vacuum in a vacuum desiccator at room temperature until the weight is constant in three consecutive readings before they were used for drug-release assays and degradation tests.

The intrinsic viscosity and molecular weight of the five PLGA and PDLLA polymers studied were DIFFERENT. The corresponding values are listed in Table 3.1. The hydrophobic polymer/dichloromethane solution made up the oil phase. The forming of an emulsion requires the expenditure of a certain amount of energy, this being partly the work required to form the interface between the two phases. The creation of the interface also requires that mechanical work is carried out against the internal friction (or viscosity) of the system⁹⁸. To keep the particle size of the different polymers constant, the viscosity of the solutions of the DIFFERENT polymers has to be kept constant. To keep the viscosity of the solutions of the DIFFERENT polymers constant, the concentration of each solution of the DIFFERENT polymer was changed and adapted to the same viscosity.

3.2.2 Pure microspheres

Similarly, microspheres without ganciclovir were also prepared to study the effect of hydrolytic degradation on the polymers in the absence of drug.

3.2.3 Particle size study

It is reported that the concentration of polymer solution from the same polymer affected the particle size⁹⁹. Thus, PLGA 75/25 I.V. 0.94 was prepared at different concentrations (0.025, 0.050, 0.100, 0.150 and 0.200 g/ml) to study the effect of polymer solution concentration on particle size. The microspheres were prepared by an oil-in-water emulsion solvent evaporation method. 0.25, 0.5, 1.0, 1.5 and 2.0 g of polymer were dissolved in 10 ml of DCM in a conical flask, respectively. As for the aqueous solution, 0.5 g of poly (vinyl alcohol) (PVA) was dissolved in 100 ml of distilled water in a 250 cm³ beaker. A propylene cover was used to cover the beaker to prevent evaporation. The dissolved polymer was emulsified in aqueous PVA solution. The emulsion was stirred at a constant speed of 1000 rpm for 1 hour. The stirring speed was then reduced to 500 rpm and stirred for another 2 hrs to allow complete evaporation of DCM. The stirring was carried out in the fume chamber because DCM was volatile and hazardous to health. The microspheres were then collected and rinsed with distilled water 3 times before they were dried in a vacuum desiccator at room temperature until the weight is constant in three consecutive readings.

The microspheres size and distribution were measured using a laser particle analyzer as described in section 3.2.4.

3.2.4 Laser Particle analyzer

Using the Fraunhofer diffraction theory, dispersed particles momentarily traversing in a collimated light beam will result in diffraction of light outside the cross section of the beam. This occurs when the particles have diameter larger than the wavelength of light. The intensity of the forward diffracted light is proportional to the squared of particle size, but the diffraction angle varies inversely with particle size. A helium-neon laser is the commonly used light source. The combination of lens and multi-element detector coupled with a microcomputer enables the particle size distribution from the diffraction data to be computed.

The microspheres size and distribution was measured using a particle analyzer (Fritsch analysette 22 compact, Germany) with a measuring range of 0.31 μm to 300.74 μm . The measurement duration used was 3 scans, the pump and stirrer were set at 100 rpm and 1 rpm, respectively. The microspheres were first homogeneously dispersed in distilled water. They were then added drop by drop to the analyzer. Particle size measurements were obtained when the microspheres concentration reached 7 % (weight/volume).

3.3 Degradation studies

The degrading medium used was phosphate buffered solution at pH 7.00. 50 mg of the microspheres samples were kept in 10 ml vessels, immersed in phosphate buffered solution and heated to 37 °C by a pre-programmed water bath set at 37 °C, for various lengths of time, from 1 month to 3 months.

3.3.1 Changes in mass of microspheres

Gravimetric analysis for polymer mass loss was accomplished using an electronic balance. Approximately 50 mg of the dry polymers were carefully weighed prior to

incubation in the degradation medium. This initial mass of microspheres, labeled m_i , was then incubated in PBS solution for a designated period of time. At fixed time intervals, the samples were removed from the degrading medium and dried for 3 days in a vacuum desiccator at room temperature until the weight is constant in three consecutive readings. The dried samples were then weighed to determine the mass after degradation, m_d , and the % mass change was calculated as

$$\text{masschange}\% = \frac{m_i - m_d}{m_i} \times 100\% . \quad (3.3)$$

3.4 Drug release Studies

The drug release medium used was phosphate buffered solution at pH 7.00. 50 mg of the microspheres samples were kept in 10 ml vessels, immersed in phosphate buffered solution and heated to 37 °C by a pre-programmed water bath. Samples for analysis (8 ml) were removed with a syringe at various time intervals. After the samples were removed for analysis, an identical volume of fresh phosphate-buffered saline (PBS) solution was added to the container with the microspheres to continue the release test.

3.5 Materials Characterization

At the end of each time period, 3 to 5 sets of samples were removed from the water bath. The polymer microspheres were characterized using thermal analysis (MDSC), SEM, GPC, gravimetric analysis to follow the effect of hydrolytic degradation on the morphology of the polymer. The pH of the degrading medium was also measured periodically using a pH meter. UV spectrometer was used to study the rate of drug release from the drug-loaded polymer samples.

3.5.1 Thermal analysis

Thermal analysis embraces all methods in which measurements are made of a physical property that changes as the temperature is varied¹⁰⁰. The techniques are ideally suited for the location and characterization of processes in which there is a change in molecular mobility in the system or when a reaction is occurring.

3.5.1.1 Differential Scanning Calorimetry (DSC)

There are two types of DSC, the heat-flux DSCs and the power-compensation DSCs. The heat-flux measuring system is a passive system, whereas the power-compensation system is active. The heat-flux DSC registers the full temperature difference between sample and reference, which is built up during sample reaction, while the power-compensation DSC 'suppresses' this difference down to a fraction, which is used as the measured signal. The DSC used in this study is the heat-flux MDSC with disk-type measuring system.

Modulated DSC (MDSC)

Modulated differential scanning calorimetry (MDSC) is a novel thermoanalytical technique which involves the application of a sinusoidal (modulated) heating signal to a sample, thereby allowing separation of the total heat flow response into the reversing and non-reversing components. The heat flow from a sample experiencing a linear heating (or cooling) programme will comprise of a heat capacity (reversing) component and a contribution from any kinetically hindered (non-reversing) thermal events.

The glass transition temperature, T_g , is a very important characteristic of amorphous polymers. T_g is a non-equilibrium property. The measurements made are sensitive to the heating rate and the method used. Thus the value of T_g obtained differs from one technique to another, over a range of several degrees, but since the transition is usually rather broad these differences are not necessarily recognized.

Many polymers are able to form ordered crystalline regions and hence exhibit melt transitions. The melting temperature is rather a broad transition reflecting a range of crystallite sizes and crystal perfection. If the polymer was cooled rapidly when the sample was formed, on reheating it may show "pre-melting crystallization". This arises because when the sample is at an elevated temperature (but still below the melt temperature) the kinetics of crystallization are sufficiently speeded up to allow some parts of the molecules initially trapped in a disordered state to crystallize. Hence it is especially valuable to conduct an initial experiment with a constant heating rate, followed by controlled cooling within the thermal analysis cell, then by a repeat run using the same heating conditions. The second run act as a reference, and reveals clearly those features in the first run that takes account of the previous thermomechanical history. The MDSC allows separation of these components during the first heating cycle, and the repeat run will allow the generation of a reference curve against which effects may be judged.

The enthalpy of fusion, ΔH_f can be measured using the C_p versus T curve from a calibrated DSC instrument by integrating under the curve over the melting range. If the curve is fairly sharp, with the peak temperature at T_m , then the entropy of fusion can be estimated as $\Delta S_f = \Delta H_f / T_m$. If the enthalpy of fusion of a semicrystalline polymer sample is H_f then the fractional crystallinity is given by $f_c = H_f / H_{f,c}$, where $H_{f,c}$ is the enthalpy of fusion of a completely crystalline sample of the same polymer.

DSC studies were performed using a modulated DSC (DSC 2920, TA Instruments, USA), with a refrigerated cooling system (RCS) attached. Nitrogen was used as the purge gas, flowing at a rate of 40 cc/min through the DSC cell, and at 150 cc/min through the RCS unit. TA Instruments aluminum hermetic DSC pans were used throughout the study. The mass of each empty sample pan was matched with the mass of the empty reference pan to

± 0.1 mg. Approximately 3 mg of sample was used for the MDSC runs. MDSC experiments were performed with modulation amplitude of ± 1 °C and a 1-minute period with a 5 °C/min underlying heating or cooling rate. The experimental methodology included an initial 20-minute isothermal period at -20 °C to allow equilibration of the sample to the programmed temperature modulation, then heating to 250 °C.

3.5.1.2 Thermo Gravimetric Analyzer (TGA)

In thermo gravimetric analytical (TGA) measurements, the mass of the sample is recorded continuously while temperature is increased at a constant rate. Weight losses occur when volatiles absorbed by the polymer are driven off and when degradation of the polymer occurs with the formation of volatile products at higher temperatures. The equipment is designed to allow precise weight measurements to be performed in a controlled environment, thus avoiding the effects of convection forces arising in the heating chamber and the changes in the density of the gaseous environment. It is important to ensure that volatiles do not condense on the weighing apparatus. It is also necessary to control the atmosphere when this has an influence on the process of degradation. Typically studies are performed using air with nitrogen as an inert atmosphere.

A Hi-Res TGA-2950 thermo gravimetric analyzer was used to investigate the temperature dependent degradation/decomposition of the drugs. The samples were heated at 10 °C/min from room temperature to 600 °C in nitrogen atmosphere. It showed the decomposition temperature of the sample. The plots obtained were the percentage weight remaining versus temperature. Here the temperature at which at least 95 % of the original weight was lost to the environment was defined as the decomposition temperature.

3.5.2 Scanning Electron Microscope (SEM)

The SEM is widely used in studies of polymers. However, there are limitations such as specimen charging when the specimen is non conductive, and structural damage caused by the high energy electron beam impinging on the specimen.

Surface morphology of microspheres during the incubation period was observed using a JEOL JSM-6340F field emission scanning electron microscope (FESEM) at 5.0 KV. The samples were first mounted on metal stubs with the help of double-sided tape, and coated with gold using a pulse plasma system (18mA for 70 seconds) to prevent sample charging.

3.5.3 Gel Permeation Chromatography (GPC)

GPC is a form of liquid chromatography in which the molecules are separated according to their molecular size or, more correctly, their hydrodynamic volume in solution. When the solvent has a constant composition, the method is termed isocratic chromatography. The procedure involves injecting a dilute solution of a polydisperse polymer into a continuous flow of solvent passing through a column containing tightly packed microporous gel particles.

The particle sizes are in the range of 5 - 10 μm for efficient packing and typically possess a range of pore sizes from 0.5 - 10 nm, which corresponds to the effective size range of polymer molecules. Separation of the molecules occurs by preferential penetration of the different sized molecules into the pores. Small molecules are able to permeate more easily through the pores compared to the larger molecules so that their rate of passage through

the column is correspondingly slower. It follows that the time or volume of elution is inversely proportional to the molecular size.

The ability of the polymer molecule to enter a pore will depend upon its size or hydrodynamic volume in solution. Change of solvent and temperature can lead to changes in the hydrodynamic volume and hence the ability to be retained by the column.

The changes in molecular weight were studied using Agilent 1100 Series, Model No. G1311A gel permeation chromatography. Molecular weights of the as-received PDLGA and PLGA polymers and the degraded samples were determined. An Agilent's Plgel 5 μm MIXED-C column with a Agilent's RI-254 refractive index detector was used. The mobile phase was a mix-solvent of 80:20 tetrahydrofuran (THF) and dichloromethane (DCM) at a flow rate of 1 ml/minute and a temperature of 35 °C. Samples were first dissolved in the mix-solvent, filtered, and then filled into 2 ml vials. The solution was then injected into the column using auto injection. The average molecular weights were calculated using a series of polystyrene standards that ranged from 640 to 4,843,000 in their molecular weight.

3.5.4 Ultraviolet-visible Spectrometer

The drug release profile of the microspheres samples was studied using ultraviolet spectrometer (SHIMADZU UV2501 (PC) S, Australia). The phosphate buffered solution was added to the optical cell and the sample was analyzed for ganciclovir (GCV) by monitoring its absorbance at 252.40 nm.

A GCV calibration curve was obtained by plotting the peak absorbance values at 252.40 nm against known GCV concentrations, as illustrated in Figure 3.1. This graph was then used to calculate the concentration of GCV in the phosphate buffered solution retrieved at various time intervals.

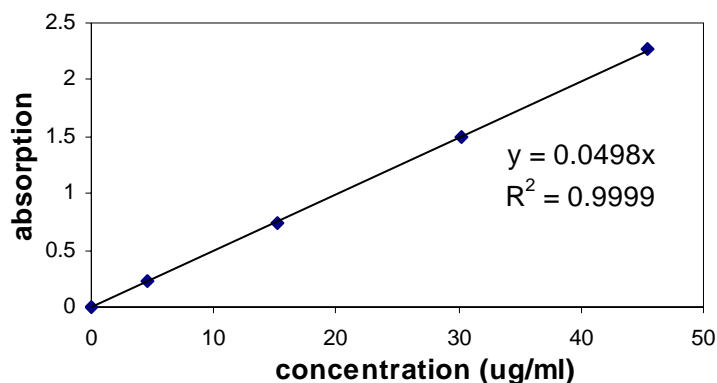


Figure 3.1 GCV Calibration Curve.

3.5.4.1 Drug Loading Efficiency Test

In order to find the true amount of GCV that was loaded into the microspheres during the fabrication process, 10 mg of the drug loaded microspheres were dissolved in 2 ml of DCM. 25 ml of deionized water was then added to the bottle and the contents were stirred overnight to allow the GCV to diffuse into the inorganic layer (water). The water phase was then retrieved from the bottle and tested for its GCV contents via UV spectrophotometer.

3.5.5 ^{13}C nuclear magnetic resonance (NMR) spectroscopy

^{13}C NMR has been a valuable technique for studying the microstructure of polymers¹⁰¹,¹⁰². Pulsed Fourier transform (FT) ^{13}C NMR has been used to specifically determine the sequence distribution of many types of copolymers^{103,104}. The technique relies on separate chemical shifts produced by carbons in specific molecular environments. Quantitative analysis requires: (1) a sufficiently powerful radiofrequency (RF) pulse to irradiate all of

the nuclei equally; (2) enough relaxation time for the nuclei of interest to completely return to equilibrium after the pulse and prior to the next pulse; and (3) elimination of differential nuclear Overhauser enhancement (NOE). As a spectrum is proton decoupled, signal enhancement of a multiplet is observed as the multiplet collapses into a single line. The extent is usually greater than would be expected due to simple collapse. This additional signal increase is termed the nuclear Overhauser enhancement and is created by ^{13}C - ^1H dipole-dipole interactions¹⁰⁵.

For ^{13}C NMR, a sufficient delay occasionally approaches 100 s, which would substantially increase the minimum experiment acquisition time from under 1 hour to 10 or more hours. Fortunately, large molecules such as polymers generally feature short relaxation times and require pulse delays of only a few seconds. Any relaxation and differential NOE problems can be overcome by the addition of a paramagnetic substance, also known as a relaxation agent, such as chromium (III) acetylacetonate ($\text{Cr}(\text{acac})_3$) and iron chelates.

3.5.5.1 Materials and methods for ^{13}C NMR

The instrument used was 100 MHz ^{13}C NMR instrument (Bruker DRX 400) and the solvent employed was deuterated chloroform (CDCl_3).

The following parameters were selected in all the runs. 90° pulse width = 8.7 ms, pulse delay = 2 s, spectral width = 13000 Hz with the decoupler mode on. Samples were prepared in deuterated CDCl_3 at concentrations of 50 mg / ml. Total acquisition time was approximately 2 hours to obtain a good signal-to-noise ratio.

The comonomer sequence distributions were obtained by comparing the relative intensities of the resonances between the GA carbonyl connected to a LA unit (GA-LA) at 166.5 ppm, and the GA carbonyl attached to another GA unit (GA-GA) at 166.6 ppm²⁷.

$$\text{The ratio, } R_{\text{cms}} = \frac{\text{Int}_{\text{GA-LA}}}{\text{Int}_{\text{GA-GA}}} \quad (3.4)$$

where, R_{cms} is the relative proportions of the lactic acid-glycolic acid units (LA-GA) and glycolic acid-glycolic acid (GA-GA), $\text{Int}_{\text{GA-LA}}$ is the intensity of the GA-LA carbonyl peak and $\text{Int}_{\text{GA-GA}}$ is the intensity of the GA-GA carbonyl peak. The lower the R_{cms} value, the higher the degree of heterogeneity or blockiness of the copolymer. In commercial samples of PLGA 50:50, the R_{cms} values ranged from 0.42 to 0.57, indicating differing degree of blockiness¹⁰⁶.

3.5.6 X-Ray Photoelectron Spectroscopy (XPS)

XPS measurements were carried out on a VG Scientific ESCA LAB Mk II spectrometer equipped with a Mg K_{α} X ray source (1235.6 eV photons) and a hemispherical energy analyzer. The source was adjusted at a powerful 280 W (power of emission of 20 mA and a tension of 14 kV). A pressure of about 1×10^{-9} mbar was maintained in the analysis unit. The use of a slit of 15×6 mm at the end of the hemispherical analyzer allowed the surface analysis of 3×2 mm of sample. The photoelectrons were exited at an angle of 90° , thus allowing probe close to 50 \AA on the material.

The Cymevene® powders, pure and GCV-loaded microspheres samples were first evenly distributed on pre-cleaned glass slides and held in place with double-sided adhesive tape. After removing the residual moisture in vacuum, the samples were tested by XPS.

Series of survey spectra were recorded over a binding energy range of 0 to 1000 eV using passive energy 20 eV. In all cases, the survey spectra recorded the presence of only oxygen (O1s 533 eV), nitrogen (N1s 398.5 eV) and carbon (C1s 285 eV) at the surface. Detailed analysis of C1s regions of each sample was recorded over a binding energy range of 280 to 300 eV.

The curve fitting was performed by the computer program Kratos provided by the equipment manufacturer. A Gaussian-Lorentzian function was applied to all data. No asymmetry component was introduced.

CHAPTER 4

AS-RECEIVED MATERIALS AND MICROSPHERES

This chapter deals with the results from the characterization of as-received polymeric granules, GCV, undegraded blank microspheres as well as undegraded GCV-loaded microspheres. The as-received polymeric granules were dissolved in dichloromethane (DCM) and fabricated into blank and GCV-loaded microspheres as described in section 3.2.1 and section 3.2.2. TGA, MDSC, GPC, SEM and particle analyzer were used to characterize the samples.

4.1 As-received materials

The results obtained from the characterization of the as-received polymer granules and commercially available Ganciclovir (GCV) were presented in this section.

4.1.1 Thermo gravimetric Analyzer (TGA)

GCV decomposed at 284 °C when heated from room temperature to 600 °C at a ramping rate of 10 °C/min. The decomposition temperatures for the as-received polymer granules are summarized in Table 4.1. These temperatures were used to determine the maximum temperatures the samples were heated to in a DSC scan. Here, the maximum temperature used in the DSC scans was 250 °C. This was to prevent the release of volatile products formed at decomposition temperatures, which would contaminate the measuring chamber and result in inaccurate readings.

Polymer	Decomposition Temperature (°C)
PDLLA I.V. 0.22	270
PLGA 75/25 I.V. 0.94	281
PLGA 75/25 I.V. 0.24	270
PLGA 50/50 I.V. 0.50	266
PLGA 50/50 I.V. 0.22	268

Table 4.1 Decomposition temperatures for as-received polymer granules

The decomposition temperature of the polymers were found to be around 270 °C except for PLGA 75/25 I.V. 0.94, which was around 280 °C. The high decomposition temperature for PLGA 75/25 I.V. 0.94 could be due to structural differences, where PLGA 75/25 I.V. 0.94 had aliphatic alcohol end groups, while the rest had uncapped carboxylic acid end groups.

As the measurements were carried out in nitrogen atmosphere, there were no oxidation reactions. At around the thermal degradation temperature, depolymerization would take place, starting from the end groups, which would leave free radicals on the polymer backbone. This would then trigger a chain reaction, releasing monomers to the surrounding. In the case of the alcohol end groups ($R-OH$) in PLGA 75/25 I.V. 0.94, higher temperature was needed to initiate the depolymerization compared to the carboxylic acid end groups ($R-COOH$) in the rest PDLLA and PLGA polymers.

4.1.2 Modulated Differential Scanning Calorimetry (MDSC)

The DSC thermograms obtained from the first heating cycle illustrates the thermal history of the samples. As all of the PDLLA and PLGA purchased were amorphous in nature, no melting peaks were observed in the DSC thermograms. There was only a glass transition temperature (T_g) observed in all the samples. The T_g of as-received polymers was summarized in Table 4.2.

Sample	LA:GA ratio	I.V.	M _w (Daltons)	T _g (°C)
PDLLA	100:0	0.22	20,000	47 ± 1
PLGA	75:25	0.94	130,000	52 ± 3
		0.24	23,000	42 ± 4
	50:50	0.50	37,000	42 ± 3
		0.22	11,000	28 ± 4

Table 4.2 Glass Transition Temperature (T_g) of the as-received polymer granules.

The initial T_g is directly related to the molecular weight and the ratio of LA to GA. For the same LA to GA ratio, the higher the I.V., the higher was the T_g. The decrease in T_g is proportional to the decrease in the molecular weight of polymer according to the Fox-Flory equation¹⁰⁷.

$$T_g = T_{g\infty} - k / \overline{M}_n \quad (4.1)$$

where, \overline{M}_n is the number average molecular weight, $T_{g\infty}$ is the T_g of the material at infinite molecular weight, k is a constant, which is related to the degree of branching for the system¹⁰⁸.

The higher molecular weight increased the glass transition temperature and this would lead to slower degradation because glassy polymers degrade slower than rubbery ones. If the polymer is in the glassy state ($T < T_g$), the mobility of the macromolecules is very slow. In this case, the free volume available for diffusion and consequently the diffusion rate of drug/ water through the polymer matrix is very slow. In contrast, if the polymer is in the rubbery state ($T > T_g$), the macromolecules are much more mobile and the resulting drug/ water diffusion coefficient are orders of magnitude higher than in the glassy state. Hence rubbery polymers should degrade faster than glassy polymers. From Table 4.2, for the same I.V., the T_g appeared to increase with decreasing glycolic acid ratio. The T_g value for all the polymers was greater than the physiological temperature of 37 °C, except for PLGA 50/50 I.V. 0.22. Devices fabricated using PLGA 50/50 I.V. 0.22 therefore would be in a rubbery state at 37 °C. The drug release rate from these devices would be

faster than devices made from the other polymers, as the latter would be in a glassy state when implanted in the body. This was supported by the ganciclovir release profile obtained from the various drug-loaded microspheres, as shown in Figure 7.1, Chapter 7.

The drug ganciclovir (GCV) with two melting peaks at 254 °C and 232 °C was highly crystalline, as observed from the DSC heating scan in Figure 4.1. These melting peaks corresponded to the GCV and the excipient, povidone melting temperatures, respectively. Upon incorporation of GCV into the polymer matrix, the originally amorphous polymer displayed the melting peak for GCV. The effect of GCV on the morphology and hydrolytic degradation of polymers is discussed in detail in Chapter 6.

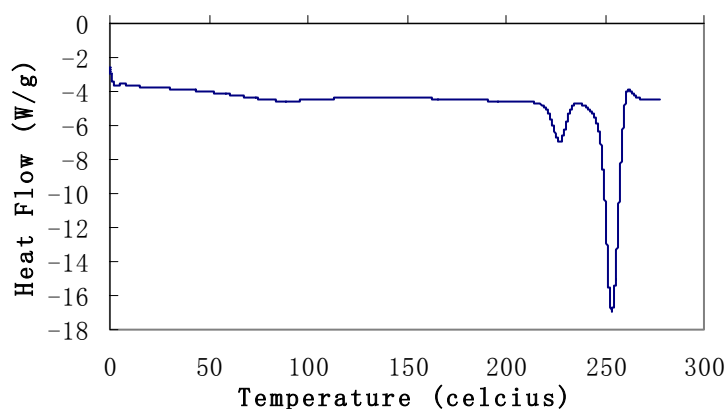


Figure 4.1 Thermogram of commercially available GCV.

4.1.3 Gel Permeation Chromatography (GPC)

The weight average molecular weight (M_w), number average molecular weight (M_n) and polydispersity index (PI) of the as-received polymers were summarized in Table 4.3.

Sample	LA:GA ratio	I.V.	M_w (Dalton)	M_n (Dalton)	PI
PDLLA	100:0	0.22	19,657	15,238	1.29
PLGA	75:25	0.94	126,720	78,708	1.61
		0.24	23,149	13,153	1.76
	50:50	0.50	35,386	22,396	1.58
		0.22	11,444	7,681	1.49

Table 4.3: Weight average molecular weight (M_w), Number average molecular weight (M_n), Polydispersity Index (PI) of the as received PDLLA and PLGA polymeric granules.

From table 4.3, it was observed that I.V. was directly related to the molecular weight of the polymer. When the I.V. decreased, both the M_w and M_n decreased accordingly. Take for example, for the PLGA with LA to GA ratio of 75:25, when the I.V. decreased from 0.94 to 0.24, the M_w decreased from 130,000 dalton to 23,000 dalton, and the M_n decreased from 79,000 dalton to 13,000 dalton.

The polydispersity, PI, of the polymer represents the breadth of the molecular weight distribution, MWD, of the polymer and can be calculated as follows

$$PI = M_w / M_n . \quad (4.2)$$

4.1.4 ^{13}C nuclear magnetic resonance (NMR) spectroscopy

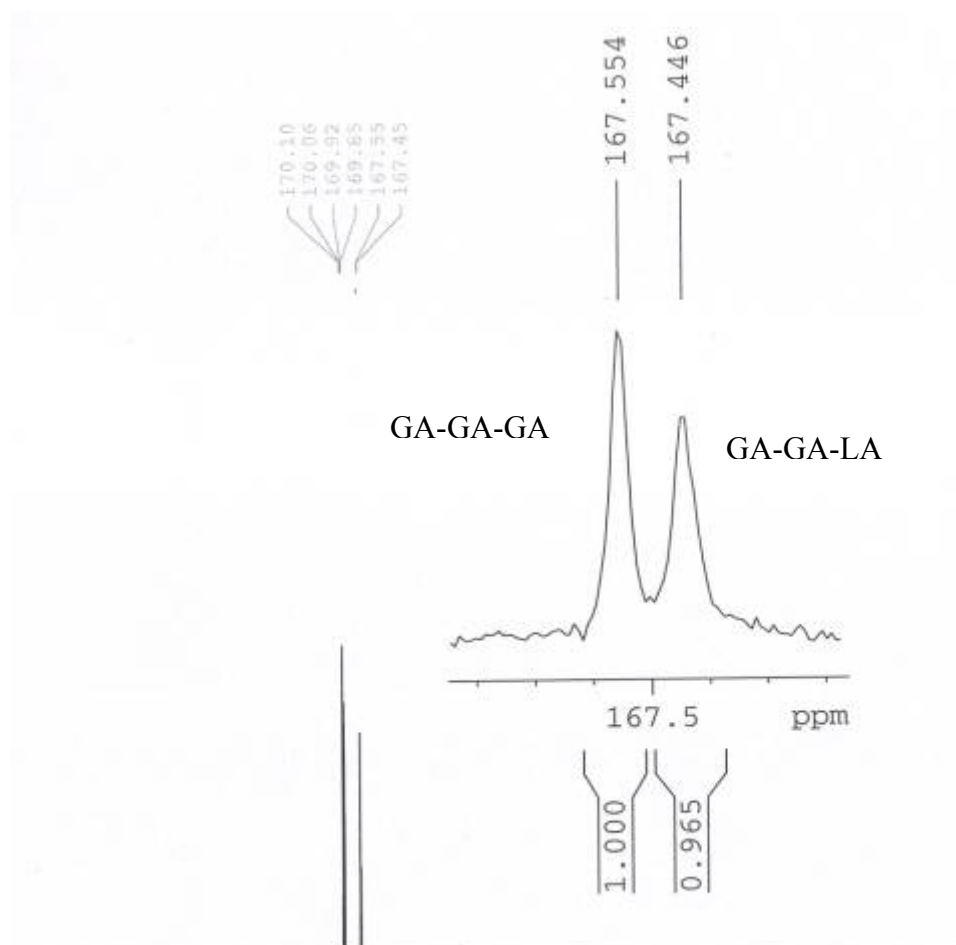


Figure 4.2 ^{13}C NMR spectra of PLGA 75/25 I.V. 0.94 and assignment of the GA carbonyl resonances; GA-LA at 167.5 ppm and GA-GA at 167.6 ppm.

The ^{13}C NMR spectroscopy was used to determine the comonomer ratio sequence distribution in the copolymers. Figure 4.2 shows the ^{13}C NMR spectrum obtained for as-received PLGA 75/25 I.V. 0.94 polymer granules. The two peaks at 167.6 and 167.5 ppm were from the carbonyls of the glycolic acid (GA) unit of the copolymer in specific environments of GA-GA-GA and GA-GA-LA (lactic acid unit), as reported by Avgoustakis *et al*²⁷. The R_{cms} calculated using equation 3.4 for the above polymer was 0.97, which was very close to 1, indicating a very low degree of blockiness for the copolymer²⁹. The PLGA 75/25 I.V. 0.94 should thus be considered a homogeneous copolymer. Due to its high molecular weight ($\sim 130,000$ dalton), the polymer was probably synthesized through ring opening polymerization of the appropriate cyclic dimers. The higher reactivity of the glycolic acid compared with L- (or D-) lactic acid during the ring opening polymerization would give the PLGA 75/25 I.V. 0.94 a segregated structure instead of a random structure.

The additional resonances near 166 ppm representing the LA-GA-LA and LA-GA-GA arrangements claimed by Avgoustakis *et al*²⁷ were missing in this spectrum. The results obtained here corresponded to the results observed by Bernix²⁸ and M Jesus Dorta *et al*²⁹.

The ^{13}C NMR spectra of the other as-received polymer granules, were similar to PLGA 75/25 I.V. 0.94, where the two distinct peaks at 167.6 and 167.5 ppm were observed in all samples. There were no additional resonances near 166 ppm observed.

The R_{cms} calculated for all these PLGA polymers were listed in Table 4.4.

Sample	LA:GA ratio	I.V.	Int _{GA-LA} (167.5ppm)	Int _{GA-GA} (167.6ppm)	$R_{cms} = \frac{Int_{GA-LA}}{Int_{GA-GA}}$
As-received PLGA granules	75:25	0.94	0.965	1.000	0.97
		0.24	0.641	1.000	0.64
	50:50	0.50	0.498	1.000	0.50
		0.22	0.634	1.000	0.63

Table 4.4 R_{cms} of PLGA microspheres

The PLGA 50/50 I.V. 0.50 had the lowest R_{cms} thus the highest degree of heterogeneity or blockiness of the copolymer. On the other hand, PLGA 75/25 I.V. 0.94 had a R_{cms} close to 1, indicating a homogeneous copolymer.

The degree of blockiness was related to the mean block length of the copolymer directly. A low degree of blockiness corresponded to short mean block length of the copolymer, whereas a high degree of blockiness corresponded to long mean block length of the copolymer. For the same PLGA with different degree of blockiness, the long mean block length means the long GA-GA or LA-LA chains. It is believed that the hydrolytic random chain scission between GA-GA bonds was much easier than the hydrolytic random chain scission occurring between the LA-LA bonds and GA-LA bonds. This was due to the methyl group in the lactic acid, which made lactic acid more hydrophobic than glycolic acid. Thus for the PLGA with the same molecular weight and same LA to GA ratio, the molecular weight of the PLGA with a higher degree of blockiness was likely to decrease faster at the beginning, and generated crystallinity at the later stages of hydrolytic degradation. The PLGA with a low degree of blockiness on the other hand, would tend to maintain the amorphous state during the later stages of hydrolytic degradation and the molecular weight would not drop as dramatically during the first stages of hydrolytic degradation. The PLGA with a lower degree of blockiness is believed to have more GA-LA connectors than the PLGA with a higher degree of blockiness. Ease of chain scission: GA-GA > GA-LA > LA-LA.

In the case of PLGA 75/25 I.V. 0.94, it was a homogeneous copolymer and had the lowest degree of blockiness or highest number of GA-LA bonds compared with the rest of the PLGA polymers investigated. Hence its molecular weight was expected to decrease slowly during the initial stages of hydrolytic degradation and the polymer would remain amorphous during the later stages of hydrolytic degradation. The PLGA 50/50 I.V. 0.50 had the highest degree of blockiness. Hence the molecular weight was expected to decrease rapidly at the beginning of degradation followed by crystallization of the shortened chains due to chain scission at the later stages of hydrolytic degradation. In the case of PLGA 75/25 I.V. 0.24 and PLGA 50/50 I.V. 0.22, both had the same degree of blockiness and very similar intrinsic viscosity. The higher concentration of LA units in PLGA 75/25 compared with PLGA 50/50 would increase the hydrolytic degradation rate of PLGA 50/50 compared with the PLGA 75/25. The higher reactivity of poly (glycolic acid) as compared to poly (lactic acid) was because the GA unit was more hydrophilic in nature than the LA unit. Furthermore, the methyl group in the lactic acid hindered the attack of water on the polymer backbone.

4.2 Size distribution of microspheres

Particle size has been reported to affect the hydrolytic degradation rate of PDLA microspheres⁵¹ where the larger the particle size, the faster the rate of degradation. Hence the particle size for pure and GCV-loaded microspheres was kept constant at around $110 \pm 20 \mu\text{m}$ by changing the concentration of polymer/DCM solution while forming the emulsion. The effects of LA to GA ratio and molecular weight on the hydrolytic degradation and drug release profile were investigated in this research.

The concentration of the polymer was found to affect the particle size and their size distribution. A decrease in polymer concentration decreased the particle size and

narrowed the size distribution, as shown in Table 4.5. The higher polymer concentration resulted in the higher viscosity, where more mechanical force was needed to break down the more viscous polymer/DCM oil phase compared to the less viscous polymer/DCM oil phase found in lower polymer concentration. Since the stirring speed was fixed at 1000 rpm, the mechanical force exerted on the emulsion was fixed. Hence the more viscous polymer/DCM oil phase resulted in larger particle size and broader size distribution.

Concentration (g/ml)	Mass of PLGA used (g)	Vol of DCM (cm ³)	Size of particles (μm)
0.025	0.25	10	24 ± 6
0.050	0.50	10	58 ± 8
0.100	1.00	10	125 ± 11
0.150	1.50	10	268 ± 16
0.200	1.0	5	870~1020*

Table 4.5: Size of PLGA Microspheres varies directly with polymer concentration.

*Measurements were made using polarizing microscope.

Figure 4.3 showed the distribution of pure PLGA 75/25 I.V. 0.94 microspheres obtained using the laser particle analyzer.

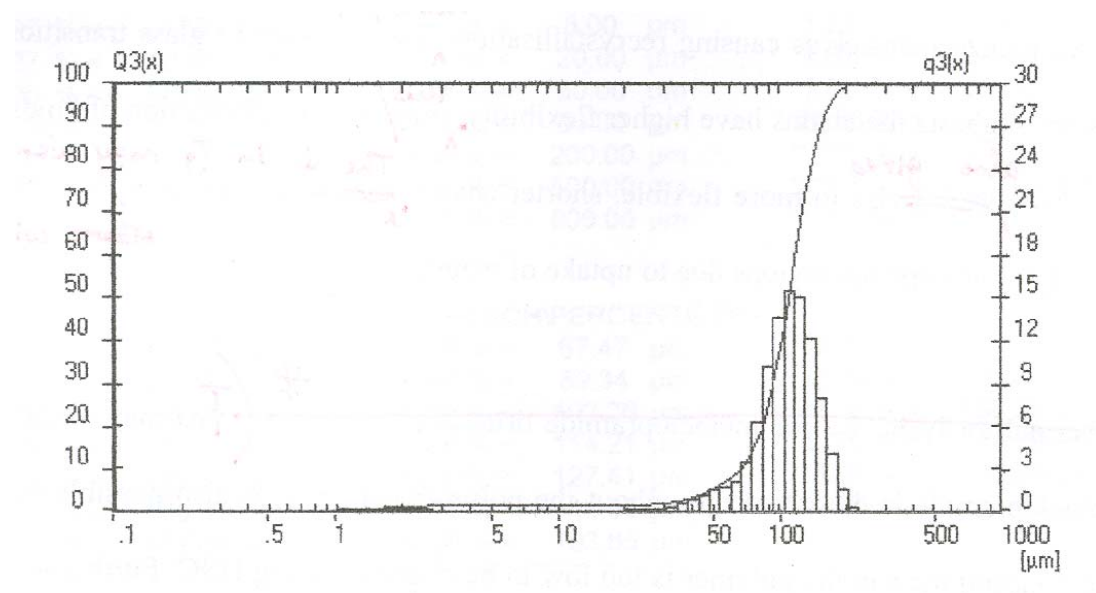


Figure 4.3 Size Distribution of PLGA 75/25 I.V. 0.94 microspheres

A single peak with a maximum distribution was observed at $110 \pm 11 \mu\text{m}$. The other pure and GCV-loaded microspheres had similar uni-modal distribution and their sizes were in the range of $90 \mu\text{m}$ to $130 \mu\text{m}$. It has been reported that by increasing the emulsification speed, there is both a decrease in the particle size and a narrowing of the size distribution¹⁰⁹. Here the emulsification speed was kept at a constant 1000 rpm during sample preparation.

The ganciclovir-loaded microspheres ($89.77 \mu\text{g}$ ganciclovir/mg) injected by Amadeo *et al*¹⁸ was in the size range of 300 to $500 \mu\text{m}$ into the eyes of rabbits inoculated with human cytomegalovirus. Here microspheres of 90 to $130 \mu\text{m}$ with similar GCV payload were successfully prepared. Even smaller sized microspheres ($< 20 \mu\text{m}$) were made, but these microspheres had a porous surface with very low GCV payload of $4.13 \mu\text{g}$ ganciclovir/mg. GCV is a polar hydrophilic compound with a solubility of 2.6 mg/ml in water at $25 \text{ }^\circ\text{C}$ ⁹³. During the formation of microspheres of $< 20 \mu\text{m}$, before the GCV particles could be dispersed in the polymer matrix, the GCV particles would have dissolved in the aqueous PVA. To prepare these small sized microspheres, higher mechanical force was required by using the homogenizer. As the GCV particles were dispersed in the polymer/DCM oil phase by the fast stirring speed, dissolution of GCV in the aqueous phase would occur. Furthermore, the large surface area of these microspheres resulted in fast dissolution of GCV from the surface of the microspheres, giving rise to the porous surface and low drug loading.

4.3 Pure microspheres

The T_g values of the pure microspheres were similar to the T_g values of their corresponding as-received polymer granules, as shown in Table 4.2. The same could be

said for the initial molecular weight and polydispersity index of the pure microspheres. These values were similar to those of as-received polymer granules, as shown in Table 4.3. Hence the oil-in-water emulsification technique used in the preparation of microspheres did not affect the morphology or initial molecular weight of the polymers.

SEM photographs were taken for the pure microspheres. Figure 4.4 showed the SEM photograph of PLGA 50/50 I.V. 0.50 microspheres before degradation. The pure microspheres were spherical in shape with a smooth surface. The rest of the PDLLA I.V. 0.22, PLGA 75/25 I.V. 0.94, PLGA I.V. 0.24 and PLGA 50/50 I.V. 0.22 microspheres before degradation were also spherical in shape with smooth surfaces, similar to the PLGA 50/50 I.V. 0.50 microspheres.

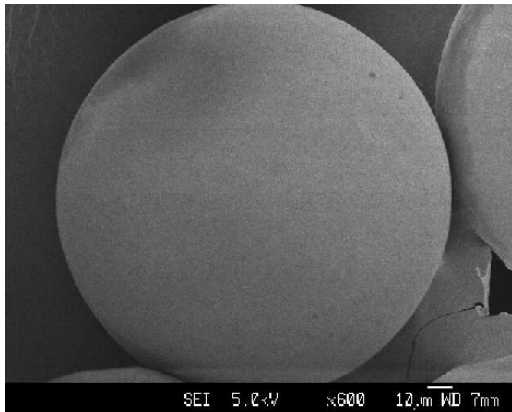


Figure 4.4 SEM photographs of PLGA 50/50 I.V. 0.50 microspheres before degradation.

4.4 GCV-loaded microspheres

4.4.1 MDSC

Sample	LA:GA ratio	I.V.	Synonym	T _g (°C)
PDLLA	100:0	0.22	PDLLA I.V. 0.22 5% GCV	47 ± 2
PLGA	75:25	0.94	PLGA 75/25 I.V. 0.94 7% GCV	51 ± 2
			PLGA 75/25 I.V. 0.94 18% GCV	54 ± 5
	50:50	0.24	PLGA 75/25 I.V. 0.24 5% GCV	43 ± 3
			PLGA 50/50 I.V. 0.50 5% GCV	41 ± 3
		0.50	PLGA 50/50 I.V. 0.50 20% GCV	41 ± 2
			0.22	PLGA 50/50 I.V. 0.22 7% GCV

Table 4.6 Glass Transition Temperature (T_g) of the GCV-loaded microspheres prepared.

The incorporation of GCV did not affect the glass transition temperatures of the polymers. Table 4.6 showed the T_g values of the GCV-loaded microspheres, which were similar, within experimental error, to the T_g values of as-received polymer granules.

4.4.2 GPC

The initial molecular weights and polydispersity index of the polymers were not affected by the incorporation of GCV. The initial molecular weight and polydispersity index values were similar, within experimental error, to the as-received polymer granules as shown in Table 4.3.

4.4.3 SEM

The GCV particles had a needle shaped structures as shown in Figure 4.5 A. The SEM photographs for the GCV-loaded microspheres before degradation were spherical and had a smooth surface, showing no GCV particles adsorbed on the surface. Hence GCV was incorporated inside the microspheres and would be released when the microspheres degraded. Figure 4.5 B showed the SEM photograph of PLGA 75/25 I.V. 0.94 microspheres with 7 % of GCV by weight.

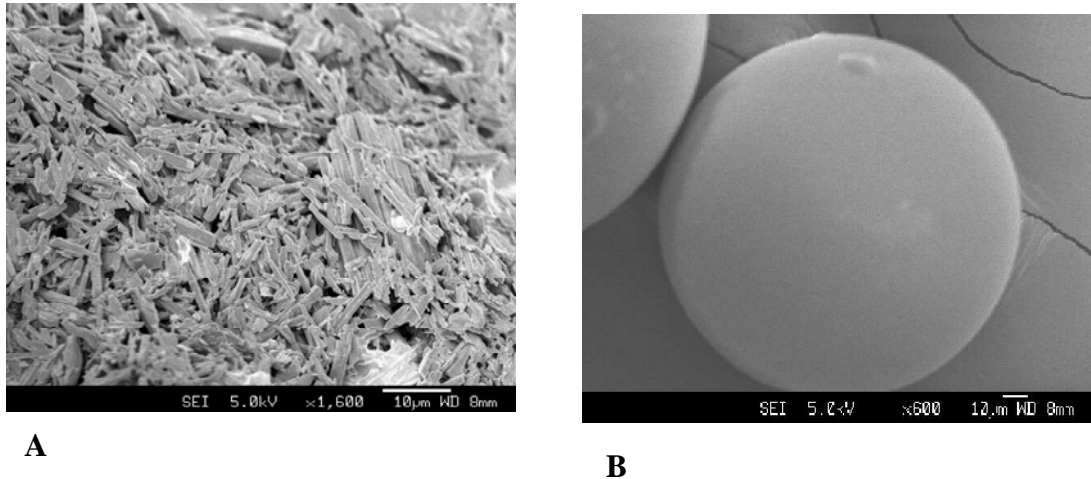


Figure 4.5 SEM photographs of A) GCV; B) PLGA 75/25 I.V. 0.94 7% GCV microspheres.

Chapter 5 and Chapter 6 investigated the degradation profiles of the pure microspheres and drug-loaded microspheres respectively. A correlation between the hydrolytic degradation of the polymers and the drug release profiles was obtained and the suitability of these microspheres as intraocular drug delivery device was discussed in the following chapters.

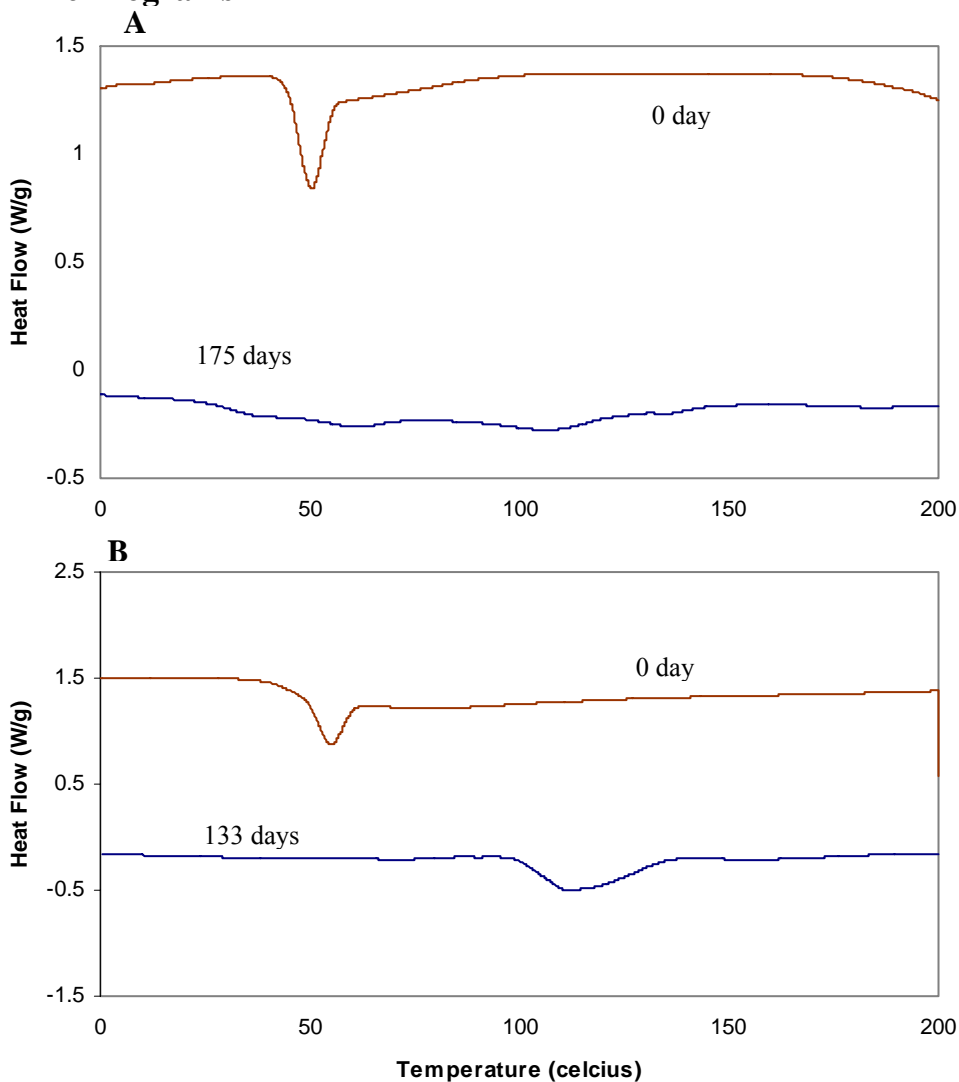
CHAPTER 5

HYDROLYTIC DEGRADATION OF BLANK MICROSPHERES

Pure microspheres of PDLGA and PLGA at different LA to GA ratio and molecular weights were degraded in phosphate buffered solution (pH=7.0) at 37°C for various length of time. Sample preparation and characterization using DSC, GPC, SEM, pH meter have been discussed in detail in Chapter 3.

5.1 Modulated Differential scanning calorimetry (MDSC)

5.1.1 Thermograms



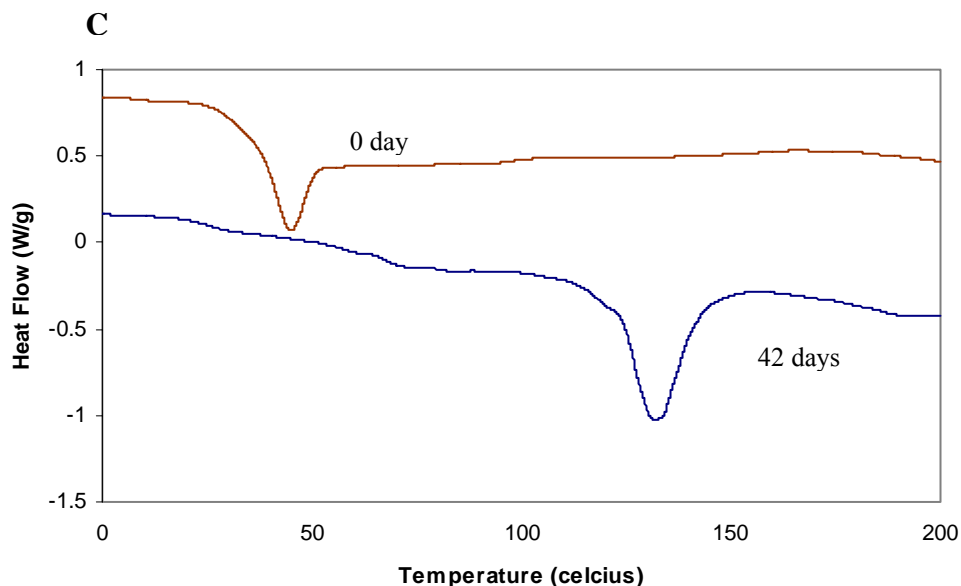


Figure 5.1 Thermograms of A) PDLLA I.V. 0.22 microspheres before degradation and after 175 days of degradation; B) PLGA 75/25 I.V. 0.94 microspheres before degradation and after 133 days of degradation and C) PLGA 50/50 I.V. 0.50 microspheres before degradation and after 42 days of degradation in phosphate buffered solution at 37 °C, Exotherm up.

All the DSC thermograms obtained were from the first heating cycle, which illustrated the thermal history of the samples. The undegraded microspheres were amorphous in nature, thus no melting peaks were observed in the 0 day samples.

All the undegraded microspheres exhibited a sharp endothermic peak at their T_g as shown in the MDSC thermograms of PDLLA and PLGA microspheres in Figure 5.1. This peak is related to the polymer chain relaxation kinetics in response to the thermal scanning rate. Since the glass transition is a kinetic phenomenon, which involves the polymer viscoelasticity, it is affected by experimental conditions such as heating rate and previous thermal history of the sample.

The degradation of PDLLA and PLGA involves chain scissions of ester bond linkages in the polymer backbone by hydrolytic attack of ester groups⁴. As the samples degraded, a melting peak appeared above the glass transition temperature in the initially amorphous PLGA 75/25 I.V. 0.94 and PLGA 50/50 I.V. 0.50 microspheres, as shown in Figures 5.1

B and C. However, no melting peaks were observed in the degraded PDLLA I.V. 0.22 (Figure 5.1 A), PLGA 75/25 I.V. 0.24 and PLGA 50/50 I.V. 0.22 microspheres.

These melting peaks were generated by the crystallization of degradation products trapped in the microspheres. As proven by ^{13}C NMR spectra in Chapter 4, all the PLGA copolymers had more or less some degree of blockiness. Since the ester bonds linking the glycolic acid units, GA-GA, and glycolic-lactic acid, GA-LA, have high reactivity with water and/or greater hydrophilicity¹¹⁰ compared with those of lactic-lactic acid (LA-LA) linked ester, this would lead to a preferential hydrolytic scission of GA-GA and GA-LA linked ester bonds. As a result, stereoregular and crystallizable D- or L-lactic acid oligomers, along with stereo-complex of D- and L-helical structures¹¹¹ are produced. The formation of these crystallizable oligomers with enriched D- or L-lactic acids in their sequence of polymer backbone gave rise to the melting endotherms observed in the long term degraded samples. Hence the appearance of melting endotherms with degradation time was believed to be due to the low-molecular-weight crystallizable polymer domain. The ^{13}C NMR results showed that PLGA 50/50 I.V. 0.50 had the highest degree of blockiness among the polymers investigated, and it was a heterogeneous copolymer. As a result, it was able to generate crystallizable oligomers as the polymer degraded, giving rise to the melting endotherm as shown in the 42 days degraded samples in Figure 5.1 C.

PLGA 75/25 I.V. 0.94 was a homogeneous copolymer and was expected to maintain its amorphous structure even during the later stages of hydrolytic degradation. However, a small and broad endotherm just above 100 °C was observed in samples after 133 days of degradation (Figure 5.1 B). This could be due to the crystallization of enriched D- or L-lactic acid chain segments left behind after the hydrolytic scission of the more hydrophilic glycolic acid units in the polymer chains.

As for the pure PDLA, no melting peak was observed even after 175 days of hydrolytic degradation (Figure 5.1A). This suggested that the chain segments formed were still stereo-complex of D- or L-lactic acids instead of crystallizable chain segments with enriched D- or L-lactic acids.

It was observed that crystallization of chain segments during the later stages of hydrolytic degradation of initially amorphous PLGA and PDLA polymers, was dependent on several factors. The existence of both D- and L-lactic acids in the polymer discouraged crystallization. Hence the absence of melting peaks in degraded PDLA I.V. 0.22 samples. Long chain heterogeneous polymer with a high degree of blockiness was able to generate crystallinity during later stages of hydrolytic degradation, as in the case of PLGA 50/50 I.V. 0.50. As for PLGA 50/50 I.V. 0.22 and PLGA 75/25 I.V. 0.24, both had the same degree of blockiness and were of lower degree of blockiness and molecular weight compared to PLGA 50/50 I.V. 0.50. Crystallization of chain fragments was not observed for these two copolymers during the later stages of hydrolytic degradation. This would suggest that the oligomers formed were stereo-complex of D- or L-lactic acids instead of crystallizable oligomers with enriched D- or L-lactic acids chain segments.

5.1.2 Glass transition temperature, T_g

The T_g was used to follow the hydrolytic degradation rate of the polymers. Figure 5.2 showed the changes in the glass transition temperatures of the PLGA 75/25 microspheres of I.V. 0.94 and I.V. 0.24 before and after exposure to PBS solution of pH 7.

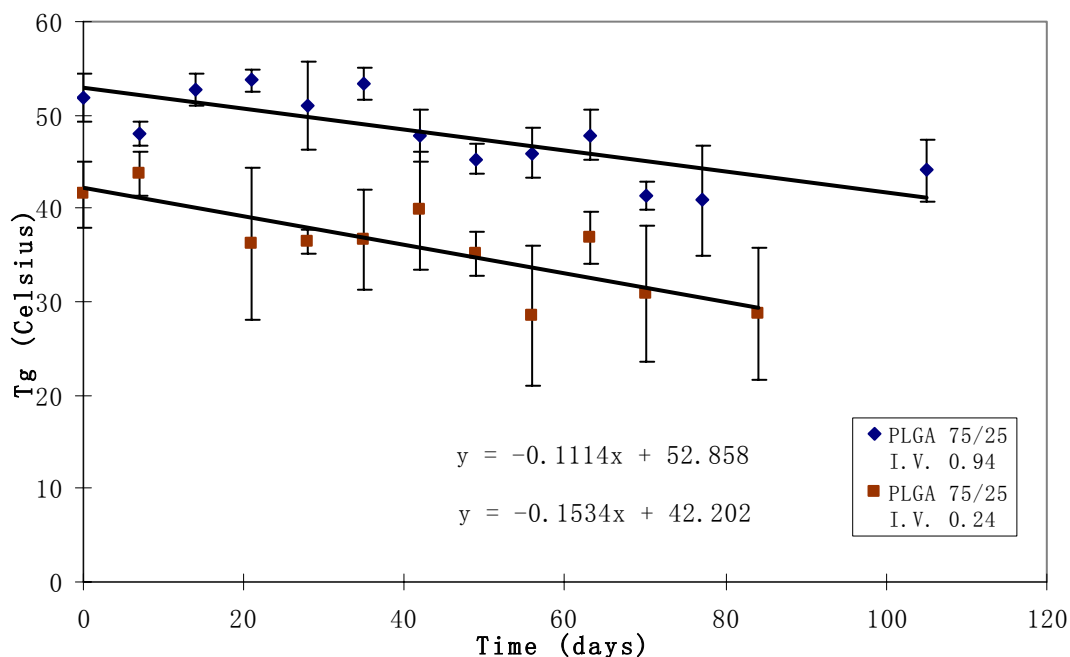


Figure 5.2 Glass transition temperatures (T_g) as a function of degradation time for PLGA 75/25 I.V. 0.94 (◆) and PLGA 75/25 I.V. 0.24 (■) microspheres degraded in phosphate buffered solution at 37 °C.

The PLGA 75/25 I.V. 0.94 had a higher molecular weight than the PLGA 75/25 I.V. 0.24. Hence the T_g for PLGA 75/25 I.V. 0.94 was larger than the T_g of the copolymer with the lower molecular weight. The decrease in T_g is proportional to the decrease in the molecular weight of polymer according to the Fox-Flory equation¹⁰⁷. The T_g for both the polymers decreased with degradation time. A straight line was fitted to each set of T_g values and the corresponding linear regression equations were as shown in Figure 5.2. The slope was used to compare the rate of change in the T_g , where steeper the slope, the faster the rate of hydrolytic degradation. From the linear fitting equations, the rate at which the T_g decreased for PLGA 75/25 I.V. 0.24 was slightly higher than that of PLGA 75/25 I.V. 0.94, indicating PLGA 75/25 I.V. 0.24 degraded faster than PLGA 75/25 I.V. 0.94. This was due to the difference in molecular weight and degree of blockiness of the polymers. PLGA 75/25 I.V. 0.24 had a lower molecular weight and higher degree of blockiness than PLGA 75/25 I.V. 0.94. The lower molecular weight meant shorter chain lengths and the higher degree of blockiness meant more GA-GA units in the polymer

backbone. These two factors would increase the hydrolytic degradation rate of PLGA. Hence PLGA 75/25 of I.V. 0.24 degraded faster than PLGA 75/25 of I.V. 0.94.

The T_g of PLGA 75/25 I.V. 0.94 remained above the degrading medium temperature (37 °C) even after 105 days of degradation, indicating that the polymer was in a glassy state throughout the time frame investigated. This glassy state “protected” the polymer from hydrolysis as all short-term chain motions were frozen. The same was observed in PLGA 75/25 I.V. 0.24. The T_g was above 37 °C up to 56 days of degradation. During this time, the polymer chains were less susceptible to hydrolysis. After 56 days of degradation, the T_g dropped below 37 °C and the polymer underwent a transition from glassy to rubbery state, which would further accelerate the degradation process. However, no obvious signs of increased rate of decrease of T_g after 56 days of hydrolytic degradation was observed in Figure 5.2. This may be due to the LA-LA and GA-LA bonds being the majority bonds left behind during the later stages of degradation, which could slow down the rate of hydrolytic degradation despite the polymer’s transition from glassy to rubbery state.

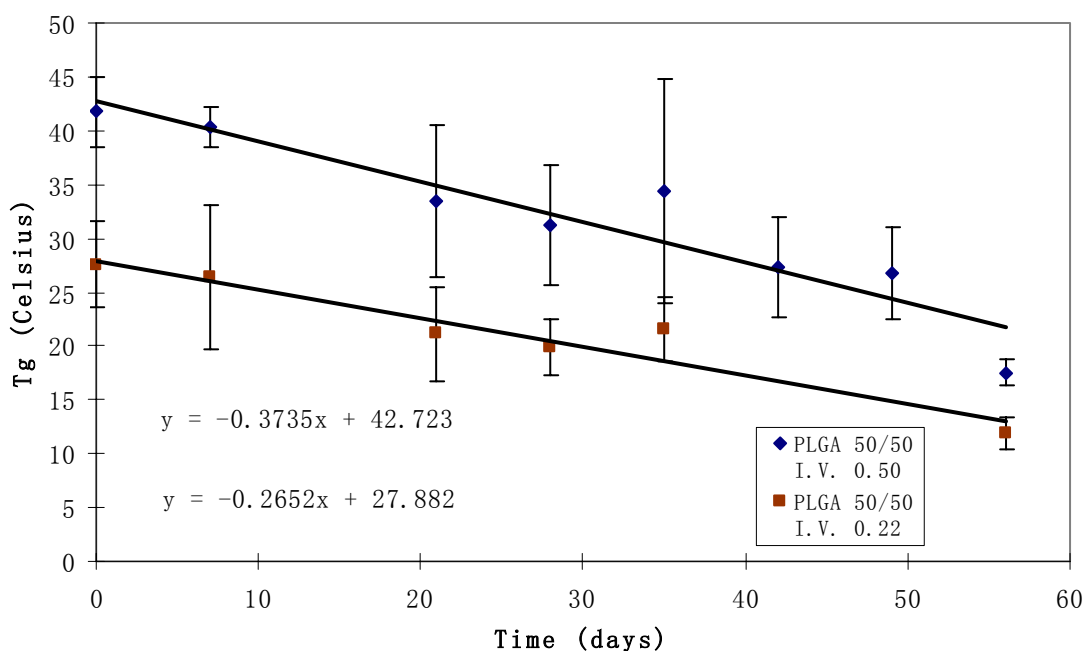


Figure 5.3 Glass transition temperatures (T_g) as a function of degradation time for PLGA 50/50 I.V. 0.50 (◆) and PLGA 50/50 I.V. 0.22 (■) microspheres degraded in phosphate buffered solution at 37 °C.

In the case of PLGA 50/50 microspheres, the T_g also decreased with degradation time as shown in Figure 5.3. The rate of change in T_g is higher for PLGA 50/50 I.V. 0.50 than PLGA 50/50 I.V. 0.22 indicating a faster degradation rate for PLGA 50/50 I.V. 0.50 than PLGA 50/50 I.V. 0.22. This was surprising as PLGA 50/50 I.V. 0.50 had higher initial molecular weight than PLGA 50/50 I.V. 0.22. Furthermore, The T_g of the PLGA 50/50 I.V. 0.22 was below the temperature of the degradation medium (37 °C) throughout the time investigated, as observed in Figure 5.3. The polymer was in the rubbery state during the time investigated. It was only after 21 days of degradation, the T_g of the PLGA 50/50 I.V.0.50 dropped to below 37 °C and was in the rubbery state. Hence PLGA 50/50 I.V. 0.50 was expected to degrade slower than PLGA 50/50 I.V. 0.22. However PLGA 50/50 I.V. 0.50 had a higher degree of blockiness compared to PLGA 50/50 I.V. 0.22. This could increase the hydrophilicity of the polymer, as there were longer GA-GA units in the polymer backbone. This in turn increased the rate of water uptake, which led to faster degradation rate. This suggested that the degree of blockiness had a larger effect on the hydrolytic degradation than the initial molecular weight.

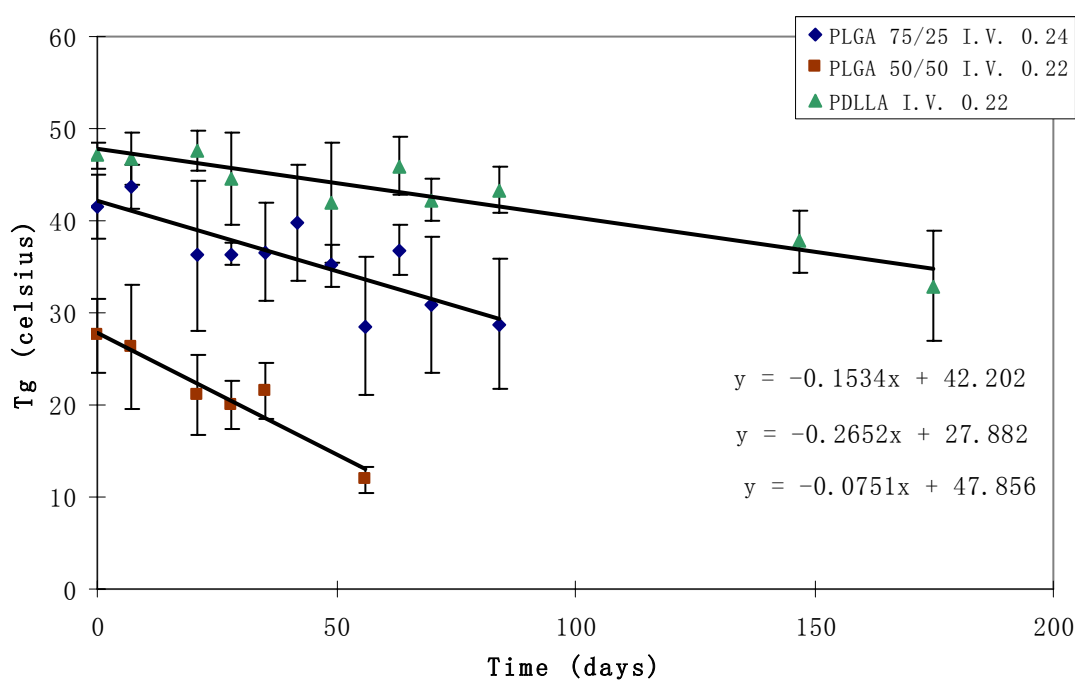


Figure 5.4 Glass transition temperatures (T_g) as a function of degradation time for PLGA 75/25 I.V. 0.24 (◆), PLGA 50/50 I.V. 0.22 (■) and PDLLA I.V. 0.22 (▲) microspheres degraded in phosphate buffered solution at 37 °C.

Figure 5.4 shows the change in the glass transition temperatures with degradation time for polymers with similar I.V. but different LA to GA ratios before and after exposure to PBS solution at pH 7 at 37 °C. The PLGA 50/50 I.V. 0.22 degraded the fastest, followed by PLGA 75/25 I.V. 0.24. The PDLLA I.V. 0.22 degraded the slowest. Since PLGA 50/50 I.V. 0.22 and PLGA 75/25 I.V. 0.24 had the same degree of blockiness, this might suggest the LA to GA ratio played a more significant role in the hydrolytic degradation rate compared to other factors such as degree of blockiness and initial molecular weight.

Poly (D,L-lactic acid) and poly (D,L-lactic-co-glycolic acid) are amorphous polymers. Changes in the hydrophilic/lipophilic balance as well as steric effects are responsible for the changes in the degradation rate of PLGA. A polymer built from two monomers A and B, for example, contains four types of bonds: A-A, B-B, A-B and B-A. This has some significance on the hydrolysis rate of the polymer, when these bonds have different hydrolysis rates. It is noteworthy that there is no linear relationship between the ratio of glycolic acid to lactic acid and the physico-mechanical properties of the corresponding copolymers. PLGA polymers containing 50:50 ratio of lactic and glycolic acids have been reported to hydrolyze much faster than those containing higher proportion of either of the two monomers^{2,32}. This phenomenon was also observed here (Figure 5.4), where PLGA 50/50 degraded the fastest, followed by PLGA 75/25 and PDLLA.

This decrease in T_g with degradation time was due to loss of amorphous material arising from hydrolytic scission of the polymer chains. Since the polymers used were amorphous in nature, water was able to penetrate easily into the polymer matrix because of the open nature and loosely packed chains. This would in turn decrease the T_g due to plasticization of the amorphous material. The hydrophilic/lipophilic balance of GA and LA units would also decide the rate of water penetration into the polymer matrix. The more GA content,

the higher degree of blockiness thus the more GA-GA units in the polymer backbone made it easier for water to penetrate. This is because the GA units are more hydrophilic than the LA units.

The T_g of the polymer and its change during degradation are very important features when elucidating the underlying degradation mechanism in controlled delivery systems. If the polymer has a T_g larger than 37 °C (body temperature), the polymer will be in a glassy state in the body. Hence the mobility of the macromolecules is very slow and the free volume available for diffusion is small. As a result, the diffusion rate of drug/water through the polymer matrix is very slow. In contrast, if the polymer has a T_g less than 37 °C, the polymer is in a rubbery state when implanted in the body. Hence the macromolecules are much more mobile, and the resulting drug/water diffusion coefficient are orders of magnitude higher than in the glassy state. Hence it is important to know the glass transition temperature of the polymers and its changes with degradation time.

5.2 Gel permeation chromatography (GPC)

Figure 5.5 showed the changes in the weight-average molecular weight, M_w , as a function of degradation time.

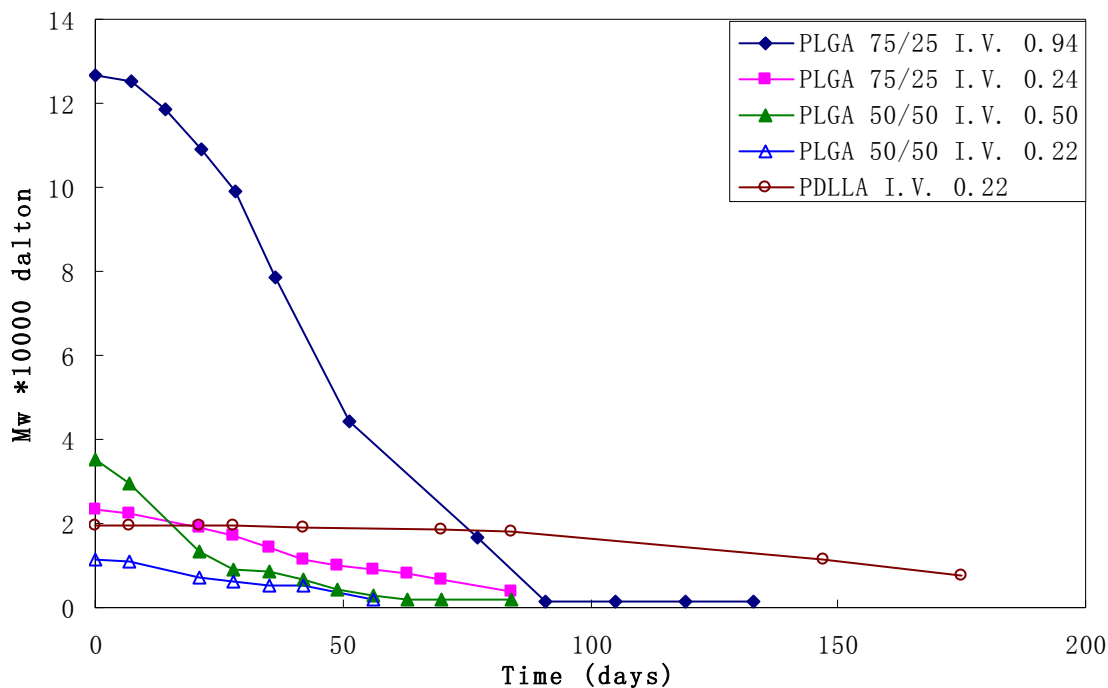


Figure 5.5 Weight-average molecular weight change of PLGA 75/25 I.V. 0.94 (◆), PLGA 75/25 I.V. 0.24 (■), PLGA50/50 I.V. 0.50 (▲), PLGA 50/50 I.V. 0.22 (△) and PDLLA I.V. 0.22 (◇) microspheres as a function of degradation time

Since the range of weight average molecular weight (M_w) for the PLGA copolymers and PDLLA was relatively broad, from around 10,000 dalton to 100,000 dalton, the normalized weight-average molecular weight (M_w/M_{w0}) was also plotted, as shown in Figure 5.6.

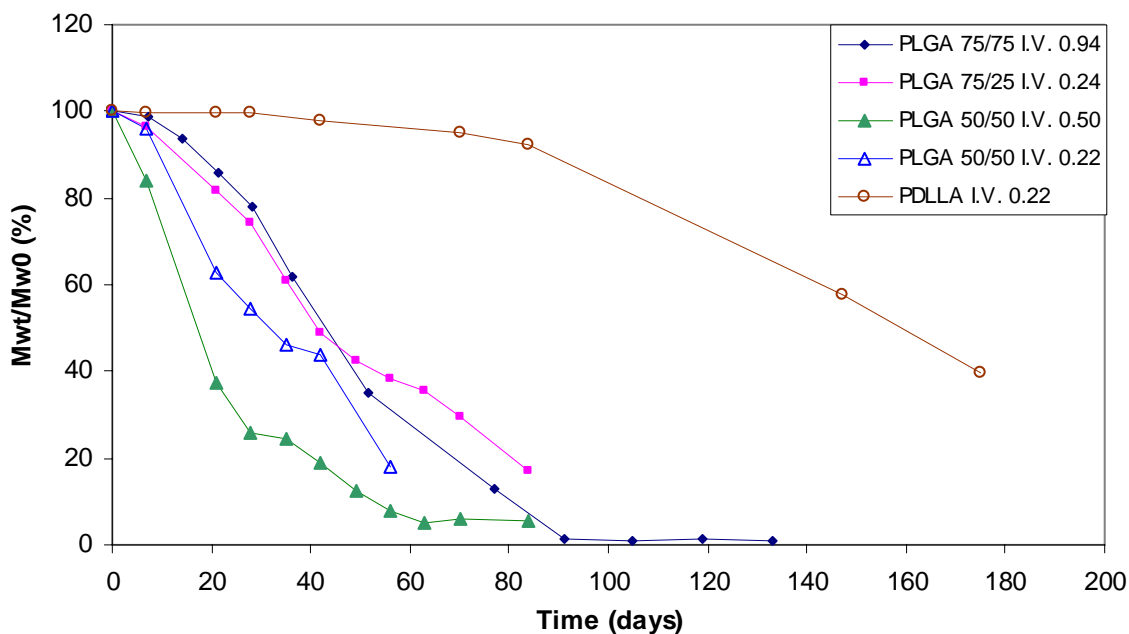


Figure 5.6 Normalized weight-average molecular weight (M_{wt}/M_{w0}) for microspheres as a function of degradation time. PLGA 75/25 I.V. 0.94 (◆), PLGA 75/25 I.V. 0.24 (■), PLGA 50/50 I.V. 0.50 (▲), PLGA 50/50 I.V. 0.22 (△) and PDLA I.V. 0.22 (◇)

It was observed that the rate of M_w decreased in the following order: PLGA 50/50 I.V. 0.50 > PLGA 50/50 I.V. 0.22 > PLGA 75/25 I.V. 0.24 \approx PLGA 75/25 I.V. 0.94 > PDLA I.V. 0.22. The decrease in molecular weight corresponded to the decrease in T_g with degradation time as observed in Figures 5.2 to 5.4.

From Figure 5.5 and 5.6, it was observed that for the polymers with similar initial I.V. of around 0.20, the lower the LA to GA ratio, the faster was the decrease of M_w with degradation time. The PDLA, with 100 % LA content, was the slowest to degrade even though it was totally amorphous and had a low initial weight-average molecular weight of 20,000 dalton. It took 175 days to decrease to 10,000 in M_w . On the other hand, PLGA 75/25 I.V. 0.94 with the highest initial weight-average molecular weight of 130,000 dalton, took 91 days to decrease to 10,000 in M_w . This suggested that the rate of hydrolytic degradation was dependent on the LA to GA ratio and that the higher the GA content, the faster was the rate of degradation. This was due to the glycolic acid inherent high reactivity with water and/or its greater hydrophilicity compared to lactic acid.

Consequently, the ester bonds linking the glycolic acid units, G-G, and glycolic-lactic acid, G-L, had high reactivity with water and/or greater hydrophilicity¹¹⁰ compared with those of lactic-lactic acid (L-L) linked ester. This would lead to a preferential hydrolytic scission of G-G and G-L linked ester bonds compared with the L-L linked ester bonds.

Sample	LA:GA ratio	I.V.	Initial M_w (Dalton)	Synonym	Time for M_w to decrease to 10,000 dalton (days)
PDLLA	100:0	0.22	20,005	PDLLA I.V. 0.22	175
PLGA	75:25	0.94	130,089	PLGA 75/25 I.V. 0.94	91
		0.24	22,787	PLGA 75/25 I.V. 0.24	49
	50:50	0.50	37,149	PLGA 50/50 I.V. 0.50	28
		0.22	11,058	PLGA 50/50 I.V. 0.22	21

Table 5.1: Time for Weight average molecular weight (M_w) of the PDLLA and PLGA microspheres to drop to 10,000 dalton.

It was also observed that a minimum M_w was required for the bulk stability of the microspheres. The polymers deformed and became brittle and fragmented in nature when their M_w reached about 10,000 dalton. Table 5.1 showed that the time taken for the M_w of PDLLA and PLGA microspheres to reach 10,000 dalton. It was observed that the higher the LA to GA ratio, the longer it took for the polymer to degrade to 10,000 dalton, irrespective of the initial M_w . In the copolymers of the same LA to GA ratio, the copolymers with larger I.V. took longer to degrade to 10,000 dalton compared to the ones with lower I.V. This was because the larger the I.V. or molecular weight, the longer the chain length and, therefore, more bonds had to be cleaved in order to generate water soluble oligomers or monomers to allow erosion to proceed. Hence the longer time taken for the copolymers with larger initial M_w to degrade to 10,000 dalton. With prolonged degradation, the fragments would then soften and become gel-like. By this time, the M_w was around 2,000 to 4,000 dalton. It was difficult to collect the M_w data beyond this point due to the soluble nature of the polymer.

From the M_w profile (Figure 5.5, Figure 5.6 and Table 5.1) and mass change profile (Figure 5.11), the onset of weight loss was observed when the M_w decreased to 10,000 dalton. Figure 5.7 A and B showed the natural logarithmic number average molecular weight ($\ln(M_n)$) of PDLLA and PLGA polymers before any mass loss was observed as a function of hydrolytic degradation time. From the graphs, linear plots showing a strong statistical linear correlation ($R^2 > 0.9$) were obtained. The results showed that the molecular weight of PDLLA and PLGA polymers decreased with hydrolytic degradation time. The degradation rate constants, k' , taken as the gradient of the linear plots, were summarized in Table 5.2.

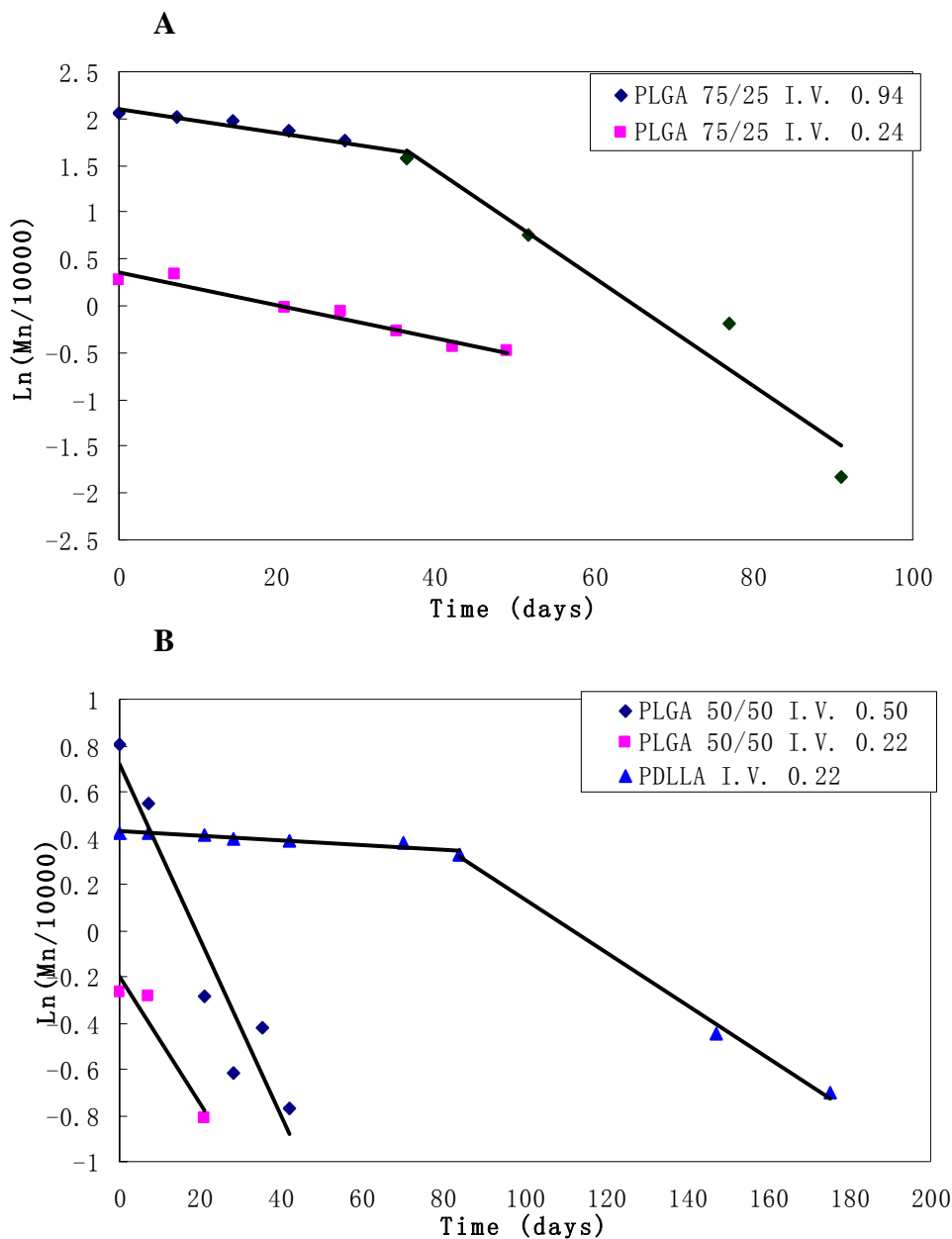


Figure 5.7 Plot of $\ln(M_n)$ of PDLLA and PLGA with hydrolytic degradation time

It was observed that for polymers which had very long degradation time frame had a combination of two different linear relationship of hydrolysis, such as PLGA 75/25 I.V. 0.94 and PDLLA I.V. 0.22.

In PDLLA I.V. 0.22, the first k' value was very close to 0, indicating very little chain scission taking place in the first 84 days of degradation. The k' value increased to 0.0115 after 84 days of degradation, which coincided with the faster drop in M_w and normalized M_w with degradation time as shown in Figure 5.5 and Figure 5.6 respectively. The initial lack of hydrolytic chain scission was due to the slow water uptake into the polymer. The inherent hydrophobic nature of LA units discouraged water absorption, thus decreasing the rate of hydrolytic chain scission.

It is believed for PLGA 75/25 I.V. 0.94, the drastic increase in hydrolysis rate after 36 days of degradation indicated auto-catalyst effect. Acidic products from the scissions of the ester bonds trapped inside the polymer matrix would increase the rate of degradation of the core in comparison to the surface of the microspheres. This is known as auto-catalysts effect^{35,50,51}.

In the case of PLGA 50/50 I.V. 0.50, PLGA 50/50 I.V. 0.22 and PLGA 75/25 I.V. 0.24, the effect of auto-catalysis was less obvious. There was only one degradation rate constant before any obvious mass loss was observed. This could be due to the much lower molecular weights compared to PLGA 75/25 I.V. 0.94, where a shorter degradation time would be required for these polymers to degrade to water soluble fragments.

Sample	LA:GA ratio	I.V.	M_{n0} (Dalton)	Synonym	Degradation rate constant k'
PDLLA	100:0	0.22	14,819	PDLLA I.V. 0.22	0.0115
PLGA	75:25	0.94	73,123	PLGA 75/25 I.V. 0.94	0.0130; 0.0576*
		0.24	12,520	PLGA 75/25 I.V. 0.24	0.0179
	50:50	0.50	22,245	PLGA 50/50 I.V. 0.50	0.0525
		0.22	7,421	PLGA 50/50 I.V. 0.22	0.0276

Table 5.2 Degradation rate constant k' of each pure polymeric microspheres.

*degradation rate constant due to auto catalyst hydrolysis.

The rate of degradation in decreasing order: PLGA 50/50 I.V. 0.50 > PLGA 50/50 I.V. 0.22 > PLGA 75/25 I.V. 0.24 > PLGA 75/25 I.V. 0.94 > PDLLA I.V. 0.22. This corresponded to the changes in T_g with degradation time (Figure 5.2 to 5.4) and the normalized M_w profile with degradation time (Figure 5.6).

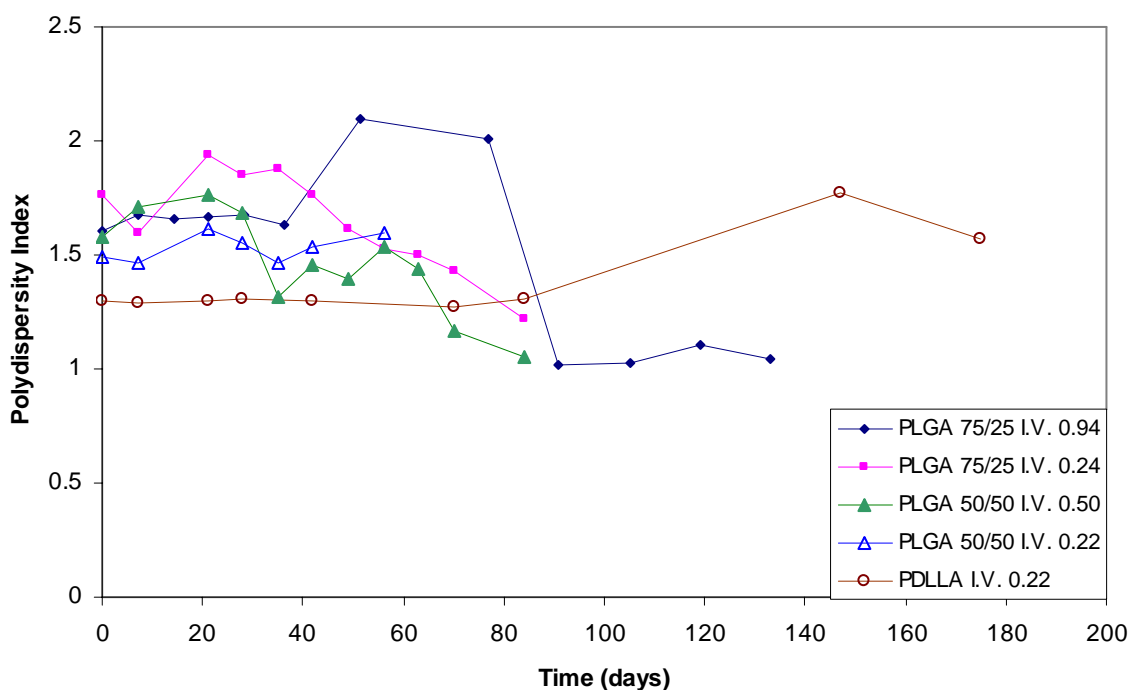


Figure 5.8 Polydispersity index (PI) of PLGA 75/25 I.V. 0.94 (◆), PLGA 75/25 I.V. 0.24 (■), PLGA50/50 I.V. 0.50 (▲), PLGA 50/50 I.V. 0.22 (Δ) and PDLLA I.V. 0.22 (◇) microspheres as a function of degradation time.

Figure 5.8 shows the changes in polydispersity index (PI) of the different microspheres with time. The PI increased first then decreased slowly with degradation time for all the polymers except for PLGA 50/50 I.V. 0.22 and PDLLA I.V. 0.22. The rate of decrease in the PI was slightly faster in the PLGA 50/50 compared with the PLGA 75/25 polymers,

which suggested the former degraded faster than the PLGA 75/25 polymers. This observation coincided with the T_g and M_w changes with degradation time.

In most of the polymers, the peak in the chromatogram broadened initially and began to narrow at longer degradation times. The initial broadening of the polydispersity index indicated a mixture of high- and low-molecular weight fractions, while the subsequent narrowing thereafter, indicated a more uniform weight fractions. These changes might be attributed to the high probability of preferential breaking of long PLGA chains during the early stages of degradation compared to the shorter chains at the later stages of degradation¹¹². There was also a sharp reduction in M_w at earlier degradation times followed by a gentle decrease in M_w at longer degradation times, as shown in Figure 5.6. Mass loss was observed when a gentle decrease in M_w at longer degradation times was observed as shown in Figure 5.10.

In the case of PDLLA I.V. 0.22, no change in the polydispersity index was observed even after 84 days of degradation. The PI increased slightly with degradation time after 84 days of degradation, indicating a broader molecular weight fraction due to the early stages of hydrolytic degradation, which resulted in a mixture of high- and low-molecular weight fractions. This coincided with the increase in the degradation rate constant (Figure 5.7) and the faster decrease in M_w (Figure 5.5) and normalized M_w (Figure 5.6) after 84 days of degradation.

5.3 Changes in pH

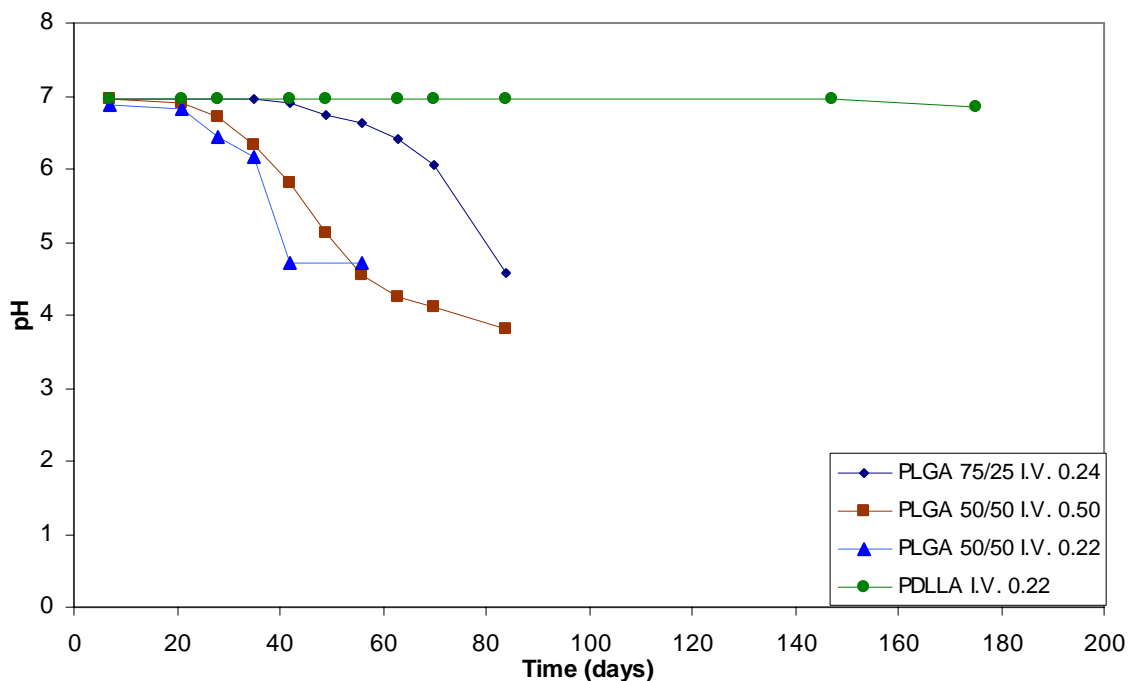
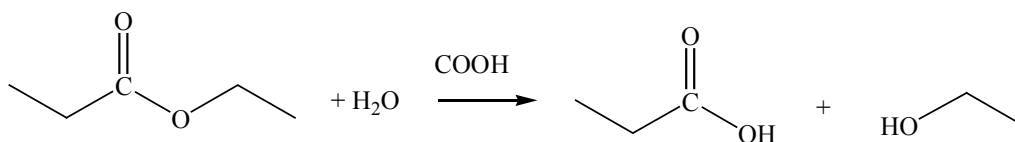


Figure 5.9 pH value of PDLLA I.V. 0.22 (●), PLGA 75/25 I.V. 0.24 (◆), PLGA 50/50 I.V. 0.50 (■) and PLGA50/50 I.V. 0.22 (▲) microspheres as a function of degradation time.

The pH values of the PBS solution were measured periodically throughout the degradation studies. The pH values were measured by a pH meter (Horiba, Kyoto, Japan, Model: D-21) and their values were plotted with respect to the degradation time, as illustrated in Figure 5.9.

The pH values of the surrounding medium for all the polymers, except for PDLLA I.V. 0.22 decreased with degradation time. The hydrolysis of ester bonds leads to the formation of monomers such as glycolic acids and lactic acids^{50,51}. The leaching of these small monomers from the polymer bulk will therefore decrease the pH of the surrounding medium.



The pH medium for the PLGA 50/50 polymers decreased much faster than the PLGA 75/25 polymers. This was due to the faster hydrolytic degradation rate of PLGA 50/50 polymers than the PLGA 75/25 polymers. GA is more hydrophilic than LA, the PLGA with higher GA ratio degraded faster than PLGA with higher LA ratio, and consequently more acidic products were produced, which decreased the pH. Furthermore, glycolic acid is more acidic than lactic acid, hence PLGA polymers with higher GA fractions decreased the pH of the surrounding medium more significantly.

The pH of the surrounding medium of PDLLA I.V. 0.22 remained approximately unchanged even after 147 days of degradation. It is believed that the sample was still in the initial stages of degradation, thus little or no acidic products were leached at this stage.

5.4 Changes in Mass

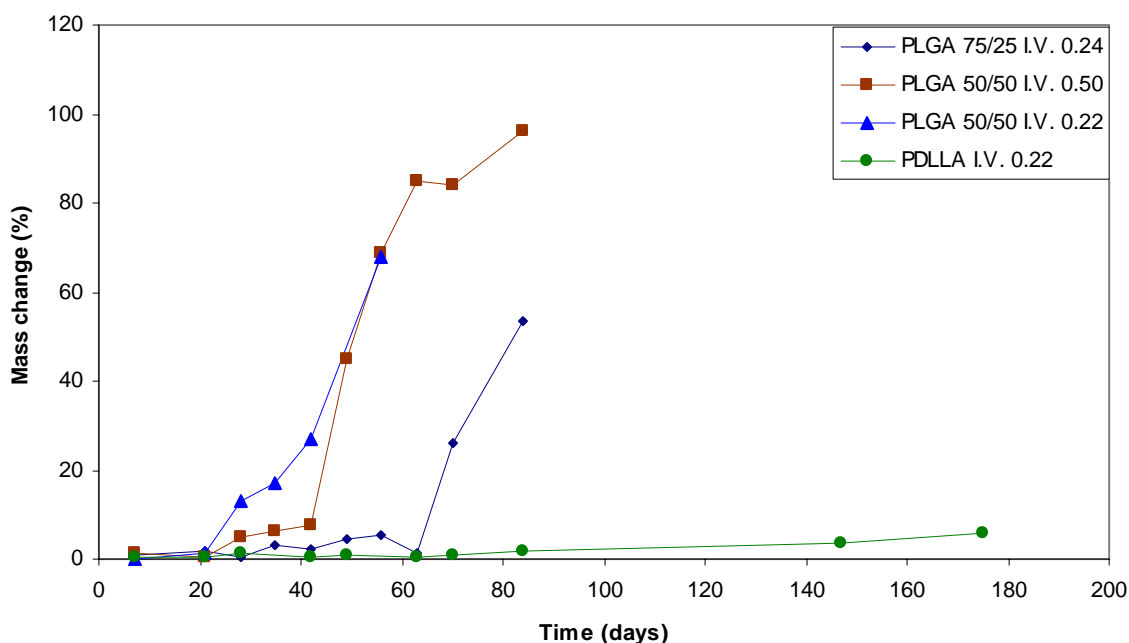


Figure 5.10 Mass change of PDLLA I.V. 0.22 (●), PLGA 75/25 I.V. 0.24 (◆), PLGA 50/50 I.V. 0.50 (■) and PLGA50/50 I.V. 0.22 (▲) microspheres as a function of degradation time.

The change in mass of the pure microspheres at different degradation times was shown in Figure 5.10. From Figure 5.10, very little mass loss was observed in all of the samples in the first 3 weeks of degradation. It was only after 3 weeks of degradation, mass loss was observed for PLGA 75/25 I.V. 0.24, PLGA 50/50 I.V. 0.50, and PLGA 50/50 I.V. 0.22 microspheres.

In the first 3 weeks of degradation, even though mass loss was negligible, the M_w of the polymers decreased with degradation time (Figure 5.5 and Figure 5.6). As water absorbed into the polymer and promoted hydrolytic chain scission, the molecular weight decreased with degradation time. This corresponded to the first and second stages of the general stages of bulk degradation profile^{34,35}. However no soluble oligomers/monomers were formed at this stage. This was supported by the lack of change in the pH of the surrounding medium (Figure 5.9).

As degradation proceeded, mass loss was observed, corresponding to the third stage in the degradation process^{34,35}, which was the loss of mass integrity which occurred when the implant had essentially no cohesive strength and began to fragment into pieces of low molecular weight polymer.

From Figure 5.5, Figure 5.6 and Figure 5.10, it was observed that a significant decrease in M_w had to occur in all the polymers before any mass loss was observed. This indicates that extensive chain scission had to take place before soluble oligomers or monomers were produced.

The degradation of PLGA involved chain scission of ester bond linkages in the polymer backbone by hydrolytic attack of water molecules. Studies on the degradation of various

PDLLA and PLGA samples showed a heterogeneous degradation mechanism^{46,113,114}. The degradation products generated in the interior of the device auto-catalytically accelerated the degradation process. This was due to an increased amount of carboxylic acid end groups, which were responsible for the faster degradation in the center of the device than at the surface.

Acidic polymeric fragments, which were formed inside the polymer mass, were unable to escape into the aqueous surrounding medium until their molecular weight was sufficiently reduced. This also explained the fact why the M_w of polymer located in the central part of the microspheres was much lower than that for polymer situated at the surface. Therefore, PLGA polymers underwent bulk degradation.

The methyl group in poly lactic acids (PLA) caused the carbonyl of the ester linkage to be sterically less susceptible to hydrolytic attack as compared to the ester linkages in poly glycolic acid (PGA). The degradation rate of PLA is also dependent on the molecular weight, degree of crystallinity, the physical geometry of the drug delivery device and the physico-chemical environment. Therefore, PLA is typically more hydrolytically stable than PGA.

5.5 SEM

SEM photographs were taken of the dried and degraded pure microspheres, as shown in Figures 5.11 to Figure 5.15.

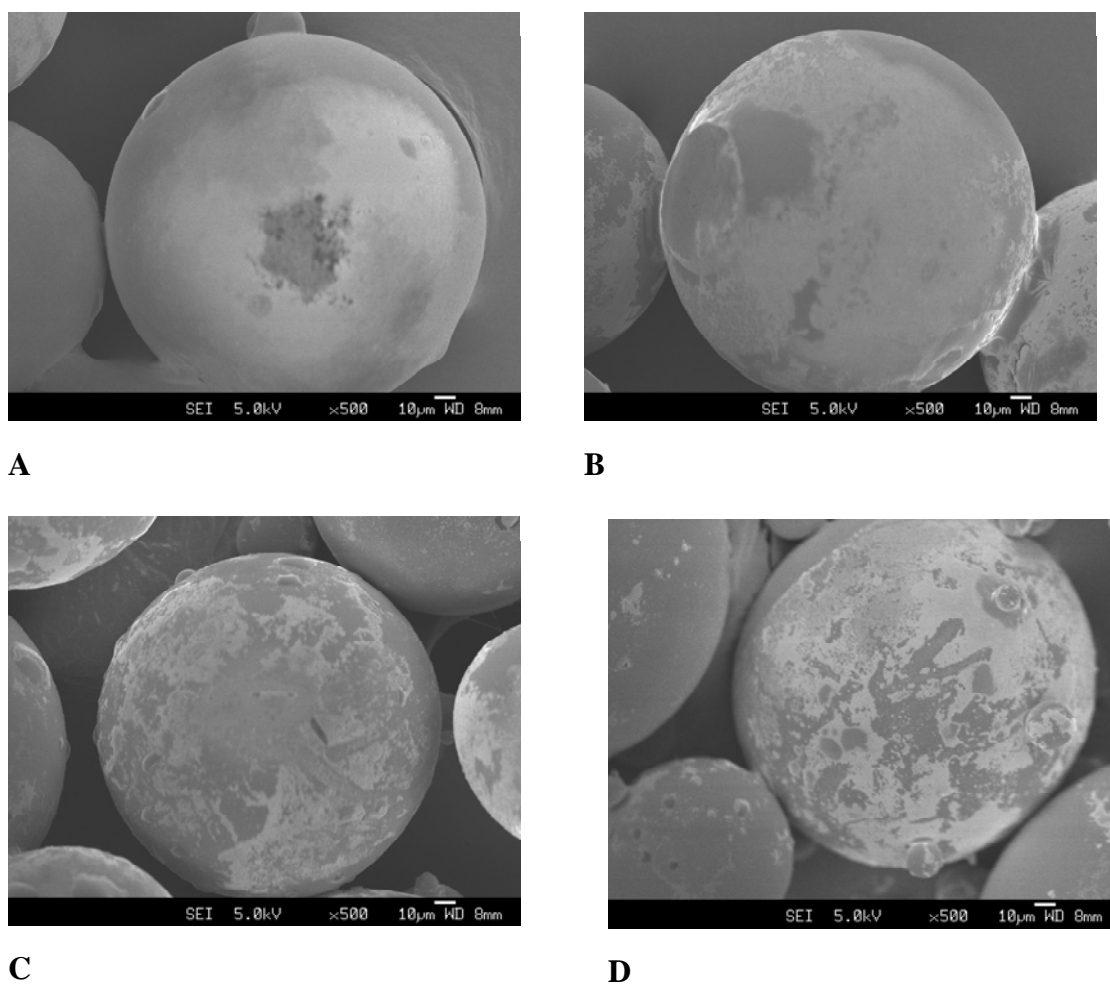


Figure 5.11 SEM photographs of PDLLA I.V. 0.22 microspheres A) 7 days; B) 21 days; C) 42 days; and D) 84 days of degradation.

After 21 days of degradation, blister-like formation was observed on the surfaces of the PDLLA I.V.0.22 microspheres as shown in Figure 5.11. The microspheres were still spherical and with little signs of degradation even after 84 days of degradation, as shown in Figure 5.11. It was only after 84 days of degradation, the M_w dropped to around 10,000 dalton (Figure 5.5) and the pH of the degrading medium (Figure 5.9) began to decrease. Mass loss was also observed at this time (Figure 5.10).

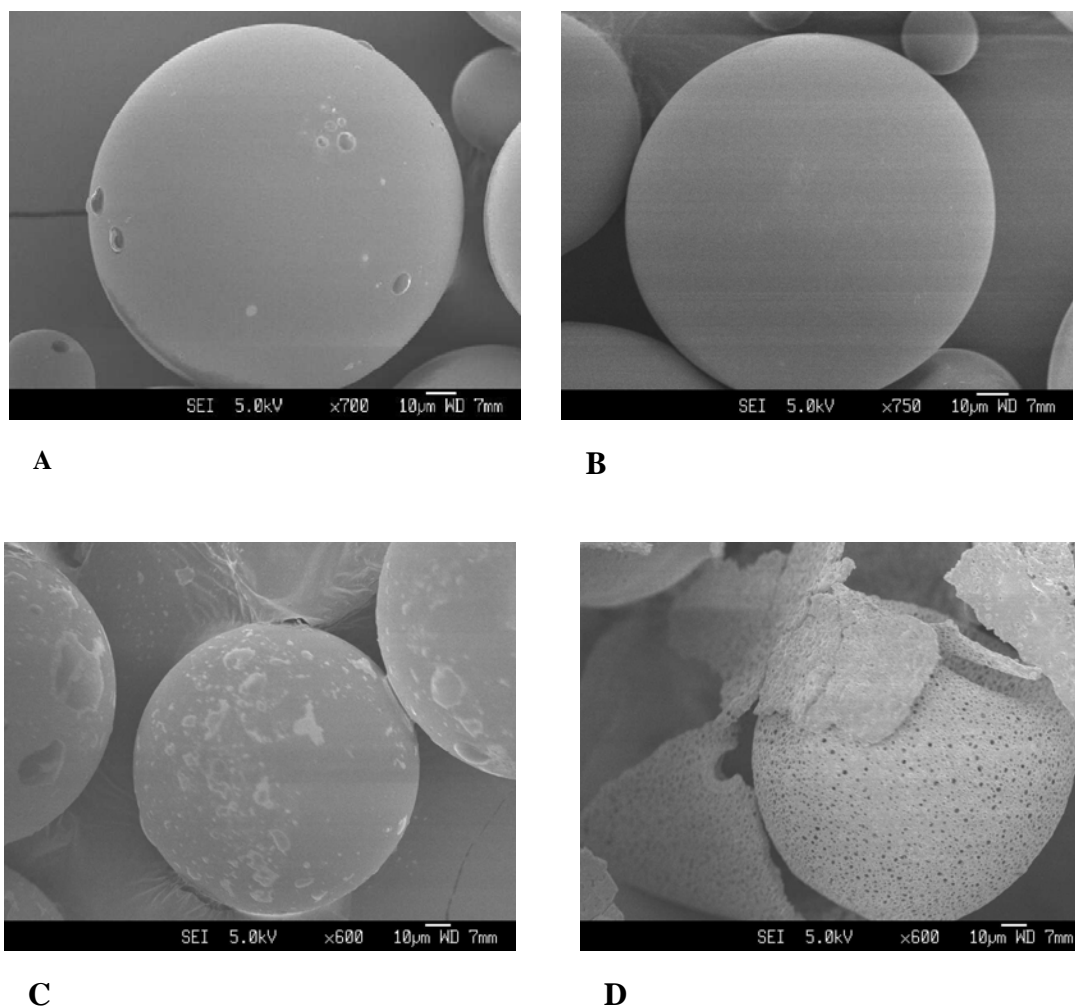


Figure 5.12 SEM photographs of degraded PLGA 75 /25 I.V. 0.94 microspheres A) 7 days; B) 35 days; C) 49 days and D) 77 days.

Figure 5.12 A) - D) showed the surfaces of the degraded pure PLGA 75/25 I.V. 0.94 microspheres. They were relatively smooth for up to about 35 days of degradation. It was only after 49 days of degradation, the microspheres showed blister-like formation on the surfaces and by 77 days, pores were observed on the surfaces. This was due to the leaching of water-soluble oligomers/monomers into the incubation medium. Depolymerization or chemical cleavage of the polymer backbone resulted in a reduction in mechanical properties (strength). Water reacted with the polymer in a hydrolytic fashion resulting in cleavage of covalent chemical bonds with a commensurate reduction in average molecular weight and physical strength. The loss of mass integrity occurred when the implant had essentially no cohesive strength and began to fragment into pieces of low molecular weight polymer. In this case the microspheres were brittle and

fragmented easily after 77 days of degradation, which corresponded to M_w of 10,000 dalton (Figure 5.5). After 91 days of degradation, the M_w dropped to around 2,000 dalton and no SEM photographs could be taken as these sample were gel-like.

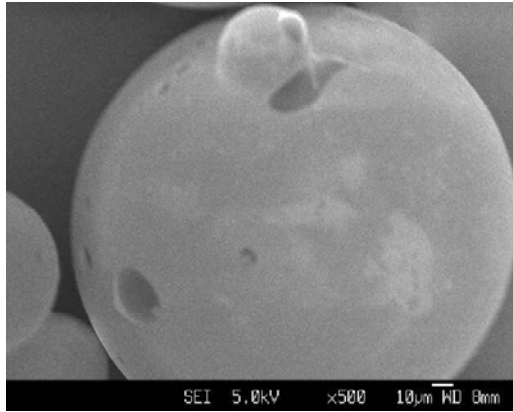
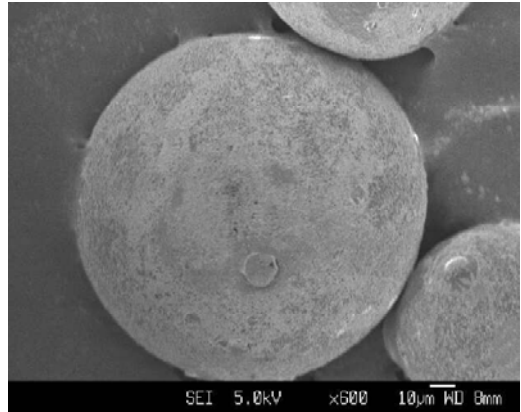
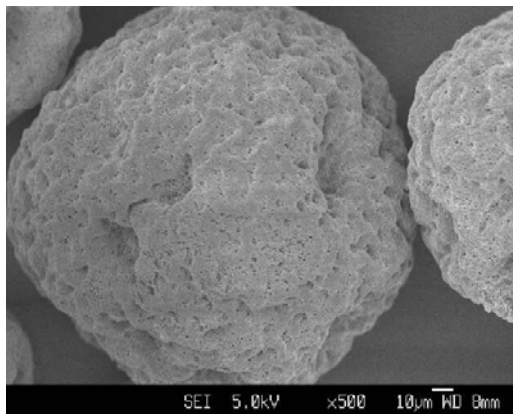
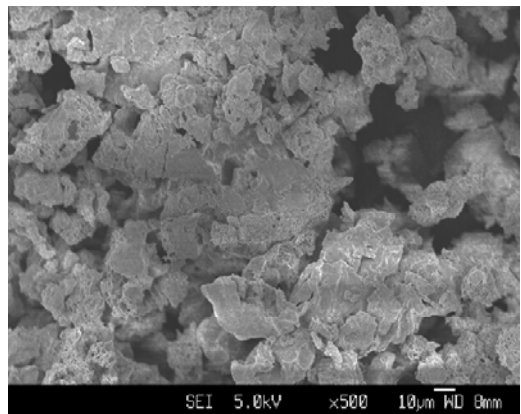
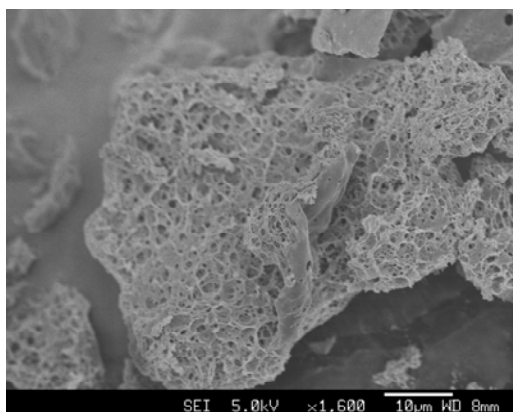
**A****B****C****D****E**

Figure 5.13 SEM photographs of PLGA 75 /25 I.V. 0.24 microspheres with respect to degradation time. A) 7 days; B) 28 days; C) 35 days; D) 56 days and E) 63 days.

In the case of the PLGA 75/25 I.V. 0.24 microspheres as shown in Figure 5.13, the surface roughened after 28 days of degradation and by the 35th day, pores were observed on the surfaces of the microspheres. This corresponded with the decrease in pH as shown in Figure 5.9. After 49 days of degradation, the microspheres were brittle and fragmented, with the M_w of around 10,000 dalton (Figure 5.5). This also coincided with the onset of mass loss as observed in Figure 5.10. The samples were gel-like in nature after 63 days of degradation, which was 14 days earlier as compared to the PLGA 75/25 I.V. 0.94 microspheres.

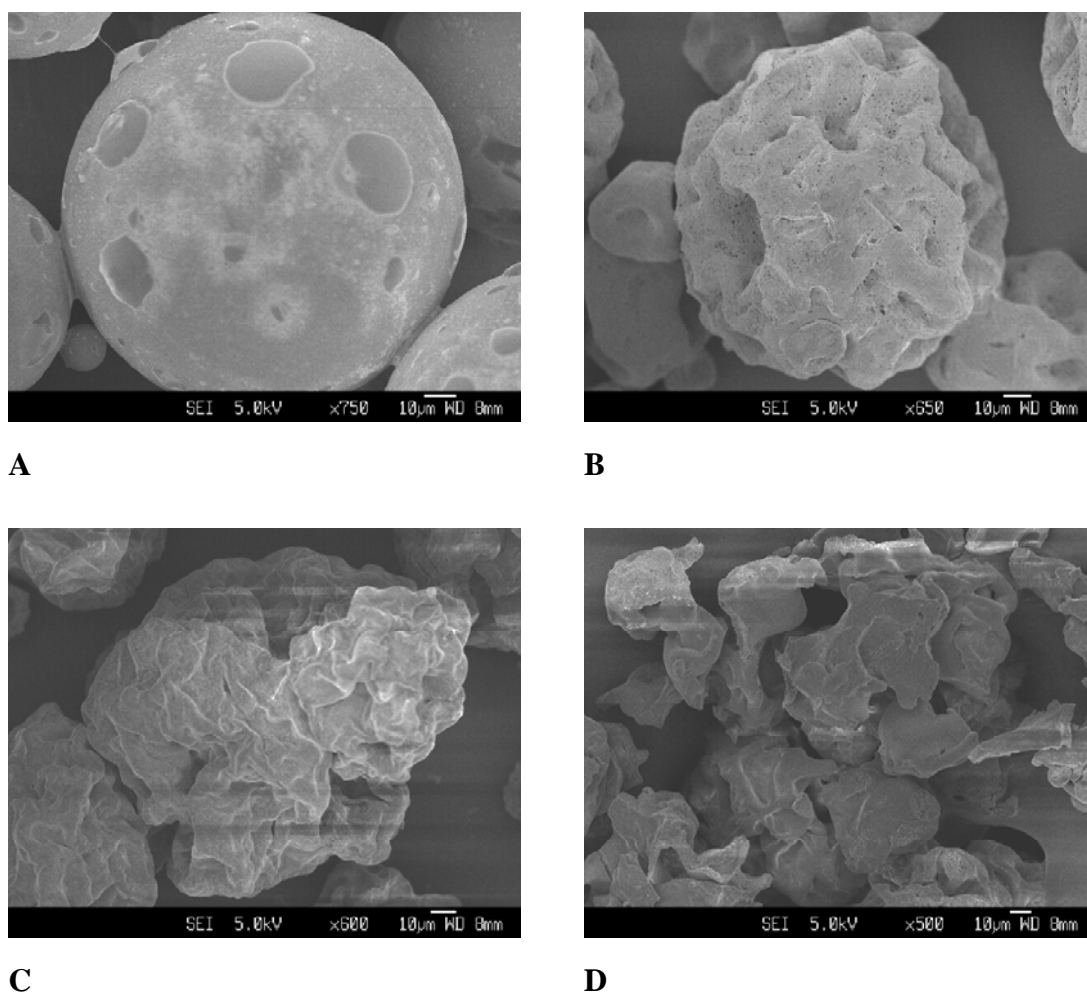


Figure 5.14 SEM photographs of PLGA 50/50 I.V. 0.50 microspheres with respect to degradation time. A) 7 days; B) 21 days; C) 28 days and D) 35 days.

In the PLGA 50/50 polymers, the microspheres with higher initial I.V. (0.50) degraded slower than the microspheres with lower I.V. (0.22). In the polymers of I.V. 0.50, pores were observed on the surface of the microspheres after 21 days of degradation (Figure

5.14 B), which also coincided with the decrease in pH of the degrading medium (Figure 5.9). The microspheres were gel-like after 28 days of degradation and the M_w dropped to around 10,000 dalton by this stage (Figure 5.5). At this time, the onset of mass loss was also observed (Figure 5.10). As for PLGA 50/50 I.V. 0.22 microspheres, the samples had turned to gel after 14 days of degradation and no SEM photographs could be taken of them.

SEM results confirmed that the microspheres from PLGA 75/25 copolymers degraded slower than the PLGA 50/50 copolymers. As for the polymers with the same LA to GA ratio, the higher the initial I.V., the longer it took for the polymers to lose its bulk integrity. PDLLA I.V. 0.22, which had the highest LA content (100 %) among the polymers investigated degraded the slowest. Even after 84 days of degradation, the shape of the microspheres was still intact with only blister-like formation observed on the surface of the microspheres.

5.6 Conclusions

The I.V. or initial molecular weight was less important compared to the LA to GA ratio in controlling the hydrolysis degradation rate of the PLGA and PDLLA polymers. For example, the rate of hydrolytic degradation for PDLLA I.V. 0.22 was the slowest even though its initial molecular weight was only 20,000 dalton.

Both the PLGA and PDLLA polymers underwent bulk degradation. The microspheres remained intact but became brittle and fragmented easily only when the M_w dropped to around 10,000 dalton. This coincided with the onset of mass loss and decrease in the pH of the degrading medium. As the M_w decreased to around 2,000 to 4,000 dalton, the microspheres became gel-like, which corresponded to a mass loss of more than 50 %.

The decrease in T_g with degradation time before the M_w decreased to 10,000 dalton, was due to plasticization of the amorphous material and decrease in chain length, resulting from hydrolysis of the polymer backbone. As for $M_w \leq 10,000$ dalton, the decrease in T_g with degradation time was mainly due to the formation of shorter chains formed by the hydrolysis of the polymer backbone and loss of amorphous material.

The natural logarithmic number average molecular weight ($\ln(M_n)$) of PDLLA and PLGA polymers before any mass loss was observed as a function of hydrolytic degradation time. PLGA 75/25 I.V. 0.94 and PDLLA I.V. 0.22 had a combination of two different linear relationship of hydrolysis. In PDLLA I.V. 0.22, the first k' value was very close to 0, indicating very little chain scission taking place in the first 84 days of degradation. The k' value increased to 0.0115 after 84 days of degradation. The initial lack of hydrolytic chain scission was due to the slow water uptake into the polymer. The inherent hydrophobic nature of LA units discouraged water absorption, thus decreasing the rate of hydrolytic chain scission. It is believed for PLGA 75/25 I.V. 0.94, the drastic increase in hydrolysis rate after 36 days of degradation indicated auto-catalyst effect. Acidic products from the scissions of the ester bonds trapped inside the polymer matrix would increase the rate of degradation of the core in comparison to the surface of the microspheres.

It was observed that crystallization of chain segments during the later stages of hydrolytic degradation of initially amorphous PLGA and PDLLA polymers, was dependent on several factors. The existence of both D- and L-lactic acids in the polymer discouraged crystallization. Hence the absence of melting peaks in degraded PDLLA I.V. 0.22 samples. Long chain heterogeneous polymer with a high degree of blockiness was able to generate crystallinity during later stages of hydrolytic degradation, as in the case of

PLGA 50/50 I.V. 0.50. As for PLGA 50/50 I.V. 0.22 and PLGA 75/25 I.V. 0.24, both had the same degree of blockiness and were of lower degree of blockiness and molecular weight compared to PLGA 50/50 I.V. 0.50. Crystallization of chain fragments was not observed for these two copolymers during the later stages of hydrolytic degradation. This would suggest that the oligomers formed were stereo-complex of D- or L-lactic acids instead of crystallizable oligomers with enriched D- or L-lactic acids chain segments.

CHAPTER 6

HYDROLYTIC DEGRADATION OF DRUG LOADED MICROSPHERES

Drug loaded microspheres of PDLLA and PLGA of different LA to GA ratio and molecular weight were degraded in phosphate buffered solution (pH=7.0) at 37°C for various length of time. Sample preparation and characterization using DSC, GPC, SEM, pH meter have been discussed in detail in Chapter 3.

The poly(D,L-lactide) PDLLA I.V. 0.22 and poly(D,L-lactide-co-glycolide) polymers investigated were amorphous in nature, with no melting peaks in the DSC thermogram. However, upon hydrolytic degradation, melting endotherms were observed in the MDSC thermograms of the degraded samples (Figure 5.1). As GCV was a highly crystalline drug, it had a melting endotherm. Since its melting endotherm might overlap with the melting endotherms of the degraded PDLLA and PLGA polymers, in order to determine if the melting peaks were due to the highly crystalline GCV or the re-crystallized polymer degradation fragments, a semi-crystalline poly(L-lactide), PLLA I.V. 1.04 and poly (L-lactide-co-glycolide) PLGA 80/20 I.V. 4.8 were used to gauge the melting temperature range for this group of poly (α -hydroxyl acids) polyesters. The thermal properties were listed in Table 6.1.

Sample	LA:GA ratio	I.V.	M _w (Dalton)	T _m (°C)	ΔH_m (J/g)	T _g (°C)
PLLA	100:0	1.04	100,000	179.8	53.62	64.0
PLGA	80:20	4.8	1,050,000	156	37.33	53.6
GCV	Nil	Nil	Nil	254.5	147.7	Nil

Table 6.1 Thermal properties of crystalline PLLA, semicrystalline PLGA and crystalline GCV.

The melting temperature of crystalline GCV was much higher than the melting temperature of the PLLA and PLGA. The heat of fusion (ΔH_m) of the crystalline GCV was also much larger than the heat of fusion of the PLLA and PLGA. If the GCV remained in the PDLLA and PLGA microspheres during later stages of hydrolytic degradation, the melting endotherm of GCV should be distinguishable from the melting endotherms of the degraded PDLLA and PLGA polymers.

According to literature^{93,94}, GCV has two pK_a values (acid dissociation constant), $pK_{a1} = 2.2$ and $pK_{a2} = 9.4$. Dr. Thomas. L Tarnowski⁹⁴ further pointed out that in very acidic medium (pH less than 2.2), ganciclovir is protonated and therefore has a single positive charge. In solutions of pH between 2.2 and 9.4 (such as pH 7.4), ganciclovir is mainly neutral, with no charged groups. It is not zwitterionic. In strongly basic solution (pH greater than 9.4), ganciclovir is deprotonated and has a single negative charge⁹⁴.

A schematic diagram of Ganciclovir molecule in different pH environment was drawn to illustrate the above (Figure 6.1).

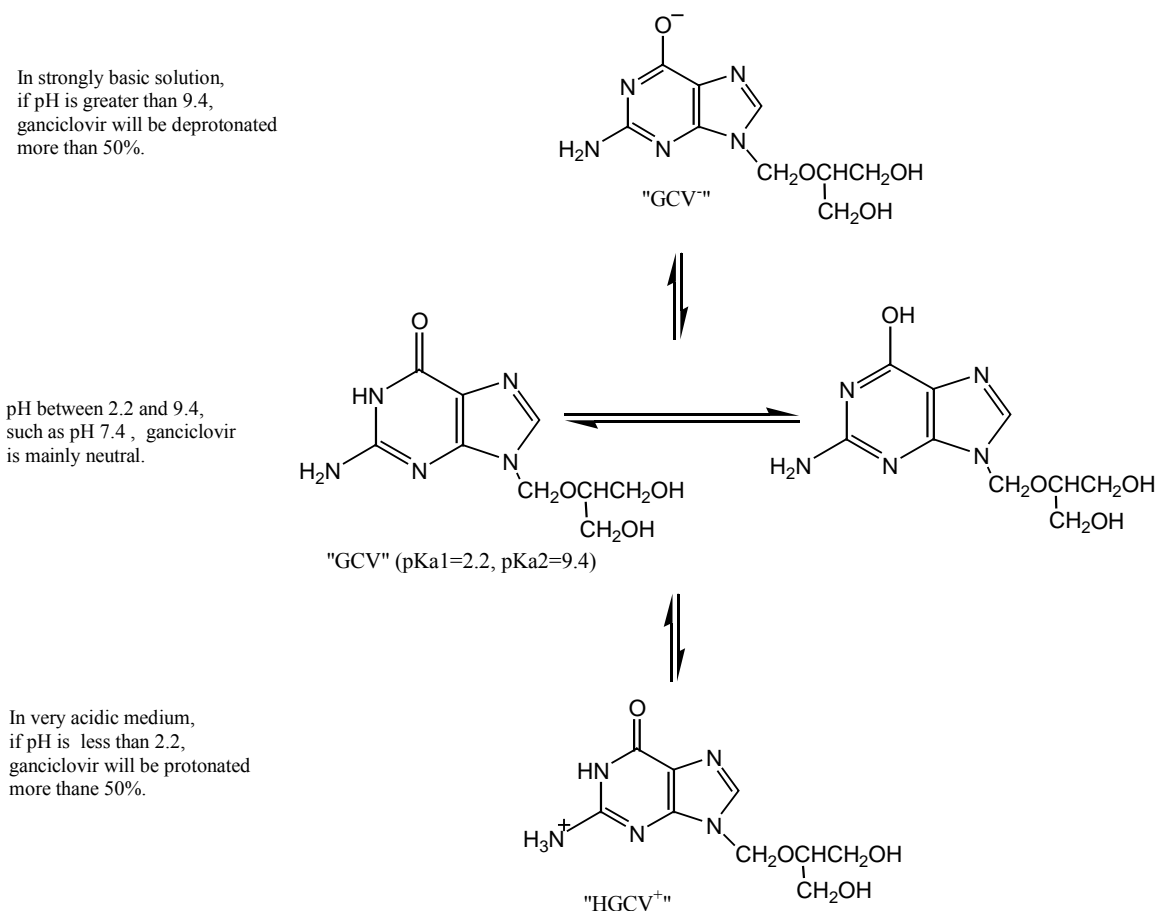


Figure 6.1 Schematic diagram of Ganciclovir molecule in different pH environment.

According to equation 6.2, in very acidic medium (pH less than 2.2) ganciclovir was protonated more than 50 % and therefore had a single positive charge. In solutions of pH between 2.2 and 9.4 (such as pH=7.0) ganciclovir had no charge and was not zwitterionic. In strongly basic solution (pH greater than 9.4) ganciclovir was deprotonated more than 50 % and had a single negative charge as shown from equation 6.4.

1. In acidic medium, ganciclovir was protonated and therefore had a single positive charge.



The basic dissociate constant *K_{b1}* can be expressed as

$$K_{b1} = \frac{[HGCV^+][OH^-]}{[GCV]}, \text{ Or } pK_{b1} = p \frac{[HGCV^+]}{[GCV]} + p[OH^-] \quad (6.1)$$

where $pK_{b1} = 14 - pK_{a1}$, $p \frac{[HGCV^+]}{[GCV]} = -\log \frac{[HGCV^+]}{[GCV]}$, $p[OH^-] = 14 - pH$ and

$pK_{a1} = 2.2$, equation (6.1) was derived as

$$\log \frac{[HGCV^+]}{[GCV]} = 2.2 - pH \quad (6.2)$$

At $pH = 2.2$, ganciclovir was protonated around 50 %.

- In basic medium, ganciclovir was deprotonated and therefore had a single negative charge.



The acid dissociate constant K_{a2} was expressed as

$$K_{a2} = \frac{[GCV^-][H^+]}{[GCV]} \text{ or } pK_{a2} = pH + p \frac{[GCV^-]}{[GCV]} \quad (6.3)$$

where $p \frac{[GCV^-]}{[GCV]} = -\log \frac{[GCV^-]}{[GCV]}$, when $pK_{a2} = 9.4$, equation (6.3) was derived as

$$\log \frac{[GCV^-]}{[GCV]} = pH - 9.4 \quad (6.4)$$

At $pH = 9.4$, ganciclovir was deprotonated around 50 %.

- By plotting equations (6.2) and (6.4) against pH values as shown in Figure 6.2, at $pH = 7$,

$$\log \frac{[GCV^-]}{[GCV]} = pH - 9.4 = -2.4, \text{ and } \log \frac{[HGCV^+]}{[GCV]} = 2.2 - pH = -4.8$$

Hence GCV was deprotonated less than 1% ($\frac{[GCV^-]}{[GCV]} = 0.4\%$) and was protonated

less than 0.01% ($\frac{[HGCV^+]}{[GCV]} = 0.002\%$) at pH 7. In other words, GCV mainly

existed as neutral molecules.

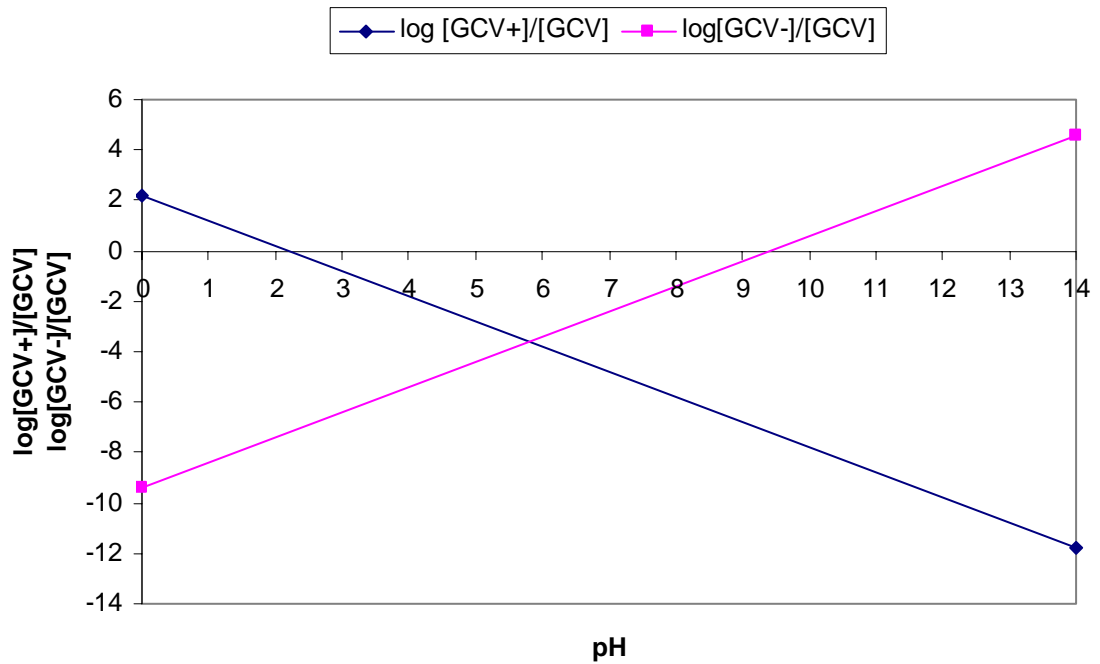


Figure 6.2 $\log \frac{[HGCV^+]}{[GCV]}$ and $\log \frac{[GCV^-]}{[GCV]}$ as a function of pH values

6.1 Modulated Differential scanning calorimetry (MDSC)

6.1.1 Thermograms

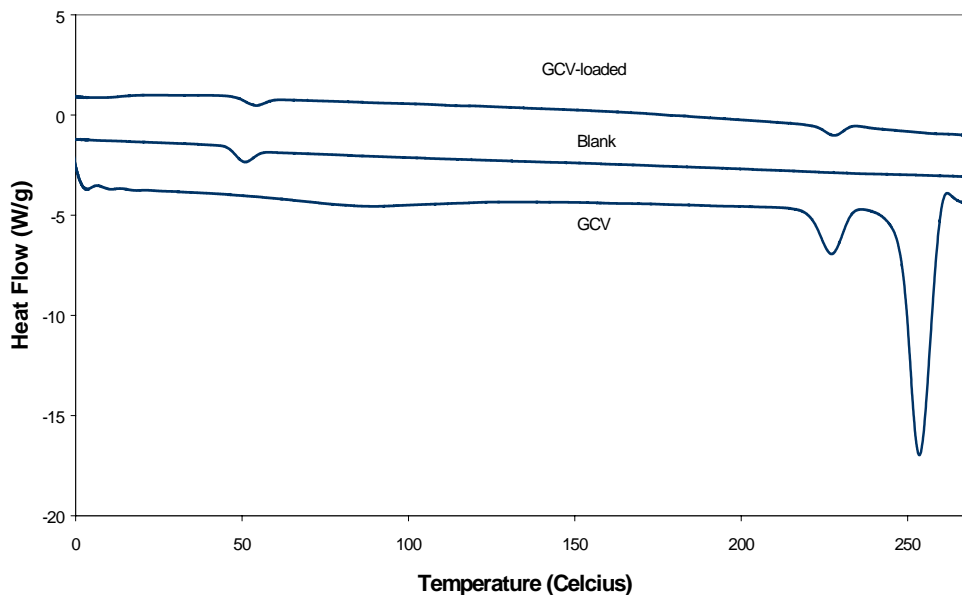


Figure 6.3 Heating profiles of ganciclovir (GCV), blank PLGA 75/25 I.V. 0.94 microspheres and ganciclovir-loaded (GCV-loaded) PLGA 75/25 I.V. 0.94 microspheres obtained from modulated differential scanning calorimetry (MDSC) at a heating rate of 5 °C/min.

MDSC thermograms for the PLGA 75/25 I.V. 0.94 microspheres, GCV and GCV-loaded PLGA 75/25 I.V. 0.94 microspheres were obtained for characterization of the physical state of the PLGA 75/25 I.V. 0.94 and GCV before and after the GCV-loaded microspheres preparation, as shown in Figure 6.3. The pure PLGA 75/25 I.V. 0.94 microspheres only showed a glass transition peak, whereas 2 endothermic peaks were observed for GCV at 232 °C and 254 °C, which corresponded to the melting phase transitions of the excipient, povidone and GCV, respectively. An endothermic peak was observed at about 220 °C to 230 °C in the heating profiles of GCV-loaded PLGA 75/25 I.V. 0.94 microspheres. Since the polymer was amorphous (Figure 5.1), this melting temperature corresponded to the melting temperature of GCV. This indicated that GCV was successfully incorporated into the polymer and was in a crystalline state in the microspheres. Figure 6.3 is a representation of changes to the physical state of amorphous

PDLLA and PLGA polymers investigated before and after the preparation of GCV-loaded microspheres.

(a) PLGA 75/25 polymers

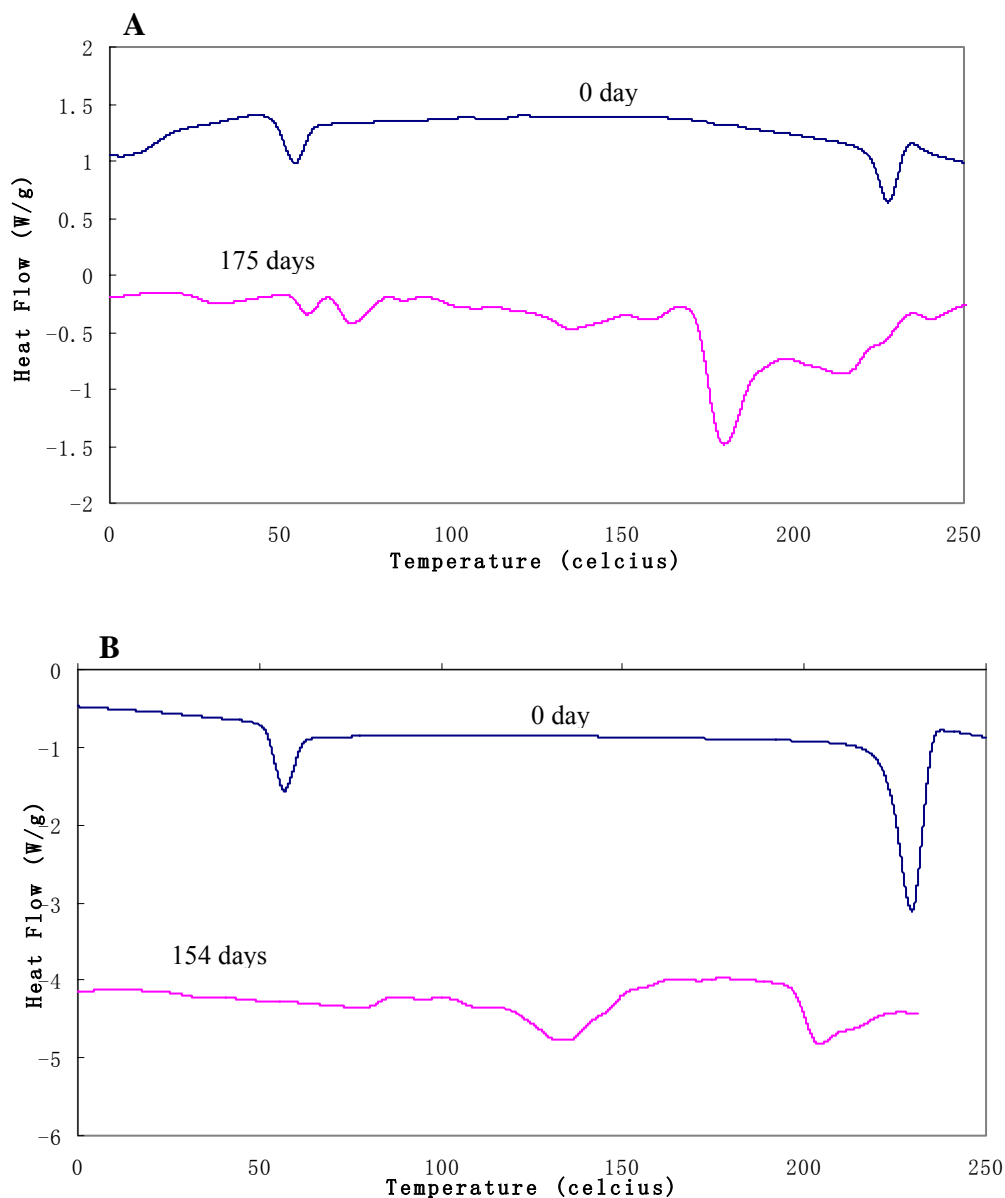
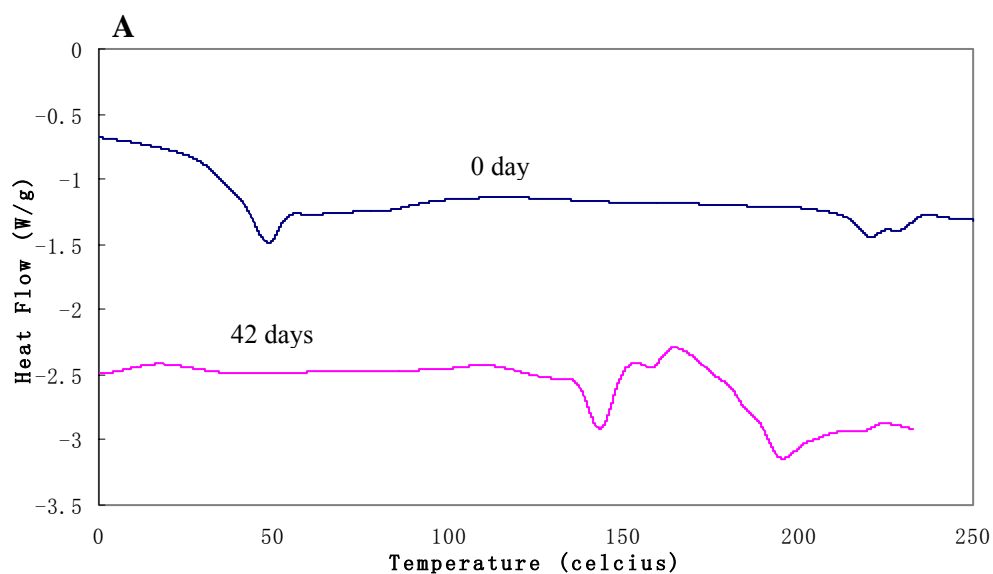


Figure 6.4 Thermograms of A) PLGA 75/25 I.V. 0.94 7% GCV microspheres before degradation and after 175 days of degradation and B) PLGA 75/25 I.V. 0.94 18% GCV microspheres before degradation and after 154 days of degradation in phosphate buffered solution at 37 °C, exotherm up.

In the undegraded GCV-loaded PLGA 75/25 I.V. 0.94 microspheres (Figure 6.4), a distinctive GCV melting peak and a glass transition peak were observed at around 230 °C and 50 °C, respectively. As the polymers underwent hydrolytic degradation, multiple

melting peaks were observed. With reference to the GCV release profiles of these polymers as shown in Figure 7.1 in chapter 7, by that time, most GCV had been released to the environment and very little remained in the microspheres. The presence of melting peaks were also observed in the degraded samples of the initially amorphous blank PLGA 75/25 I.V. 0.94 microspheres as shown in Figure 5.1 B. Hydrolytic chain scission of the polymer backbone generated shorter chains, which could then reorientate and recrystallize. These melting peaks were generated by the crystallization of these shorter chains trapped in the microspheres.

(b) PLGA 50/50 polymers



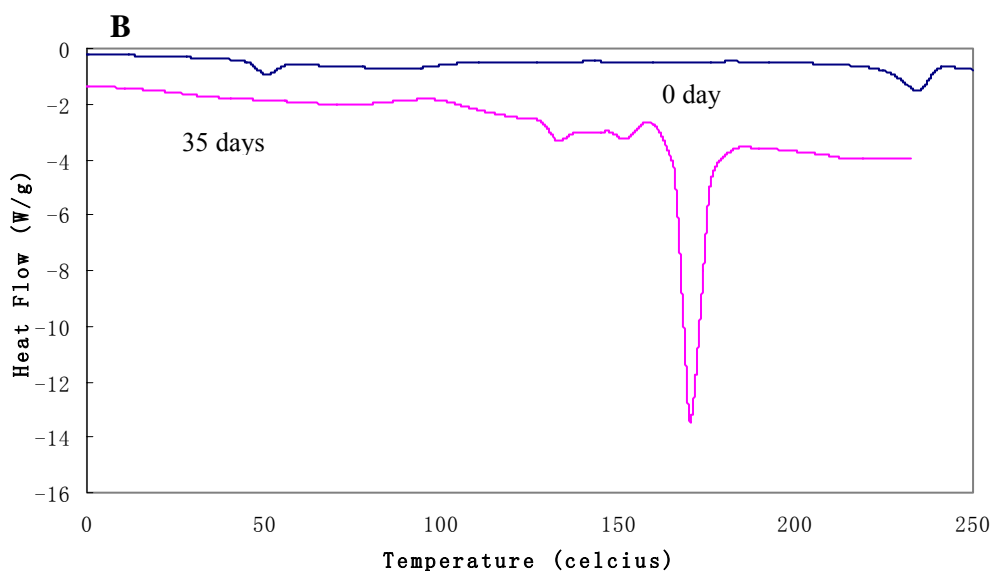
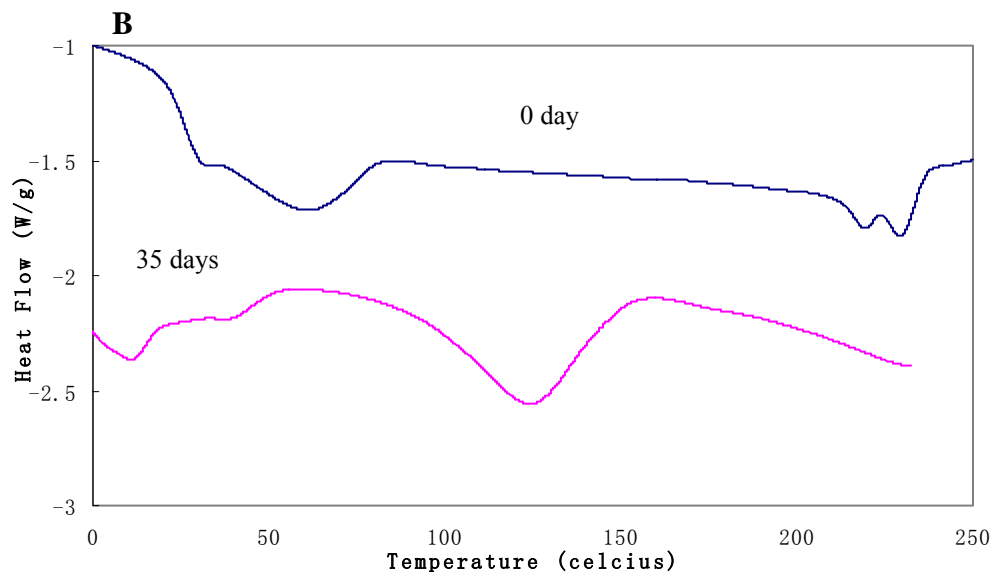
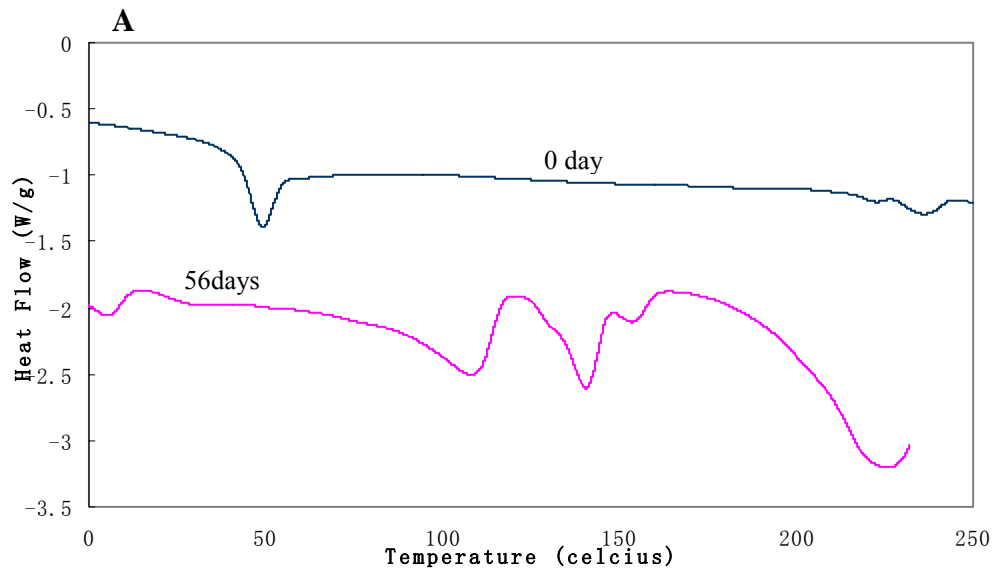


Figure 6.5 Thermograms of A) PLGA 50/50 I.V. 0.50 5% GCV microspheres before degradation and after 42 days of degradation and B) PLGA 50/50 I.V. 0.50 20% GCV microspheres before degradation and after 35 days of degradation in phosphate buffered solution at 37 °C, exotherm up.

In the undegraded GCV-loaded PLGA 50/50 I.V. 0.50 microspheres (Figure 6.5), a distinctive melting peak and a glass transition peak were also observed at around 230 °C and 50 °C, respectively. Since the PLGA 50/50 I.V. 0.50 polymers were also amorphous in nature (Figure 5.1 C), the melting peaks observed at 230 °C for the GCV-loaded PLGA 50/50 I.V. 0.50 microspheres were due to the incorporated GCV. As the polymers underwent hydrolytic degradation, multiple melting peaks were observed for all the GCV-loaded microspheres (Figure 6.5). These melting peaks were generated by the crystallization of fragments of degraded chains trapped in the microspheres.

(c) PLGA and PDLLA polymers of similar I.V. and GCV content



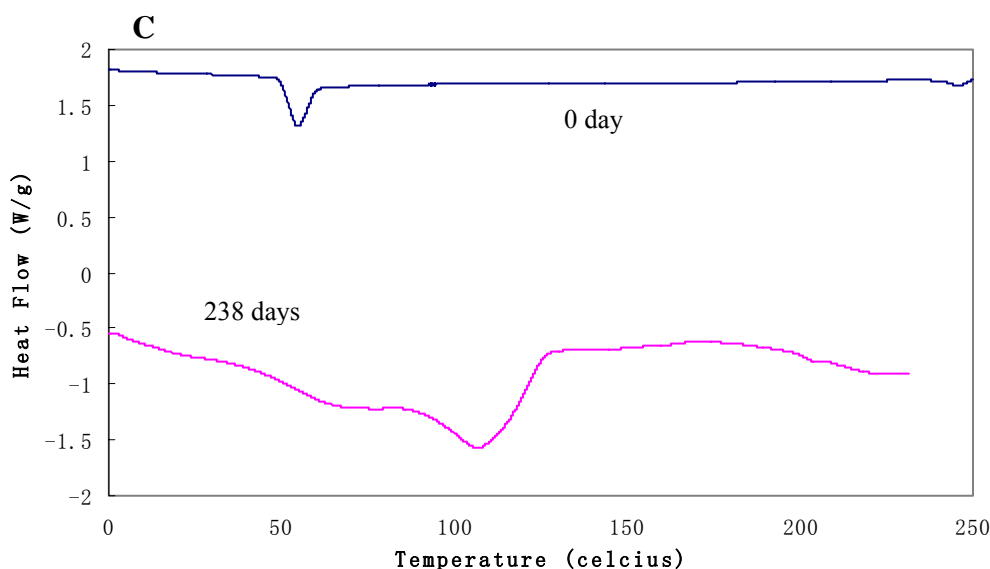


Figure 6.6 Thermogram of A) PLGA 75/25 I.V. 0.24 5% GCV microspheres before degradation and after 56 days of degradation; B) PLGA 50/50 I.V. 0.22 7% GCV microspheres before degradation and after 35 days of degradation and C) PDLLA I.V. 0.22 5% GCV microspheres before degradation and after 238s of degradation in phosphate buffered solution at 37 °C, exotherm up.

In the undegraded PLGA 75/25 I.V. 0.24 5% GCV microspheres, a melting peak and a glass transition peak were both observed at around 230 °C and 50 °C, respectively in the thermogram (Figure 6.6 A). The melting peak observed at 230 °C for the GCV-loaded PLGA 75/25 I.V. 0.24 microspheres was due to the incorporated GCV. After 56 days of degradation, multiple endothermic peaks were observed from 100 °C to 150 °C (Figure 6.6 A). These melting peaks were generated by the crystallization of degradation products trapped in the microspheres. However, no melting peak was observed in the degraded blank PLGA 75/25 I.V. 0.24 microspheres.

Similar observations were made for PLGA 50/50 I.V. 0.22 7% GCV microspheres. A bimodal melting peak was observed at around 230 °C in the thermogram (Figure 6.6 B), corresponding to the incorporated GCV. After 35 days of degradation, a broad endothermic peak was observed at around 100 °C (Figure 6.6 B). The melting peak was generated by the crystallization of degradation products trapped in the microspheres.

In the undegraded PDLLA I.V. 0.22 5% GCV microspheres, there was only a distinctive glass transition peak at around 50 °C (Figure 6.6 C). However, after 238 days of degradation, a broad endothermic peak was observed at around 100 °C. No endothermic peak was observed in the blank PDLLA I.V. 0.22 microspheres after 175 days of degradation (Figure 5.1 A). The PDLLA I.V. 0.22 took much longer time to degrade compared to the other PLGA polymers, thus a melting peak appeared above the glass transition temperature in the initially amorphous PDLLA I.V. 0.22 microspheres only after 238 days of degradation.

6.1.2 Glass transition temperature, T_g

All the DSC thermograms obtained were from the first heating cycle, which illustrated the thermal history of the samples.

The incorporation of the GCV into the polymers did not significantly change the initial T_g of the respective polymers as shown in Figure 6.7. For the same polymer, the increase in GCV content did not affect the T_g significantly. This may be due to the small amount of GCV in the polymer ($\leq 182 \mu\text{g}/\text{mg}$). The glass transition temperatures of the GCV-loaded PDLLA and PLGA microspheres were listed in Table 4.8 in Chapter 4 respectively.

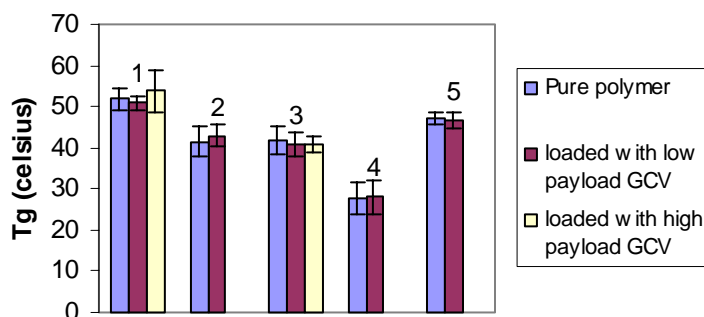


Figure 6.7 Glass transition temperatures (T_g) of undegraded pure, low payload (5 - 7 % wt/wt) GCV-loaded microspheres and high payload (18-20 % wt/wt) GCV-loaded microspheres. 1- PLGA 75/25 I.V. 0.94; 2- PLGA 75/25 I.V. 0.24; 3- PLGA 50/50 I.V. 0.50; 4- PLGA 50/50 I.V. 0.22; 5- PDLLA I.V. 0.22.

As the microspheres were amorphous in nature, only the T_g was used to follow the degradation rate of the polymers. The T_g decreased with degradation for all the GCV-loaded microspheres, as shown in Figures 6.8 to 6.10.

(a) PLGA 75/25 polymers

The changes in T_g with respect to degradation time for GCV-loaded PLGA 75/25 microspheres were illustrated in Figure 6.8.

Figure 6.8 showed the changes in the glass transition temperatures of the PLGA 75/25 I.V. 0.94 7% GCV, PLGA 75/25 I.V. 0.94 18% GCV and PLGA 75/25 I.V. 0.24 5% GCV microspheres with degradation time in PBS solution at pH 7.0 and at 37 °C. The GCV-loaded PLGA 75/25 microspheres with a higher molecular weight (I.V. = 0.94) had a higher T_g (53 ± 5 °C) compared with the copolymer with lower molecular weight (I.V.= 0.24). The T_g for the latter copolymer was 43 ± 3 °C. The T_g for all the polymers decreased with degradation time. The rate at which the T_g decreased was different in the polymers due to the large differences in molecular weight and GCV content. From Figure 6.8, linear plots showing strong statistical linear correlation ($R^2 > 0.90$) were obtained. From the gradient of the linear plots, it was observed that the gradient for PLGA 75/25 I.V. 0.24 5% GCV > PLGA 75/25 I.V. 0.94 18% GCV > PLGA 75/25 I.V. 0.94 7% GCV. This order suggested that the effects of I.V. and degree of blockiness on the change in T_g with degradation time, as previously discussed in chapter 5, were more significant than the effect of GCV content.

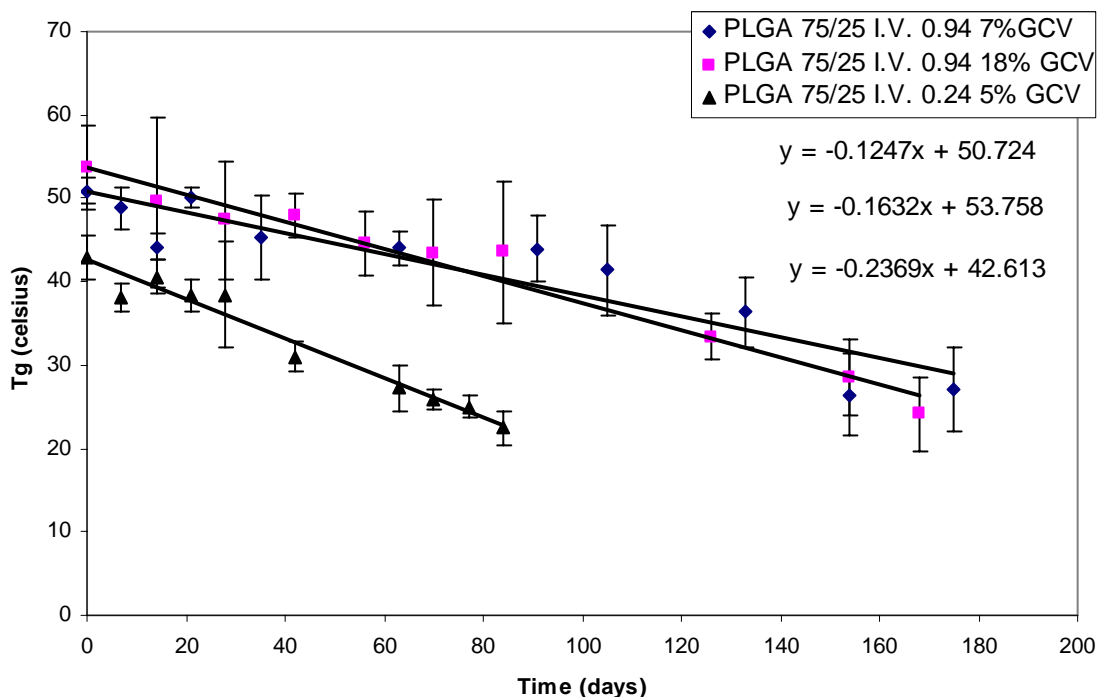


Figure 6.8 Glass transition temperature (T_g) as a function of degradation time for PLGA 75/25 I.V. 0.94 7% GCV (◆), PLGA 75/25 I.V. 0.94 18% GCV (■) and PLGA 75/25 I.V. 0.24 5% GCV (▲) microspheres degraded in phosphate buffered solution at 37 °C.

The rate in which T_g decreased with degradation time was faster in the higher (18% wt/wt) GCV-loaded PLGA 75/25 I.V. 0.94 microspheres compared to the lower (7% wt/wt) GCV-loaded ones. It is believed that as GCV dissolved and released to the surrounding medium, small pores or micro-channels were left behind within the polymeric matrix. This would in turn, accelerate the water uptake rate into the polymer, resulting in more water molecules acting as plasticizers to further lower the T_g . Furthermore, the increase in water uptake would result in more water molecules attacking the polymer backbone, thus accelerating the hydrolysis process. Table 6.2 summarized the gradient value, k , of the linear T_g plots with degradation time of the pure microspheres and GCV-loaded microspheres.

From Table 6.2, it was observed that the gradient of the linear T_g plots with degradation time of pure PLGA 75/25 microspheres was lower than the GCV-loaded PLGA 75/25 microspheres. Hence incorporation of GCV accelerated the PLGA 75/25 degradation rate.

The effect of GCV on the T_g decrease profile of PLGA 75/25 I.V. 0.24 was more significant than of PLGA 75/25 I.V. 0.94. The higher molecular weight PLGA 75/25 took longer time to produce shorter chains via hydrolysis compared to the lower molecular weight PLGA 75/25. Furthermore, PLGA 75/25 I.V. 0.24 had higher degree of blockiness compared with PLGA 75/25 I.V. 0.94, as discussed in Chapter 5. The lower molecular weight meant shorter chain lengths and the higher degree of blockiness meant more GA-GA units in the polymer backbone. These two factors would increase the hydrolytic degradation rate of PLGA. Hence when GCV accelerated the hydrolysis for both PLGA 75/25, the accelerated hydrolysis of the copolymer of I.V. 0.24 was more significant than the copolymer of I.V. 0.94.

Sample	LA:GA ratio	I.V.	Synonym	Gradient value k of T_g
PDLLA	100:0	0.22	PDLLA I.V. 0.22	0.0751
			PDLLA I.V. 0.22 5% GCV	0.0231; 0.2482
PLGA	75:25	0.94	PLGA 75/25 I.V. 0.94	0.1114
			PLGA 75/25 I.V. 0.94 7% GCV	0.1247
			PLGA 75/25 I.V. 0.94 18% GCV	0.1632
		0.24	PLGA 75/25 I.V. 0.24	0.1534
			PLGA 75/25 I.V. 0.24 5% GCV	0.2369
			PLGA 50/50 I.V. 0.50	0.3735
	50:50	0.50	PLGA 50/50 I.V. 0.50 5% GCV	0.5164
			PLGA 50/50 I.V. 0.50 20% GCV	0.2579
			PLGA 50/50 I.V. 0.22	0.2652
		0.22	PLGA 50/50 I.V. 0.22 7% GCV	0.5141

Table 6.2 The gradient value k of the linear T_g plots with degradation time of pure and GCV-loaded polymeric microspheres.

(b) PLGA 50/50 polymers

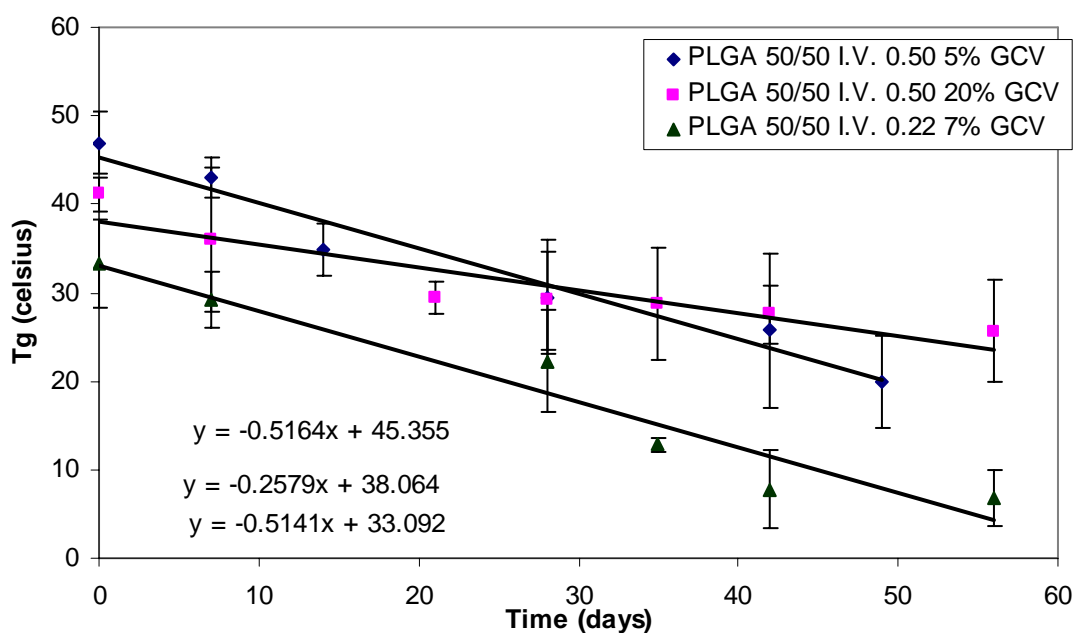


Figure 6.9 Glass transition temperature (T_g) as a function of degradation time for PLGA 50/50 I.V. 0.50 5% GCV (◆), PLGA 50/50 I.V. 0.50 20% GCV (■) and PLGA 50/50 I.V. 0.22 7% GCV (▲) microspheres degraded in phosphate buffered solution at 37 °C.

The T_g as a function of degradation time for GCV-loaded PLGA 50/50 microspheres was as illustrated in Figure 6.9. Significant differences in the gradient value, k , of the linear T_g plots with degradation time were observed due to the different I.V. and GCV content. From Table 6.2, the k values for PLGA 50/50 I.V. 0.50 5% GCV ($k = 0.5164$) and PLGA 50/50 I.V. 0.22 7% GCV ($k = 0.5141$) were similar within experimental error. In Chapter 5, it was observed that the gradient value, k , for the pure PLGA 50/50 I.V. 0.50 microspheres ($k = 0.3735$) was higher than that of pure PLGA 50/50 I.V. 0.22 ($k = 0.2652$). This was due to the higher degree of blockiness of PLGA 50/50 I.V. 0.50 than PLGA 50/50 I.V. 0.22, as discussed in detail in section 5.1.1, Chapter 5. It is believed that the incorporation of GCV affected the T_g decrease profile due to accelerated water uptake rate caused by small pores and channels left behind after GCV had dissolved and released to the surrounding medium. Since PLGA 50/50 I.V. 0.22 7% GCV had a higher GCV content compared to PLGA 50/50 I.V. 0.50 5% GCV, more small pores and channels

were formed as GCV dissolved. This resulted in larger uptake of water molecules, which would increase the hydrolytic degradation rate of the polymer. Hence the similar k values for PLGA 50/50 I.V. 0.50 5% GCV and PLGA 50/50 I.V. 0.22 7% GCV. However, as seen from Table 6.2, the k values for the GCV-loaded PLGA 50/50 I.V. 0.50 20% was lower than that of the GCV-loaded PLGA 50/50 I.V. 0.50 5% and pure PLGA 50/50 I.V. 0.50 microspheres. The PLGA 50/50 I.V. 0.50 20% GCV was expected to have the highest k value compared to PLGA 50/50 I.V. 0.50 5% GCV and pure PLGA 50/50 I.V. 0.50 due to the larger number of small pores and channels formation after GCV dissolved and was released. The contradiction observed was analyzed together with the other degradation profiles such as M_w and morphology, and discussed in the later sections.

(C) PDLLA and PLGA polymers of similar I.V. and GCV content.

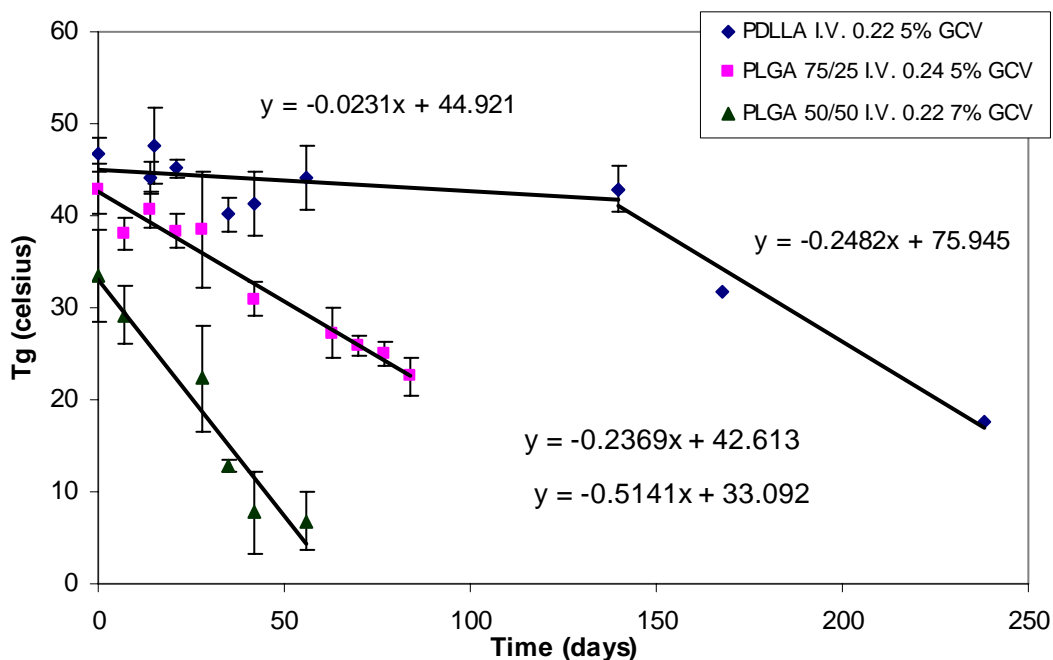


Figure 6.10 Glass transition temperature (T_g) as a function of degradation time for PDLLA I.V. 0.22 5% GCV (◆), PLGA 75/25 I.V. 0.24 5% GCV (■) and PLGA 50/50 I.V. 0.22 7% GCV (▲) microspheres degraded in phosphate buffered solution at 37 °C.

Figure 6.10 shows the profiles related to the decrease of T_g of the GCV-loaded microspheres with similar I.V. and GCV content but different LA to GA ratio. From

Table 6.2, the incorporation of GCV increased the k values of all the pure PLGA 50/50 I.V. 0.22, PLGA 75/25 I.V. 0.24 and PDLLA I.V. 0.22 microspheres. It was also observed that the order in which the k values decrease was: PLGA 50/50 I.V. 0.22 7% GCV > PLGA 75/25 I.V. 0.24 5% GCV > PDLLA I.V. 0.22 5% GCV.

Differential scanning calorimetry (DSC) is a very useful technique for determining the form of the polymer and drug in a microparticle formulation. For microspheres prepared from poly(L-lactic acid) or poly(D-lactic acid), this technique may be used to determine the degree of crystallinity of the polymer in the microparticles. However, in cases where the microspheres are prepared from poly(DL-lactic acid) or PLGA, the measurements will be more useful in determining the glass transition temperature of the polymer as the polymer is amorphous. This glass transition temperature is dependent on the molecular weight of the polymer as well as on the presence of solvents or plasticizers such as water.

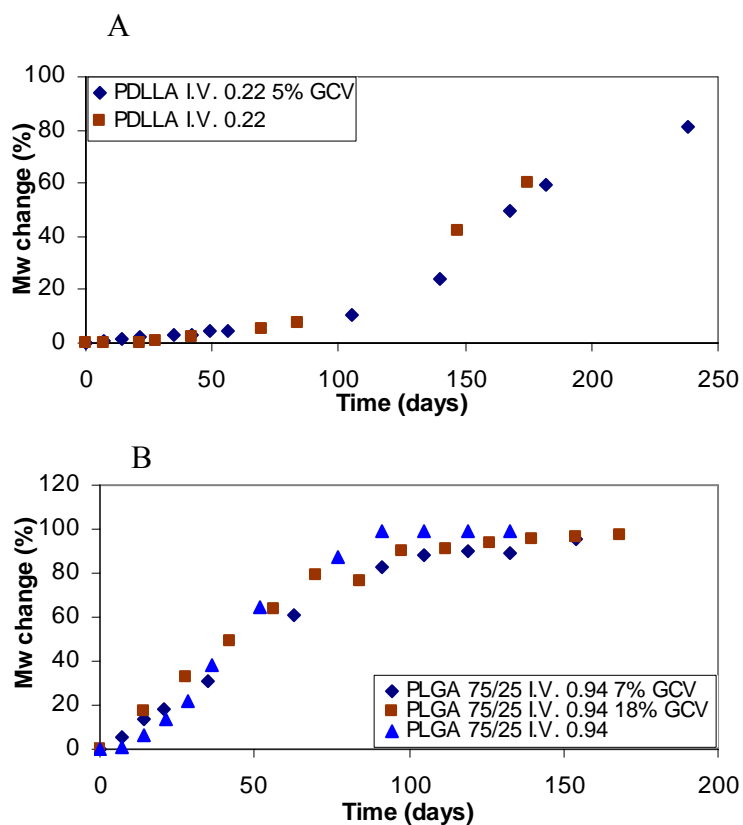
As the PLGA degraded and its molecular weight decreased throughout the bulk of the polymer, Park¹¹⁵ *et al.* reported that the glass transition temperature of the original PLGA microspheres with a molecular weight of 17,000, dropped from 41.7 °C to 10 °C over 33 days. As the glass transition temperature of the polymer approached and went below the temperature of its environment, degradation and the release behavior changed dramatically.

As degradation progressed, multiple endotherms were observed in the thermograms of all the initially amorphous GCV-loaded PDLLA and PLGA microspheres as shown in Figures 6.3 to 6.5. These peaks were due to the crystallization of degradation products trapped in the microspheres. At the same time, the GCV melting peak at around 230 °C became indistinguishable with degradation time. From the plot of the cumulative release

curve of GCV-loaded microspheres (Figure 7.1 in Chapter 7), it was observed that by the time these multiple endotherms were observed in the thermograms, more than 90 % of the incorporated GCV had been released to the surrounding medium and only a small amount of GCV remained in the microspheres. These multiple endotherms were also observed in the thermograms of pure microspheres during the late stages of degradation, as shown in Figure 5.1. Hence these peaks were likely due to changes in polymer and not due to the drug GCV.

6.2 Gel permeation chromatography (GPC)

6.2.1 % Normalized change in weight-average molecular weight (ΔM_w)



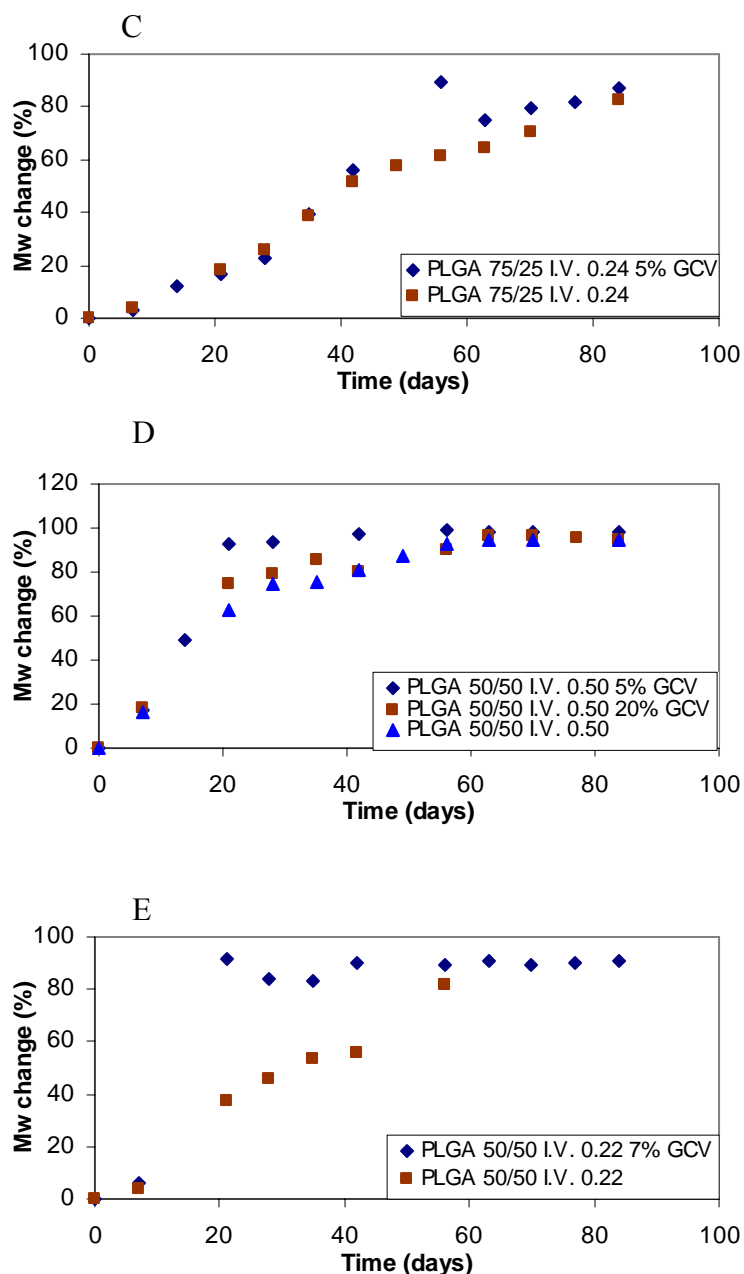


Figure 6.11 Normalized change in weight-average molecular weight (ΔM_w) of A) PDLLA 0.22 5% GCV (◆) and PDLLA 0.22 (■); B) PLGA 75/25 I.V. 0.94 7% GCV (◆), PLGA 75/25 I.V. 0.94 18% GCV (■) and PLGA 75/25 I.V. 0.94 (▲); C) PLGA 75/25 I.V. 0.24 5% GCV (◆) and PLGA 75/25 I.V. 0.24 (■); D) PLGA 50/50 I.V. 0.50 5% GCV (◆), PLGA 50/50 I.V. 0.50 20% GCV (■) and PLGA 50/50 I.V. 0.50 (▲); E) PLGA 50/50 I.V. 0.22 7% GCV (◆) and PLGA 50/50 0.22 (■) microspheres as a function of degradation time.

The initial weight-average molecular weight of microspheres were labeled M_{wi} , the weight-average molecular weight of microspheres after degradation, M_{wd} , and the % normalized change in weight-average molecular weight, ΔM_w was calculated using equation 6.5:

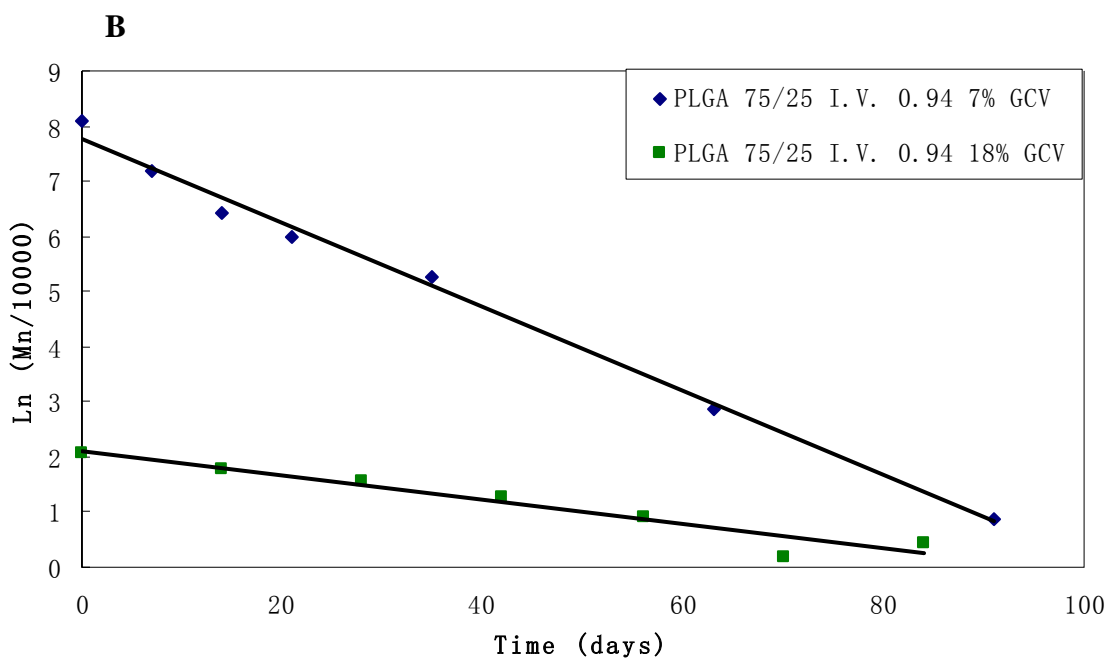
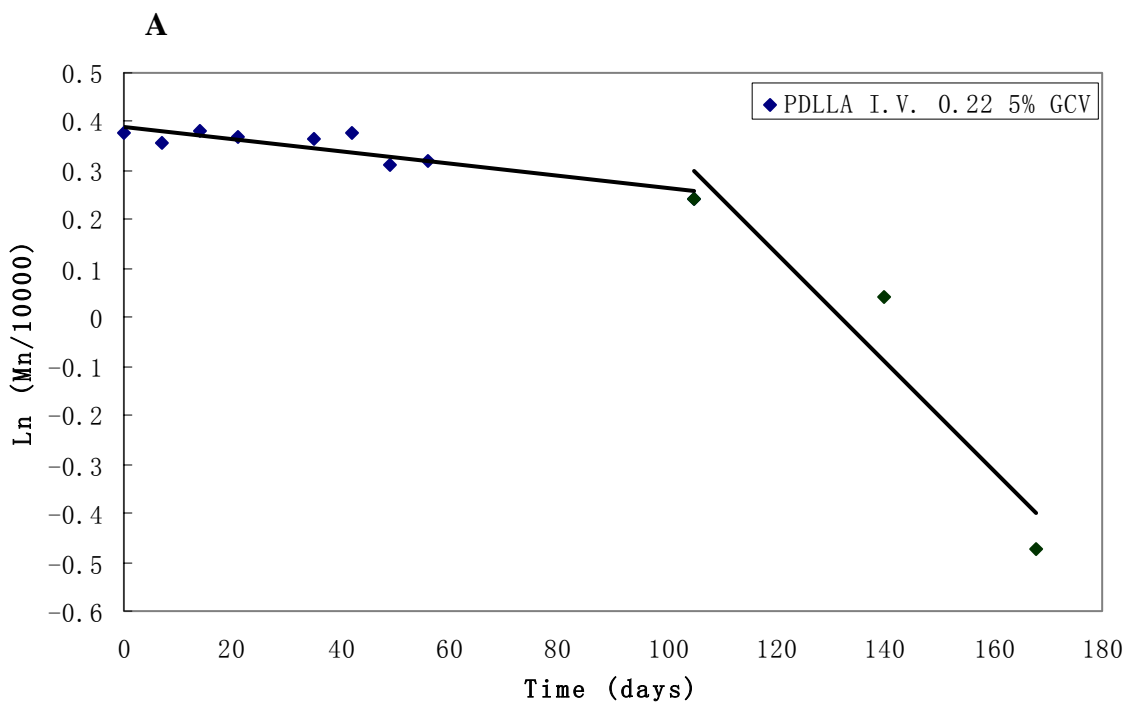
$$\Delta M_w \% = \frac{M_{wi} - M_{wd}}{M_{wi}} \times 100\% \quad (6.5)$$

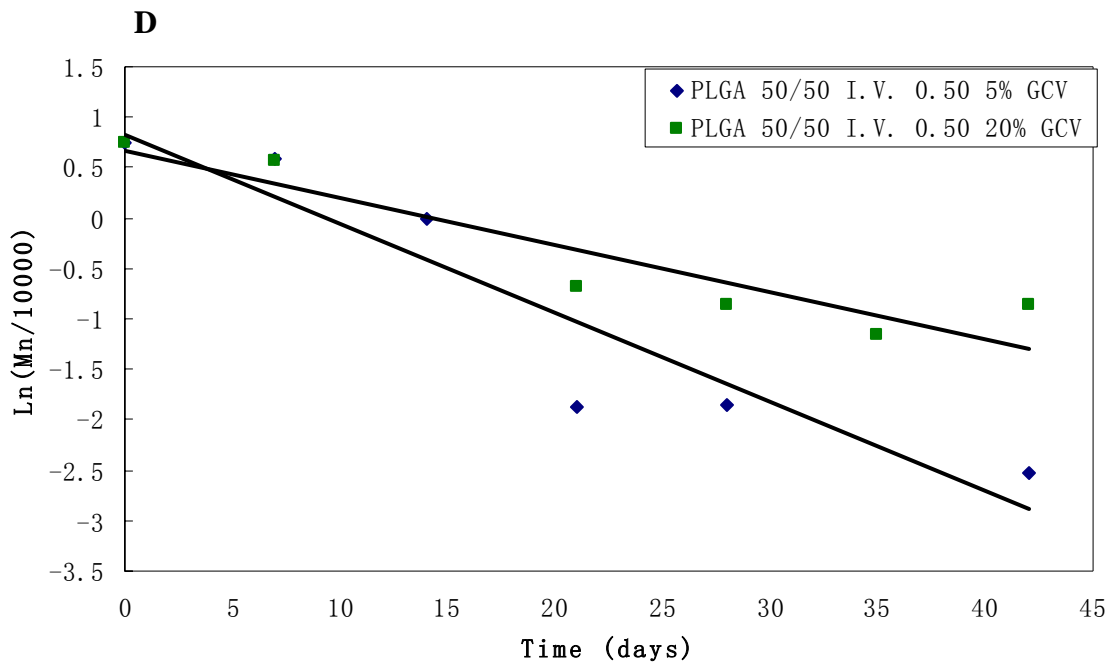
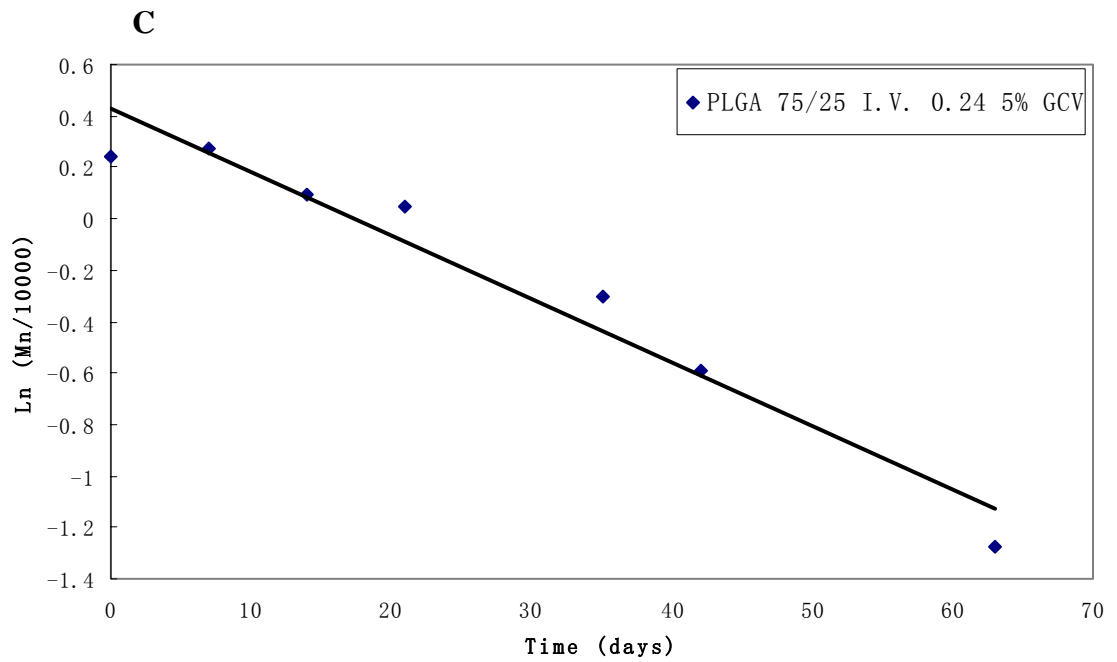
The ΔM_w profiles were plotted against degradation time for all samples to compare the degradation process of GCV-loaded and pure microspheres as shown in Figure 6.11. GCV incorporated PDLLA, PLGA 75/25 and PLGA 50/50 I.V 0.50 polymers were not significantly different from the normalized ΔM_w of the respective pure polymers. However for PLGA 50/50 I.V. 0.22, the addition of GCV accelerated the decrease in M_w , where the ΔM_w was 80 % after 3 weeks of degradation.

The pH of the degradation medium was maintained within the range between 2.2 and 9.4 during the entire time of investigation. In this pH range, the GCV was mainly neutral, with no-charged groups. Attention had to be paid to drugs and other substances with an acid or base functionality when they were incorporated into degradable polymers because they might alter degradation rates as well. However, the drug GCV had little effect on the hydrolytical chain scission of the polyester backbone due to the neutral status of the GCV between the pH 2.2 and pH 9.4. Theoretically, GCV would not alter degradation through chemically affecting the hydrolysis.

In the case of PLGA 50/50 I.V. 0.22 7% GCV, from the plot of the cumulative release curve of GCV-loaded microspheres (Figure 7.1 in Chapter 7), the microspheres released 16 % of the GCV to the surrounding medium at day 21, and 93 % by day 28. The T_g for the microspheres was lower than 37 °C throughout the period investigated. Therefore PLGA 50/50 I.V. 0.22 was in rubbery state and could absorb large quantity of water easily, resulting in fast dissolution and diffusion of GCV. The fast release of GCV left small pores and micro-channels inside the microspheres, thus increasing the water uptake rate of the polymer matrix, and accelerating the decrease of M_w .

By plotting the $\ln(M_n)$ against degradation time, as shown in Figures 6.12 A to E, the degradation rate constant, k' , for the GCV-loaded microspheres was calculated from the gradient of the linear plots. The k' values were summarized in Table 6.3. The M_n values were taken before any significant mass loss was observed.





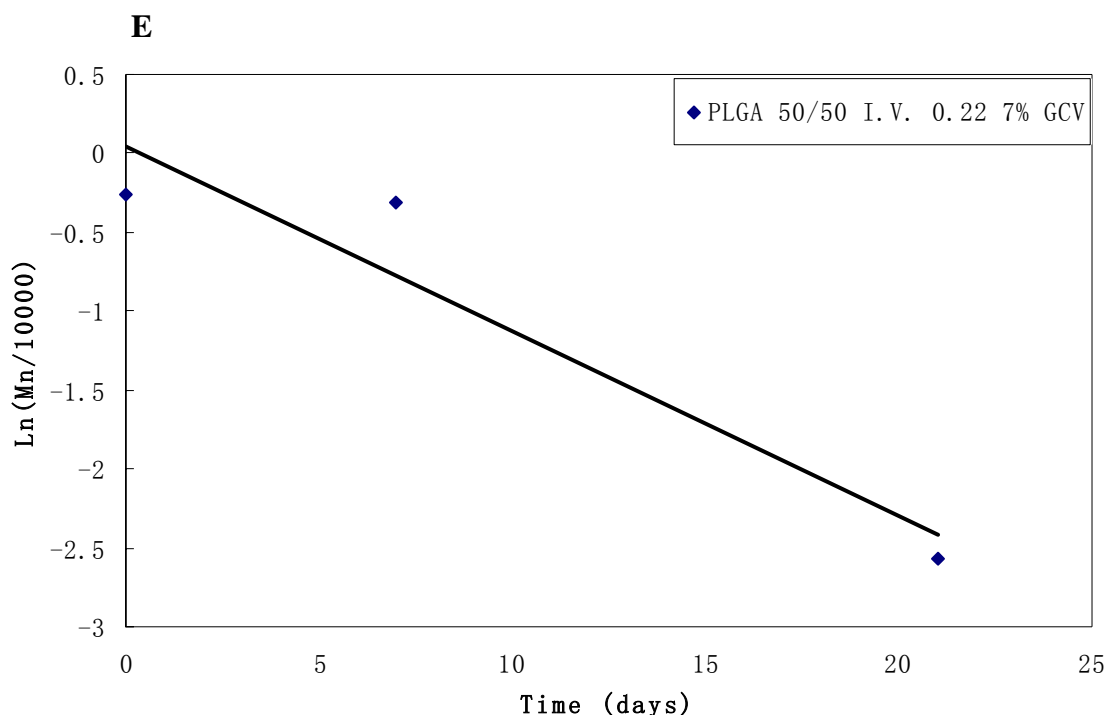


Figure 6.12 $\ln(M_n)$ against degradation time before commencement of significant mass loss for GCV-loaded PDLLA and PLGA microspheres. A) PDLLA I.V. 0.22 5% GCV; B) PLGA 75/25 I.V. 0.94 7% and 18% GCV; C) PLGA 75/25 I.V. 0.24 5% GCV; D) PLGA 50/50 I.V. 0.50 5% and 20% GCV; E) PLGA 50/50 I.V. 0.22 7% GCV microspheres.

Sample	LA:GA ratio	I.V.	Synonym	Degradation rate constant k'
PDLLA	100:0	0.22	PDLLA I.V. 0.22	0.0115
			PDLLA I.V. 0.22 5% GCV	0.0111
PLGA	75:25	0.94	PLGA 75/25 I.V. 0.94	0.0130; 0.0576
			PLGA 75/25 I.V. 0.94 7% GCV	0.0764
		PLGA 75/25 I.V. 0.94 18% GCV	0.0222	
		0.24	PLGA 75/25 I.V. 0.24	0.0179
	PLGA 75/25 I.V. 0.24 5% GCV	0.0248		
	50:50	0.50	PLGA 50/50 I.V. 0.50	0.0525
			PLGA 50/50 I.V. 0.50 5% GCV	0.0887
		PLGA 50/50 I.V. 0.50 20% GCV	0.0469	
0.22		PLGA 50/50 I.V. 0.22	0.0276	
PLGA 50/50 I.V. 0.22 7% GCV	0.1174			

Table 6.3 Degradation rate constant k' of each GCV-loaded and pure polymeric microspheres.

Figure 6.12 A clearly showed that the $\ln(M_n)$ profile of PDLLA I.V. 0.22 5% GCV was similar to that of the pure PDLLA I.V. 0.22 as shown in Figure 5.7. The k' value before 105 days of degradation was very close to 0, indicating very little chain scission had

occurred. This would be due to the slow water uptake into the polymer because of the inherent hydrophobic nature of LA units. A significant drop in the M_w was observed only after 105 days of degradation as shown in Figure 6.12 A. This decrease in M_w with degradation time signified the hydrolysis of the PDLLA. Hence incorporation of GCV did not significantly affect the degradation rate constant of PDLLA, as shown in Table 6.3.

The incorporation of the drug GCV increased the degradation rate constant k' of PLGA 75/25 I.V. 0.94, as shown in Table 6.3. Linear plots were obtained for both PLGA 75/25 I.V. 0.94 7% GCV and PLGA 75/25 I.V. 0.94 18% GCV microspheres. This was unlike the $\ln(M_n)$ profile of the pure PLGA 75/25 I.V. 0.94 microspheres, where, two k' values were obtained, the k' value before 35 days of degradation (0.013) was much smaller than the k' value after 35 days of degradation (0.0576). This might be seen as a first indication that auto-catalytic effect accelerating polymer degradation at the center of the microspheres did not play a major role in the drug-loaded systems. Pronounced auto-catalytic effect would only lead to deviations from the first order kinetics of polymer degradation instead (increasing degradation rate constant with time) as observed in the pure PLGA 75/25 I.V. 0.94 microspheres in Figure 5.7 and discussed in Chapter 5.

In the case of the PLGA 75/25 I.V. 0.94 18% GCV, according to the plot of the cumulative release curve of GCV-loaded microspheres (Figure 7.1 in Chapter 7), the release pattern exhibited a huge initial burst release, followed by a long diffusive phase. It is believed that the initial burst release of GCV left behind small pores and micro-channels on and near the surface. This allowed for larger water uptake, thus increasing the dissolution and diffusion of GCV and water-soluble degradation products from the matrix. This allowed the hydrolysis of the polymer backbone to occur with little and/or no auto-catalyst effect.

As for PLGA 75/25 I.V. 0.94 7% GCV, no initial burst of GCV was observed. Hence the water uptake rate should be similar to that of the pure PLGA 75/25 I.V. 0.94 microspheres. It is believed that the hydrolysis of the ester bonds gradually resulted in shorter polymer chains with free carboxylic acid end groups. This would in turn, decrease the pH at the core where they were trapped inside the polymeric matrix. From Figure 6.1, GCV in an acidic environment would be protonated as $\text{GCV} + \text{H}_2\text{O} \rightleftharpoons \text{HGCV}^+ + \text{OH}^-$. Here GCV behaved as a weak alkaline, where it would react with H^+ , decreasing the concentration of the acid in the core. The basic-catalyst effect due to protonated GCV was more significant in the hydrolytic degradation rate of PLGA 75/25 I.V. 0.94 7% GCV ($k'=0.0764$) than the auto-catalyst effect in the hydrolytic degradation rate of PLGA 75/25 I.V. 0.94 ($k'=0.0576$).

From the organic synthesis standpoint, esterification is a reversible chemical reaction, where the reverse reaction is hydrolysis. Equilibrium exists for both sides of reaction, hydrolysis and esterification. In order to shift the equilibrium to the hydrolysis side, excess water, ester and acid catalyst are needed. Another way to shift the equilibrium and promote hydrolysis is to continuously remove the carboxylic acid product. Here the GCV behaved as a weak alkaline, neutralizing the carboxylic acid and shifting the equilibrium towards hydrolysis. This accounted for the accelerated hydrolysis observed in PLGA 75/25 I.V. 0.94 7% GCV compared to the pure microspheres which underwent auto-catalyst effect of the carboxylic acid products.

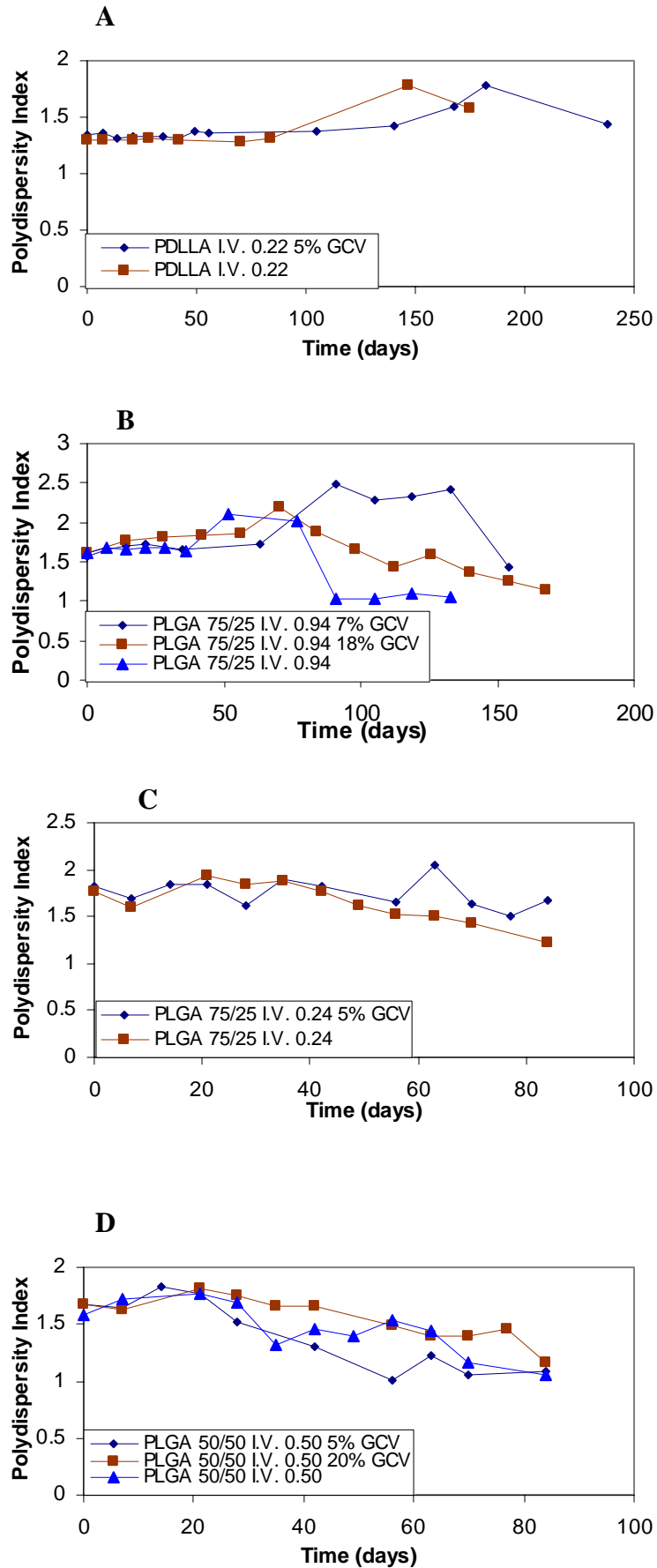
The same could be applied to PLGA 75/25 I.V. 0.24 5% GCV, PLGA 50/50 I.V. 0.50 5% GCV and PLGA 50/50 I.V. 0.22 7% GCV. Although no auto-catalyst effect was observed on the polymer hydrolysis of the corresponding pure polymeric microspheres, the protonated GCV is believed to accelerate the hydrolysis process of the low GCV-loaded

microspheres due to basic-catalyst effect, resulting in the larger k' values as shown in Table 6.3.

In the case of PLGA 50/50 I.V. 0.50 20% GCV, the degradation rate constant k' (0.0469) was similar to the k' of the pure PLGA 50/50 I.V. 0.50 (0.0525) within experimental error. The release pattern exhibited a huge initial burst release, followed by a long diffusive phase. It is believed that the initial burst release of GCV left behind small pores and micro-channels on and near the surface. This allowed for larger water uptake, thus increasing the dissolution and diffusion of GCV and water-soluble degradation products from the matrix. This allowed the hydrolysis of the polymer backbone to occur with little and/or no basic-catalyst effect or auto-catalyst effect on the hydrolytic degradation rate. This would explain for the similarity in the k' value for PLGA 50/50 I.V. 0.50 20% and pure PLGA 50/50 I.V. 0.50 microspheres.

As shown in Table 6.2 and Table 6.3, T_g decrease rate constant k and the degradation rate constant k' coincided with each other in most cases, where k' and the corresponding k for one specific microspheres indicated the same degradation tendency. The exception was the PLGA 75/25 I.V. 0.94 7% GCV and PLGA 75/25 I.V. 0.94 18% GCV, where the k' indicated that the former degraded faster, while the k indicated that the later degraded faster. The decrease in T_g was a combination of plasticization of amorphous material, decrease in M_w and loss of amorphous material. While, the incorporation of GCV accelerated the hydrolysis mostly due to the basic-catalyst effect instead of due to the small pores and micro-channels allowing more water uptake thus hastening the hydrolysis.

6.2.2 Polydispersity Index (PI)



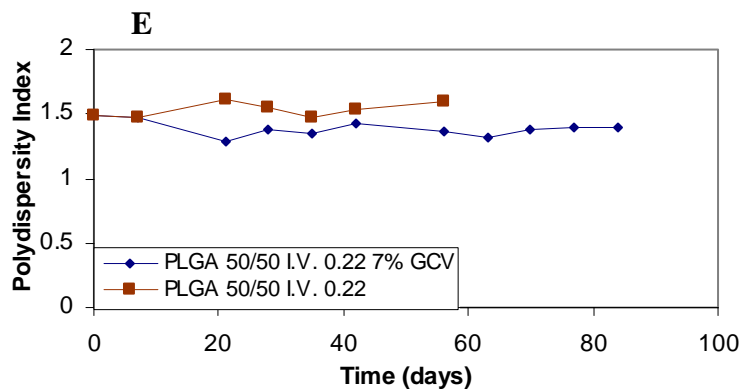


Figure 6.13 Polydispersity Index of A) PDLLA I.V. 0.22 5% GCV(◆) and PDLLA I.V. 0.22(■); B) PLGA 75/25 I.V. 0.94 7% GCV (◆), PLGA 75/25 I.V. 0.94 18% GCV (■) and PLGA 75/25 I.V. 0.94 (▲); C) PLGA 75/25 I.V. 0.24 5% GCV (◆) and PLGA 75/25 I.V. 0.24 (■); D) PLGA 50/50 I.V. 0.50 5% GCV (◆), PLGA 50/50 I.V. 0.50 20% GCV (■) and PLGA 50/50 I.V. 0.50 (▲); E) PLGA 50/50 I.V. 0.22 7% GCV (◆) and PLGA 50/50 I.V. 0.22 (■) microspheres as a function of degradation time.

The PI profile for PDLLA I.V. 0.22 was similar to PLGA 75/25 I.V. 0.94, where a maximum was observed with degradation time. The PI of the pure PDLLA I.V. 0.22 microspheres increased very slowly and reached a maximum only after 182 days of degradation. As for the 5% GCV-loaded microspheres, the PI increased and reached its maximum after 147 days of degradation before decreasing again. From Table 6.3, when the k' values for the GCV-loaded and pure PDLLA microspheres were compared, the k' values indicated that the GCV incorporated had little and/or no effect on the degradation profile. Since the PI profiles only showed the distribution of molecular weight fractions, where larger PI meant a broader distribution while a smaller PI indicated a narrower distribution, the k' values obtained from the change in the natural logarithm of number-average molecular weight with degradation time was more reliable in the comparison of degradation rates.

For PLGA 75/25 I.V. 0.94, the PI of the pure microspheres increased after 52 days of degradation and decreased after 91 days of degradation. As for the polymer with the GCV content of 7%, the PI increased only after 91 days of degradation and began to decrease

after 133 days. When the GCV content was increased to 18%, the PI reached a maximum after 70 days of degradation and decreased thereafter. Similar to PDLA I.V. 0.22, the change in the PI profiles of these polymers did not tally with the k' values. The k' values obtained from $\ln(M_n)$ versus degradation time profile was more reliable in predicting the degradation rate.

For the PLGA 75/25 with the lower initial intrinsic viscosity of 0.24, the addition of GCV in the polymer did not significantly affect the PI profile with degradation time. It was similar to that of pure PLGA 75/25, I.V. 0.24, where the PI decreased continuously with degradation time. The same was observed for the PLGA 50/50 polymers, where the PI for both GCV-loaded and pure polymers decreased at the same rate with degradation time irrespective of initial molecular weight.

The initial increase in the polydispersity index was due to a mixture of high- and low-molecular weight fractions, while the subsequent decrease thereafter, was due to a more uniform weight fractions. These changes could be attributed to the high probability of preferential breaking of long PLGA chains during the early stages of degradation compared to the shorter chains at the later stages of degradation¹¹¹. This was observed in the sharp reduction in M_w at short degradation times followed by a gentle decrease in M_w at long degradation times. The polydispersity index decreased, indicating a more uniform molecular weight fraction with longer degradation time due to hydrolytic scission of the polymer chains. The rate of decrease in the polydispersity index was slightly faster in the PLGA 50/50 series as compared with the PLGA 75/25 series, which indicates that PLGA 50/50 degraded faster than PLGA 75/25. The PDLA degraded the slowest.

6.3 Changes in pH

The pH of saturated GCV in distilled water aqueous solution (2.6 mg/ml) measured at 20 °C is 7.48 while the pH of the saturated GCV in PBS buffer solution (2.6 mg/ml) (pH=7.00 at 20 °C) measured at 20 °C is 6.97. Although GCV is slightly basic in nature due to the amino groups in its chemical structure, the buffer solution was able to neutralize the base in GCV. This in turn would prohibit basic-catalyst effect on hydrolytic degradation due to high pH during the initial stages of degradation³⁷. However as degradation progressed and soluble acidic products were formed from the hydrolytic chain scission of ester bonds, the amino groups would help neutralize these acidic oligomers/monomers. This would in turn stabilize the pH of the degrading medium at around pH=7.0.

Lactic acid, a degradation product of poly(lactic acid) and poly(lactic-co-glycolic acid), for example, has a very high water solubility. Due to the α -hydroxyl group, the pK_a of 3.8 is lower than that of unsubstituted aliphatic carboxylic acids which usually have pK_a values of about 4.5⁴⁵. The low pK_a in combination with high water solubility gives lactic and glycolic acid the potential to substantially decrease the pH inside an eroding polymer matrix. The decreased pH and the generated carboxylic acids would cause auto-catalyst effect, leading to the faster erosion inside poly(α -hydroxyl acids) as compared to their surface³⁷.

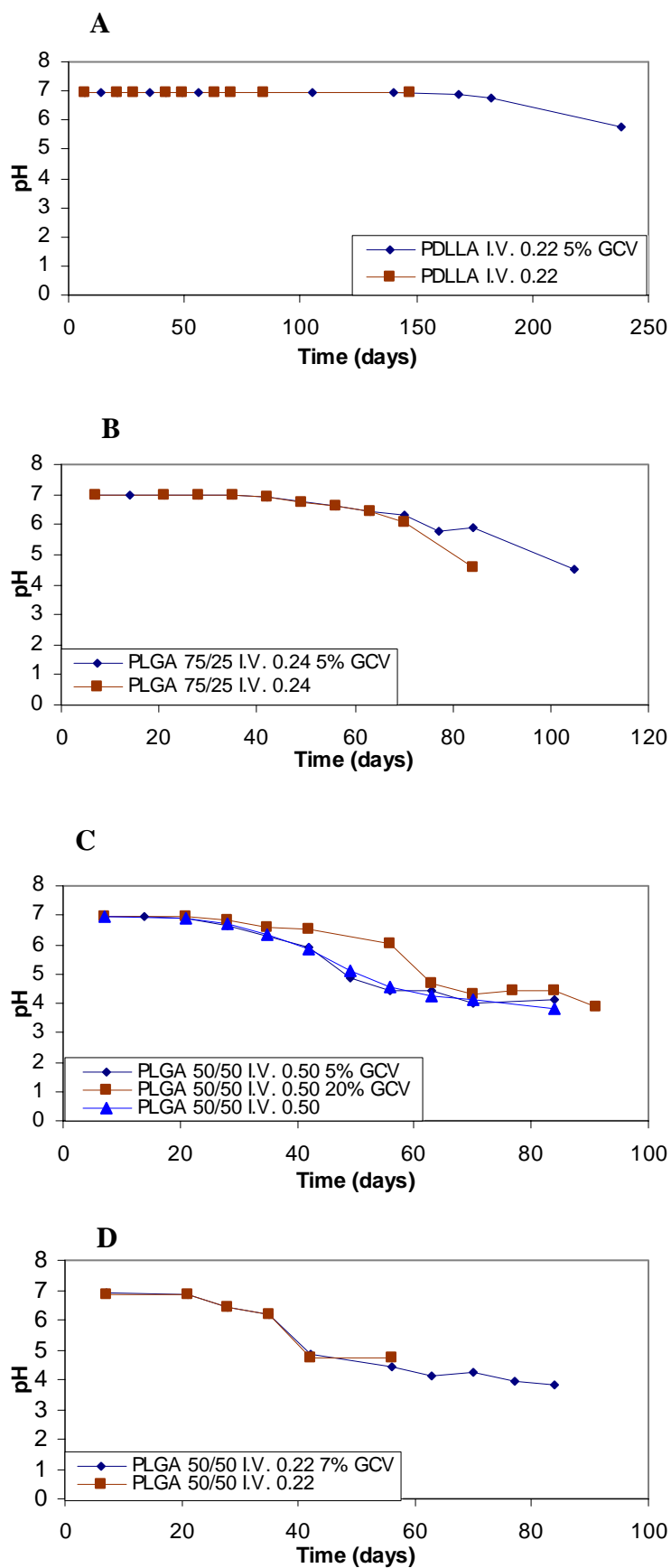


Figure 6.14 pH value of A) PDLLA I.V. 0.22 5% GCV (◆) and PDLLA I.V. 0.22 (■); B) PLGA 75/25 I.V. 0.24 5% GCV (◆) and PLGA 75/25 I.V. 0.24 (■); C) PLGA 50/50 I.V. 0.50 5% GCV (◆), PLGA 50/50 I.V. 0.50 20% GCV (■) and PLGA 50/50 I.V. 0.50 (▲); D) PLGA 50/50 I.V. 0.22 7% GCV (◆) and PLGA 50/50 I.V. 0.22 (■) microspheres as a function of degradation time.

Figure 6.14 showed the pH profiles of pure and GCV-loaded PDLLA and PLGA microspheres. In all the samples, GCV-loaded and pure microspheres, the pH decreased with degradation time. The decrease in pH with degradation indicated the release of acidic oligomers/monomers via hydrolytic degradation. Hydrolysis of ester bond linkage lead to formation of shorter chains with carboxylic acidic end groups that would finally lead to formation of monomers such as glycolic acids and lactic acids.

Looking at the changes in mass with degradation time (Figure 6.15), it was observed that the drastic drop in pH began when mass loss started.

The decrease in pH for PDLLA I.V. 0.22 was the slowest among the polymers investigated. The pH of the PDLLA I.V. 0.22 5% GCV microspheres remained unchanged up to 168 days of degradation and was 5.78 after 238 days of degradation. The incorporation of GCV did not affect the pH profiles of PDLLA I.V. 0.22 significantly.

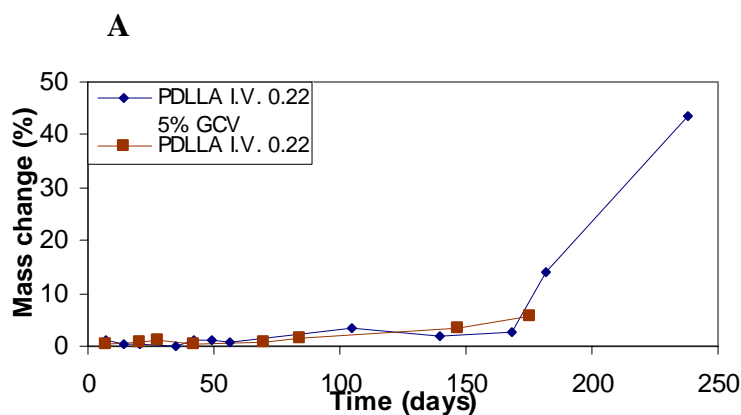
In the PLGA 75/25 I.V. 0.24 and PLGA 50/50 I.V. 0.50, the GCV retarded the rate in which pH decreased. The pH profile of both GCV-loaded and pure PLGA 75/25 I.V. 0.24 microspheres were similar to one another up to 63 days of degradation. The pH of the pure PLGA 75/25 I.V. 0.24 microspheres dropped to 6.05 after 70 days of degradation, while, the pH was only 6.33 for the PLGA 75/25 I.V. 0.24 5% GCV microspheres.

In the case of the PLGA 50/50 I.V. 0.50 microspheres, the pure PLGA 50/50 I.V. 0.50 microspheres and the PLGA 50/50 I.V. 0.50 5% GCV had similar pH versus degradation time profile as shown in Figure 6.14 D. The pH remained approximately unchanged in the first 28 days of degradation, followed by a decrease in pH to 4.24 after 63 days of degradation. In the case of PLGA 50/50 I.V. 0.50 20% GCV, the pH decreased much

slower than the pure and 5% GCV microspheres. From Figure 6.12 and Table 6.2, it was concluded that the lower GCV-loaded microspheres hydrolyzed faster due to the basic-catalyst effect of protonated GCV. The slower decrease in the pH for the higher GCV-loaded microspheres due to little an/or no catalyst effect (auto- and basic-) on their hydrolytic degradation further supported the basic-catalyst effect due to the GCV protonating process in the lower GCV-loaded microspheres.

As for the PLGA 50/50 I.V. 0.22, the GCV did not significantly affect the pH versus degradation time profile as of the pure microspheres (Figure 6.14 E). According to the changes in mass with respect to degradation time for the pure and GCV-loaded PLGA 50/50 I.V. 0.22 microspheres (Figure 6.15 E), the onset of mass loss for both microspheres was observed after 21 days of degradation. This corresponded with the slight decrease in pH with degradation time. From the cumulative GCV release curve (Figure 7.1, Chapter 7), it was observed that GCV was released between 21 and 35 days of degradation. This GCV released could neutralize acidic products from hydrolysis. Hence the slight decrease in pH with degradation. After 35 days of degradation, no more GCV was found in the surrounding medium. Hence the fast pH decrease was simply due to the hydrolysis of the polymer chains.

6.4 Changes in Mass



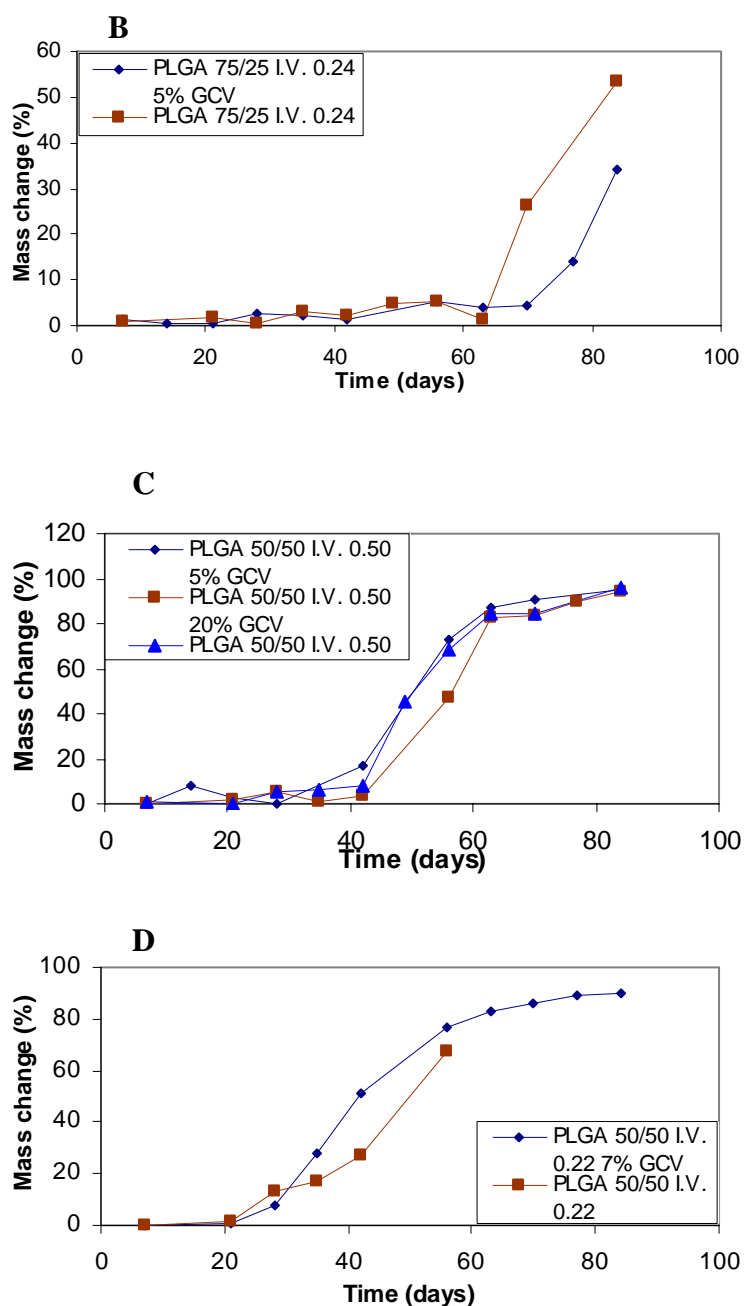


Figure 6.15 Mass change of A) PDLLA I.V. 0.22 5% GCV (◆) and PDLLA I.V. 0.22 (■); B) PLGA 75/25 I.V. 0.24 5% GCV (◆) and PLGA 75/25 I.V. 0.24 (■); C) PLGA 50/50 I.V. 0.50 5% GCV (◆), PLGA 50/50 I.V. 0.50 20% GCV (■) and PLGA50/50 I.V. 0.50 (▲); D) PLGA 50/50 I.V. 0.22 7% GCV (◆) and PLGA 50/50 I.V. 0.22 (■) microspheres as a function of degradation time.

From Figure 6.15, the mass loss for PDLLA was much slower than the PLGA 50/50 and PLGA 75/25 polymers irrespective of the initial I.V. or molecular weight used. Similar to PLGA, PDLLA degraded through bulk erosion by hydrolytic cleavage of ester bond linkages. Mass loss occurred when the molecular weight had decreased to the point such that fragments were small enough to diffuse out from the polymer bulk.

From Figure 6.15A, no significant mass loss was observed for PDLLA I.V. 0.22 pure and 5% GCV-loaded even after 150 days of degradation. It was only after 180 days of degradation that the mass loss increased as a function of time.

The hydrophobic nature of polymer and steric effects modified hydrolysis rates. For example, the higher reactivity of poly (glycolic acid) as compared to poly(lactic acid) appeared to be due to the methyl groups present in PDLLA which hindered the attack of water.

No significant mass loss was detected for the pure and 5% GCV-loaded PLGA 75/25 I.V. 0.24 up to 40 days of degradation despite the decrease in molecular weight with degradation time (Figure 6.16 B). This might be because the short segments produced via hydrolysis were not small enough to leach out and were still trapped inside the polymer matrix. After 40 days of degradation, there was a slow increase in mass loss, which continued up to 70 days of degradation. After 70 days of degradation, the mass loss increased drastically with further degradation. This would be due to the leaching out of the degradation products from the polymer matrix.

As for PLGA 50/50 I.V. 0.50, no significant mass loss was observed for the pure and GCV-loaded microspheres in the first 30 days of degradation. The mass loss that followed after 30 days of degradation increased as a function of time, reaching 100 % after 84 days of degradation. The mass loss observed was attributed to the leaching of GCV and degradation products into the surrounding medium for the GCV-loaded microspheres. The degradation pattern of PLGA was bulk erosion, in which the rate for water penetrating the device exceeded the rate for the polymer to be converted into water-soluble materials. It is believed that the degradation of the PLGA polymers started as

soon as it was placed in the PBS buffer medium with the hydrolytic cleavage of ester bond linkages. This hydrolysis rate would increase with degradation time due to the basic-catalyst effect of the protonated GCV. The molecular weight would continue to decrease to the point that fragments were small enough to be diffused out from the polymer bulk, causing mass loss. The mass change profiles for the 5% and 20% GCV-loaded PLGA 50/50 I.V. 0.50 microspheres were similar to the mass change profile of the pure microspheres. This could be due to the high experimental error in the mass readings where small changes to the mass could not be determined within experimental error.

As for PLGA 50/50 I.V. 0.22 microspheres (Figure 6.15 E), both the pure and 7% GCV-loaded microspheres showed mass loss after 21 days of degradation. The mass loss was due to the leaching of the degradation products for the pure microspheres. In the GCV-loaded microspheres, the mass loss was due to the leaching of GCV and degradation products into the surrounding medium. The degradation by hydrolysis commenced once the polymers were placed in the medium. However, mass loss was only observed when hydrolytic chain scission of ester links had reached a stage whereby the molecular weight loss had decreased to the point such that fragments were small enough to diffuse out from the polymer.

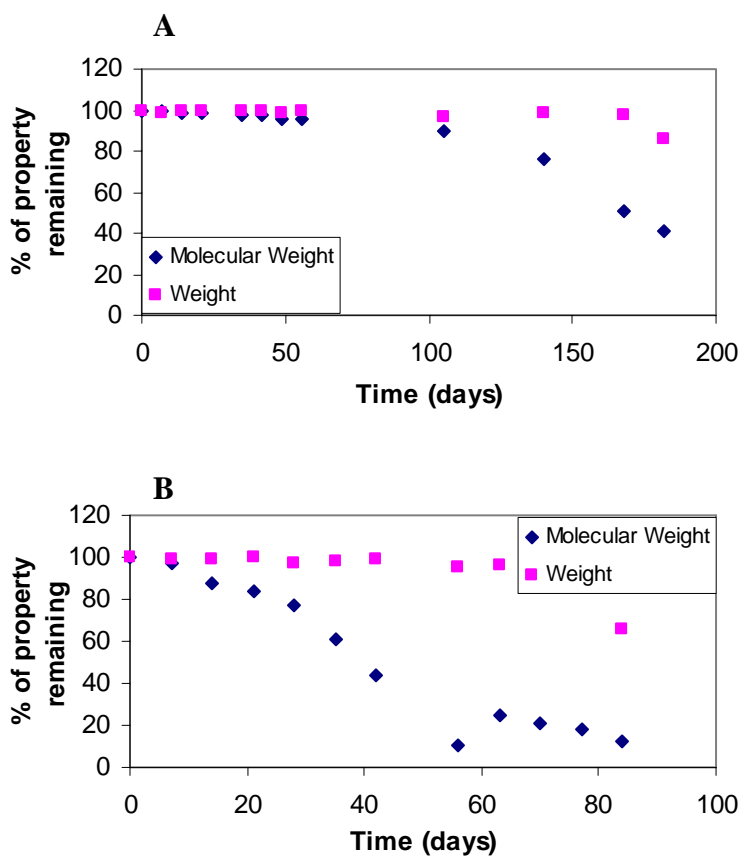
The time when mass loss for all the pure and GCV-loaded PLGA and PDLLA microspheres started was listed in Table 6.4.

Sample	LA:GA ratio	I.V.	GCV content (%)	Commence time of mass loss (days)
PDLLA	100:0	0.22	0	147
			5	140
PLGA	75:25	0.24	0	49
			5	56
	50:50	0.50	0	42
			5	42
			20	42
	0.22	0.22	0	28
7			28	

Table 6.4 Commence time of mass loss for pure and GCV-loaded PLGA, PDLLA microspheres

From Table 6.4, PDLLA degraded the slowest, followed by PLGA 75/25 and PLGA 50/50. In addition to it, GCV did not significantly affect the onset of mass loss and did not increase the rate of mass loss for most of the samples.

6.4.1 Comparison between molecular weight and changes in mass.



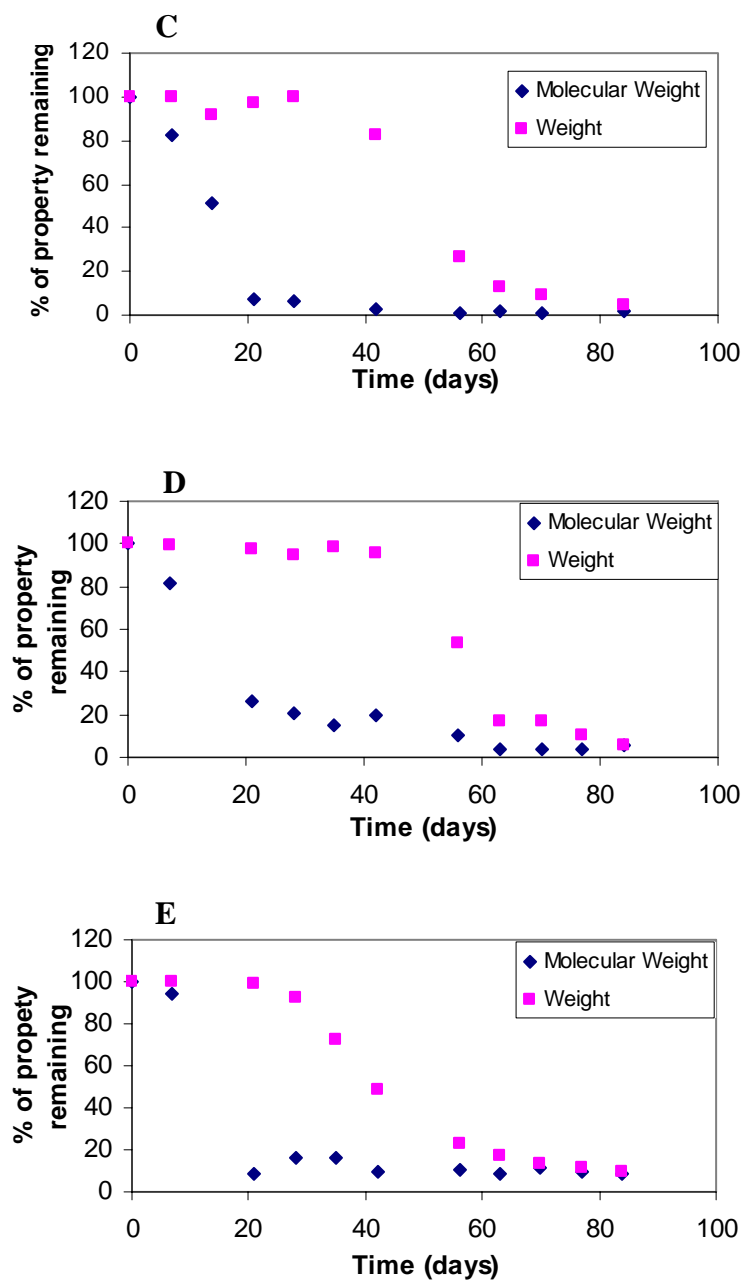


Figure 6.16 Changes in percentage of normalized M_w (◆) and normalized weight (■) of A) PDLGA I.V. 0.22 5% GCV; B) PLGA 75/25 I.V. 0.24 5% GCV; C) PLGA 50/50 I.V. 0.50 5% GCV; D) PLGA 50/50 I.V. 0.50 20% GCV; E) PLGA 50/50 I.V. 0.22 7% GCV microspheres during degradation at 37 °C.

It was observed that the M_w of all the PLGA microspheres had to decrease to about 10 % to 20 % of its initial M_w before any obvious mass loss was observed (Figure 6.16 B to E). This suggested that the acidic polymeric fragments produced during hydrolysis were trapped inside the polymer and were unable to escape into the aqueous surrounding medium. Extensive hydrolysis of the polymer chains had to occur before soluble

oligomers or monomers were released into the surrounding medium, causing mass loss. Therefore the molecular weight of the polymers had to be sufficiently reduced before mass loss can be detected. This process corresponded to bulk degradation, which is commonly observed in PLGA polymers. While for the PDLLA I.V. 0.22 pure and GCV-loaded microspheres, the M_w only decreased to about 30 % to 40 % of its initial M_w before mass loss was observed (Figure 6.16 A). PDLLA I.V. 0.22 was homopolymer with only LA-LA units in its backbone, the hydrolytic chain scission of the polymer backbone was uniform and steady. As for the PLGA copolymers, because of the existence of GA-GA units and GA-LA units in their backbones, the preferential hydrolytic chain scission of these units resulted in the drastic decrease in M_w during early stages of degradation. The degradation time frame for the PDLLA I.V. 0.22 was much longer than the PLGA copolymers, the degradation was not finished during the investigation time frame (182 days). When the M_w of the PDLLA I.V. 0.22 5% GCV microspheres decreased to 30 % to 40 % of its initial M_w , the SEM photograph showed that the microspheres were disintegrated (Figure 6.17 D). The mass loss of the PDLLA I.V. 0.22 5% GCV microspheres by this time was due to the sample disintegration rather than polymer degradation.

6.5 SEM

SEM photographs taken of the dried degraded GCV-loaded microspheres were shown in Figures 6.17 to 6.22 respectively. The surface of the undegraded GCV-loaded microspheres for all polymers were smooth and without any drug particles as shown in Figure 4.4 in Chapter 4, suggesting that the drugs were encapsulated inside the polymer matrix.

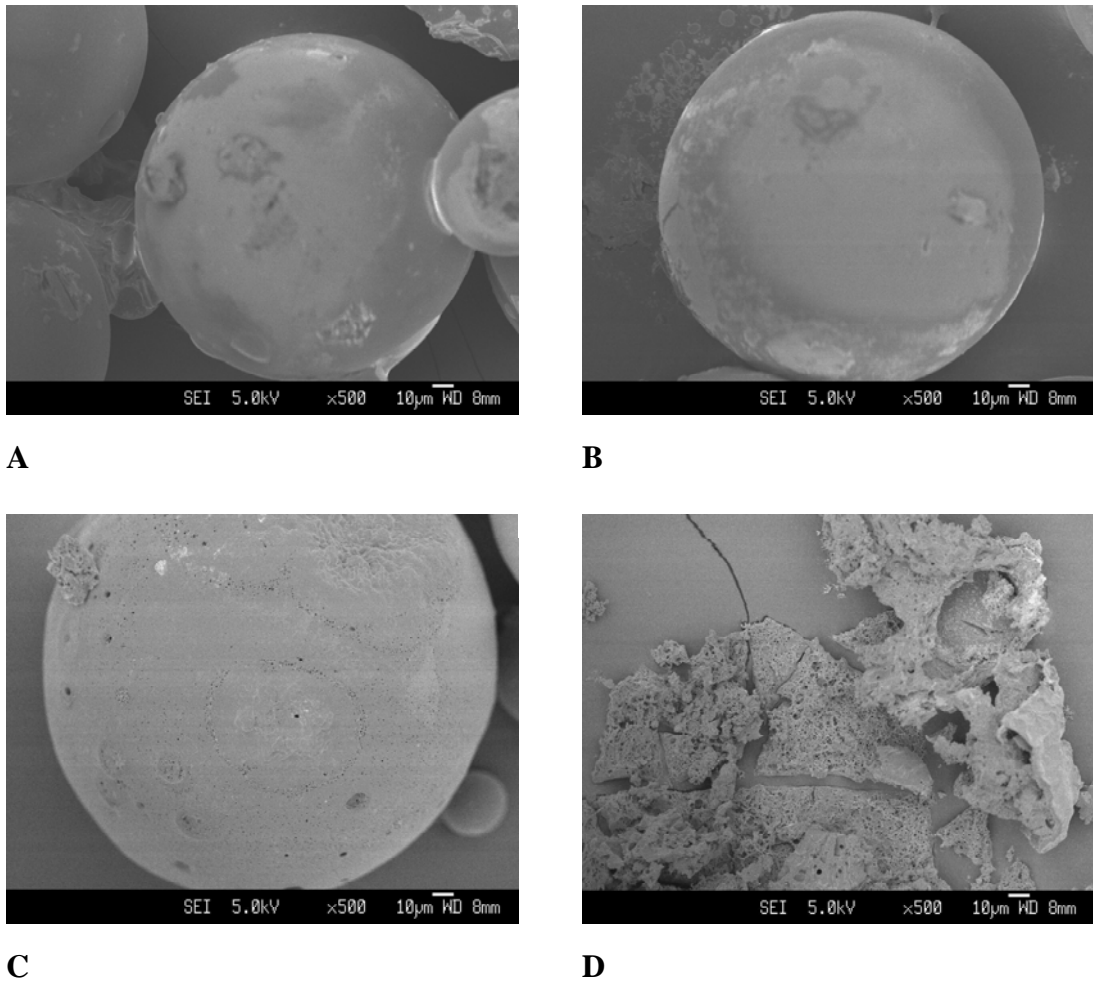
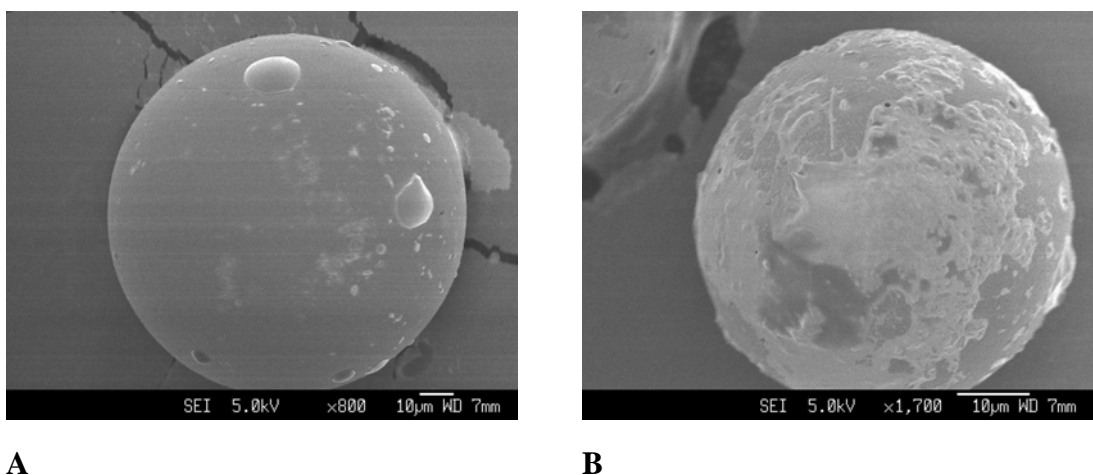


Figure 6.17 SEM photographs of PDLLA I.V. 0.22 5% GCV microspheres A) 7 days; B) after 105 days; C) 168 days and D) 182 days of degradation.

For PDLLA I.V. 0.22 5% GCV microspheres, only blister-like formation was observed on the surface of the microspheres even after 168 days of degradation. By this time, the M_w had dropped to 9,900 dalton and the microspheres were brittle and fragmented easily. The samples were gel-like after 182 days of degradation.



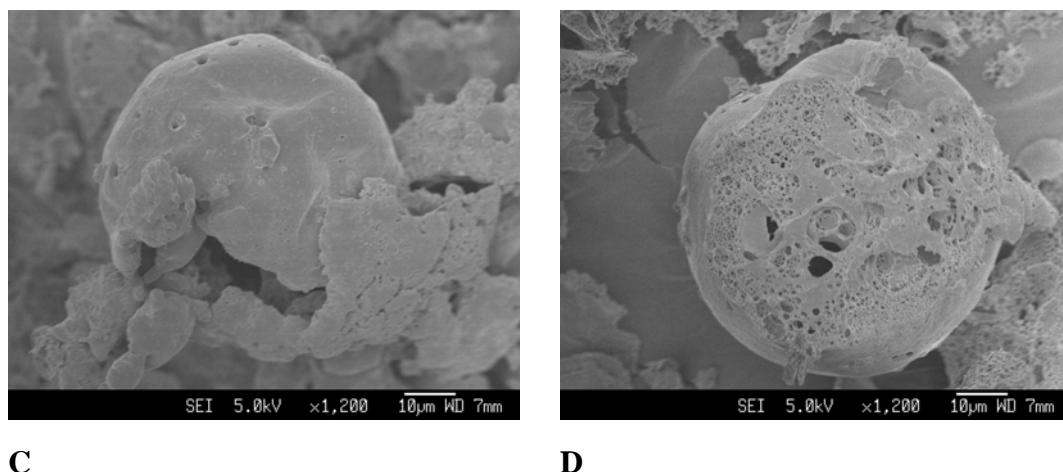
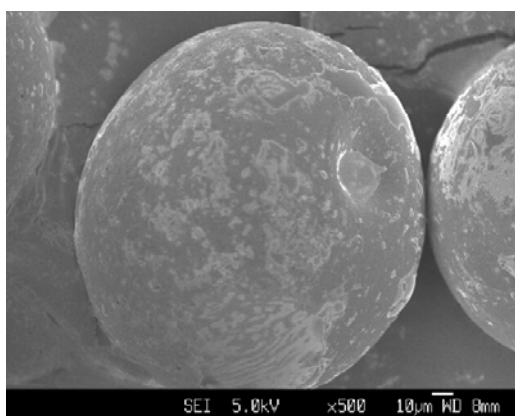
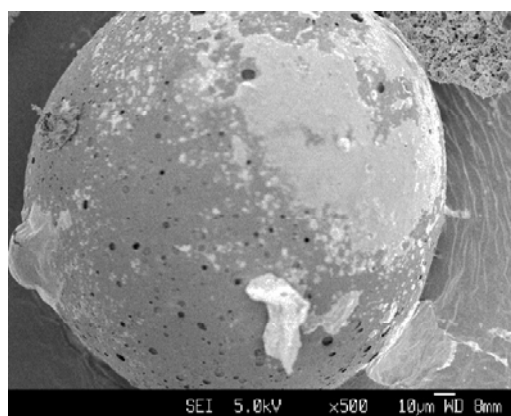
**C****D**

Figure 6.18 SEM photographs of PLGA 75/25 I.V. 0.94 7% GCV microspheres A) 7 days; B) 105 days; C) 119 days and D) 154 days of degradation.

The surface of the degraded PLGA 75/25 I.V. 0.94 7% GCV microspheres remained relatively smooth to about 63 of degradation. After 105 days of degradation, the microspheres showed blister-like formations on the surface, and by 119 days, pores were observed on the surface and throughout the microspheres. By this time, the M_w had dropped to about 13,000 dalton and the microspheres were brittle and fragmented easily. No SEM photographs could be taken after 154 days of degradation as the sample were gel-like with further degradation. The M_w at this time was 6,000 dalton.

**A****B**

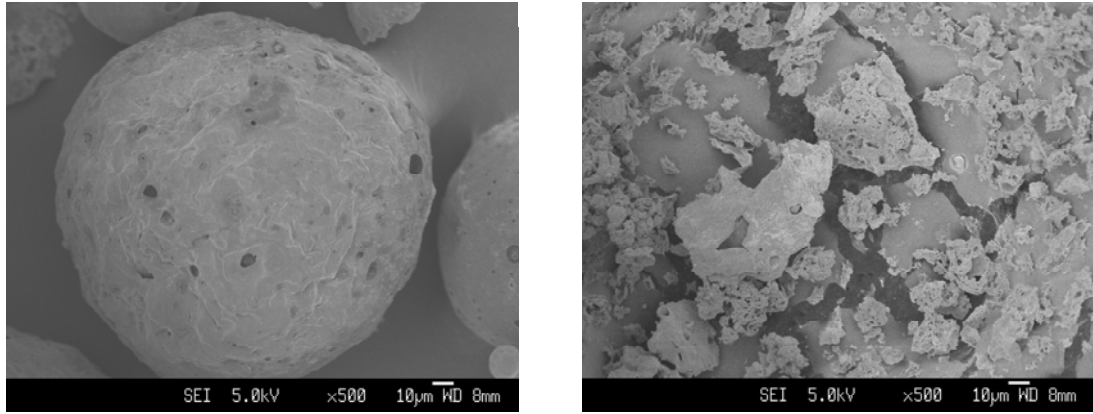
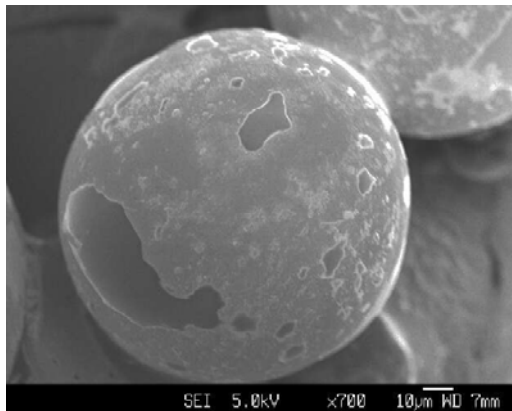
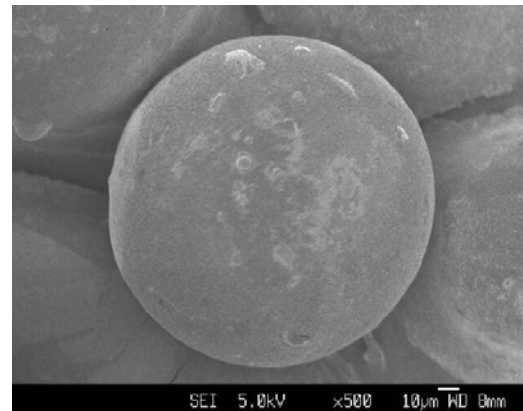
**C****D**

Figure 6.19 SEM photographs of PLGA 75/25 I.V. 0.94 18% GCV microspheres A) 14 days; B) 70 days; C) 84 days and D) 98 days of degradation.

In the case of the PLGA 75/25 I.V. 0.94 18% GCV microspheres, the degraded microspheres had blister-like formations on the surface after 70 days of degradation and after 84 days of degradation, the surface of the microspheres were uneven with pores clearly observed on the surface and throughout the microspheres. After 98 days of degradation, the M_w drop to about 13,000 dalton and the microspheres were brittle and fragmented easily. The samples were gel-like after 112 days of degradation.

**A****B**

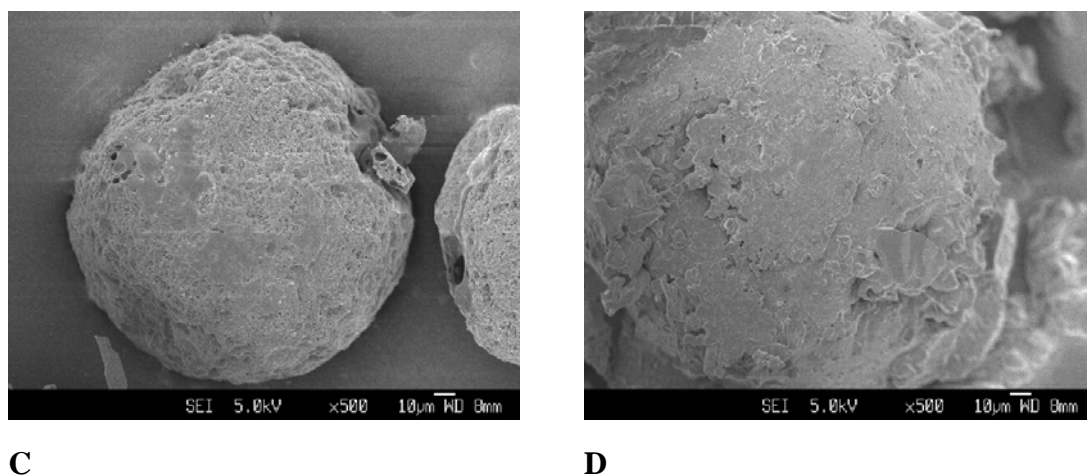


Figure 6.20 SEM photographs of PLGA 75/25 I.V. 0.24 5% GCV microspheres A) 7 days; B) 28 days; C) 35 days and D) 42 days of degradation.

In the case of the PLGA 75/25 I.V. 0.24 5% GCV microspheres, the degraded microspheres showed blister-like formations on the surface after 14 days of degradation and after 35 days of degradation, pores were observed on the surface and throughout the microspheres. By this time, the microspheres were brittle and fragmented easily. The corresponding M_w was about 14,000 dalton. The samples were gel-like after 42 days of degradation, corresponding to the M_w of about 10,000 dalton.

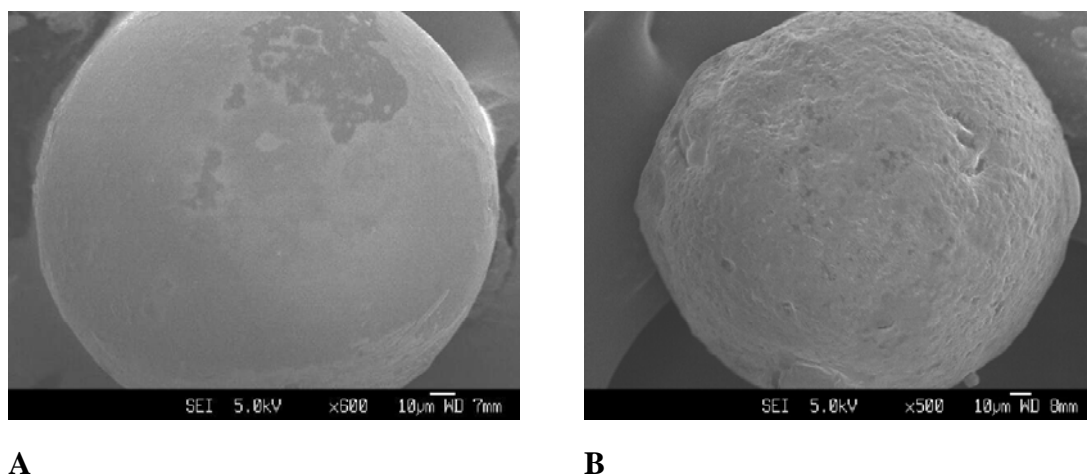


Figure 6.21 SEM photographs of PLGA 50/50 I.V. 0.50 5% GCV microspheres A) 7 days and B) 14 days of degradation.

As for the PLGA 50/50 I.V. 0.50 5% GCV, no SEM photographs could be taken after 14 days of degradation as the samples were already brittle and fragmented easily. Roughening of surface was observed after 14 days of degradation, with the corresponding

M_w of about 18,000 dalton. By 21 days of degradation, the M_w had decreased to 2,700 dalton and the microspheres were gel-like.

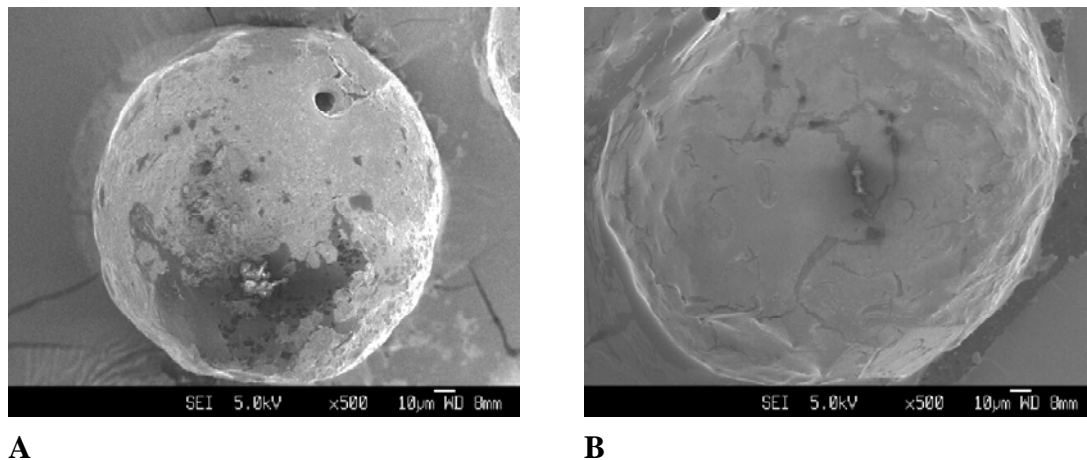


Figure 6.22 SEM photographs of PLGA 50/50 I.V. 0.50 20% GCV microspheres A) 7 days and B) 21 days of degradation.

As for the PLGA 50/50 I.V. 0.50 20% GCV, no SEM photographs could be taken after 28 days of degradation as the samples had become gel-like by this stage. The M_w at this time was 7,400 dalton.

No SEM photographs were taken for PLGA 50/50 I.V. 0.22 7% GCV microspheres as the samples had become gel-like in nature after 1 week of degradation. The M_w drop to 11,000 dalton after 1 week of degradation and dropped drastically to 2,000 dalton after 21 days of degradation.

SEM results confirmed that the degradation rate of GCV-loaded microspheres from the PLGA 75/25 series was slower than the GCV-loaded microspheres from the PLGA 50/50 series. The degradation rate of GCV-loaded PDLLA was the slowest.

The incorporation of GCV inside the microspheres affected the surface morphology of degradation. The GCV-loaded microspheres could only maintain their spherical shape at a M_w of about 13,000 to 14,000 dalton, as compared to the pure microspheres which

maintained their spherical shape up to a M_w of about 10,000 dalton. The GCV-loaded microspheres were gel-like when their M_w decreased to just below 10,000 dalton, while the pure microspheres were gel-like only when the M_w decreased to 3,000 to 4,000 dalton.

6.6 Conclusions

GCV was successfully incorporated into the polymer and was in a crystalline state in the microspheres. The incorporation of GCV showed an effect in the thermograms. An endothermic peak for GCV at about 220 °C to 230 °C was detected in the heat scans of GCV-loaded microspheres for all the polymers used. As the polymers underwent hydrolytic degradation, multiple melting peaks were observed for all the GCV-loaded microspheres. These melting peaks were generated by the crystallization of fragments of degraded chains trapped in the microspheres.

Before the GCV-loaded microspheres were used for the degradation test, the characterization of these microspheres showed that the incorporation of GCV into the microspheres did not significantly change the initial T_g and M_w of the polymers. The incorporation of GCV, however, affected the T_g and M_w profile with respect to degradation time. It is believed that the incorporation of GCV affected the T_g decrease profile due to accelerated water uptake rate caused by small pores and channels left behind after GCV had dissolved and released to the surrounding medium. Hence incorporation of GCV accelerated the T_g decrease rate of PLGA 75/25, PLGA 50/50 and PDLLA.

The pH of the degradation medium was maintained within the range between 2.2 and 9.4 during the entire time of investigation in. In this pH range, the GCV was mainly neutral,

with no-charged groups. Theoretically, GCV would not alter degradation through chemically affecting the hydrolysis.

The incorporation of GCV did not significantly affect the degradation rate constant of PDLLA. The incorporated GCV was believed to accelerate the hydrolysis process of the low GCV-loaded PLGA microspheres due to basic-catalysis, which resulted in larger k' values compared with pure and high GCV-loaded PLGA microspheres. In the high GCV-loaded PLGA microspheres, the initial burst left behind small pores and micro-channels on and near the surface. This allowed for larger water uptake, thus increasing the dissolution and diffusion of GCV and water soluble degradation products from the matrix. This allowed the hydrolysis of the polymer backbone to occur with little and/or no auto-catalyst effect. Hence the smaller k' values in high GCV-loaded PLGA microspheres were obtained compared with low GCV-loaded PLGA microspheres. The incorporation of GCV increased the k' value but to a certain limit, where excess GCV decelerated and/or had no affect on the k' value.

The rate of decrease in the polydispersity index was slightly faster in the PLGA 50/50 series as compared with the PLGA 75/25 series, which indicates that PLGA 50/50 degraded faster than PLGA 75/25. The PDLLA degraded the slowest.

In all the samples, GCV-loaded and pure microspheres, the pH decreased with degradation time. The decrease in pH with degradation indicated the release of acidic oligomers/monomers via hydrolytic degradation. Hydrolysis of ester bond linkage lead to formation of shorter chains with carboxylic acidic end groups that would finally lead to formation of monomers such as glycolic acids and lactic acids. The incorporation of GCV did not affect the pH profiles of PDLLA I.V. 0.22 significantly. In the PLGA 75/25 I.V.

0.24 and PLGA 50/50 I.V. 0.50, the GCV retarded the rate in which pH decreased. As for the PLGA 50/50 I.V. 0.22, the GCV did not significantly affect the pH versus degradation time profile as of the pure microspheres.

The mass loss for PDLA was much slower than the PLGA 75/25 and PLGA 50/50 polymers irrespective of the initial I.V. or molecular weight used. PDLA degraded the slowest, followed by PLGA 75/25 and lastly PLGA 50/50. The addition of GCV did not significantly affect the onset of mass loss neither did it increase the rate of mass loss.

It was observed that the M_w of all the PLGA microspheres had to decrease to about 10 % to 20 % of its initial M_w before any obvious mass loss was observed (Figure 6.16 B to E). While for the PDLA I.V. 0.22 pure and GCV-loaded microspheres, the M_w only decreased to about 30 % to 40 % of its initial M_w before mass loss was observed (Figure 6.16 A).

The GCV-loaded microspheres required a higher M_w (13,000 to 14,000 dalton) to maintain their spherical shape than the pure microspheres (10,000 dalton).

CHAPTER 7

CONTROLLED RELEASE OF DRUG LOADED MICROSPHERES

7.1 Drug Release Studies (*in vitro*)

All the drug release tests were carried out in multiplicity (n=5) to verify the homogeneity of the drug release and the results obtained were averaged.

7.1.1 Fractional Cumulative Release Curve of GCV-loaded microspheres

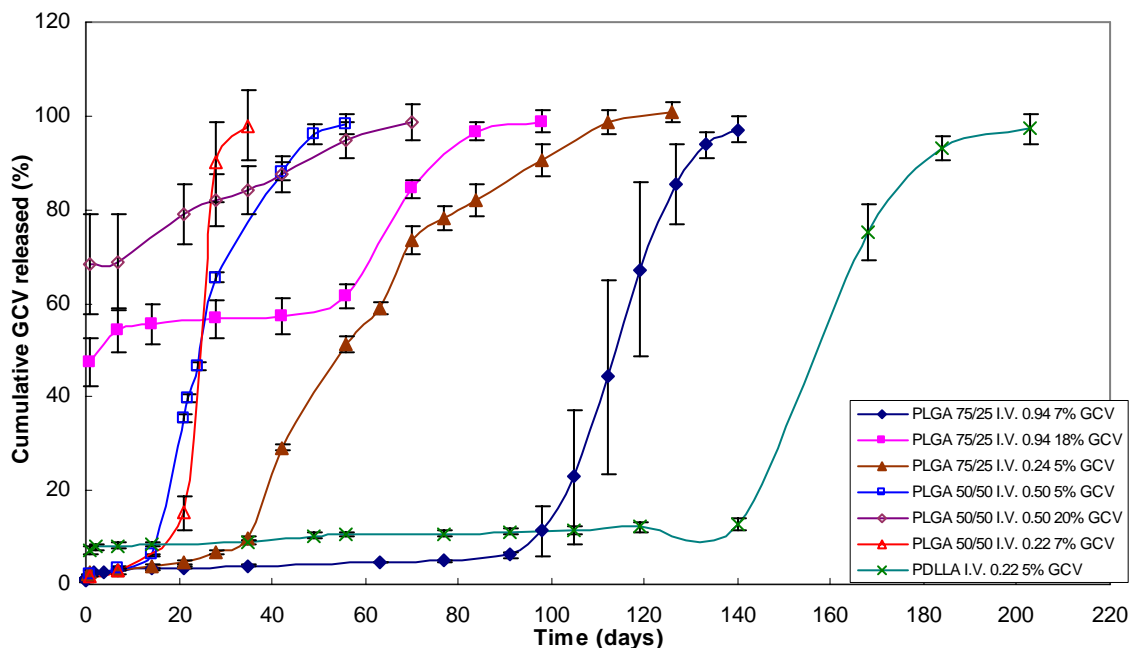


Figure 7.1 Fractional cumulative release of GCV from the PLGA and PDLLA microspheres in phosphate-buffered solution (pH 7.0) at 37 °C. The values are shown as mean \pm SD of n = 5, PLGA 75/25 I.V. 0.94 7% GCV (\blacklozenge), PLGA 75/25 I.V. 0.94 18% GCV (\blacksquare), PLGA 75/25 I.V. 0.24 5% GCV (\blacktriangle), PLGA 50/50 I.V. 0.50 5% GCV (\square), PLGA 50/50 I.V. 0.50 20% GCV (\diamond), PLGA 50/50 I.V. 0.22 7% GCV (\triangle), PDLLA I.V. 0.22 5% GCV (\times).

The microspheres with low GCV payload (5% - 7% wt/wt), such as PLGA 75/25 I.V. 0.94 7% GCV, PLGA 75/25 I.V. 0.24 5% GCV, PLGA 50/50 I.V. 0.50 5% GCV and PLGA 50/50 I.V. 0.22 7% GCV displayed a biphasic release pattern, i.e. a diffusive phase

followed by a burst release. There was no initial burst of GCV in all the low GCV payload PLGA microspheres.

In the PLGA 75/25 I.V. 0.94 7% GCV, the first phase was the diffusive phase which occurred during the first 91 days of immersion, where 6.20 % of GCV was released into the surrounding medium. The rate of GCV released during this period was 0.07 %/day. This was followed by a sharp release of GCV, where 90.92 % of GCV was released in the next 49 days, giving a release rate of 1.86 %/day. After 140 days of immersion, 97.12 % GCV had been released to the surrounding medium. The microspheres continued releasing GCV and by 175 days of immersion, all GCV had been released to the surrounding medium.

As for PLGA 75/25 I.V. 0.24 5% GCV, no initial release of GCV was observed after 1 day of immersion. The diffusive phase lasted for 35 days of immersion, with 9.81 % of GCV released into the PBS solution during that time. The release rate during the diffusive stage was 0.28 %/day. This was followed by a burst release phase due to degradation of the polymer matrix. This stage lasted up to 112 days of immersion and the release rate was 1.16 %/day. By the end of 112 days, 98.78 % of GCV of GCV had been released. No GCV was recorded after 126 days of immersion, indicating all GCV had released into the PBS solution.

In the case of PLGA 50/50 I.V. 0.50 5% GCV, the diffusive phase was even shorter compared with the PLGA 75/25 polymers. The diffusive phase occurred immediately upon immersion up to 14 days of immersion, with the release rate of 0.45 %/day. This was followed by the burst release phase, which occurred in the next 35 days, releasing

95.94 % of GCV into the PBS solution, with the release rate of 2.47 %/day. All GCV was released by the 70th day of immersion.

In PLGA 50/50 I.V. 0.22 7% GCV, during the first 7 days of immersion, only 2.78 % of GCV was released, which amounted to 0.40 %/day. This was followed by burst release of to the 35th day, with the release of up to 97.29 % of GCV, resulting in the release rate of 3.38 %/day. All GCV was released by the 56th day of immersion.

The shorter diffusive phase and faster burst release in the PLGA 50/50 polymers compared to the PLGA 75/25 polymers were due to the faster hydrolytic degradation rate in the PLGA 50/50 polymers. The higher GA content in the PLGA 50/50 polymers made the polymers more hydrophilic in nature. This increased the water uptake, which in turn, increased the rate of hydrolytic degradation. According to Yasukawa, *et al.*⁵³, the large total surface area of microspheres resulted in a severe initial burst of drugs when hydrophilic drugs were used. However, no initial release was observed in all these four groups of PLGA microspheres with low GCV payload (5% - 7% wt/wt). Since these microspheres were of relatively low payload, it was possible that very little GCV were distributed on and near the surface of the microspheres with the bulk of the drug trapped in the polymer matrix, which resulted in almost no initial release. The low concentration of GCV on and near the surface was further supported by the XPS data, where no obvious binding peak and atomic concentration for nitrogen was displayed.

The diffusive phase exhibited stable GCV release, which was achieved by the outward diffusion of GCV through the polymer network and/or diffusion of GCV newly dissolved by water under osmotic pressure. The GCV release in the diffusive phase was affected by the molecular weight and the composition of the polymers. PLGA 50/50 microspheres

exhibited shorter diffusive phase than PLGA 75/25 microspheres. For the polymers with the same LA to GA ratio, e.g. PLGA 50/50, the microspheres of PLGA 50/50 I.V. 0.22 exhibited shorter diffusive phase than PLGA 50/50 I.V. 0.50 microspheres. The same was observed for PLGA 75/25 polymers, where the microspheres from polymers of lower I.V. (0.24) had shorter diffusive phase than the microspheres of the polymer of higher I.V. (0.94). Similar observations were made by Yasukawa *et al.*⁵³ in their investigation.

The bulk erosion accompanied hydrolysis of PLGA throughout the matrix during the diffusive phase, resulting in the final burst due to the disintegration of the polymer matrix when inner hydrolysis of polymers proceeded to a critical point. The presence of GCV in the matrix could affect the PLGA degradation as hydrophilic GCV could dissolve faster than the degradation products and subsequently increase the permeability of the polymer matrix. This was observed in the GCV-loaded PLGA microspheres mentioned above. The presence of GCV increased the PLGA degradation rate due to the improved water permeability and most importantly due to the basic-catalyst effect. Other factors that affected the PLGA degradation were the molecular weight and the LA to GA ratio.

As for the microspheres with high GCV payload (18% - 20% wt/wt), such as PLGA 75/25 I.V. 0.94 18% GCV and PLGA 50/50 I.V. 0.50 20% GCV, they displayed a huge initial burst release of GCV to the surrounding medium after a day of immersion in PBS solution. This was followed by a biphasic release pattern, similar to that of the microspheres with low GCV payload. It is believed that the huge initial burst was due to GCV loosely bounded on the surface or embedded in the surface of the microspheres.

In the PLGA 75/25 I.V. 0.94 18% GCV, 47.49 % of GCV was released into the PBS solution within the first day of immersion. This huge release was mostly due to the

leaching of GCV particles from the surface of the microspheres. The initial burst was followed by a diffusive phase which lasted for 56 days, where the release rate was 0.15 %/day. A burst release was observed after 56 days of degradation, where the release rate increased to 1.26 %/day for the next 28 days. This burst release was attributed to the hydrolytic degradation of the polymer matrix. At the end of 132 days of degradation, all of the GCV had been released into the PBS solution.

When compared to PLGA 75/25 I.V. 0.94 7% GCV, the microspheres with the higher payload (18% wt/wt) displayed a much shorter diffusive phase as well as a final burst release phase. From Table 6.2, PLGA 75/25 I.V. 0.94 18% GCV had a larger T_g decrease rate constant ($k=0.1632$) than PLGA 75/25 I.V. 0.94 7% GCV ($k=0.1247$). This was possibly due to more water absorbed into the polymer and behaving as plasticizer for the PLGA 75/25 I.V. 0.94 18% GCV microspheres. The huge initial burst release of GCV would create small pores and micro-channels, which would improve the permeability of water. The short diffusive phase for PLGA 75/25 I.V. 0.94 18% GCV was also due to the diffusion of GCV newly dissolved by water under osmotic pressure. The short final burst release phase of PLGA 75/25 I.V. 0.94 18% was due to the disintegration of the polymer matrix when these hydrolysis of polymers proceeded to a critical point. From the SEM photographs of microspheres, pores were observed on the originally smooth surface of microspheres after 10 weeks of degradation. GCV along with the degradation products were able to move through these channels and into the surrounding medium through these pores.

As discussed in Chapter 6, PLGA 75/25 I.V. 0.94 7% GCV had a larger degradation rate constant ($k'=0.0764$) compared with PLGA 75/25 I.V. 0.94 18% GCV ($k'=0.0222$), indicating faster hydrolysis for the low GCV payload PLGA 75/25 I.V. 0.94

microspheres. Since there were no initial burst release for these microspheres, no pores or micro-channels were formed after the first day of immersion as compared to PLGA 75/25 I.V. 0.94 18% GCV. Hence water penetration into the polymer matrix occurred more slowly and a longer diffusion phase was obtained for PLGA 75/25 I.V. 0.94 7% GCV microspheres. As the GCV behaved as a weak alkaline and was protonated by the trapped acidic degradation products with degradation time, basic-catalyst effect occurred, thus accelerating the hydrolysis rate. On the other hand, in the high GCV payload microspheres, the huge initial burst formed small pores and micro-channels, resulting in easier release of the degradation products and GCV to the surrounding environment. This would result in little and/or no auto-catalyst and basic-catalyst effect. Hence the GCV release time for the PLGA 75/25 I.V. 0.94 18% GCV was shorter than PLGA 75/25 I.V. 0.94 7% GCV even though it degraded slower.

As for PLGA 50/50 I.V. 0.50 with GCV payload of 20% wt/wt, a huge initial burst was observed on the first day of immersion, with 68.38 % of GCV released into the surrounding medium. This was followed by a very short diffusive phase, which lasted from day 1 to day 7, with only 0.3 % of GCV released. A more gradual release of GCV of 0.47 %/day was observed after 7 days of degradation, which lasted until all GCV had released into the PBS solution.

Looking at the change in T_g with degradation time for PLGA 50/50 I.V. 0.50 (Figure 6.9) the T_g of the polymer decreased to below 37 °C after 7 days of degradation in the PBS solution. By this time, the polymer was in a rubbery state and was more permeable to water than in glassy state. It was observed from the change in $\ln(M_n)$ with degradation time (Figure 6.12 D), PLGA 50/50 I.V. 0.50 20% GCV degraded slower than PLGA 50/50 I.V. 0.50 5% GCV. Even though the onset of mass loss occurred at about the same

time in both the GCV-loaded microspheres, the PLGA with 5% GCV lost 17 % of mass while the mass loss for PLGA with 18% GCV was only 4 % mass after 42 days of degradation. It is believed that the PLGA microspheres with 5% GCV underwent hydrolysis affected by basic-catalyst effect. The microspheres with 20% GCV on the other hand, degraded slower because of the huge initial burst, which created pores and micro-channels that assisted the diffusion of acidic degradation products and GCV from the microspheres core into the surrounding medium. This would in turn, decrease auto-catalyst effect and basic-catalyst effect, thus decrease the degradation rate of PLGA 50/50 I.V. 0.50 20% GCV microspheres.

The PDLLA I.V. 0.22 5% GCV microspheres displayed an initial burst release after the first day of immersion into the PBS solution, with the release of 7.23 % of GCV incorporated. This was followed by a much longer diffusive phase, which lasted to the 140th day, where only 12.81 % of GCV was released into the surrounding environment. The burst release was observed only after 140 days of immersion, with the release rate of 1.34 %/day. The percentage of GCV released was 97.25 % after 203 days of immersion.

It was not surprising to observe the longest release time frame was from PDLLA I.V. 0.22 5% GCV microspheres. As discussed earlier in Chapter 5 and Chapter 6, both pure and GCV-loaded PDLLA I.V. 0.22 microspheres decreased the slowest. Even though with the low GCV payload of 5%, the microspheres exhibited an initial burst, unlike the other PLGA microspheres with similar GCV payload. Although all of these PLGA and PDLLA microspheres were amorphous in nature, more GCV was found on an/or near the surface of the PDLLA microspheres, while in PLGA, the GCV was more homogeneously dispersed within the microspheres. This might suggest the PLGA copolymers were more efficient to be used as particulate DDS than the homopolymer PDLLA.

As observed from Figure 7.1, most of the GCV incorporated in the microspheres were released into the PBS solution during the burst release phase through polymer degradation. However, the time taken for complete release of GCV into the surrounding was determined by the length of the diffusive phase. During the diffusive phase, GCV was released slowly and in small quantity.

7.1.2 X-Ray Photoelectron Spectroscopy (XPS) study of GCV-loaded microspheres

The XPS technique allowed the elucidation of the surface structure of the GCV-loaded microspheres. The polymers, PLGA, displayed carbon and oxygen binding peaks at 282.20 eV and 529.65 eV, respectively in their molecular structure while Ganciclovir showed carbon, oxygen and nitrogen at 396.80 eV in their molecular structure. XPS analysis of pure PLGA microspheres showed no nitrogen binding peak at 396.80 eV¹¹⁶. Hence, if no nitrogen binding peak was detected in the GCV-loaded microspheres, it could be concluded that there was no GCV on the surface of the microspheres. It should be kept in mind that with this technique, an analysis of the surface with a depth close to 50 Å, could be achieved.

Table 7.1 illustrated the binding energies for carbon, nitrogen and oxygen for Ganciclovir (Cymevene®) and the GCV-loaded microspheres. It was observed that the binding peak for nitrogen for GCV was at 396.80 eV and the atomic concentration was 17.94 %.

No obvious binding peak for nitrogen was observed for PLGA 75/25 I.V. 0.94 7% GCV microspheres, and the atomic concentration of nitrogen was 0.47 %, which suggested that only trace amount of GCV was found on the surface of the microspheres. This corresponded to the absence of initial burst release as observed in Figure 7.1.

The binding peak for nitrogen was observed in both the PLGA 75/25 and PLGA 50/50 microspheres with high GCV payload. On the PLGA 75/25 I.V. 0.94 18% GCV microspheres, the atomic concentration of nitrogen was 3.54 %. The atomic concentration of nitrogen was 3.87 % for PLGA 50/50 I.V. 0.50 20% GCV microspheres. This indicated that GCV was found on the surface of the microspheres, which would explain for the huge initial burst release observed after one day of immersion in PBS solution (Figure 7.1).

As for PLGA 50/50 I.V. 0.50 5% GCV microspheres, the binding peak for nitrogen was observed at 397.40 eV and the atomic concentration was 2.32 %. Since Figure 7.1 showed no initial burst for these microspheres, it is believed that the binding peak for nitrogen was due to GCV, which were incorporated inside the microspheres but were within the depth close to 50 Å beneath the surface.

The XPS analysis supported the release profile shown in Figure 7.1. The lower the binding peak of nitrogen, the lower the GCV content on the surface of the microspheres. These microspheres did not show an initial burst. As for the microspheres with high GCV payload, they displayed the binding peak and atomic concentration for nitrogen, and showed an initial burst.

Sample	Peak	Atomic Concentration (%)
GCV (Cymevene®)	O 1s	18.73
	N 1s	17.94
	C 1s	63.33
PLGA 75/25 I.V. 0.94 7% GCV microspheres	O 1s	30.13
	N 1s	0.47
	C 1s	69.40
PLGA 75/25 I.V. 0.94 18% GCV microspheres	O 1s	27.56
	N 1s	3.54
	C 1s	62.79
PLGA 50/50 I.V. 0.50 5% GCV microspheres	O 1s	21.80
	N 1s	2.32
	C 1s	75.87
PLGA 50/50 I.V. 0.50 20% GCV microspheres	O 1s	31.66
	N 1s	3.87
	C 1s	64.47

Table 7.1 Quantification report of surface analysis of GCV (Cymevene®), PLGA 75/25 I.V. 0.94 7% GCV and PLGA 75/25 I.V. 0.94 18% GCV microspheres.

7.1.3 Median effective dose (ED₅₀) of GCV-loaded microspheres

10 mg GCV-loaded microspheres were incubated in 10 ml, pH = 7.0 PBS solutions at 37 °C. The GCV concentration was thus calculated based on 10 mg microspheres/10 ml PBS solution. The median effective dose (ED₅₀), is the dosage of a drug that is pharmacologically effective for 50 % of the population exposed to the drug or a 50 % response in a biological system that is exposed to the drug. The ED₅₀ of GCV for human CMV has been determined to be 0.1 – 3.0 µg/ml^{17,117}. The GCV concentrations at various time intervals for each GCV-loaded microspheres were shown in Figure 7.2 to Figure 7.4.

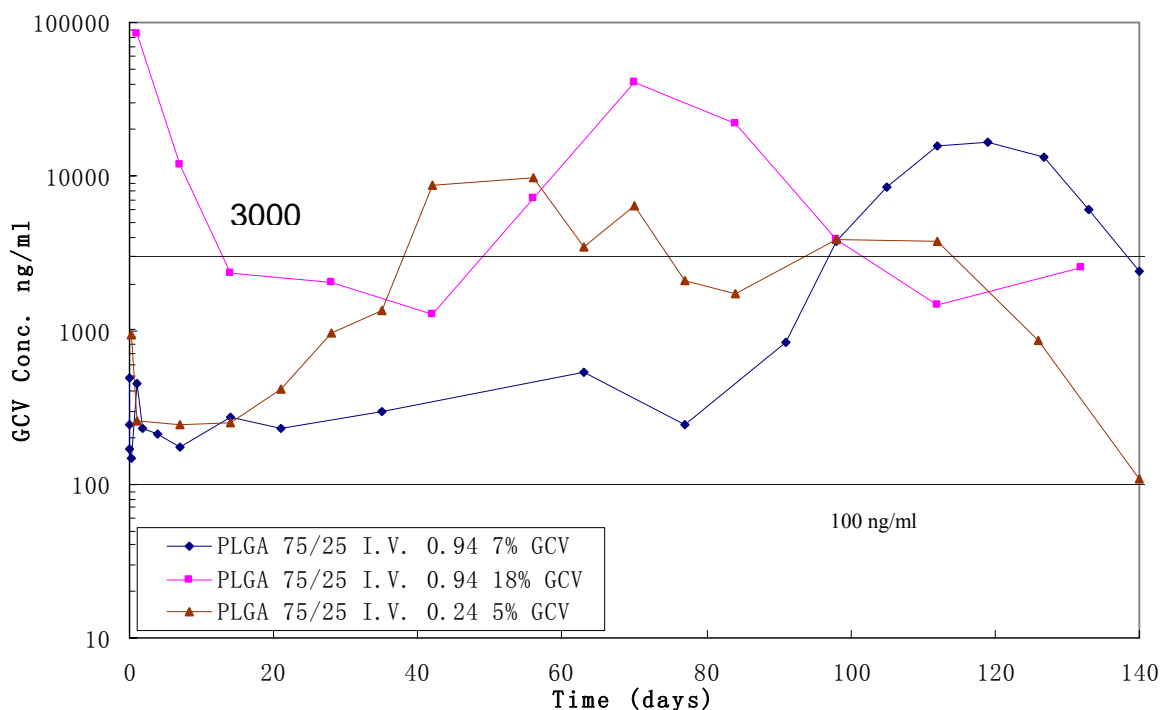


Figure 7.2 Semi logarithmic plots of GCV concentrations in phosphate-buffered solution (pH 7.0) at 37 °C. The values are shown as mean of n = 5, PLGA 75/25 I.V. 0.94 7% GCV (◆), PLGA 75/25 I.V. 0.94 18% GCV (■), PLGA 75/25 I.V. 0.24 5% GCV (▲), the area between the two lines (100 ng/ml, 3000ng/ml) indicates a 50% effective dose (ED₅₀) of ganciclovir for human cytomegalovirus replication.

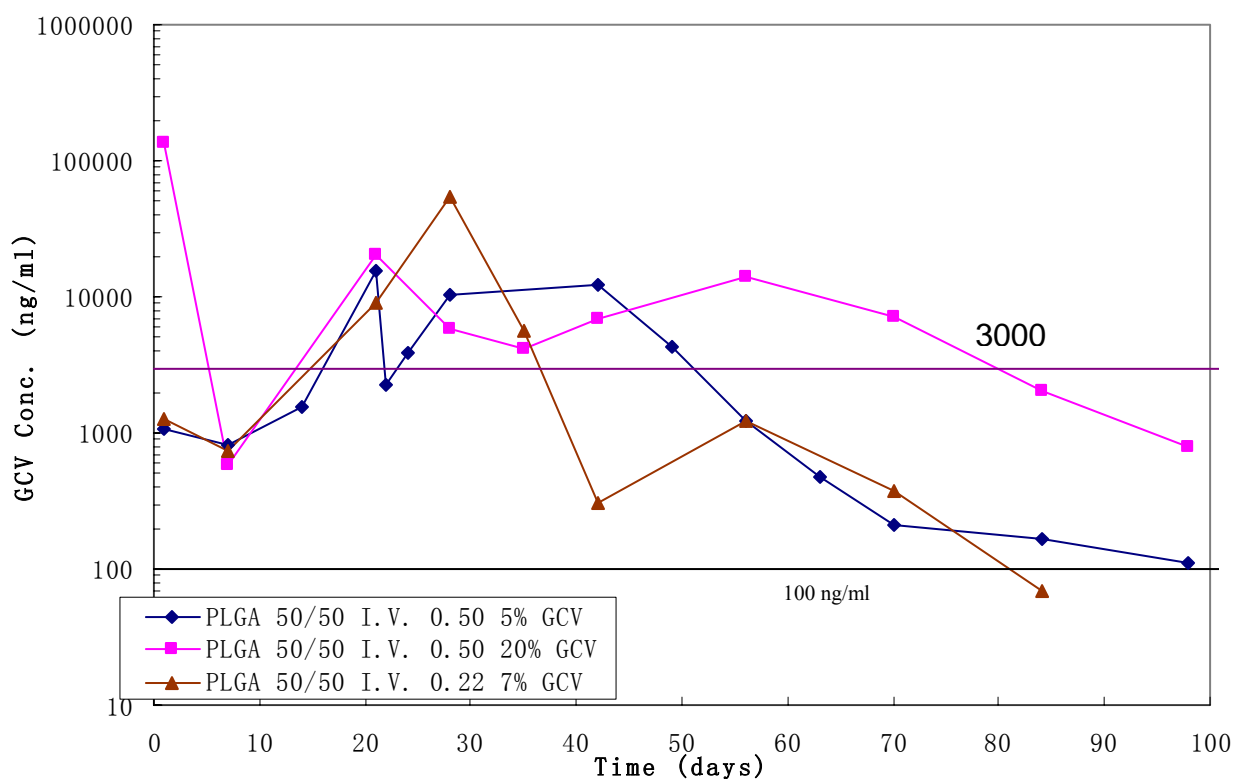


Figure 7.3 Semi logarithmic plots of GCV concentrations in phosphate-buffered solution (pH 7.0) at 37 °C. The values are shown as mean of n = 5, PLGA 50/50 I.V. 0.50 5% GCV (◆), PLGA 50/50 I.V. 0.50 20% GCV (■), PLGA 50/50 I.V. 0.22 7% GCV (▲), the area between the two lines (100 ng/ml, 3000ng/ml) indicates a 50% effective dose (ED₅₀) of ganciclovir for human cytomegalovirus replication.

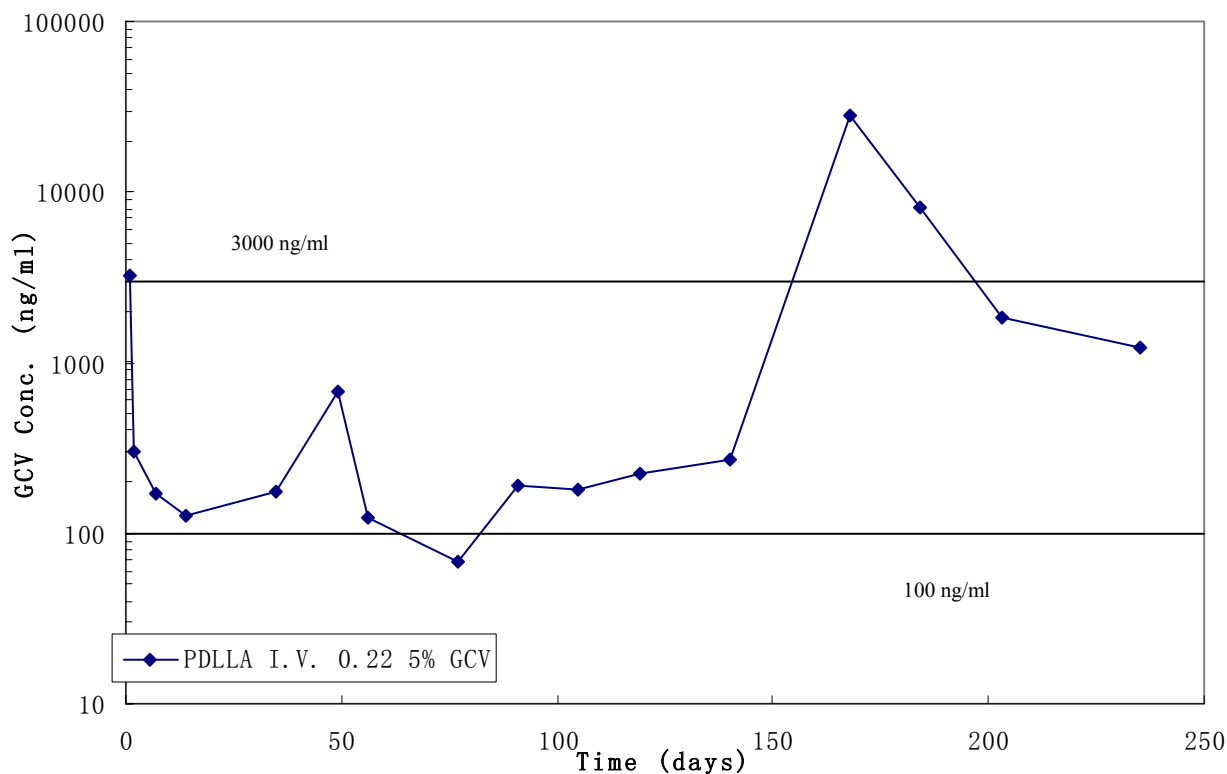


Figure 7.4 Semi logarithmic plots of GCV concentrations in phosphate-buffered solution (pH 7.0) at 37 °C. The values are shown as mean of $n = 5$, PDLLA I.V. 0.22 5% GCV (\blacklozenge), the area between the two lines (100 ng/ml, 3000 ng/ml) indicates a 50% effective dose (ED_{50}) of ganciclovir for human cytomegalovirus replication.

The initial amount of ganciclovir per 10 mg of microspheres for each group of GCV-loaded microspheres was listed in table 7.2. For the low GCV payload microspheres, the GCV:polymer ratio is 1:10, which resulted in 1000 μg GCV for every 11 mg GCV-loaded microspheres (909.1 μg GCV for every 10 mg GCV-loaded microspheres) theoretically, but since some of the GCV was dissolved in the PVA aqueous solution and was not incorporated in the polymeric microspheres during processing GCV-loaded microspheres, the experimental initial GCV amount per 10 mg of microspheres was obtained by extraction method and was listed in Table 7.2. The GCV payload and loading efficiency were consequently calculated. For the high GCV payload microspheres, the GCV:polymer ratio is 5:10, which resulted in 5000 μg GCV for every 15 mg GCV-loaded microspheres (3333.3 μg GCV for every 10 mg GCV-loaded microspheres) theoretically.

Sample	LA:GA ratio	I.V.	GCV $\mu\text{g}/10\text{mg}$ (theoretical)	GCV $\mu\text{g}/10\text{mg}$ (experimental)	GCV payload (%)	Loading Efficiency (%)
GCV- loaded microspheres	75:25	0.94	909.1	707	7	78
			3333.3	1817	18	55
PLGA	50:50	0.24	909.1	454	5	50
		0.50	909.1	542	5	60
			3333.3	1959	20	59
0.22	909.1	728	7	80		
PDLLA	100:0	0.22	909.1	449	5	49

Table 7.2 Initial GCV amount per 10 mg of microspheres before immersion in PBS solution.

The ganciclovir concentration were maintained within the range of ED_{50} of human CMV for PLGA 75/25 I.V. 0.94 7% GCV for up to 91 days, where it ranged from 150 ng/ml to 840 ng/ml. This stable release of GCV at small amount was due to the diffusive release before polymeric matrix degradation took place, corresponding with the diffusive phase in the cumulative GCV release versus time plot as shown in Figure 7.1. After 98 days of immersion, unwanted burst release stage of GCV was observed due to the disintegration of the polymeric matrix, and the concentration of GCV during this time frame exceeded ED_{50} range, resulted in overdosed release.

As for the other PLGA 75/25 microspheres, the concentration of GCV was observed to exceed the ED_{50} range during the burst release stage. Ganciclovir concentration were maintained within the range from 240 ng/ml to 9900 ng/ml for PLGA 75/25 I.V. 0.24 5% GCV for 126 days. The GCV concentration exceeded the ED_{50} range from 42 to 70 days of immersion, which corresponded to the burst release stage for the microspheres. However, by reducing the initial amount of microspheres used from 10 mg to 4 mg and considering the volume of the human vitreous is 4.5 ml^{17} , it would be possible to maintain the ganciclovir concentration within the ED_{50} range for 126 days.

In the case of PLGA 75/25 I.V. 0.94 18% GCV, the ganciclovir concentration was within the range of 1300 $\mu\text{g}/\text{ml}$ to 41400 ng/ml from day 7 to day 132. From Figure 7.2, it was

observed that the GCV concentration was on the upper limit and exceeded the ED₅₀ range in the time investigated. However, by reducing the amount of the microspheres used from 10 mg to 0.35 mg and taking into account that the vitreous humor is 4.5 ml¹⁷, it would be possible to reduce the ganciclovir concentration within the range of ED₅₀ of human CMV of 99 ng/ml to 3200 ng/ml for up to 132 days. The initial burst release of GCV could be removed by pre-incubating the microspheres in PBS solution for several hours before application.

In the case of the PLGA 50/50 polymers, the effective range was shorter than the PLGA 75/25 polymers. For PLGA 50/50 I.V. 0.50 5% GCV, the ganciclovir concentration was within a range of 1100 ng/ml to 15800 ng/ml for up to 98 days. The GCV concentration exceeded the ED₅₀ range from 21 to 49 days of immersion, which corresponded to the burst release stage for the microspheres. By reducing the amount of the microspheres used from 10 mg to 0.9 mg, it would be possible to reduce the ganciclovir concentration to 96 ng/ml to 3150 ng/ml, which was within the range of ED₅₀ of human CMV for up to 63 days.

As for PLGA 50/50 I.V. 0.50 20% GCV, with the exception of the initial burst release of GCV, the ganciclovir concentration was within a range of 600 ng/ml to 20300 ng/ml for 98 days. The GCV concentration exceeded the ED₅₀ range from 21 to 49 days of immersion, which corresponded to the burst release stage for the microspheres. By reducing the amount of the microspheres used from 10 mg to 0.675 mg, it would be possible to reduce the ganciclovir concentration to 86 ng/ml to 3000 ng/ml, which was within the range of ED₅₀ of human CMV for 98 days. The initial burst release of GCV could be removed through pre-incubation of the microspheres in PBS solution for several hours before application. Hence, by reducing the initial amount of microspheres used,

both the PLGA 50/50 I.V. 0.50 microspheres with the payload of 5% and 20% are suitable for sustained release in treatment of human CMV.

The ganciclovir concentration was maintained within the range of ED_{50} of human CMV for PDLLA I.V. 0.22 5% GCV for 140 days. The concentration ranged from 70 ng/ml to 3200 ng/ml. After 168 days of degradation, the burst release of GCV resulted in concentrations above the ED_{50} range.

The release profile of PDLLA I.V. 0.22 5% GCV, PLGA 50/50 I.V. 0.22 7% GCV and PLGA 75/25 I.V. 0.94 7% GCV microspheres were not ideal to be served as sustained release drug delivery systems (DDS). The high concentration of GCV during the burst release phase was unwanted and un-avoided.

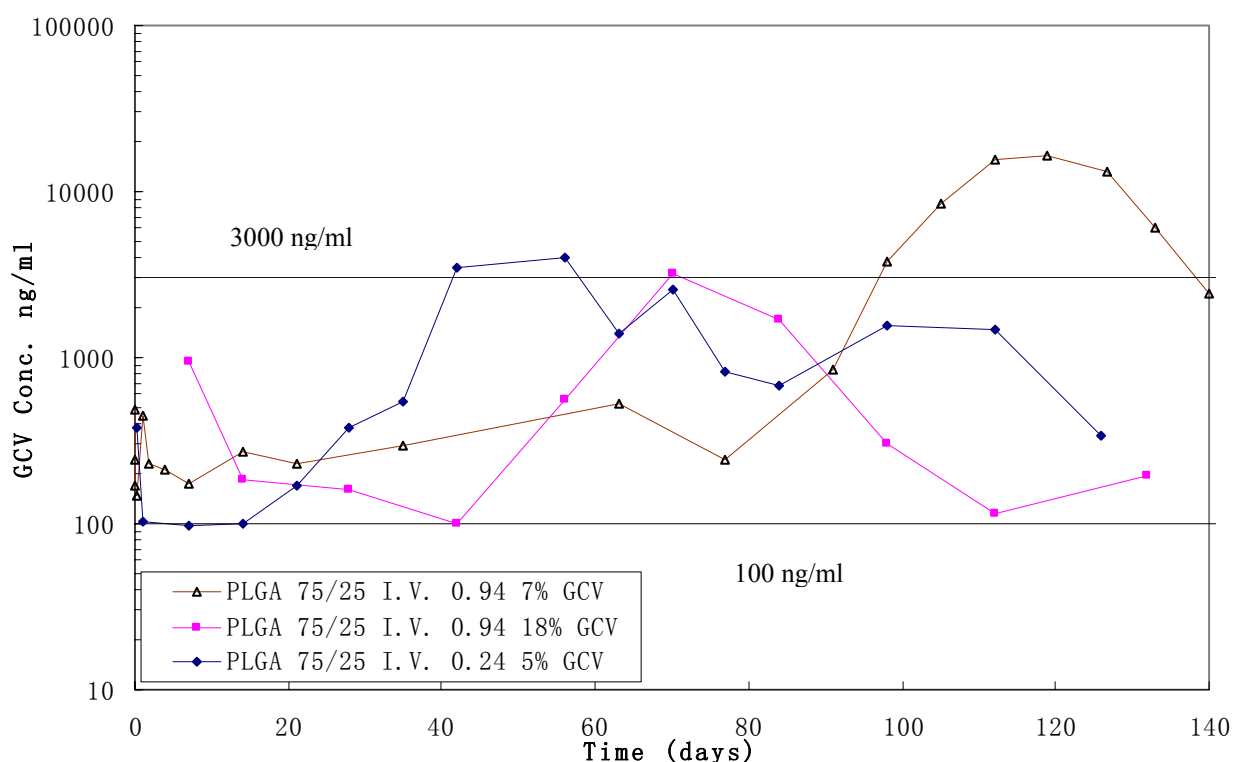


Figure 7.5 Semi logarithmic plots of GCV concentrations in phosphate-buffered solution (pH 7.0) at 37 °C. The values are shown as mean of $n = 5$, PLGA I.V. 0.24 5% GCV (\blacklozenge), PLGA 75/25 I.V. 0.94 18% GCV (\blacksquare) and PLGA 75/25 I.V. 0.94 7% GCV (\triangle) microspheres. The area between the two lines (100 ng/ml, 3000ng/ml) indicates a 50% effective dose (ED_{50}) of ganciclovir for human cytomegalovirus replication.

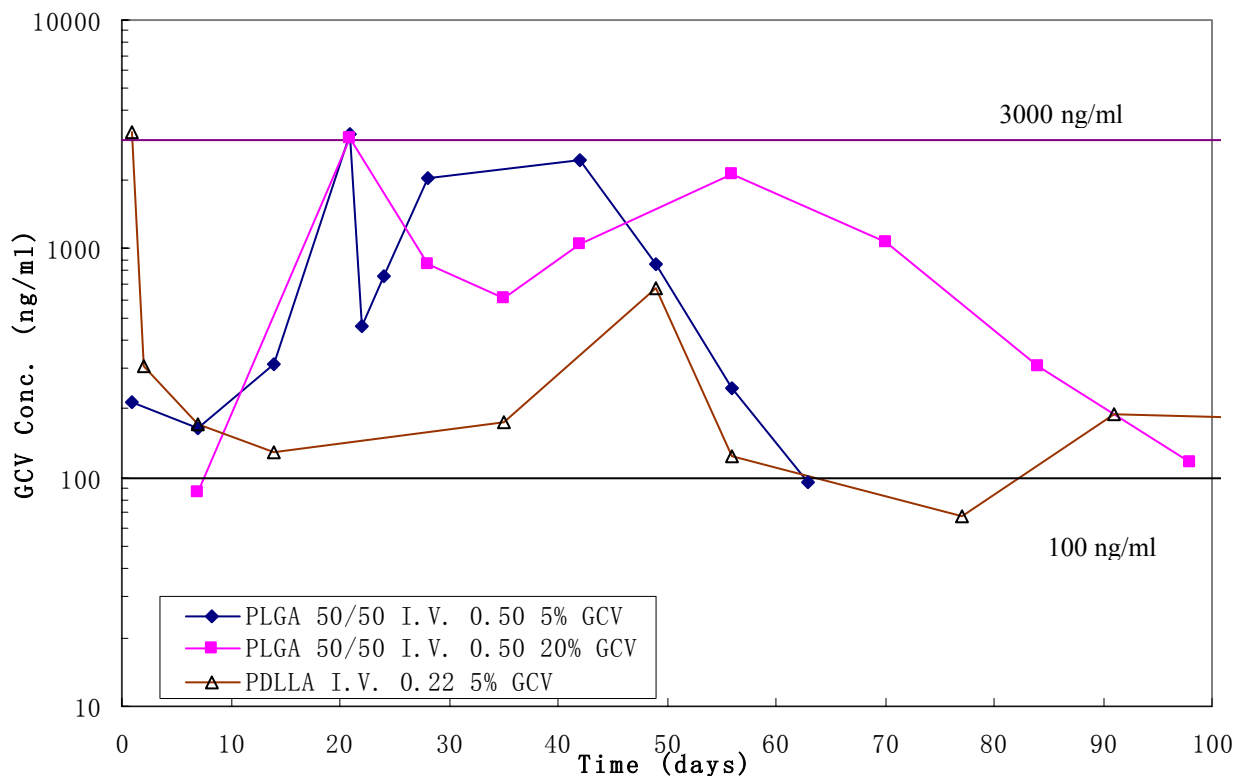
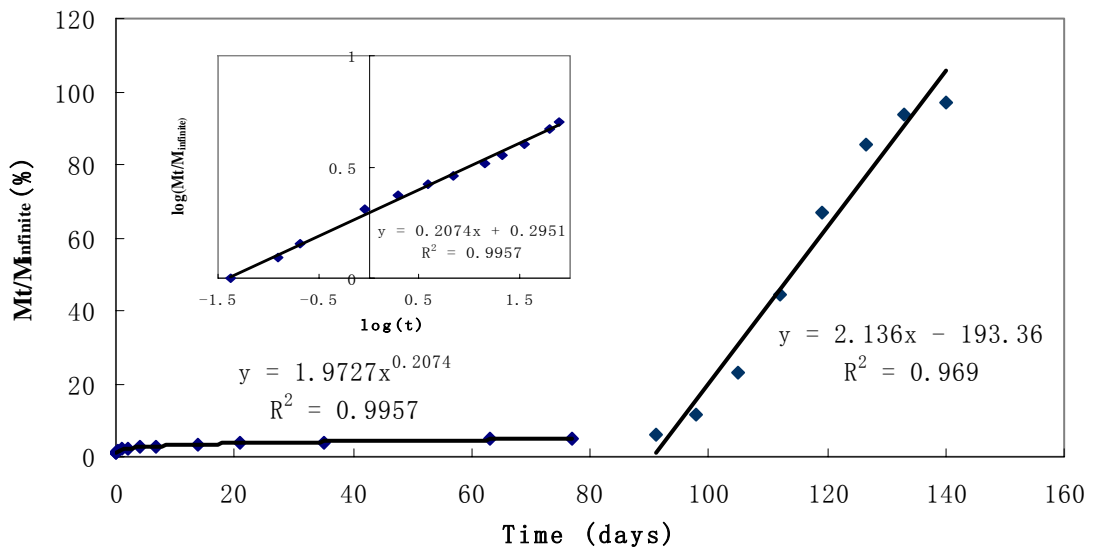


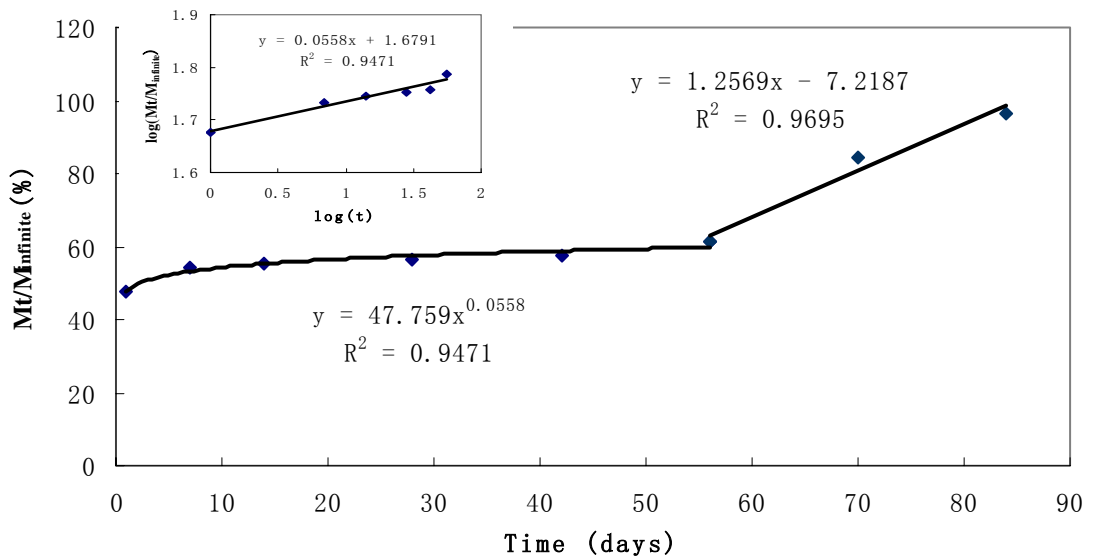
Figure 7.6 Semi logarithmic plots of GCV concentrations in phosphate-buffered solution (pH 7.0) at 37 °C. The values are shown as mean of $n = 5$, PLGA 50/50 I.V. 0.50 5% GCV (\blacklozenge), PLGA 50/05 I.V. 0.50 20% GCV (\blacksquare) and PDLLA I.V. 0.22 5% GCV (\triangle) microspheres. The area between the two lines (100 ng/ml, 3000ng/ml) indicates a 50% effective dose (ED_{50}) of ganciclovir for human cytomegalovirus replication.

PLGA 75/25 I.V. 0.94 18% GCV, PLGA 75/25 I.V. 0.24 5% GCV, PLGA 50/50 I.V. 0.50 5% GCV and PLGA 50/50 I.V. 0.50 20% GCV microspheres were ideal to be used for sustained release of GCV to treat CMV. By reducing the initial amount of microspheres used, the GCV concentrations were maintained with the range of ED_{50} of human CMV, as shown in Figure 7.5 and Figure 7.6. The elimination of initial burst effect had to be carried out for PLGA 75/25 I.V. 0.94 18% GCV and PLGA 50/50 20% GCV microspheres through pre-incubation of the microspheres in PBS solution for several hours. In summary, GCV-loaded microspheres were successfully processed and were ideal for long term sustained release for treatment of human CMV. From the GCV release profiles (Figure 7.5 and Figure 7.6), these microspheres released GCV for 63 days (PLGA 50/50 I.V. 0.50 5% GCV) to 132 days (PLGA 75/25 I.V. 0.94 18% GCV), which was equivalent to 2 months and 4 months respectively.

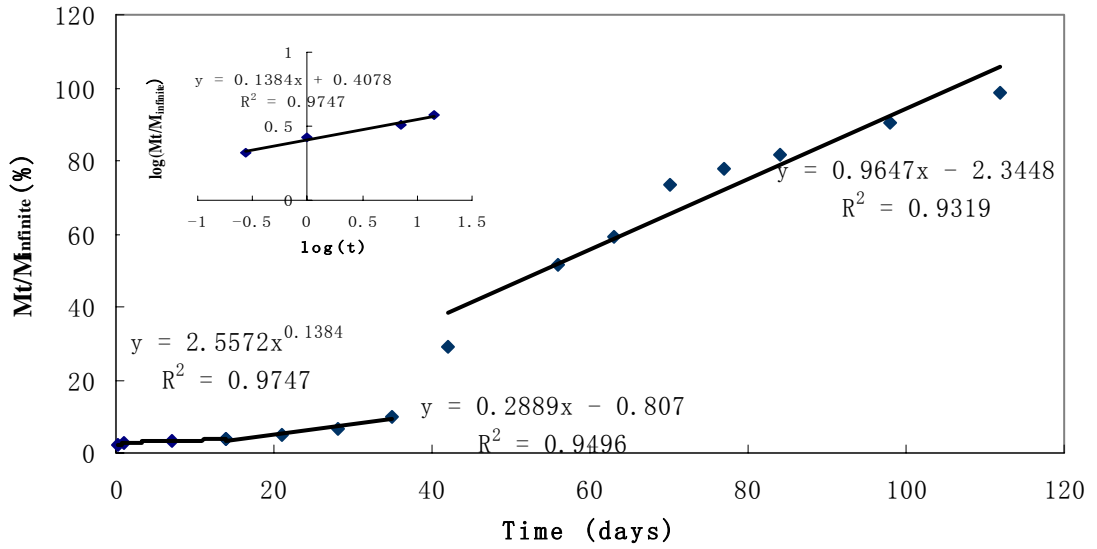
B PLGA 75/25 I. V. 0.94 7% GCV



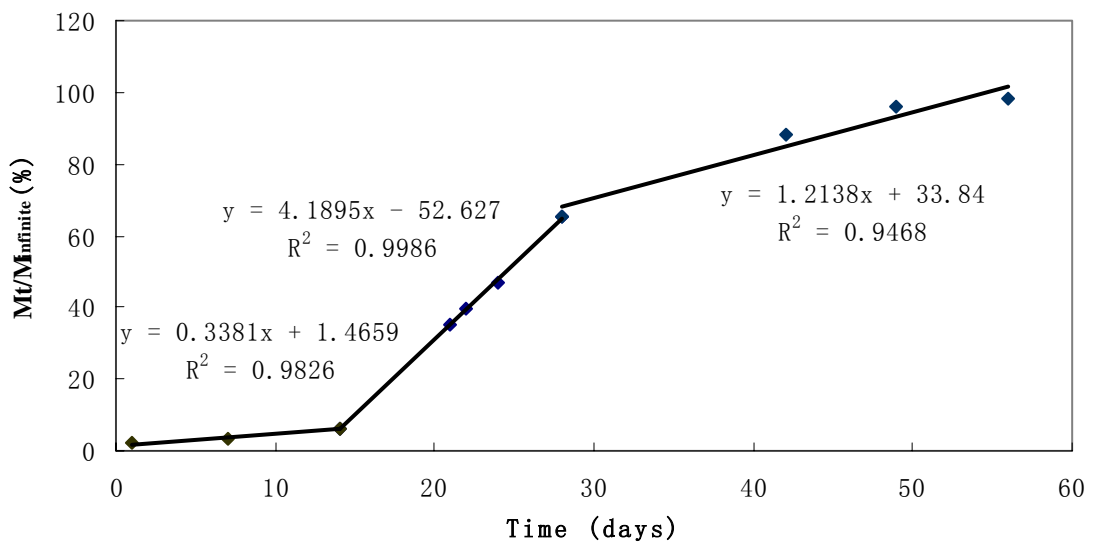
C PLGA 75/25 I. V. 0.94 18% GCV



D PLGA 75/25 I. V. 0.24 5% GCV



E PLGA 50/50 I. V. 0.50 5% GCV



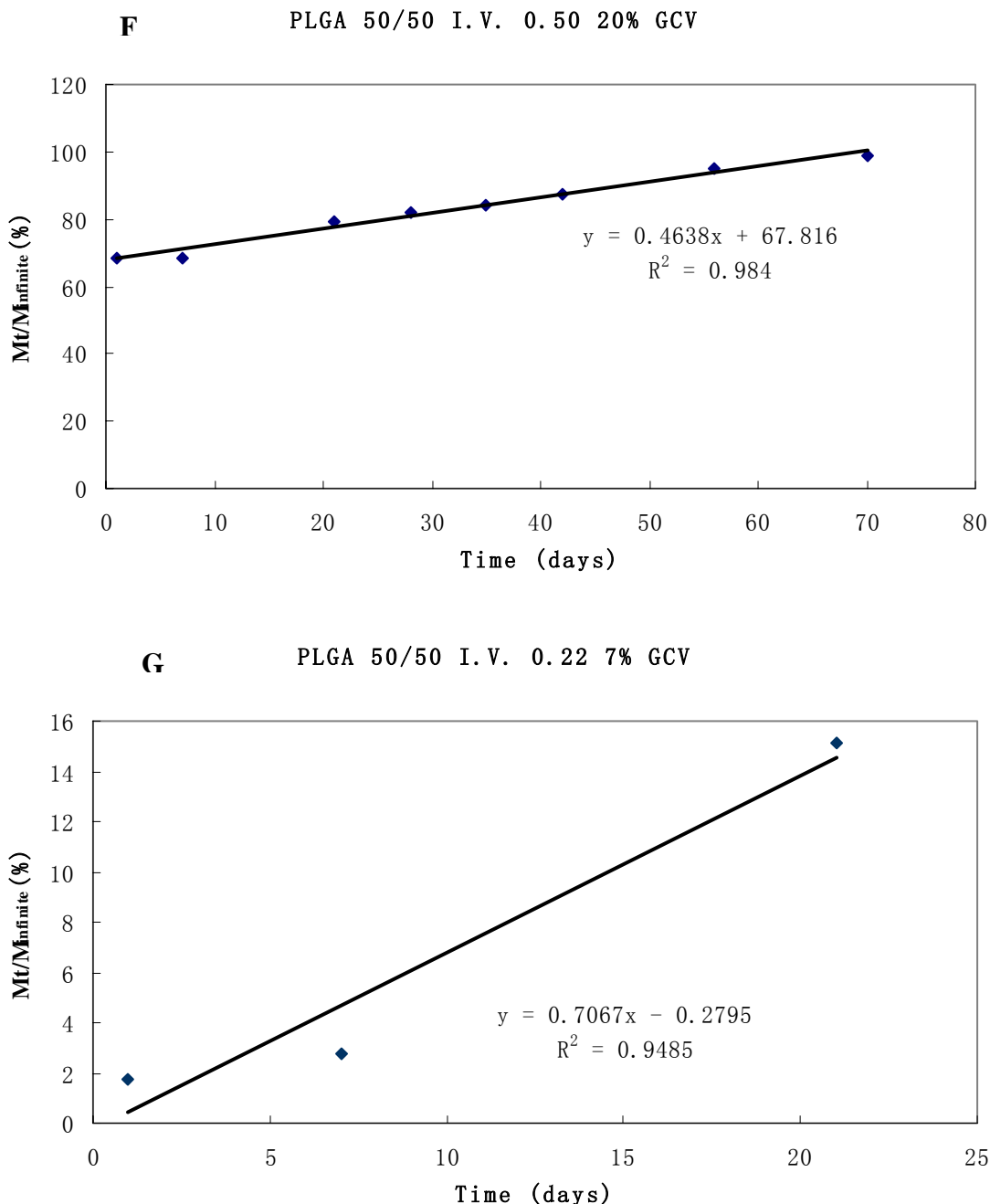


Figure 7.7 Fitting curves (both M_t/M_{∞} versus t and $\log(M_t/M_{\infty})$ versus $\log(t)$) of A) PDLGA I.V. 0.22 5% GCV; B) PLGA 75/25 I.V. 0.94 7% GCV; C) PLGA 75/25 I.V. 0.94 18% GCV; D) PLGA 75/25 I.V. 0.24 5% GCV; E) PLGA 50/50 I.V. 0.50 5% GCV; F) PLGA 50/50 I.V. 0.50 20% GCV; and G) PLGA 50/50 I.V. 0.22 7% GCV microspheres.

Figure 7.7 analyzes the whole release profile ($0 \leq M_t/M_{\infty} \leq 1.00$) which combines both diffusion release phase and burst release phase due to matrix bulk degradation. The results showed that only data obtained from PDLGA I.V. 0.22 5% GCV, PLGA 75/25 I.V. 0.94 7% GCV, PLGA 75/25 I.V. 0.94 18% GCV and PLGA 75/25 I.V. 0.24 5% GCV microspheres could be fitted to equation 2.11. The release exponent, n , for these

microspheres was less than 0.43, indicating that the release of the GCV was through diffusion and was highly dependent on the amount of the GCV that remained in the microspheres, corresponding to the fact that GCV is dispersed in the polymeric matrix, which resulted in the initial drug concentration was greater than the solubility of the GCV within the system.

In the PDLLA I.V. 0.22 5% GCV microspheres, the diffusion phase lasted for 140 days, with 12.8 % of GCV incorporated released to the environment. After 140 days of degradation, a linear fit to the release curve was preferred as shown in Figure 7.7 A, indicating the onset of disintegration of the polymeric matrix due to hydrolysis. The degradation of polymer changed the release profile of diffusion to zero-order release.

Similar observations were made for PLGA 75/25 I.V. 0.94 7% GCV, PLGA 75/25 I.V. 0.94 18% GCV, and PLGA 75/25 I.V. 0.24 5% GCV microspheres. The release of GCV was first due to diffusion, followed by zero-order release kinetics due to the polymer degradation.

In the PLGA 75/25 I.V. 0.24 5% GCV and PLGA 50/50 I.V. 0.50 5% GCV microspheres, the burst release phase was fitted with 2 linear curves. These two linear releases were believed to be due to the polymer degradation.

A small amount of the total GCV incorporated in the microspheres was released to the environment through diffusion. The diffusion phase lasted for more than 70 days for PLGA 75/25 I.V. 0.94 7% GCV and PDLLA 0.22 5% GCV microspheres. This phase coincided with the stage where the M_w of the polymer decreased with degradation time but no changes to the mass was observed. The bulk of GCV released to the environment

through polymer degradation. During this stage, obvious loss to the polymer mass was observed, along with a decrease in the pH of the surrounding medium. Since PLGA 75/25 I.V. 0.24 microspheres had a lower I.V. than the PLGA 75/25 I.V. 0.94 microspheres, the hydrolytic degradation rate of the former was larger, which accounted for the shorter diffusion release period. The GCV released from all the microspheres was mostly due to a combination of diffusion and polymer degradation.

For PLGA 50/50 I.V. 0.50 5% GCV, PLGA 50/50 I.V. 0.50 20% GCV and PLGA 50/50 I.V. 0.22 7% GCV microspheres, linear fit of the release curves showing a strong statistical linear correlation ($R^2 > 0.90$) were obtained, indicating a zero-order release profile due to a combination of diffusion and polymer degradation, but predominantly polymer degradation. This would suggest that for the PLGA 50/50 polymers, the rate of water penetration into the polymer matrix was equivalent to the polymer chain scission rate, thus the GCV was released through diffusion and polymer degradation.

As for PLGA 50/50 I.V. 0.50 20% GCV, the initial large burst release of GCV would leave behind holes and micro-channels in the microspheres, further increasing the rate of water penetration and the hydrolysis rate through polymer chain scission. Hence the GCV was released predominantly through polymer degradation.

In the PLGA 50/50 I.V. 0.22 7% GCV, the polymer was always in the rubbery state because the T_g was lower than 37 °C. This allowed for a higher water penetration rate. This in turn, would increase the hydrolysis rate through polymer chain scission and the GCV was released predominantly through polymer degradation.

7.3 Physical Model of Drug Release Profile for GCV-loaded Microspheres

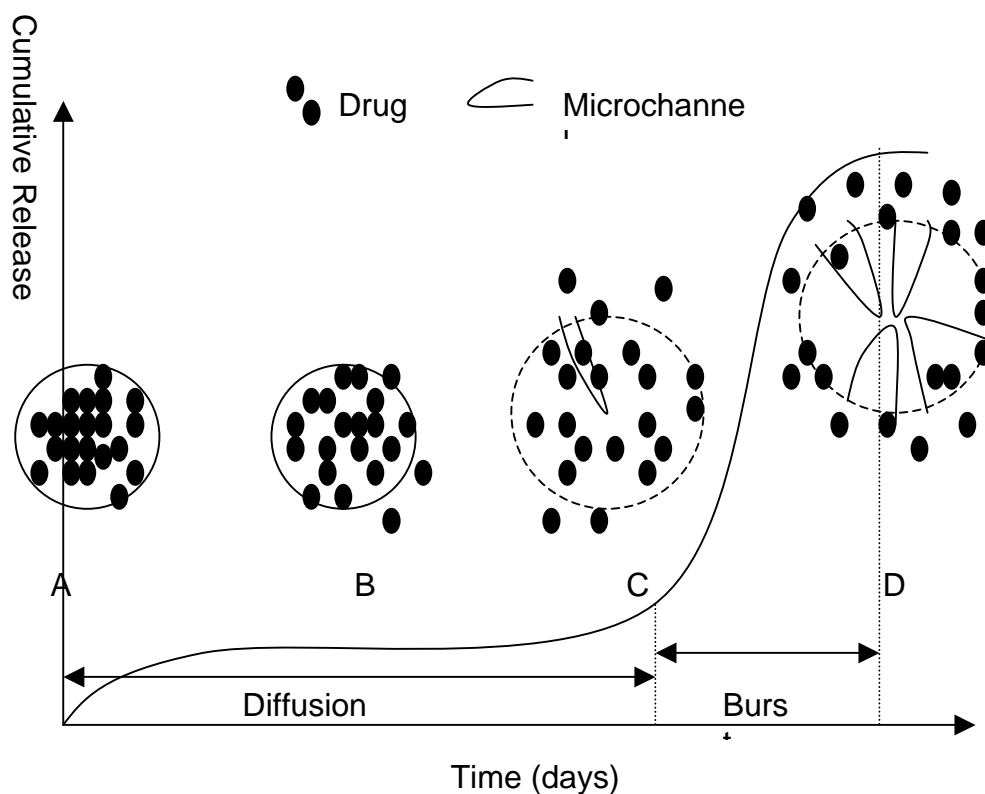


Figure 7.8 Physical model of drug release for the GCV-loaded microspheres. A) Upon immersion into the PBS solution. B) During the diffusion release phase. C) Polymeric matrix swells and cracks, small pores or micro-channels formed with further degradation. D) Final burst release phase.

Figure 7.8 is the schematic illustration of the drug release for the GCV-loaded microspheres. Upon immersion into the PBS solution (Figure 7.8 A)), the drug which is loosely bounded on the surface or embedded in the surface of the microspheres comes into contact with water and is released. During the diffusion phase (Figure 7.8 B)), the drug migrates from the core to the surface of the polymeric matrix and is released to the environmental PBS solution. This migration is due to the drug concentration gradient and/or the newly dissolved drug by water under osmotic pressure. With further immersion in the PBS solution (Figure 7.8 C) and D)), polymeric matrix swells with further water uptake and cracks, small pores or micro-channels are formed within the polymeric matrix due to hydrolytic degradation. During the final burst release phase, most of the drug

dispersed is dissolved and released to the environmental PBS solution upon the disintegration of the polymeric matrix due to further hydrolytic degradation.

7.4 Conclusions

The microspheres with low GCV payload (5% - 7% wt/wt) displayed a biphasic release pattern, i.e. a diffusive phase followed by a burst release. There was no initial burst of GCV in all the low GCV payload microspheres. For the polymers with the same LA to GA ratio the microspheres from polymers of lower I.V. had shorter diffusive phase than the microspheres from the polymers of higher intrinsic viscosity. As for the microspheres with high GCV payload, they displayed a huge initial burst release of GCV to the surrounding medium after a day of immersion in PBS solution. This was followed by a biphasic release pattern, similar to that of the microspheres with low GCV payload. It is believed that the huge initial burst was due to GCV loosely bounded on the surface or embedded in the surface of the microspheres.

Most of the GCV incorporated in the microspheres released into the PBS solution during the burst release phase through polymer degradation. However, the time taken for the complete release of GCV into the surrounding was determined by the length of the diffusive phase. During the diffusive phase, GCV was released slowly and in small quantity.

The XPS analysis supported the release profile shown in Figure 7.1. The lower the binding peak of nitrogen the lower the GCV content on the surface of the microspheres. These microspheres did not show an initial burst. As for the microspheres with high GCV payload, they displayed the binding peak and atomic concentration for nitrogen, and showed an initial burst.

The GCV-loaded microspheres ideal for long term sustained release for treatment of human CMV were successfully processed. From the GCV release profiles (Figure 7.5 and Figure 7.6), these microspheres released GCV for 63 days (PLGA 50/50 I.V. 0.50 5% GCV) to 132 days (PLGA 75/25 I.V. 0.94 18% GCV), which was equivalent to 2 months and 4 months respectively.

The results showed that only data obtained from PDLLA I.V. 0.22 5% GCV, PLGA 75/25 I.V. 0.94 7% GCV, PLGA 75/25 I.V. 0.94 18% GCV and PLGA 75/25 I.V. 0.24 5% GCV microspheres could be fitted to equation 2.11. The release exponent, n , for these microspheres was less than 0.43, indicating that the release of the GCV was through diffusion and was highly dependent on the amount of the GCV that remained in the microspheres.

For PLGA 50/50 I.V. 0.50 5% GCV, PLGA 50/50 I.V. 0.50 20% GCV and PLGA 50/50 I.V. 0.22 7% GCV microspheres, linear fit of the release curves showing a strong statistical linear correlation ($R^2 > 0.90$) were obtained, indicating a zero-order release profile due to the combination of diffusion and polymer degradation, but predominantly polymer degradation. This would suggest that for the PLGA 50/50 polymers, the rate of water penetration into the polymer matrix was equivalent to the polymer chain scission rate, thus the GCV was released through diffusion and polymer degradation.

CHAPTER 8

DRUG LOADED POLYMERIC TABLETS

GCV-loaded polymer tablets were prepared from GCV-loaded PLGA and PDLLA microspheres and their GCV release profile along with the *in vitro* degradation of the tablets were studied. The tablets with a diameter of 13 mm and thickness of 340 to 420 μm were prepared using a FTIR die using a maximum force of 12 tons. At least seven tablets of each GCV-loaded PLGA/PDLLA microspheres were prepared. The weight of each pellet was 50 mg. The tablets were then placed in an oven and annealed under the following conditions as listed in table 8.1, to improve the handling properties.

Sample	Temperature ($^{\circ}\text{C}$)	Period in oven (min)
PDLLA, I.V.0.22, 5 %GCV	95 \pm 5	~1-2
PLGA 75/25, I.V.0.94, 7%GCV	110 \pm 5	~20-30
PLGA 75/25, I.V. 0.24, 5% GCV	100 \pm 5	~15-20
PLGA 50/50, I.V. 0.50, 5% GCV	100 \pm 5	~30
PLGA 50/50, I.V. 0.22, 7% GCV	100 \pm 5	~30

Table 8.1 Parameters for sample annealing

It was noticed from Table 8.2 that PDLLA I.V. 0.22 5% GCV microspheres required lower annealing temperature and time to be fabricated into tablets than the GCV-loaded PLGA microspheres. The homopolymer PDLLA had better handling properties than PLGA copolymers.

Tablets from microspheres with high GCV payload (> 18%) were not prepared due to the presence of high initial burst which exceeded the ED₅₀ range by 10 times.

8.1 Modulated Differential Scanning Calorimetry (MDSC)

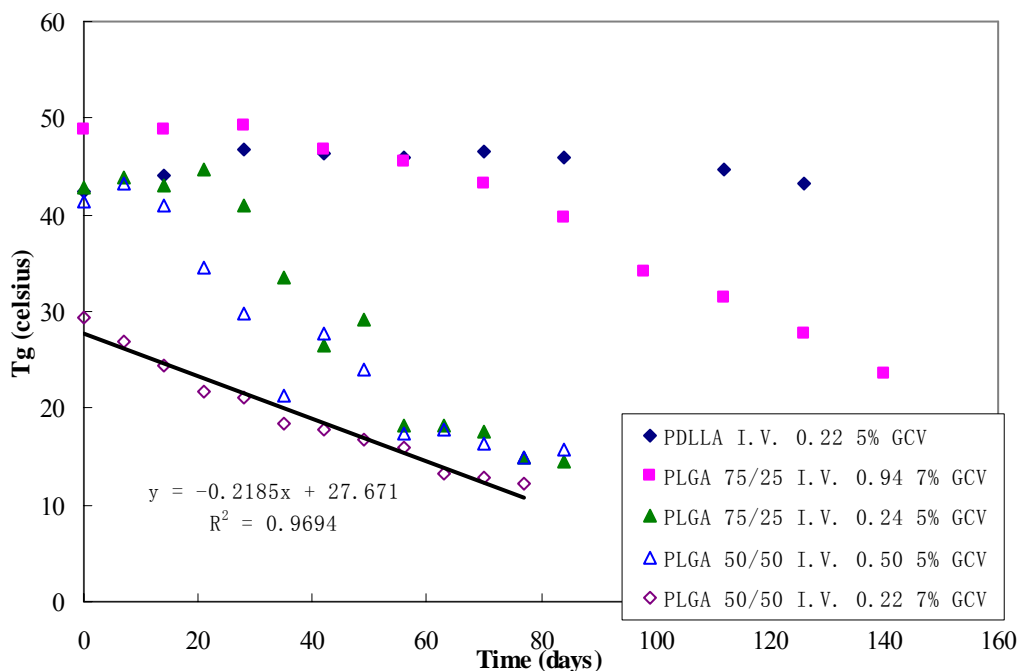


Figure 8.1 Glass transition temperature (T_g) as a function of degradation time for PDLLA I.V. 0.22 5% GCV tablets (◆), PLGA 75/25 I.V. 0.94 7% GCV tablets (■), PLGA 75/25 I.V. 0.24 5% GCV tablets (▲), PLGA 50/50 I.V. 0.50 5% GCV tablets (△) and PLGA 50/50 I.V. 0.22 7% GCV tablets (◇) degraded in PBS at 37 °C.

In the GCV-loaded microspheres, linear fit to the change in T_g with degradation time could be carried out on all the samples, while in the case of the GCV-loaded tablets, a lag time was observed in most of the samples, followed by a decrease in T_g with degradation time. A linear fit was obtained only for PLGA 50/50 I.V. 0.22 7% GCV tablets.

The lag time was due to slower water uptake into the tablets compared to the microspheres. The lag time for PLGA 50/50 I.V. 0.50 5% GCV tablets was only 7 days, which was much shorter than PLGA 75/25 I.V. 0.24 5% GCV tablets (21 days), PLGA 75/25 I.V. 0.94 7% GCV tablets (28 days) and PDLLA I.V. 0.22 5% GCV tablets (77 days). The high GA content in PLGA 50/50 polymers made the polymers more hydrophilic. Hence the PLGA 50/50 polymers required much shorter time for water uptake compared to the PLGA 75/25 polymers and PDLLA polymers.

8.2 Changes in Mass

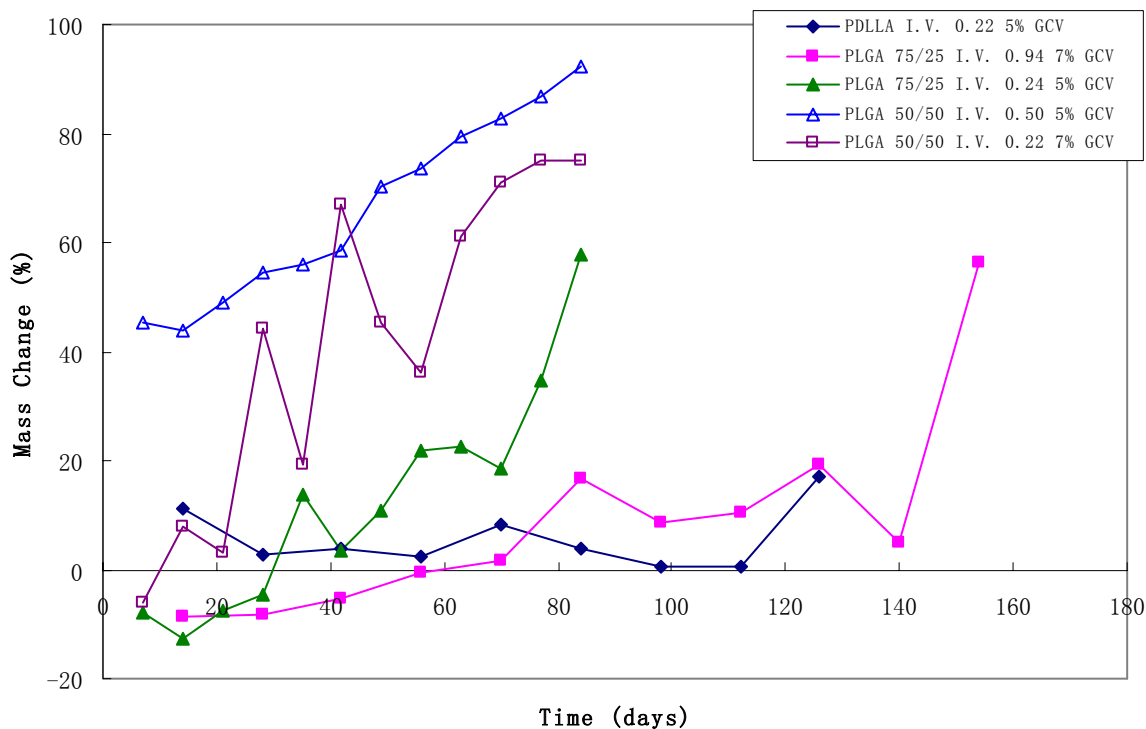


Figure 8.2 Changes in mass as a function of degradation time for PLGA 75/25 I.V. 0.24 5% GCV tablets (\blacktriangle), PLGA 75/25 I.V. 0.94 7% GCV tablets (\blacksquare), PDLLA I.V. 0.22 5% GCV tablets (\blacklozenge), PLGA 50/50 I.V. 0.22 7% GCV tablets (\diamond) and PLGA 50/50 I.V. 0.50 5% GCV tablets (\triangle) degraded in PBS at 37 °C.

The changes in mass with respect to degradation time for the tablets were shown in Figure 8.2. The changes in mass profile were different from those obtained for the microspheres. Here, the tablets had higher volume to total surface area ratio than the microspheres. Hence it was easier for the absorbed water to remain inside the tablets, causing the slight weight gain after the immersion in PBS solution, as observed in PLGA 75/25 I.V. 0.94 7% GCV and PLGA 75/25 I.V. 0.24 5% GCV tablets. As for the microspheres, no increase in mass was observed. Instead the mass decreased steadily with degradation time (Figure 6.15).

PLGA 50/50 I.V. 0.50 5% GCV and PLGA 50/50 I.V. 0.22 7% GCV tablets showed mass loss at very early stages of degradation. When compared with the changes in mass for the respective microspheres (Figure 6.15), insignificant mass loss was observed in the

first 21 to 35 days of degradation. The huge mass loss for PLGA 50/50 I.V. 0.50 5% GCV and PLGA 50/50 I.V. 0.22 7% GCV was probably be due to sample disintegration instead of degradation. Furthermore, when the normalized M_w profile of the tablets (Figure 8.3) and respective microspheres (Figure 6.16) were compared, the normalized M_w profiles of the tablets and microspheres of PLGA 50/50 I.V. 0.50 GCV were similar to one another. Hence the initial huge loss in mass for the tablets was due to sample disintegration.

No obvious changes in mass profile could be seen for PDLLA I.V. 0.22 5% GCV tablets even after 116 days of degradation. As PDLLA I.V. 0.22 was composed of 100 % LA units, and LA was more hydrophobic than GA, PDLLA I.V. 0.22 had much less water uptake compared to the other PLGA samples. This in turn, slowed down the rate of degradation for PDLLA I.V. 0.22 5% GCV tablet.

8.3 Gel Permeation Chromatography (GPC)

As seen from Figure 8.3, the rate of decrease for the normalized M_w graph for GCV-loaded tablets with respect to degradation time had the following order: PLGA 50/50 I.V. 5% GCV > PLGA 50/50 I.V. 0.22 7% GCV > PLGA 75/25 I.V. 0.24 5% GCV > PLGA 75/25 I.V. 0.94 7% GCV > PDLLA I.V. 0.22 5% GCV. This was similar to the normalized M_w profile for the low GCV payload microspheres as shown in Figure 6.16 in Chapter 6. Basically, the tablets are closely packed microspheres which adhered to each other. The hydrolysis degradation profile of each polymer was thus not affected.

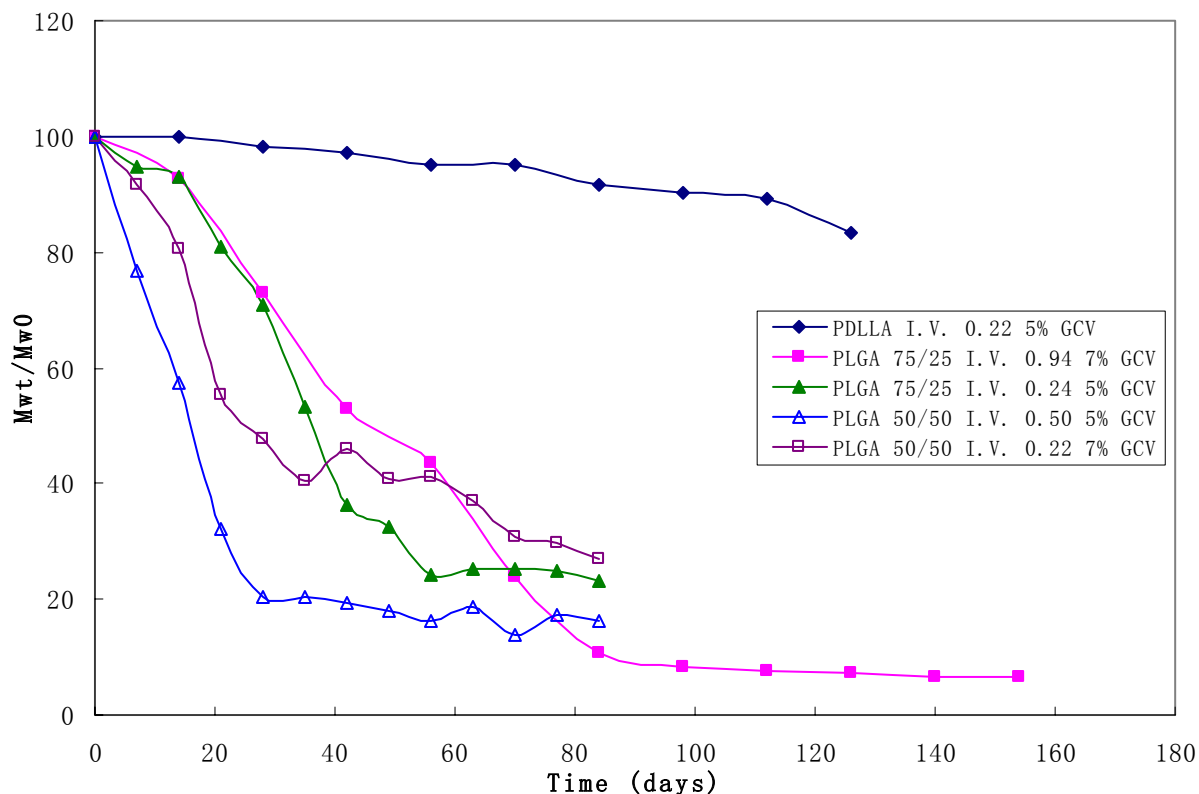


Figure 8.3 Normalized Weight Average Molecular Weight (M_w) as a function of degradation time for PLGA 75/25 I.V. 0.24 5% GCV tablet (\blacktriangle), PLGA 75/25 I.V. 0.94 7% GCV tablet (\blacksquare), PDLLA I.V. 0.22 5% GCV tablet (\blacklozenge), PLGA 50/50 I.V. 0.22 7% GCV tablet (\diamond) and PLGA 50/50 I.V. 0.50 5% GCV tablet (\triangle) degraded in PBS at 37 °C.

Figure 8.4 plots the natural logarithmic number average molecular weight ($\ln(M_n)$) against time. Only M_n before any mass loss occurred were taken. From the graphs, linear plots showing strong statistical linear correlation ($R^2 > 0.90$) were obtained. The results showed that the molecular weight of both PLGA and PDLLA polymers decreased with hydrolytic degradation time. The degradation rate constant, k' , taken as the gradient of the linear plots, for PDLLA I.V. 0.22 5% GCV, PLGA 75/25 I.V. 0.94 7% GCV and PLGA 75/25 I.V. 0.24 5% GCV tablets, was summarized in Table 8.2. The degradation rate constant, k' , for the respective microspheres was also included as comparison.

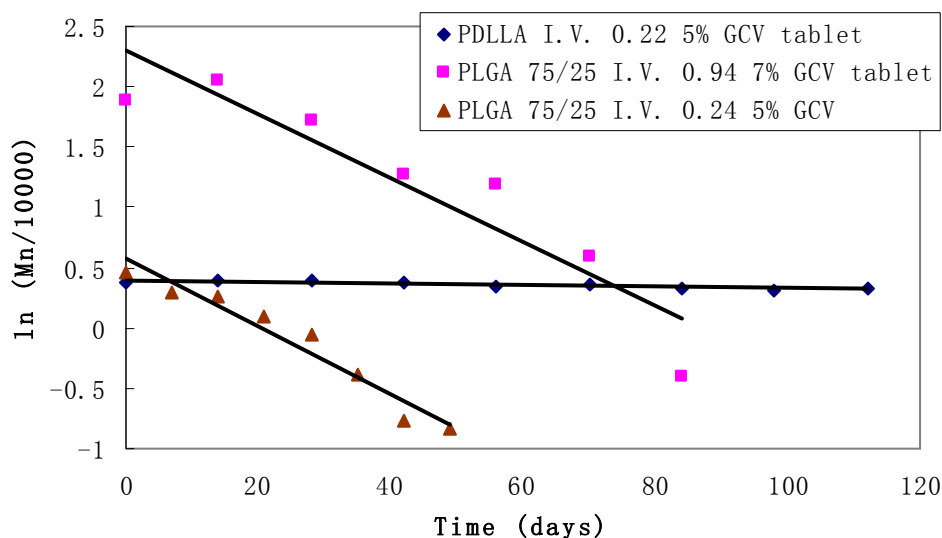


Figure 8.4 $\ln(M_n)$ vs. Degradation time for PDLLA I.V. 0.22 5% GCV (\blacklozenge); PLGA 75/25 I.V. 0.94 7% GCV (\blacksquare) and PLGA 75/25 I.V. 0.24 5% GCV (\blacktriangle) tablets.

Sample	k' of Tablets	k' of Microspheres
PDLLA, I.V.0.22, 5 %GCV	0.0007	0.0013;0.0111
PLGA 75/25, I.V.0.94, 7%GCV	0.0264	0.0764
PLGA 75/25, I.V. 0.24, 5% GCV	0.028	0.0248

Table 8.2 Degradation rate constant k' of the tablets and microspheres.

From Table 8.2, the results showed that the k' values of PDLLA I.V. 0.22 5% GCV tablet were very small, indicating very little chain scission had occurred. From the normalized M_w as a function of degradation time graph (Figure 8.3), no obvious decrease of M_w was observed even after 116 days of degradation. The slow degradation rate was due to the slow water uptake into the polymer because of the inherent hydrophobic nature of the LA units. These results corresponded with the lack of change in the mass profile for the tablets (Figure 8.2). Furthermore, the tablets were made by annealing and compressing of the PDLLA I.V. 0.22 5% GCV microspheres. These tablets had a denser structure and a larger volume to total surface area ratio than the microspheres. Hence the slower water uptake and rate of hydrolytic degradation were observed.

As for PLGA 75/25 I.V. 0.24 5% GCV tablet, the k' value was similar to the k' value of the respective microspheres. Processing the microspheres into tablet did not significantly affect the hydrolytic degradation rate of the PLGA 75/25 I.V. 0.24 polymer with 5% GCV loading.

In PLGA 75/25 I.V. 0.94 7% GCV tablet, the k' value was also significantly reduced when compared with the microspheres. The tablets were made by annealing and compressing of the PLGA 75/25 I.V. 0.94 7% GCV microspheres. These tablets had a denser structure and a larger volume to total surface area ratio than the microspheres. Hence the slower water uptake and rate of hydrolytic degradation were observed.

8.4 Changes in pH

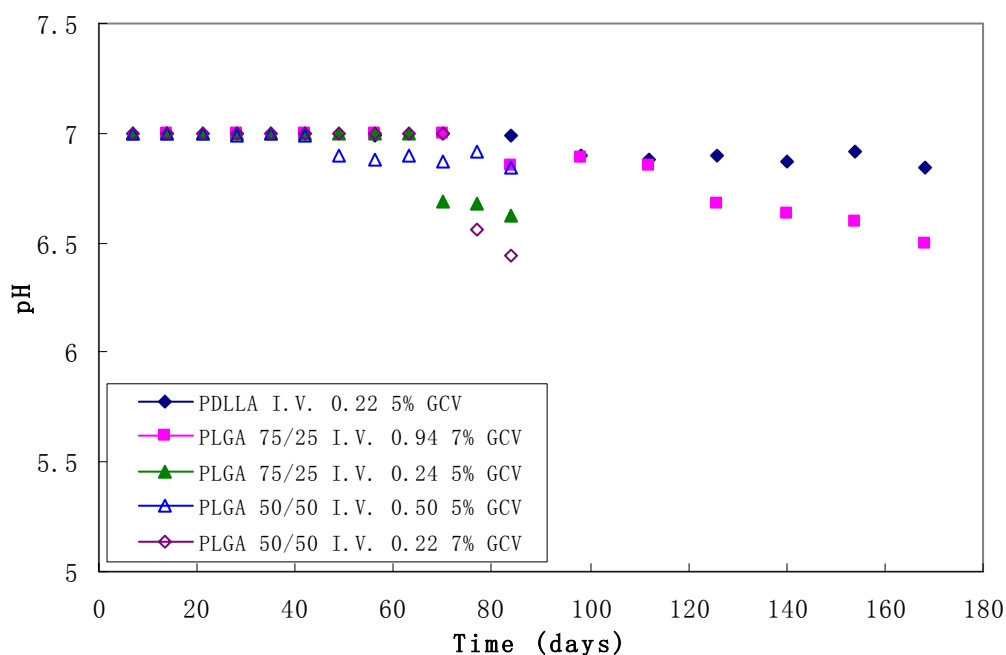


Figure 8.5 pH as a function of degradation time for PLGA 75/25 I.V. 0.24 5% GCV tablets (\blacktriangle), PLGA 75/25 I.V. 0.94 7% GCV tablets (\blacksquare), PDLLA I.V. 0.22 5% GCV tablets (\blacklozenge), PLGA 50/50 I.V. 0.22 7% GCV tablets (\diamond) and PLGA 50/50 I.V. 0.50 5% GCV tablets (\triangle) degraded in PBS at 37 °C.

Figure 8.5 showed the change of pH with respect to degradation time for the GCV-loaded tablets *in vitro* in PBS solution at 37 °C. The change in pH for PDLLA I.V. 0.22 5% GCV

tablet was very small with degradation time, where the pH decreased from 7.00 to 6.99 after 168 days of degradation. This very small change corresponded with the lack of change also observed in the T_g , M_w , and mass change with degradation time.

In comparison to the change in pH with degradation time for the GCV-loaded microspheres (Figure 6.14), the tablets had a smaller change in pH with degradation time. The pH only dropped to around 6.5 at later stages of degradation for these GCV-loaded tablets. This was due to the slower degradation rate observed in the tablets compared with the microspheres.

8.5 Fractional Cumulative Release Curve

Tablets weighing 10 mg each were immersed into 10 ml of PBS (pH 7.0) at 37 °C for release study. All the GCV release tests were carried out in multiplicity (n=5) to verify the homogeneity of the GCV release and the results obtained were averaged.

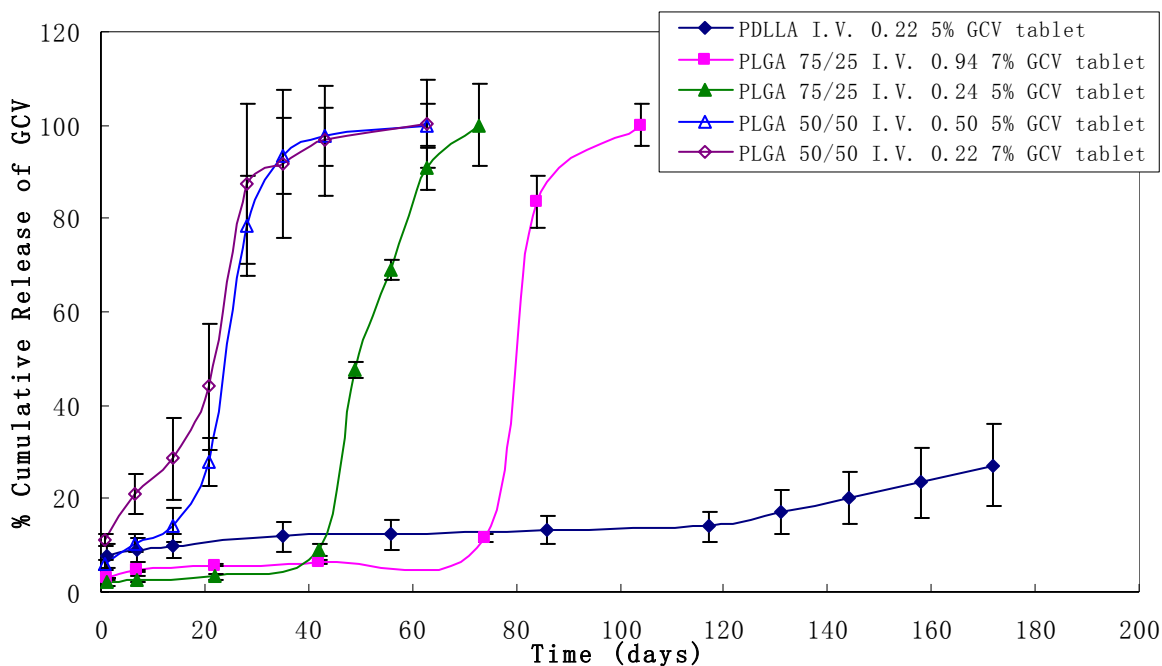


Figure 8.6 Fractional cumulative release of GCV from the PLGA, PDLLA tablets in phosphate-buffered solution (pH 7.0) at 37 °C. The values are shown as mean \pm SD of n=5, PLGA 75/25 I.V. 0.24 5% GCV

tablet (▲), PLGA 75/25 I.V. 0.94 7% GCV tablet (■), PDLLA I.V. 0.22 5% GCV tablet (◆), PLGA 50/50 I.V. 0.22 7% GCV tablet (◇) and PLGA 50/50 I.V. 0.50 5% GCV tablet (Δ).

Figure 8.6 showed the fractional cumulative release curve of GCV-loaded PDLLA and PLGA tablets. It was observed that the time taken for PLGA tablets to release all the GCV was significantly shorter than the time taken for PLGA microspheres as shown in Figure 7.1. A comparison between the time frames for diffusion and burst release phases for the respective GCV-loaded tablets and microspheres was summarized in Table 8.3.

Sample		Diffusion phase (days)	Burst release (days)
PDLLA, I.V.0.22, 5% GCV	*Microspheres	113	65
	**Tablets*	111	From day 117
PLGA 75/25, I.V.0.94, 7% GCV	Microspheres	91	42
	Tablets	74	33
PLGA 75/25, I.V. 0.24, 5% GCV	Microspheres	35	91
	Tablets	22	51
PLGA 50/50, I.V. 0.50, 5% GCV	Microspheres	14	42
	*Tablets	14	29
PLGA 50/50, I.V. 0.22, 7% GCV	Microspheres	7	28
	*Tablets	7	29

Table 8.3 Release time frame differences of microspheres and tablets.

*Initial burst was observed for * marked samples. **Release profile was not finished for ** marked sample.

From Table 8.3, it was observed that the diffusion phase for PLGA 75/25 I.V. 0.94 7% GCV and PLGA 75/25 I.V. 0.24 5% GCV was much shorter than their respective microspheres. In other words, the onset of burst release from the tablets occurred earlier than the microspheres. This was possibly due to disintegration of the tablets at the adhesion points rather than advance hydrolytic degradation of the polymer.

The differences in time frame were likely due to the processing techniques used in making the tablets. The pressure applied could have crushed some of the microspheres, changing the internal structure of the microspheres and exposing some of the GCV initially encapsulated by the polymer matrix. The annealing step was to enable particle

adhesion so as to improve the handling properties of the tablet. From the change in mass profile (Figure 8.2), it was observed that some of the samples showed significant mass loss at the very early stages of degradation due to sample disintegration. This was more pronounced in PLGA 50/50 I.V. 0.50 5% GCV and PLGA 50/50 I.V. 0.22 7% GCV tablets. These tablets had partially disintegrated into particles. Hence it wasn't surprising that these samples had similar release profiles with their respective microspheres.

The time frames for the initial burst release and following diffusion phase obtained for PDLLA I.V. 0.22 5% GCV tablets were similar to the microspheres. There was no obvious mass loss and little changes were observed to the M_w , T_g and pH of the degrading medium with degradation time during the diffusion phase. The sample remained intact and with little hydrolysis during this phase. Similar observations were made for the drug release and degradation studies of the PDLLA I.V. 0.22 5% GCV microspheres. This could account for the similarities in time frame for the initial burst release and following diffusion phase obtained for PDLLA I.V. 0.22 5% GCV tablets and microspheres.

The PLGA 50/50 I.V. 0.22 7% GCV tablets exhibited an initial burst release of 11.2 % after 1 day of immersion. Unlike the corresponding microspheres, which exhibited no initial burst as shown in Figure 7.1. The same was observed for PLGA 50/50 I.V. 0.50 5% GCV tablets, where 5.8 % of the GCV was released after 1 day of immersion. This was unlike the PLGA 50/50 I.V. 0.50 5% GCV microspheres, which exhibited no initial burst as shown in Figure 7.1.

The initial burst release from the tablets would suggest that GCV was distributed on or close to the surface of the tablets. The pressing also formed the channels and drains

throughout the polymer matrix, hence it was easier for the GCV to migrate to the lower GCV concentration area like the surface of the tablets due to the concentration gradient.

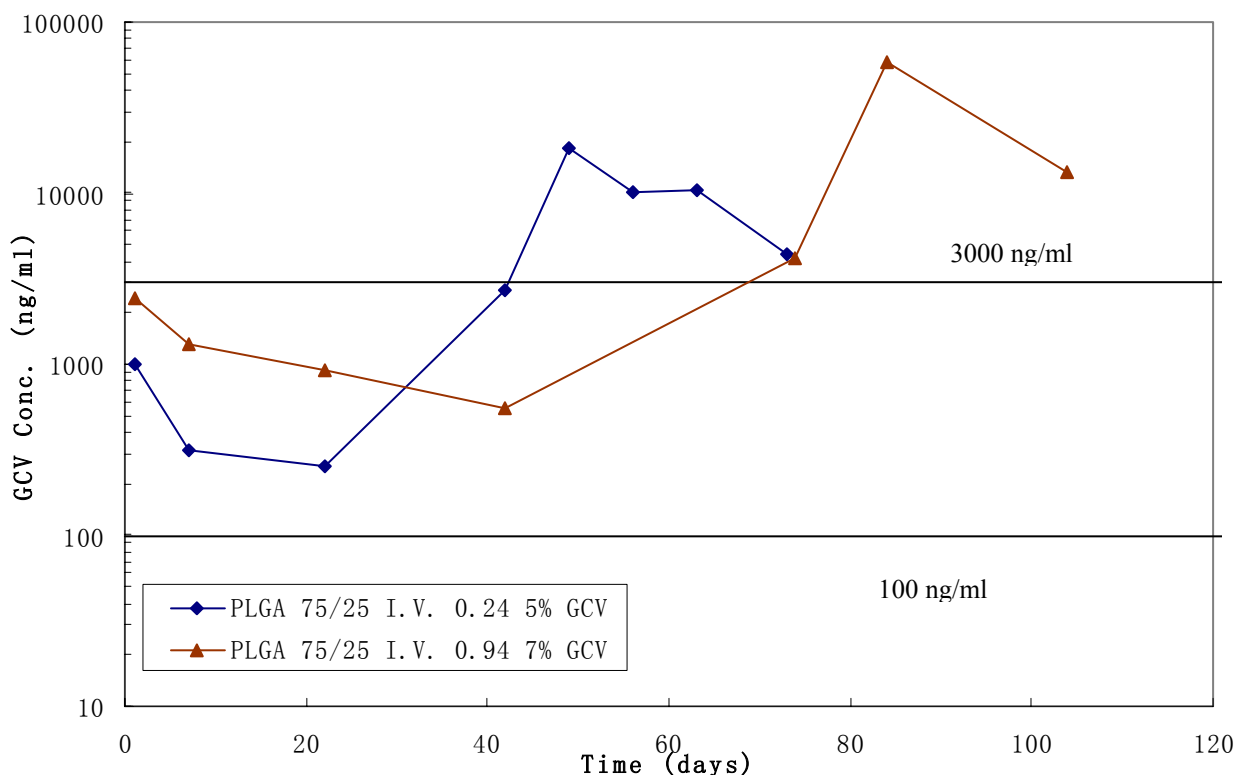


Figure 8.7 GCV concentration as a function of time during drug release for PLGA 75/25 I.V. 0.94 7% GCV tablet (\blacktriangle) and PLGA 75/25 I.V. 0.24 5% GCV tablet (\blacklozenge).

As shown in Figure 8.7, PLGA 75/25 I.V. 0.94 7% GCV tablets and PLGA 75/25 I.V. 0.24 5% GCV tablets were able to maintain their GCV concentration within the ED_{50} range for up to 42 days and 74 days respectively. The sudden burst release after that is undesirable, as an overdose of GCV was released, which was toxic to the human body.

When the initial amount of GCV-loaded tablets were reduced from 10 mg to 1.35 mg for the PLGA 75/25 I.V. 0.24 5% GCV tablet and from 10 mg to 0.45 mg for the PLGA 75/25 I.V. 0.94 7% GCV tablet while taking into account that the vitreous humor is 4.5 ml¹⁷, it was still not possible to maintain the GCV concentration within the ED_{50} range throughout the release time frame, as shown in Figure 8.8. Hence The PLGA 75/25 I.V.

0.94 7% GCV tablet and PLGA 75/25 I.V. 0.24 5% GCV tablet were not ideal to be used as the sustained release implants for the treatment of CMV retinitis.

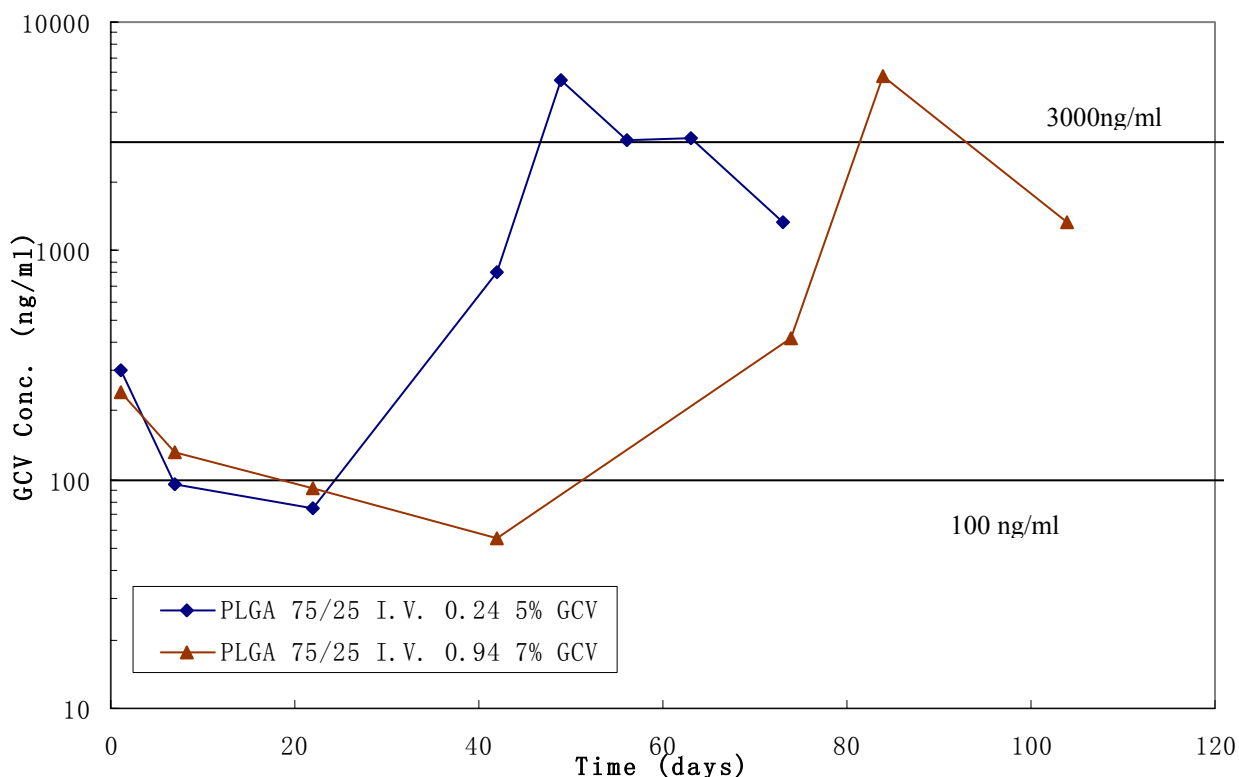


Figure 8.8 GCV concentration as a function of time during drug release for PLGA 75/25 I.V. 0.94 7% GCV tablet (▲) and PLGA 75/25 I.V. 0.24 5% GCV tablet (◆) after modification of amount.

As shown in Figure 8.9, PLGA 50/50 I.V. 0.50 5% GCV tablet was within the therapeutic range required for treatment of CMV retinitis before the onset of burst release at 28 days of degradation, which released an overdose of GCV. PLGA 50/50 I.V. 0.22 7% GCV tablet, on the other hand, failed to maintain the GCV concentration within the therapeutic range throughout the studies. The overdose of GCV concentration in both polymers was undesirable, as it would cause toxicity. However, if the initial amount of the GCV-loaded tablets was reduced from 10 mg to 0.45 mg and taking into account that the vitreous humor is 4.5 ml¹⁷, the release would be within the therapeutic range, as shown in Figure 8.10.

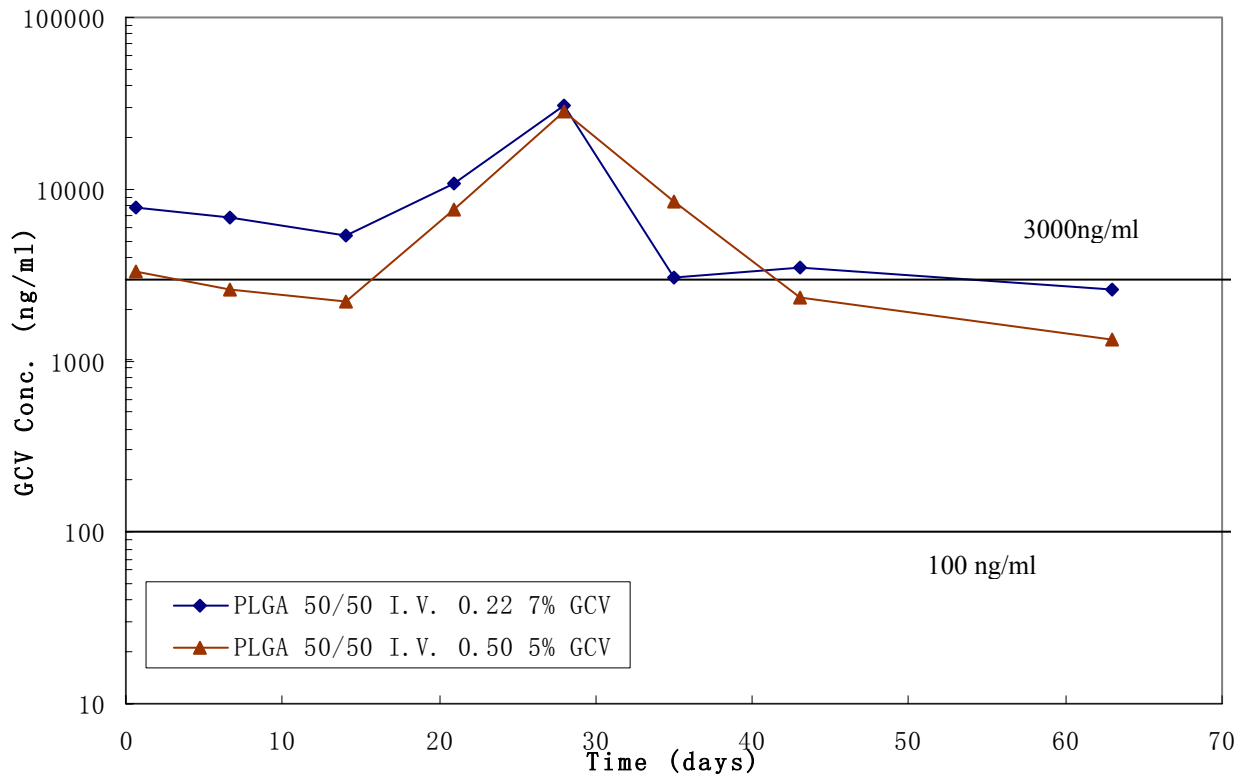


Figure 8.9 GCV concentration as a function of time during drug release for PLGA 50/50 I.V. 0.50 5% GCV tablet (▲) and PLGA 50/50 I.V. 0.22 7% GCV tablet (◆).

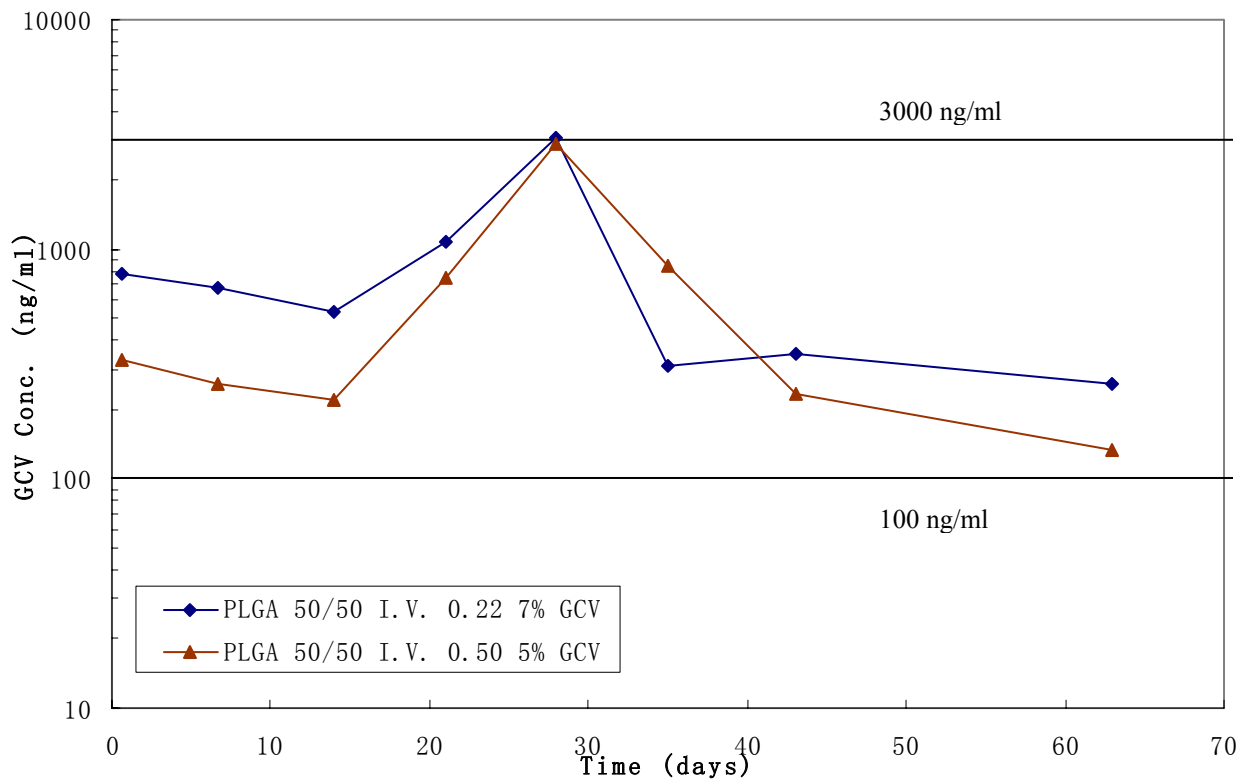
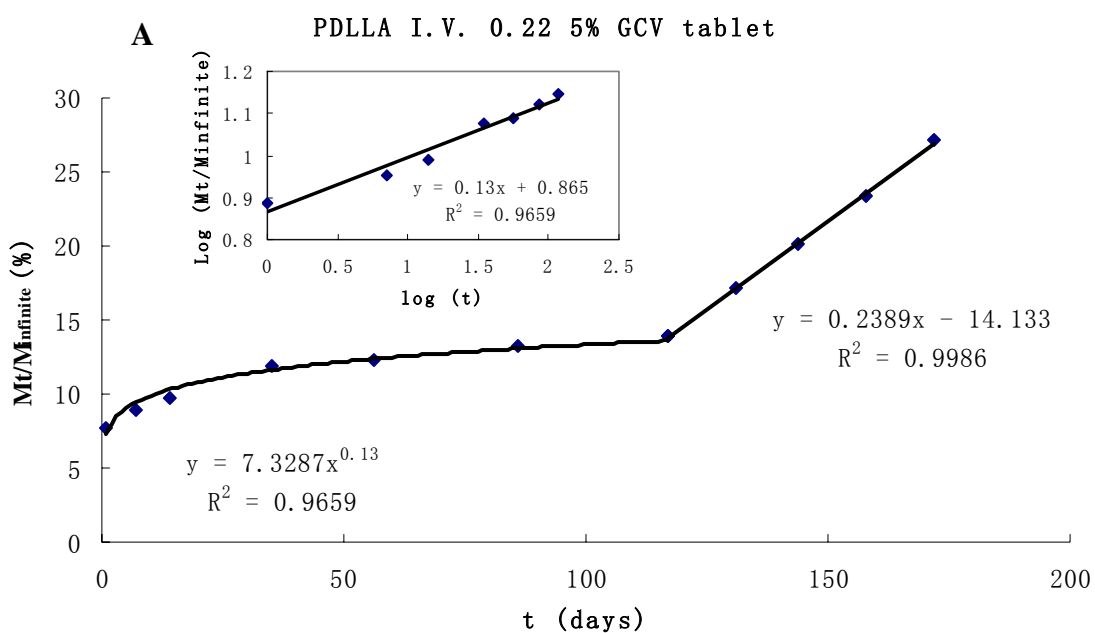


Figure 8.10 GCV concentration as a function of time during drug release for PLGA 50/50 I.V. 0.50 5% GCV tablet (▲) and PLGA 50/50 I.V. 0.22 7% GCV tablet (◆) after modification of amount.

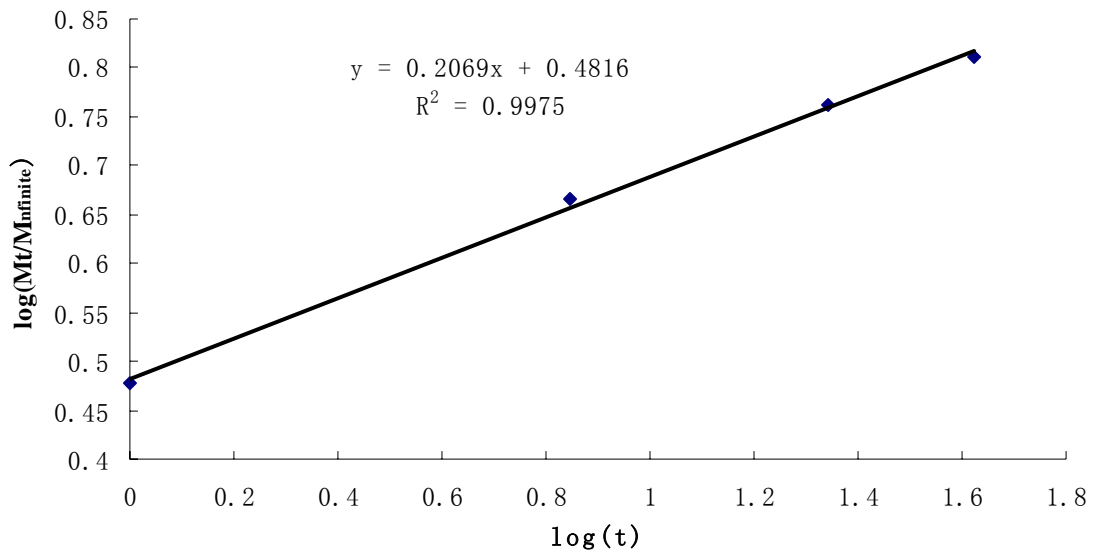
The PLGA 50/50 I.V. 0.22 7% GCV tablet and PLGA 50/50 I.V. 0.50 5% GCV tablet were ideal as sustained release intraocular devices for the treatment of CMV retinitis. The release was within the therapeutic range for 63 days, when 0.45 mg of the tablets was used.

8.6 Release mechanisms of GCV-loaded tablets

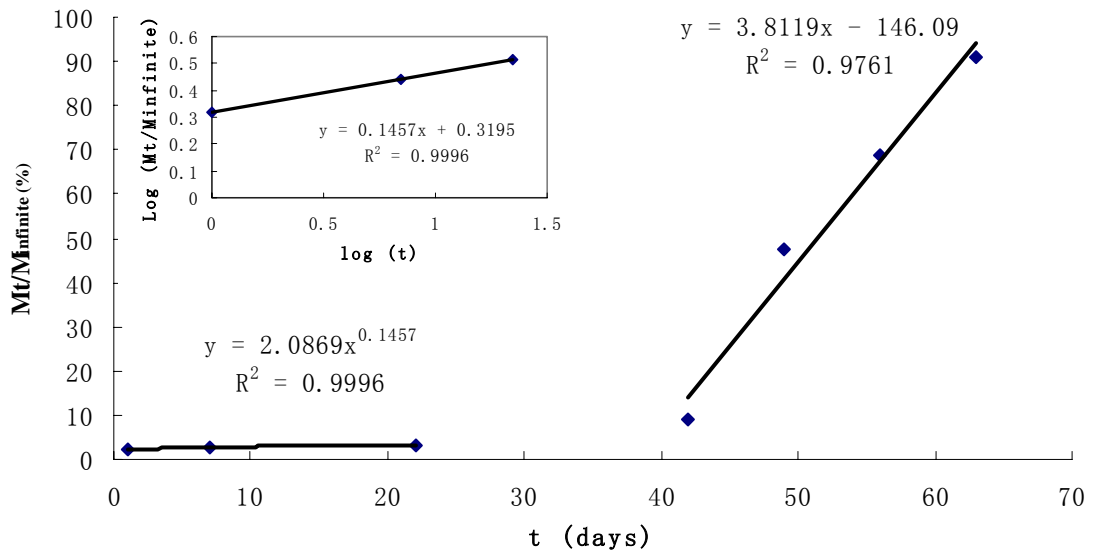
Figure 8.11 A) to E) plotted the logarithm of the fractional drug release, $\log (M_t/M_\infty)$ of GCV-loaded PDLLA and PLGA tablets respectively as function of logarithm of the hydrolytic degradation time $\log (t)$ to determine the release exponent, n . From the graphs, the fitted curves showing a strong statistical correlation ($R^2 > 0.9$) were obtained.



B PLGA 75/25 I.V. 0.94 7% GCV tablet



C PLGA 75/25 I.V. 0.24 5% GCV tablet



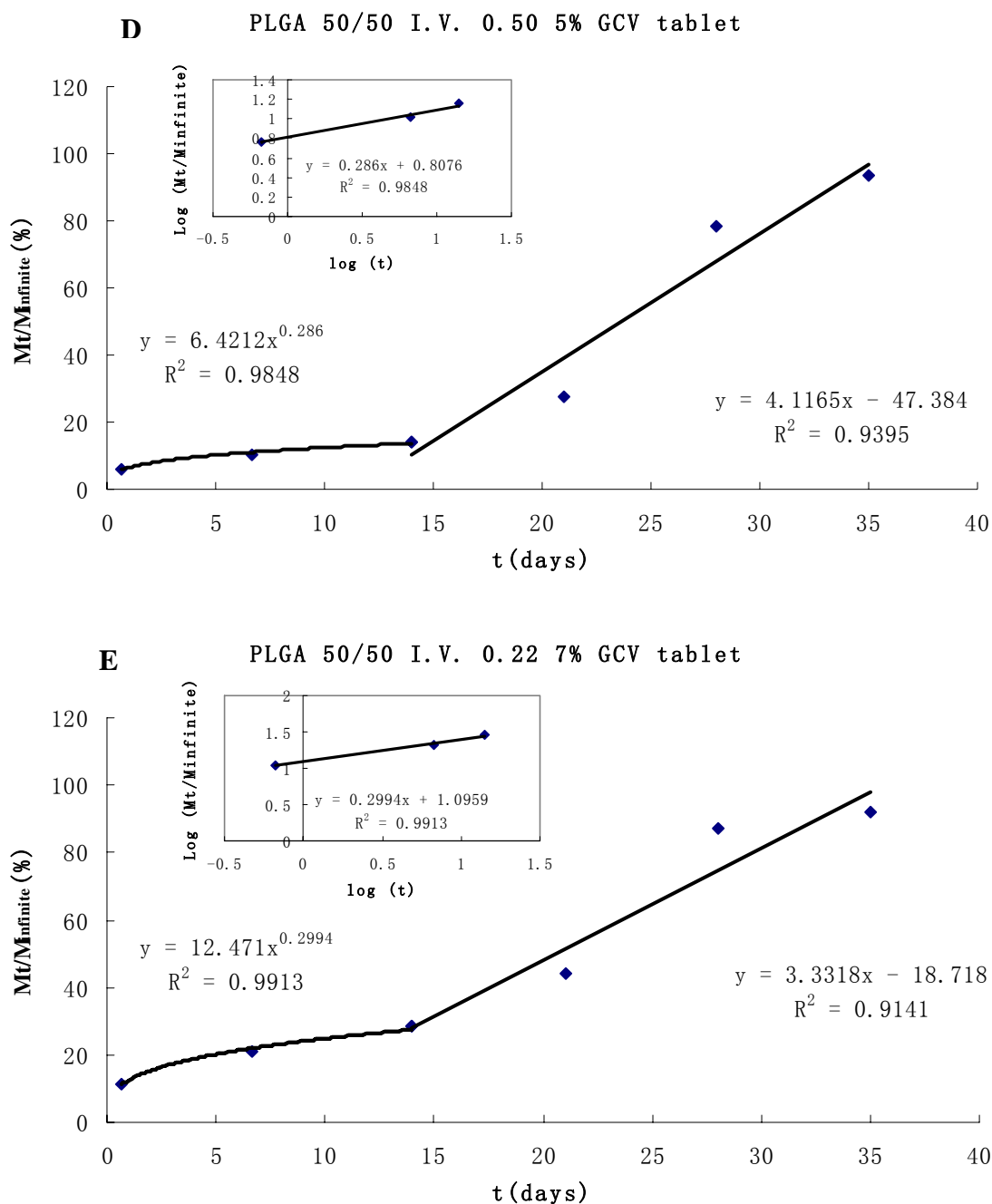


Figure 8.11 Fitting curves (both M_t/M_{∞} versus t and $\log(M_t/M_{\infty})$ versus $\log(t)$) of A) PDLLA I.V. 0.22 5% GCV; B) PLGA 75/25 I.V. 0.94 7% GCV; C) PLGA 75/25 I.V. 0.24 5% GCV; D) PLGA 50/50 I.V. 0.50 5% GCV and E) PLGA 50/50 I.V. 0.22 7% GCV tablets.

The results showed that all these five GCV-loaded tablets could be fitted to equation 2.11.

The release exponent (n) values obtained for these tablets were all less than 0.50, indicating that the release of the GCV was through diffusion and was highly dependent on the amount of the GCV that remained in the tablets.

A linear fit to the release curve was obtained during the later stages of degradation for PDLLA I.V. 0.22 5% GCV, PLGA 75/25 I.V. 0.24 5% GCV, PLGA 50/50 I.V. 0.50 5% GCV and PLGA 50/50 I.V. 0.22 7% GCV tablets, indicating the onset of disintegration of the polymeric matrix due to hydrolysis. The release of GCV was first due to diffusion, followed by zero-order release kinetics due to the polymer degradation.

Unlike their respective microspheres, the release exponent, n , can be obtained for the PLGA 50/50 I.V. 0.50 5% GCV and PLGA 50/50 I.V. 0.22 7% GCV tablets, while no release exponent, n , can be obtained for the GCV-loaded microspheres. This may be due to the difference in geometry shape resulting in different total surface area to volume ratio, which would in turn result in different water uptake rate and affect the polymeric matrix degradation rate. The tablets were made by annealing and compressing of the respective microspheres. These tablets had a denser structure and a larger volume to total surface area ratio than the microspheres. Hence a diffusive release is observed for the tablets due to the slower water uptake and rate of hydrolytic degradation compared to the microspheres.

8.7 SEM

The PLGA tablets (original tablets as well as those after *in vitro* degradation for different lengths of time) were observed under SEM, to follow the changes to the surface morphology as shown in Figure 8.11 to Figure 8.14. Within the investigation time frame, no significant changes to the surface morphology were observed for the GCV-loaded PDLLA tablets.

The morphological differences for PLGA 75/25 I.V. 0.24 5% GCV tablet and PLGA 75/25 I.V. 0.94 7% GCV tablet were quite obvious. The original tablets, which had an

initial smooth surface roughened through erosion with degradation time. As degradation proceeded, the extent of erosion was sufficient to leave a network of interconnected channels and pores as observed in Figure 8.11 and Figure 8.12.

In the PLGA 75/25 I.V. 0.24 5% GCV tablets (Figure 8.11), roughening of the surface was observed after 49 days of degradation and pores were formed on the surface. The swelling of polymers was clearly noted after 70 days of degradation.

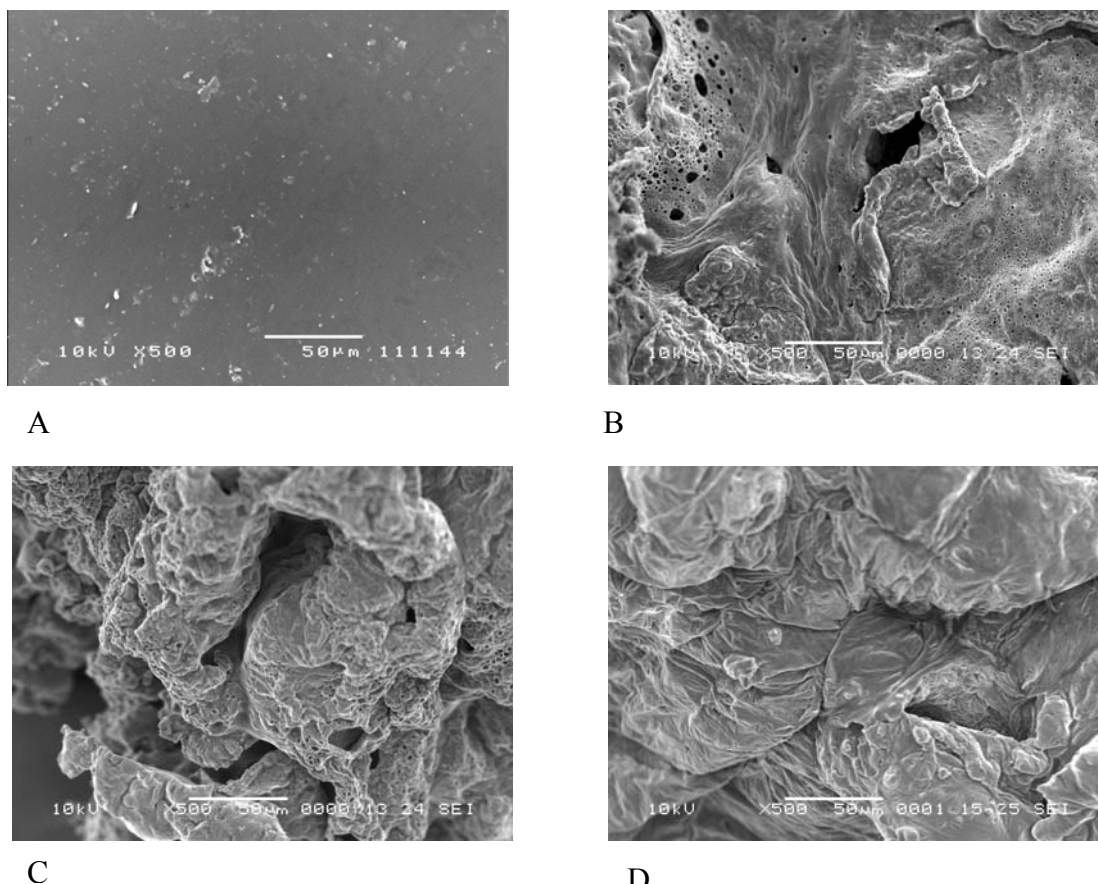
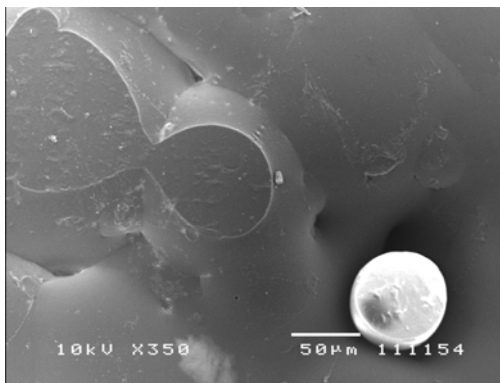
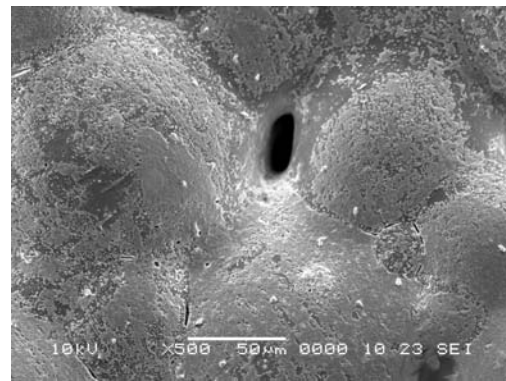


Figure 8.12 SEM photographs of PLGA 75/25 I.V. 0.24 5% GCV tablets A) 0 day; B) 49 days; C) 70 days and D) 77 days of degradation.

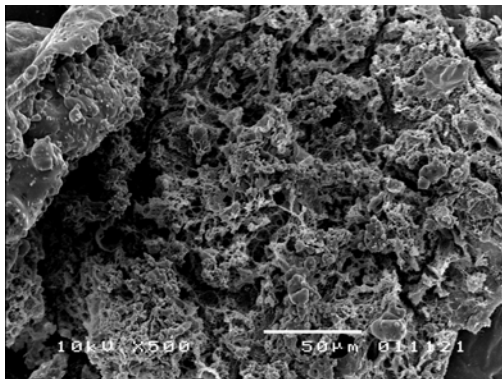
In the PLGA 75/25 I.V. 0.94 7% GCV tablet (Figure 8.12), the smooth surface was clearly observed even after 70 days of degradation. With further degradation, the surface became rougher. Finally, a network of interconnected pores and swelling of polymers were observed after 112 days of degradation.



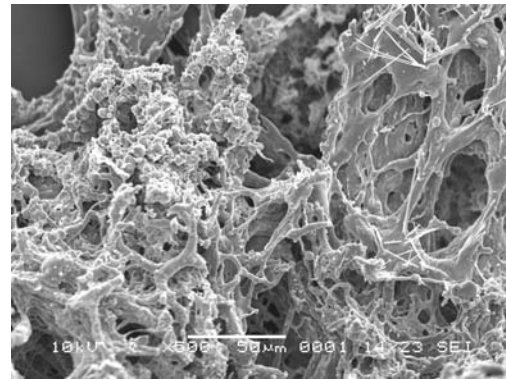
A



B



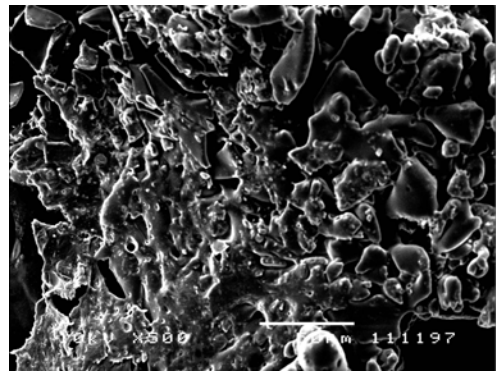
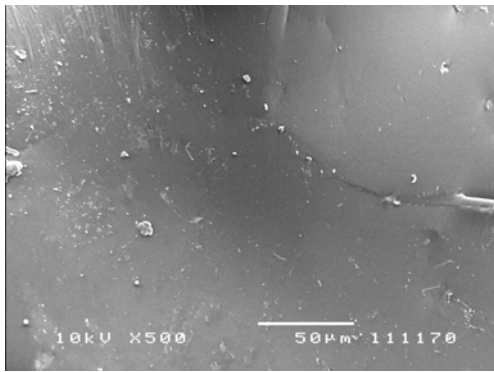
C



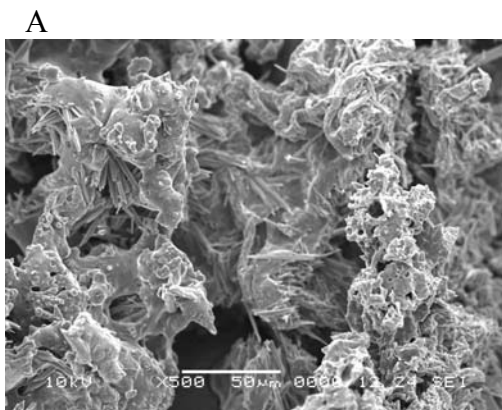
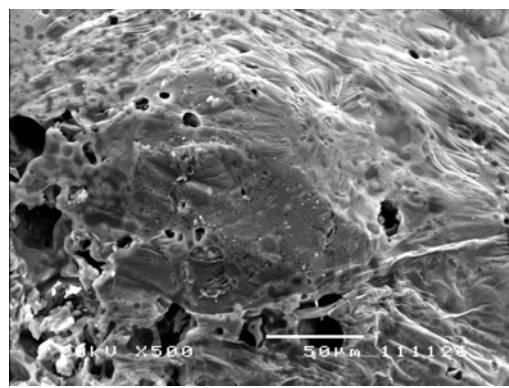
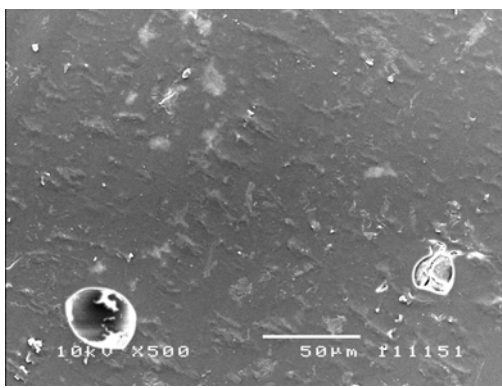
D

Figure 8.13 SEM photographs of PLGA 75/25 I.V. 0.94 7% GCV tablets A) 0 day; B) 70 days; C) 98 days and D) 112 days of degradation.

The morphological differences for PLGA 50/50 I.V. 0.22 7% GCV tablet and PLGA 50/50 I.V. 0.50 5% GCV tablet were also distinct. In the PLGA 50/50 I.V. 0.22 7% GCV tablets (Figure 8.13), the sample became gel-like after 42 days of degradation and no SEM photographs could be obtained. In the PLGA 50/50 I.V. 0.50 5% GCV tablets (Figure 8.14), the initial smooth surface roughened after 14 days of degradation. Finally, a network of interconnected pores and swelling of polymers were observed after 42 days of degradation.



A B
Figure 8.14 SEM photographs of PLGA 50/50 I.V. 0.22 7% GCV tablets A) 0 day; B) 14 days of degradation.



A B C
Figure 8.15 SEM photographs of PLGA 50/50 I.V. 0.50 5% GCV tablets A) 0 day; B) 14 days and C) 42 days of degradation.

8.8 Conclusions

In the GCV-loaded microspheres, linear fit to the change in T_g with degradation time could be carried out on all the samples, while in the case of the GCV-loaded tablets, a lag time was observed in most of the samples, followed by a decrease in T_g with degradation

time. A linear fit was obtained only for PLGA 50/50 I.V. 0.22 7% GCV tablets. The lag time was due to slower water uptake into the tablets compared to the microspheres. These tablets had a denser structure and a larger volume to total surface area ratio than the microspheres. Hence the slower water uptake and rate of hydrolytic degradation were observed. The high GA content in PLGA 50/50 polymers made the polymers more hydrophilic. Hence the PLGA 50/50 polymers required much shorter time for water uptake compared to the PLGA 75/25 polymers and PDLLA polymers.

Slight weight gain after the immersion in PBS solution was observed for some GCV-loaded tablets, unlike in the microspheres where the mass decreased steadily with degradation time. No weight gain was observed for the respective microspheres. Here, the tablets had higher volume to total surface area ratio than the microspheres. Hence it was easier for the absorbed water to remain inside the tablets, causing the slight weight gain after the immersion in PBS solution, as observed in PLGA 75/25 I.V. 0.94 7% GCV and PLGA 75/25 I.V. 0.24 5% GCV tablets.

Processing the microspheres into tablet did not significantly affect the hydrolytic degradation rate of the PLGA 75/25 I.V. 0.24 polymer with 5% GCV loading. In PDLLA I.V. 0.22 5% GCV and PLGA 75/25 I.V. 0.94 7% GCV tablets, the k' values were significantly reduced when compared with the microspheres due to slower water uptake and rate of hydrolytic degradation.

In comparison to the change in pH with degradation time for the GCV-loaded microspheres (Figure 6.14), the tablets had a smaller change in pH with degradation time. The pH only dropped to around 6.5 at later stages of degradation for these GCV-loaded

tablets. This was due to the slower degradation rate observed in the tablets compared with the microspheres.

The onset of burst release from the PLGA 75/25 tablets occurred earlier than the microspheres. This was possibly due to disintegration of the tablets at the adhesion points rather than advance hydrolytic degradation of the polymer. The differences in time frame for tablets and microspheres were likely due to the processing techniques used in making the tablets. The pressure applied could have crushed some of the microspheres, changing the internal structure of the microspheres and exposing some of the GCV initially encapsulated by the polymer matrix. The annealing step was to enable particle adhesion so as to improve the handling properties of the tablet. The time frames for the initial burst release and following diffusion phase obtained for PDLLA I.V. 0.22 5% GCV tablets were similar to the microspheres. The PLGA 50/50 I.V. 0.22 7% GCV and PLGA 50/50 I.V. 0.50 5% GCV tablets exhibited an initial burst release after 1 day of immersion. Unlike the corresponding microspheres, which exhibited no initial burst as shown in Figure 7.1. The initial burst release from the tablets would suggest that GCV was distributed on or close to the surface of the tablets. The pressing also formed the channels and drains throughout the polymer matrix, hence it was easier for the GCV to migrate to the lower GCV concentration area like the surface of the tablets due to the concentration gradient.

The release exponent, n , can be obtained for PDLLA I.V. 0.22 5% GCV, PLGA 75/25 I.V. 0.94 7% GCV, PLGA 75/25 I.V. 0.24 5% GCV, PLGA 50/50 I.V. 0.50 5% GCV and PLGA I.V. 0.22 7% GCV tablets. The exponent values for these tablets were all less than 0.50, indicating that the release of the GCV was through diffusion and was highly dependent on the amount of the GCV that remained in the tablets. The release of GCV

was first due to diffusion, followed by zero-order release kinetics due to the polymer degradation. Unlike their respective microspheres, the release exponent, n , can be obtained for the PLGA 50/50 I.V. 0.50 5% GCV and PLGA 50/50 I.V. 0.22 7% GCV tablets, while no release exponent, n , can be obtained for the GCV-loaded microspheres. These tablets had a denser structure and a larger volume to total surface area ratio than the microspheres. Hence a diffusive release is observed for the tablets due to the slower water uptake and rate of hydrolytic degradation compared to the microspheres.

The PLGA 50/50 I.V. 0.22 7% GCV tablet and PLGA 50/50 I.V. 0.50 5% GCV tablet were ideal to be used as sustained release intraocular devices for the treatment of CMV retinitis. The release was within the therapeutic range for 63 days, when 0.45 mg of the tablets was used.

CHAPTER 9

CONCLUSIONS

9.1 Degradation Studies

9.1.1 Pure microspheres

Pure PDLA microspheres and PLGA 75/25, PLGA 50/50 microspheres of size of $110 \pm 20 \mu\text{m}$ were successfully produced using oil/water emulsion technique¹⁸. By decreasing the concentration of the polymer during emulsification, the particle size decreased along with narrowing of the size distribution.

All of the as-received PDLA, PLGA 75/25, PLGA 50/50 polymers and the pure microspheres in this study were totally amorphous.

The effects of the degradation on the thermal, morphological and surface properties of the PDLA, PLGA 75/25, PLGA 50/50 pure microspheres were studied. The PDLA was the slowest to degrade, followed by PLGA 75/25 and PLGA 50/50. The slowest degradation rate was due to the presence of methyl groups in the lactic acid. The voluminous alkyl hindered the attack of water³⁶, which caused the polymer to be more hydrophobic than the other two copolymers, thus decreasing the rate of water uptake. For the PLGA copolymers with the same LA to GA ratio but different intrinsic viscosity (I.V.), the polymer with higher I.V. was slower to hydrolytically degrade than the polymer with lower intrinsic viscosity. This phenomenon was observed for both the PLGA 75/25 and PLGA 50/50 polymers investigated in this study. PLGA 50/50 had the fastest degradation rate among the polymers investigated because the I.V. played a less

significant role as compared to the LA to GA ratio in affecting the rate of hydrolytic degradation of the PLGA and PDLA polymers.

The PLGA 50/50 I.V. 0.50 had the lowest R_{cms} , thus the highest degree of heterogeneity or blockiness among the copolymers investigated. This resulted in a faster decrease of the molecular weight during the early stages of degradation when compared to the other copolymers. This in turn, enabled earlier crystallization of glycolic and lactic units compared to the other copolymers. Chain scissions during hydrolytic degradation would enable the fragments with shorter chains to move and reorganize themselves from a disordered to an ordered state. Crystallization could thus be induced in the formerly amorphous polymer. The PLGA 75/25 I.V. 0.94 had the highest R_{cms} value, which was close to 1, indicating a homogeneous copolymer. It would tend to maintain the amorphous state during the later stages of hydrolytic degradation and the molecular weight would not drop as dramatically during the first stages of hydrolytic degradation. The PLGA with a lower degree of blockiness is believed to have more GA-LA connectors than the PLGA with a higher degree of blockiness.

The PLGA and PDLA microspheres underwent bulk degradation. The glass transition temperature, T_g , of the polymers decreased with degradation time.

In the PDLA I.V.0.22, hydrolytic degradation was observed only after 84 days of degradation, where the k' value increased from 0 to 0.0115. The initial lack of hydrolytic chain scission was due to the inherent hydrophobic nature of LA units, which discouraged water absorption, thus decreasing the rate of hydrolytic chain scission. In the PLGA 75/25 I.V. 0.94, the drastic increase in hydrolysis rate after 36 days of degradation indicated auto-catalyst effect. Acidic products from the scissions of the ester bonds trapped inside

the polymer matrix increased the rate of degradation of the core in comparison to the surface of the microspheres 5.

9.1.2 GCV-loaded microspheres

GCV was successfully incorporated in the polymer and was in a crystalline state in the microspheres. As the polymers underwent hydrolytic degradation, multiple melting peaks were observed for all the GCV-loaded microspheres. These melting peaks were generated by the crystallization of fragments of degraded chains trapped in the microspheres.

The incorporation of GCV, affected the T_g and M_w profile with respect to degradation time. It is believed that the incorporation of GCV affected the T_g decrease profile due to accelerated water uptake rate caused by small pores and channels left behind after GCV had dissolved and released to the surrounding medium.

The pH of the degradation medium was maintained within the range between 2.2 and 9.4 during the entire time of investigation in. In this pH range, the GCV was mainly neutral, with no-charged groups. Theoretically, GCV would not alter degradation through chemically affecting the hydrolysis.

The incorporation of GCV did not significantly affect the degradation rate constant of PDLLA. The incorporated GCV was believed to accelerate the hydrolysis process of the low GCV-loaded PLGA microspheres due to basic-catalysis, which resulted in larger k' values compared with pure and high GCV-loaded PLGA microspheres. In the high GCV-loaded PLGA microspheres, the initial burst left behind small pores and micro-channels on and near the surface. This allowed for larger water uptake, thus increasing the dissolution and diffusion of GCV and water-soluble degradation products from the

matrix. This allowed the hydrolysis of the polymer backbone to occur with little and/or no auto-catalyst effect. Hence the smaller k' values in high GCV-loaded PLGA microspheres were obtained compared with low GCV-loaded PLGA microspheres. The incorporation of GCV increased the k' value but to a certain limit, where excess GCV decelerated and/or had no effect on the k' value.

In all the samples, GCV-loaded and pure microspheres, the pH decreased with degradation time. The decrease in pH with degradation indicated the release of acidic oligomers/monomers via hydrolytic degradation.

9.2 Drug release studies

The size range of the ganciclovir-loaded microspheres was from 90 to 130 μm . The microspheres with low GCV payload (5% - 7% wt/wt) displayed a biphasic release pattern, i.e. a diffusive phase followed by a burst release. There was no initial burst of GCV in all the low GCV payload microspheres. As for the microspheres with high GCV payload (18% - 20% wt/wt), they displayed a very high initial burst release, where 47.49% to 68.38% of GCV was released after 24 hours of incubation. This was followed by a biphasic release pattern, similar to that of the microspheres with low GCV payload. The initial burst release was due to the large amount of GCV found on the surface of the microspheres, which was confirmed from the XPS profiles.

The burst release phase released most of the GCV incorporated in the microspheres. The onset of this phase coincided with the onset of rapid decrease in M_w . The time taken for the complete release of GCV into the surrounding was determined by the length of the diffusive phase, where the polymers with the same LA to GA ratio the microspheres from

polymers of lower I.V. had shorter diffusive phase than the microspheres from the polymers of higher intrinsic viscosity.

The release exponent, n , of less than 0.43 was only obtained for PDLLA I.V. 0.22 5% GCV ($n=0.1074$), PLGA 75/25 I.V. 0.94 7% GCV ($n=0.2074$), PLGA 75/25 I.V. 0.94 18% GCV ($n=0.0558$) and PLGA 75/25 I.V. 0.24 5% GCV ($n=0.1384$) microspheres, indicating the release of GCV for these microspheres was through diffusion and was highly dependent on the amount of the GCV that remained in the microspheres.

For PLGA 50/50 I.V. 0.50 5% GCV, PLGA 50/50 I.V. 0.50 20% GCV and PLGA 50/50 I.V. 0.22 7% GCV microspheres, a zero-order release profile was obtained. In these polymers, the rate of water penetration into the polymer matrix was equivalent to the polymer chain scission rate, thus the GCV was released through diffusion and polymer degradation.

PLGA 50/50 I.V. 0.22 7% GCV microspheres were not ideal as sustained release DDS for CMV retinitis. Similar conclusions could be made for PDLLA I.V. 0.22 5% GCV and PLGA 75/25 I.V. 0.94 7% GCV microspheres. The drastic burst release of GCV during the burst release phase was unwanted and un-avoided.

It was concluded that PLGA 75/25 I.V. 0.94 18% GCV, PLGA 75/25 I.V. 0.24 5% GCV, PLGA 50/50 I.V. 0.50 5% GCV and PLGA 50/50 I.V. 0.50 20% GCV microspheres were ideal to be used for sustained delivery of GCV to treat CMV retinitis. These microspheres released GCV for 63 days (PLGA 50/50 I.V. 0.50 5% GCV) to 132 days (PLGA 75/25 I.V. 0.94 18% GCV).

9.3 GCV-loaded tablets

With the exception of PDLLA I.V. 0.22 5% GCV microspheres, the GCV-loaded PLGA had significantly different T_g , M_w , mass change, pH and release profiles from their corresponding GCV-loaded microspheres.

In the GCV-loaded tablets, a lag time was observed in most of the samples, followed by a decrease in T_g with degradation time. A linear fit was obtained only for PLGA 50/50 I.V. 0.22 7% GCV tablets. The lag time was due to slower water uptake into the tablets compared to the microspheres. These tablets had a denser structure and a larger volume to total surface area ratio than the microspheres. Hence the slower water uptake and rate of hydrolytic degradation were observed.

Slight weight gain after the immersion in PBS solution was observed for some GCV-loaded tablets, unlike in the microspheres where the mass decreased steadily with degradation time. Here, the tablets had higher volume to total surface area ratio than the microspheres. Hence it was easier for the absorbed water to remain inside the tablets, causing the slight weight gain after the immersion in PBS solution, as observed in PLGA 75/25 I.V. 0.94 7% GCV and PLGA 75/25 I.V. 0.24 5% GCV tablets.

The onset of burst release from the PLGA 75/25 tablets occurred earlier than the microspheres. This was possibly due to disintegration of the tablets at the adhesion points rather than advance hydrolytic degradation of the polymer. During the processing steps, the pressure applied to the microspheres would have changed the internal structure of the microspheres and exposed some of the GCV initially encapsulated by the polymer matrix. Only the time frames for the initial burst release and following diffusion phase obtained for PDLLA I.V. 0.22 5% GCV tablets were similar to the microspheres. The rest of the

tablets exhibited an initial burst release after 1 day of immersion, unlike the corresponding microspheres. It was possible that during the processing of the tablets, some of this GCV particles, which were previously encapsulated by the polymer matrix were no longer encapsulated due to the pressure and heating applied, resulting in some aggregation near the surface of the tablets.

The release exponent, n , can be obtained for PDLLA I.V. 0.22 5% GCV, PLGA 75/25 I.V. 0.94 7% GCV, PLGA 75/25 I.V. 0.24 5% GCV, PLGA 50/50 I.V. 0.50 5% GCV and PLGA I.V. 0.22 7% GCV tablets. The exponent values for these tablets were all less than 0.50, indicating that the release of the GCV was through diffusion and was highly dependent on the amount of the GCV that remained in the tablets. The release of GCV was first due to diffusion, followed by zero-order release kinetics due to the polymer degradation. Unlike their respective microspheres, the release exponent, n , can be obtained for the PLGA 50/50 I.V. 0.50 5% GCV and PLGA 50/50 I.V. 0.22 7% GCV tablets.

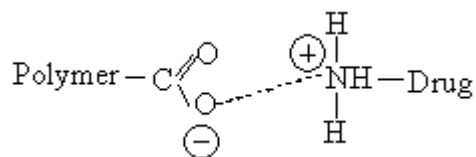
Among the tablets, the PLGA 50/50 I.V. 0.22 7% GCV and PLGA 50/50 I.V. 0.50 5% GCV tablets were the most ideal to be used as sustained release intraocular devices for the treatment of CMV retinitis. The release was within the therapeutic range for 63 days, when 0.45 mg of the tablets was used. Hence PLGA 50/50 polymers were the most suitable polymers to be used for sustained release of GCV in the treatment of CMV retinitis.

CHAPTER 10

FUTURE WORK

From the *in vitro* investigations carried out, several systems have been identified as suitable candidates for sustained release of GCV in treatment of CMV retinitis. The next important step would be the *in vivo* tests. *In vivo* tests have to be carried out to evaluate the degradation and GCV release profile of the suitable candidates. *In vivo* and/or *in-vitro* bioequivalence testing is required for most multisource (generic) pharmaceutical drug products submitted for marketing approval. A proposed multisource (generic) pharmaceutical drug product must be compared *in vivo* and/or *in vitro* to the officially designated reference drug product. Hence, the *in vivo* test is important before the systems could be used in treatment of CMV retinitis.

The presence of an amino group on GCV molecule and free carboxylic groups on the polymers suggest the possibility of salt formation. Possible interaction products may have the following structure:



It would be interesting to chemically attach GCV to the polymer backbone. The chain length of the polymer backbone and the drug attachment ratio to the polymer backbone could be investigated. Further investigation of the drug release mechanism and polymer degradation of this kind of drug delivery device could also be carried out. As Robert Langer⁵⁵ pointed out, drugs can be released when the bonds between the drug and a polymer backbone are cleaved. Jorge Heller² classified such pendant-chain systems to chemically controlled delivery systems. In the pendant-chain systems the drug is

covalently attached to a biodegradable polymer backbone. Such systems are toxicologically complicated because the FDA requires unambiguous proof that the chemically attached drug is released in its native form and not as a chemical derivative. Pendant-chain systems are not currently under development with the exception of polymer conjugates used in tumor targeting.

Other biodegradable polymers besides PLGA/PLA could be investigated as possible matrix for drug delivery. The polyanhydrides, such as poly (PCPP-SA anhydride), are possible candidates. Poly (PCPP-SA anhydride) is among the five approved distinct synthetic, degradable polymers for use in a narrow range of clinical applications by the FDA⁴. Aliphatic polyanhydrides degrade within days, whereas some aromatic polyanhydrides degrade over several years. Many polyanhydrides degrade by surface erosion without the need to incorporate various catalysts or excipients into the device formulation³. The advantage of surface eroding polymers is the predictability of the erosion process. This is desirable for drug delivery application, where the release of drugs can be related directly to the rate of polymer erosion.

Kunouk, N., Ogura⁹⁶ developed a new GCV-loaded implantable device by combining PLGA copolymers of different molecular weight. Such device provided both a higher release rate of drugs and a prolonged diffusive phase as well as eliminated the final burst. A cocktail made up of microspheres of different molecular weight, LA to GA ratio and GCV payload could be investigated to obtain the degradation and the GCV release profile to fit the ED₅₀ range in order to treat the CMV retinitis. This can be achieved by mixing PLGA polymers of different molecular weight and different LA to GA ratio first. The mixture is then dissolved in DCM with GCV homogeneously dispersed within the polymer solutions. The solution is further processed into microspheres. This cocktail can

also be achieved by physically mixing GCV-loaded PLGA microspheres of different molecular weight and LA to GA ratio, for example, mixing PLGA75/25 I.V. 0.94 7% GCV with PLGA 50/50 I.V. 0.22 7% microspheres. With the help of linear relationship and two component algebra, the release profile of the mixtures can be predicted.

Besides the loose microspheres described above, the tablet form of the mixed microspheres could also be investigated to obtain the degradation and the GCV release profile to fit the ED₅₀ range for treatment of the CMV retinitis.

REFERENCES

1. Drew WL. (1992), Cytomegalovirus infection in patients with AIDS. *Clinical Infectious Diseases*, 14, 608-615.
2. Jorge Heller, & Allan S. Hoffman, (2004a), Drug Delivery Systems. In Buddy D. Ratner, Allan S. Hoffman, Frederick J. Schoen, etc. (Eds.), *Biomaterials Science, An Introduction to Materials in Medicine, 2nd edition*, (pp. 629-649). New York: Elsevier.
3. Bret Berner, & Steve Dinh, (1992), Fundamental Concepts in Controlled Release. In Agis Kydonieus (Ed.), *Treatise on controlled drug delivery: fundamentals, optimization, applications*, (pp.1-35). New York: Marcel Dekker.
4. Joachim Kohn, Sascha Abramson, & Robert Langer, (2004b), Bioresorbable and Bioerodible Materials. In Buddy D. Ratner, Allan S. Hoffman, Frederick J. Schoen, etc. (Eds.), *Biomaterials Science, An Introduction to Materials in Medicine, 2nd edition*, (pp. 115-127). New York: Elsevier.
5. L.G.Griffith, (2000). Polymeric Biomaterials. *Acta Materialia*, 48 (1), 263-277.
6. Rajeev A. Jain, (2000). The manufacturing techniques of various drug loaded biodegradable poly (lactide-co-glycolide) (PLGA) devices. *Biomaterials*, 21 (23), 2475-2490.
7. Toshiro Heya, Yasushi Mikura, & Akihiro Nagai, et al, (1994). Controlled release of thyrotropin releasing hormone from microspheres: evaluation of release profiles and pharmacokinetics after subcutaneous administration. *Journal of Pharmaceutical Sciences*, 83 (6), 798-801.
8. Hayley Jeffery, Stanley S. Davis, & Derek T. O'Hagan, (1993). The preparation and characterization of Poly (lactide-co-glycolide) microparticles. II. The entrapment of a model protein using a (water-in-oil)-in-water emulsion solvent evaporation technique. *Pharmaceutical Research*, 10, 362-368.
9. Takahiro Uchida, Stephen Martin, & Todd P. Foster, et al, (1994). Dose and load studies for subcutaneous and oral delivery of poly (lactide-co-glycolide) microspheres containing ovalbumin. *Pharmaceutical Research*, 11(7), 1009-1015.
10. C.X. Song, V. Labhasetwar, & H. Murphy, et al, (1997). Formulation and characterization of biodegradable nanoparticles for intravascular local drug delivery. *Journal of Controlled release*, 43 (2-3), 197-212.
11. Rocio Herrero-Vanrell, & Miguel F. Refojo, (2001). Biodegradable microspheres for vitreoretinal drug delivery. *Advanced Drug Delivery Reviews*, 52 (1), 5-16.
12. Bochot, A., Couvreur, & P., Fattal, E., (2000). Intravitreal administration of antisense oligonucleotides: potential of liposomal delivery. *Progress in Retinal and eye Research*, 19 (2), 131-147.
13. Nasr Anaizi, (1997). The drug monitor. Ganciclovir [On-line]. Available: <http://www.thedrugmonitor.com/ganciclovir.html>.
14. Musch, D.C., Martin, D.F., & Gordon, J.F., etc., (1997). Ganciclovir implant study group: treatment of cytomegalovirus retinitis with a sustained-release ganciclovir implant. *The New England Journal of Medicine*, 335, 83-90.
15. Noriyuki Kunou, Yuichiro Ofura, & Yoshihito Honda, etc., (2000). Biodegradable sclera implant for controlled intraocular delivery of betamethasone phosphate. *Journal of Biomedical Materials Research*, 51 (4), 635-641.
16. Eiji Sakurai, Yoshito Matsuda, & Hironori Ozeki, etc., (2001). Sclera plug of biodegradable polymers containing ganciclovir for experimental cytomegalovirus retinitis. *Investigative Ophthalmology and Visual Science*, 42 (9), 2043-2048.
17. Rocio Herrero-vanrell, Loreto Ramirez, & Ana fernandez-Carballido, etc., (2000). Biodegradable PLGA microspheres loaded with ganciclovir for intraocular

- administration. Encapsulation technique, in vitro release profiles, and sterilization process, *Pharmaceutical Research*, 17 (10), 1323-1328.
18. Amadeo A.S, Veloso, Jr., & Qi Zhu, etc., (1997), Ganciclovir-loaded polymer microspheres in rabbit eyes inoculated with human cytomegalovirus, *Investigative Ophthalmology and Visual Science*, 38 (3), 665-675.
 19. Giordano, G.G., Chevez-Barrios, & P., Refojo, M.D., etc., (1995). Biodegradation and tissue reaction to intravitreal biodegradable poly(D,L-lactic-co-glycolic)acid microspheres. *Current Eye Research*, 14, 761-768.
 20. Moritera, T., Ogura, Y., & Yoshimura, N., Honda, etc., (1991). Microspheres of biodegradable polymers as a drug-delivery system in the vitreous. *Investigative Ophthalmology and Visual Science*, 32, 1785-1790.
 21. Kulkarni, R. K., Moore, E. G., & Hegyeli, A. F.etc., (1971), Biodegradable poly(lactic acid) polymers. *Journal of Biomedical Materials Research*, 5 (3), 169-181.
 22. Gilding, d. K. and Reed, A. M., (1979). Biodegradable polymers for use in surgery-polyglycolic/poly(lactic acid)homo-and copolymers, part 1, *Polymer*. 20 (12), 1459-1464.
 23. Tice TR, & Cowsar DR, (1984), Biodegradable controlled-release parenteral systems. *Pharmaceutical Technology*, 11, 26-35.
 24. Leenslag, J.W., Pennings, A..J., Bos, & R.R.M., Rozema, etc., (1987), Resorbable materials of poly (L-lactide). VI. Plates and screws for internal fracture fixation, *Biomaterials*, 8 (1), 70-73.
 25. Reed, A.M. & Gilding, D.K., (1981), Biodegradable polymers for use in surgery poly (glycolic)/poly(lactic acid) homo- and copolymers. Part 2: in vitro degradation. *Polymer*, 22(4), 494-498.
 26. Frazza, E.J., Schmitt, E.E., (1971), A new absorbable suture, *Journal of Biomedical Materials Research Symposium*, 1, 43-58.
 27. Argoustakis K., and Nixon J. R., (1991). Biodegradable controlled release tablets 1: Preparative variables affecting the properties of poly(lactide-co-glycolide) copolymers as matrix forming material. *International Journal of Pharmaceutics*. 70 (1-2), 77-85.
 28. Bendix, D., (1990) Analytical studies on the solubility problem of poly(DL-lactide-co-glycolide) 50:50. *Proceedings of International Symposium on Controlled Release Bioactive Materials*, 17, 248-249.
 29. Dorta M. J., Munguia O., & Llabres M., (1993). Effects of polymerization variables on PLGA properties: molecular weight, composition and chain structure. *International Journal of Pharmaceutics*, 100 (1-3), 9-14.
 30. R.L. Chasin Ma., (Ed.) (1990). *Biodegradable Polymers and Drug Delivery Systems* (pp. 71-120). New York: Marcel Dekker.
 31. B. Kalb, & A. J. Pennings., (1980). General Crystallization behavior of Poly (L-lactic Acid), *Polymer*. 21 (6), 607-612.
 32. Lisa Brannon-Peppas, & Michel Vert., (2000). Polylactic and Polyglycolic Acids as Drug Delivery Carriers. In Donald L. Wise (Ed.), *Handbook of Pharmaceutical Controlled Release Technology* (pp. 99-129). New York: Marcel Dekker.
 33. Achim Gopferich, (1996). Mechanisms of polymer degradation and erosion. *Biomaterials*. 17 (2), 103-114.
 34. Kronenthal. R.L., (1975). Biodegradable polymers in medicine and surgery. In R.L. Kronenthal, Z. Oser, and E. Martin, (Eds.), *Polymers in Medicine and Surgery*, (pp. 119-137). New York: Plenum Publishing.
 35. Pitt. C. G., Gratzel. M.M., & Kimmel, G. L., (1981). Aliphatic polyesters II. The degradation of poly (DL-lactide), poly (-caprolactone), and their copolymers in vivo, *Biomaterials*, 2 (4), 215-220.

36. Tamada J, Langer R. (1993). Erosion kinetics of hydrolytically degradable polymers. *Proceedings of the National Academy of Sciences of the USA*, 90 (2), 552-556.
37. Banford CH, & Tipper CFH. (Ed.). (1972). *Comprehensive Chemical Kinetics (Vol 14: Degradation of Polymers)*. New York: Elsevier.
38. Grassie N, Scott G. (1985). *Polymer Degradation and Stabilization*. New York: Cambridge University Press.
39. Seppala j, Linko Y-Y, & Su T, (1991). Photo- and biodegradation of high volume thermoplastics. *Acta Polytechnica Scandinavica*. 198, 10-12.
40. Spenleauer G, Vert M. Benoit JP, & Boddaert A. (1989). In vitro and in vivo degradation of poly (D,L-lactide/glycolide) type microspheres made by solvent evaporation method. *Biomaterials*, 10. 557-563.
41. Chatfield DA, Einhorn IN. (1981). Stepwise thermal degradation of a polybenzimidazole foam. *Journal of Polymer Science: Polymer Chemistry Edition*, 19 (3), 601-618.
42. Brandwood A, Noble KR, & Schindhelm K et al, (1992). Influences of stress on biodegradation of novel biomedical polyurethanes. *Advanced Biomaterials*, 10, 413-420.
43. Miler ND, & Williams DF, (1984). The in vivo and in vitro degradation of PGA suture material as a function of applied strain. *Biomaterials*, 5 (6), 365-368.
44. Von Michaela Schulz, Torsten Blunk und Achim Göpferich, (1992a). Träger für Arzneiformen und künstliche lebende Gewebe. In M. Vert, J. Feijen, & A. C. Albertsson, (Eds.), *Biodegradable Polymers and Plastics*. (pp. 73-92). Melksham: Redwood Press Ltd.
45. Arthur J. Coury. (2004c). Chemical and Biochemical Degradation of Polymers. In Buddy D. Ratner, Allan S. Hoffman, Frederick J. Schoen, etc.(Eds.), *Biomaterials Science, An Introduction to Materials in Medicine, 2nd edition*, (pp. 411-430). New York: Elsevier.
46. Michel Therin & Pascal Christel, (1992). In vivo degradation of massive poly(α -hydroxyl acids):validation of in vitro findings, *Biomaterials*, 13 (9), 594-600.
47. Li SM. Garreau H, Vert M, (1992b). In vivo degradation mechanism of massive aliphatic polyesters derived from lactic and glycolic acids. In M. Vert, J. Feijen, & A. C. Albertsson, (Eds.), *Biodegradable polymers and plastics*, (pp. 7-20). Melksham: Redwood Press Ltd.
48. Li SM. & Vert M. (1994), Morphological changes resulting from the hydrolytic degradation of stereocopolymers derived from L- and DL-lactides. *Macromolecules*, 27. 1307-1310.
49. Yasin M, & Tighe BJ, 1993, Strategies for the design of biodegradable polymer systems: manipulation of polyhydroxybutyrate-based materials. *Plastic rubber Comp Proc Appl*, 19, 15-27.
50. Xichen Zhang, Urs P. Wyss, & David Pichora, etc., (1994), An Investigation of Poly (lactic acid) Degradation. *Journal of Bioactive and Compatible Polymers*. 9, 80-100.
51. Grizzi, I., Garreau, H., Li, S., & Vert, M., (1995). Hydrolytic degradation of devices based on poly(DL-lactic acid) size-dependence. *Biomaterials*, 16 (4). 305-311.
52. Vert, M., (1998). Bioresorbable synthetic polymers and their operation field, In G. Walenkamp (Ed), *Biomaterials in Surgery*. (pp. 97-101). Stuttgart: Georg Thieme.
53. Tsutomu Yasukawa, Uuichiro Oguar, & Uasuhiko Tabata, etc. (2004), Drug delivery systems for vitreoretinal diseases, *Progress in Retinal and Eye Research*, 23 (3), 253-281.

54. Alekha K. Dash & Greggory C. Cudworth II. (1998), Therapeutic Applications of Implantable Drug Delivery Systems, *Journal of Pharmacological and Toxicological Methods*, 40, 1-12.
55. Robert Langer, (1990), New methods of drug delivery, *Science*, 249, 1527-1533.
56. N.A. Peppas, (1984), Drug Product Design and Performance, In V.F. Smolen & L.A. Ball, (Eds.), *Controlled Drug bioavailability, vol.1.* (pp. 203-237). New York: Wiley.
57. R. Langer & N.A. Peppas, (1983). Chemical and physical structure of polymers as carriers for controlled release of bioactive agents. *Journal of Macromolecular Science, Part C-Reviews in Macromolecular Chemistry and physics.* 23, 61-126.
58. Philp L. Ritger & N.A. Peppas, (1987), A simple equation for description of solute release. I. Fickian and non-Fickian release from non-swellable devices in the form of slabs, spheres, cylinders or discs. *Journal of Controlled Release*, 5 (1), 23-36.
59. Ritger, P.L. and Peppas, N.A., 1987, A simple equation for description of solute release. II. Fickian and anomalous release form swellable devices. *Journal of Controlled Release*, 5 (1), 37-42.
60. Peppas, N.A., (1984), Mathematical modeling of diffusion processes in drug delivery polymeric systems. In: Langer, R.S. and Wise, D. (Eds), *Medical Applications of Controlled Release Technology, Vol. 2*, (pp169-187). Boca Raton, Florida: CRC Press.
61. N.A. Peppas & Jennifer J. Sahlin, (1989), A simple equation for the description of solute release, III. Coupling of diffusion and relaxation. *International Journal of Pharmaceutics*, 57 (2), 169-172.
62. J.Crank,(1975), *The Mathematics of Diffusion*, Oxford: Clarendon Press.
63. Baker, R. W. & Lonsdale, H.K., (1974), Controlled release: mechanisms and rates. In Tanquary, A.C. and Lacry, R.E. (Eds.), *Controlled Release of Biologically Active Agents*, (pp.15-71). New York: Plenum.
64. N.A. Peppas, (1985), Analysis of Fickian and non-Fickian drug release from Polymers, *Pharmaceutica Acta Helvetiae*, 60, 110.
65. Drew Myers, (1988), Emulsions, *Surfactant science and technology*, (pp.209-250). New York, N.Y.: VCH Publishers, Inc..
66. Becher, P., (1965), *Emulsions: Theory and Practice*, 2nd ed., New York, Reinhold.
67. Griffith, W. C., (1954). *J. Soc. Cosmetic Chemists* 5, 249.
68. V. Labhaset war et al. (1997). Nanoparticle drug delivery system for restenosis. *Advanced Drug Delivery Reviews*, 24 (1), 63-85.
69. D. Lemoine, & V. Preat. (1998). Polymeric nanoparticles as delivery system for influenza virus glycoproteins. *Journal of Controlled Release*, 54 (1), 15-27.
70. J. Molpeceres, M. R. Abertural & Guzman. (2000). Biodegradable nanoparticles as a delivery system for cyclosporine: preparation and characterization. *Journal of Microencapsulation*, 17 (5), 599-614.
71. A. Lamprecht, N. Ubrich, & M. Hombreiro Perez, et al, (2000). Influences of process parameters on nanoparticle preparation performed by a double emulsion pressure homogenization technique. *International Journal of Pharmaceutics*, 196 (2), 177-182.
72. Thirumala Govender, Snjezana Stolnik, & Martin C. Garnett, et al, (1999). PLGA nanoparticles prepared by nanoprecipitation: drug loading and release studies of a water soluble drug. *Journal of Controlled Release*, 57 (2). 171-185.
73. Eric Allemann, Jean-Christophe Leroux, & Robert Gurny, et al. (1993). In vitro Extended-release Properties of Drug-Loaded Poly (DL- Lactic Acid) nanoparticles Produced by a Salting-Out Procedure. *Pharmaceutical Research*, 10 (12), 1732-1737.

74. Rainer Alex & Roland Bodmeier. (1990). Encapsulation of water-soluble drugs by a modified solvent evaporation method. I Effect of process and formulation variables on drug entrapment. *Journal of Microencapsulation*, 7 (3), 347-355.
75. W.W. Thompson, D.B. Anderson, & M. L. Heiman, (1997). Biodegradable microspheres as a delivery system for rismorelin porcine, a porcine-growth-hormone-releasing-hormone. *Journal of Controlled Release*, 43 (1). 9-22.
76. Smadar Cohen, Toshio Yoshioka, & Melissa Lucarelli, et al, (1991). Controlled delivery Systems for Proteins Based on Poly (Lactic/glycolic Acid) Microspheres. *Pharmaceutical Research*, 8 (6), 713-720.
77. Jean-Christophe Leroux, Patricia gravel, & Luc Balant, et al, (1994). Internalization of poly (D,L-lactic acid) nanoparticles by isolated human leukocytes and analysis of plasma proteins adsorbed onto the particles. *Journal of Biomedical Materials Research*, 28 (4), 471-481.
78. E. Allemann, R. Gurny & E.Doelker. (1992). Preparation of aqueous polymeric nanodispersions by a reversible salting-out process: influence of process parameters on particle size. *International Journal of Pharmaceutics*, 87 (1-3), 247-253.
79. Eric Allemann, Eric Doelker & Rober Gurny. (1993). Drug loaded poly(lactic acid) nanoparticles produced by a reversible salting –out process: purification of and injectable dosage form. *European Journal of Pharmaceutics and Biopharmaceutics*, 39(1). 13-18.
80. O'Donnell, P.B., Iwata, M., & McGinity, J. W., (1995). Properties of multiphase microspheres of poly (D,L-lactic-co-glycolic acid) prepared by a potentiometric dispersion technique. *Journal of Microencapsulation*, 12. 155-163.
81. Doane, J., (1980). Interaction of eyelids and tears in corneal wetting and the dynamics of the normal human eyeblink, *American Journal of Ophthalmology*, 89, 507-516
82. Annick Ludwig, (2005). The use of mucoadhesive polymers in ocular drug delivery, *Advanced Drug Delivery Reviews*, 57(11), 1595-1639.
83. Shell, J. W., (1982). Pharmacokinetics of topically applied ophthalmic drugs, *Survey of Ophthalmology*. 26 (4), 207-218.
84. Baum, J., Peyman, G. A., & Barza, M., (1982). Intravitreal administration of antibiotic in the treatment of bacterial endophthalmitis, III: consensus. *Survey of Ophthalmology* 26 (4), 204-206.
85. Ussery, F. M., Gibson, S.R., & Conklin, R. H., etc., (1988). Intravitreal ganciclovir in the treatment of AIDS-associated cytomegalovirus retinitis. *Ophthalmology* 95, 640-648.
86. Peyman, G. A., Khoobehi, B., & Tawakol M, etc., (1987). Intravitreal injection of liposome-encapsulated ganciclovir in a rabbit model. *Retina* 7 (4), 227-229.
87. Moritera, T., Ogura, Y., & Honda, Y., etc., (1991). Microspheres of biodegradable polymers as a drug delivery system in the vitreous. *Investigative Ophthalmology & Visual Science*. 32 (6), 1785-1790.
88. Sanborn, G. E., Anand, R., & Torti, R. E., etc., (1992). Sustained-release ganciclovir therapy for treatment of cytomegalovirus retinitis. *Archives of Ophthalmology*, 110 (2), 188-195.
89. Hashizoe, M., Ogura, Y., & Takanashi T, etc., (1995). Biodegradable polymeric device in the treatment of experimental proliferative vitreoretinopathy. *Current Eye Research*. 14 (6), 473-477.
90. Jacobson M. A., Mills. J. (1988). Serious cytomegalovirus disease in the acquired immunodeficiency syndrome (AIDS). *Annals of Internal Medicine*, 108 (4), 585-594.

91. Bloom J. N, Palestine A. G. (1988). The diagnosis of cytomegalovirus retinitis. *Annals of Internal Medicine*, 109 (12), 963-969.
92. Hoover, D. R., Saah A. J., & Bacellar H, etc. (1993). Clinical manifestation of AIDS in the era of pneumocystis prophylaxis: Multicenter AIDS cohort study. *The New England Journal of Medicine*. 329, 1922-1926.
93. CYTOVENE®-IV (ganciclovir sodium for injection) FOR INTRAVENOUS INFUSION ONLY; CYTOVENE® (ganciclovir capsules) FOR ORAL ADMINISTRATION. [On-line]. Available: <http://www.transplantbuddies.org/library/drugs/full/cytovene.html>
94. PharmPK Discussion List Archive - PK2003343.html – 2003. [On-line]. Available: <http://www.boomer.org/pkin/PK03/PK2003343.html>
95. Lim, J. I., Wolitz, R. A., & Dowling, A. H., etc., (1999). Visual and anatomic outcomes associated with posterior segment complications after ganciclovir implant procedures in patients with AIDS and cytomegalovirus retinitis. *American Journal of Ophthalmology*. 127 (3), 288-293.
96. Kunou, N., Ogura, Y., & Yasukawa, T., etc. (2000). Long-term sustained release of ganciclovir from biodegradable sclera implant for the treatment of cytomegalovirus retinitis. *Journal of Controlled Release*. 68 (2), 263-271.
97. Iwao Teraoka, (2002), Chapter 3 Dynamics of Dilute Polymer Solutions. In *Polymer Solutions: An Introduction to Physical Properties*, (pp. 167-275). John Wiley & Sons, Inc.
98. Paul Becher, (2001), Chapter 12 Techniques of Emulsification. In *Emulsions: Theory and Practice, 3rd edition*. (pp. 373-428). Washington, DC: American Chemical Society: Oxford University Press.
99. Ruan Gang, Feng Si-Shen and Qui Tian Li, (2002), "Effects of Materials Hydrophobicity on Physical Microspheres Formed by Double Emulsion Process", *Journal of Controlled Release*, 84, 151-160.
100. D. Campbell; R.A. Pethrick; & J.R. White; (2000). *Polymer Characterization: physical techniques. 2nd Ed.*. Cheltenham: Stanley Thornes Publishers.
101. F. Billmeyer, Jr, (1984), *Textbook of Polymer Science, 3rd Ed.*. New York: John Wiley & Sons.
102. A.E. Tonelli, M.A. Gomez, & H. Tanaka, etc, (1990), Spectroscopic and Chromatographic Methods. In C.D. Laven & T. Prorder, (Eds.), *Polymer Characterization: Physical Property*. Washington, D.C: American Chemical Society.
103. Hsieh E. T, and Randall J. C., (1982). Ethylene-1-butene copolymers. 1. Comonomer sequence distribution. *Macromolecules*, 15 (2), 353-360.
104. A. Brandolini, (1987), Chemical and physical characterization of polymer systems by p13sC NMR spectroscopy. In C. Dybowski and R.L. Lichter (Eds), *NMR Spectroscopy Techniques*. (pp. 331-373). New York: Maral Pekker.
105. R.J. Abraham, J. Fisher & P. Loftus, (1988), *Introduction to NMR Spectroscopy*, Chichester; New York: John Wiley & Sons.
106. Hansberger A. G., and Deluca P. P., (1995). Characterization of biodegradable poly(D, L-lactide-co-glycolide) polymers and microspheres. *Journal of Pharmaceutical & Biomedical Analysis*, 13 (6), 747-760.
107. Jamshidi K, Hyon S. H, Ikada Y, (1988). Thermal characterization of polylactides. *Polymer*, 29 (12), 2229-2234.
108. H.G., Elias, (1984), *Macromolecules: Structure and Properties, Vol. 1, 2nd ed.*, New York: Plenum.
109. P.D.Scholes, A.G. A. Coombes, & M.C.Davies, etc., (1997), Particle Engineering of Biodegradable Colloids for Site-Specific Drug Delivery. In Kinam

- Park (Ed.), *Controlled drug delivery: challenges and strategies*. (73-106). Washington, DC: American Chemical Society.
110. Reed A. M., and Gilding D. K., (1981). Biodegradable polymers for use in surgery-poly(glycolic)/poly(lactic acid) homo and copolymers: 2. In vitro degradation. *Polymer*, 22 (4), 494-498.
111. Ikada Y, Jamshidi K., & Tsuji H., et al, (1987). Stereocomplex formation between enantiomeric poly(lactides). *Macromolecules*. 20 (4), 904-906.
112. Park T. G., Degradation of poly(lactic-co-glycolic acid) microspheres: effect of copolymer composition. (1995). *Biomaterials*. 16 (15), 1123-1130.
113. Li S. M., Garreau H., & Vert M., (1990). Structure-property relationships in the case of degradation of massive aliphatic poly(α -hydroxyl acids) in aqueous media. Part 1: poly(DL-lactic acid). *Journal of Materials Science. Materials in Medicine*. 1, 123-130.
114. Li S. M., Garreau H., & Vert M., (1990). Structure-property relationships in the case of degradation of massive aliphatic poly(α -hydroxyl acids) in aqueous media. Part 2. Degradation of lactide-glycolide copolymers. *Journal of Materials Science. Materials in Medicine*. 1, 131-139.
115. Park, T. G., (1994). Degradation of Poly(D,L-lactic acid) microspheres: effect of molecular weight. *Journal of Controlled Release*. 30 (2), 161-173.
116. Mu L., and Feng S. S., (2003). A novel controlled release formulation for the anticancer drug paclitaxel (Taxol®): PLGA nanoparticles containing vitamin E TPGS. *Journal of Controlled Release*. 86 (1), 33-48.
117. Hashizoe M., Ogura Y., & Takanashi T., et al, (1997). Biodegradable polymeric device for sustained intravitreal release of ganciclovir in rabbits. *Current Eye Research*. 16 (7), 633-639.
118. Rizk S., Duru C., & Gaudy D., et al., (1994). Natural polymer hydrophilic matrix: influencing drug release factors. *Drug Developments and Industrial Pharmacy*. 20, 2563-2574.

BIBLIOGRAPHY

Journal Papers Overseas

X. Chen, C. P. Ooi, W. S. Lye, T. H. Lim, *Sustained Release of Ganciclovir from Poly(lactide-co-glycolide) microspheres*, Journal of Microencapsulation. 22(6):621-631, 2005 Dec 20.

X. Chen, C. P. Ooi, T. H. Lim, Effect of Ganciclovir on the hydrolytic degradation of poly(lactide-co-glycolide) microspheres, J. Biomat. Appl. Jan 2006; 20: 287 - 302

Conference Papers

Biodegradable Ganciclovir Loaded Poly(lactide-co-glycolide) Microspheres for Intraocular Administration

Xi Chen, Chui Ping Ooi

2nd International Conference on Materials for Advanced Technologies,

Suntec Singapore International Convention and Exhibition Centre

7 – 13th December 2003

The Effect of Hydrolytic Degradation on Ganciclovir Release from PLGA microspheres

C. P. Ooi, X. Chen, Y. C. Lim, T. H. Lim

2nd International Conference on Materials Processing for Properties and Performance (MP³),

Yokohama International Conference Centre, Japan,

11 – 13th October 2003

In vitro Release Behaviour of Ganciclovir from PLGA Microspheres and Tablets,

X. Chen, C. P. Ooi, T. C. Chan and T. H. Lim

4th International Conference on Materials Processing for Properties and Performance (MP³),

Tsukuba Science City, Ibraki, Japan

30 Nov – 2 Dec 2005

Conference Poster

Biodegradable Ocular Implants for Treatment of CMV Retinitis

HC Ng, X Chen and C.P. Ooi

5th Annual NTU-SGH Biomedical Engineering Symposium

College of Medicine Building, Singapore, 25 April 2002